MATHEMATICAL MODELLING ON EFFECTS OF TOXICANTS AND GLOBAL WARMING ON AQUATIC POPULATION DYNAMICS

A Thesis

Submitted to

For the award of

DOCTOR OF PHILOSOPHY (Ph.D.)
in

Mathematics

By

Shreya

Registration Number 41500172

Supervised By

Dr. Preety Kalra

LOVELY FACULTY OF TECHNOLOGY AND SCIENCES
LOVELY PROFESSIONAL UNIVERSITY
PUNJAB
2020

DECLARATION BY THE CANDIDATE

I declare that the thesis entitled **"MATHEMATICAL MODELLING ON EFFECTS OF TOXICANTS AND GLOBAL WARMING ON AQUATIC POPULATION DYNAMICS"** submitted for award of degree of Doctor of Philosophy in Mathematics, Lovely Professional University, Phagwara, is my own work conducted under the supervision of Dr. Preety Kalra (Supervisor), Assistant Professor in Department of Mathematics at School of Chemical Engineering and Physical Sciences, Lovely Professional University, Phagwara, Punjab. I further declare that to the best of my knowledge the thesis does not contain any part of any work which has been submitted for the award of any degree in this University or in any other University/Deemed University without proper citation.

Signature of the Supervisor

(Dr. Preety Kalra)

Signature of the Candidate

(Shreya)

CERTIFICATE

This is to certify that the work entitled **"MATHEMATICAL MODELLING ON EFFECTS OF TOXICANTS AND GLOBAL WARMING ON AQUATIC POPULATION DYNAMICS"** is a piece of research work done by Ms. Shreya under my guidance and supervision for the degree of Doctor of Philosophy of Mathematics , Lovely Professional University, Phagwara (Punjab) India. To the best of my knowledge and belief the thesis:

1. Embodies the work of the candidate herself.
2. Has duly been completed.
3. Fulfills the requirements of the ordinance relating to the Ph.D. degree of the University, and
4. Is up to the standard both in respect of contents and language for being referred to the examiner.

Signature of the Supervisor
(Dr. Preety Kalra)
School of Chemical Engineering and Physical Sciences
Lovely Professional University, Phagwara, Punjab.

ABSTRACT

In the proposed work, the study of the underlying system consisting of major inter-related components, viz. aquatic population, global warming, acidification, eutrophication, pollutants and toxicants is carried out. The system is analysed and studied by defining its borders, by distinguishing its major components, characterizing the change in them by mathematical equations and then interconnecting the representative equations in order to obtain a model of the original system. For the proposed study, deterministic and dynamic mathematical models are constructed using systems of ordinary differential equations in order to predict the changes in the attributes of the inter-related objects of the system. The population growth dynamics is modelled independently, taking into account the factors such as toxicity of water, rising temperature of water, pH of water, dissolved oxygen in water etc. and then these models are used to predict the effects of toxicant concentration, acidification and global warming on the process rates affecting the growth of an aquatic organism.

Once the model is governed by differential equations, these equations are solved assuming the initial positivity of all the state variables as initial conditions and by using mathematical techniques related to the system of non-linear differential equations. The system of differential equations constituting the models is analyzed using stability theory. The boundedness of all the solutions obtained and the processes involved is checked using comparison principles. The local stability is checked using Jacobian and Lyapunov's method and the global stability is analysed using Lyapunov function. Also, numerical solutions of the models are obtained by using numerical techniques and MATLAB. For the models, the sensitivity analysis is also conducted in order to estimate the sensitivity of state variables with respect to model parameters. Further, for the verification and validation of the results/outcomes of the model, they are compared with the existing experimental results and the available data in research papers related to our field in order to verify that whether the model assembly really represents the functioning of the system or not.

The objective of the research work includes the study of:

1. Mathematical modelling on effects of water pollutants and toxicants on single aquatic population.

2. Mathematical modelling on effects of water pollutants and toxicants on interacting aquatic populations.

3. Mathematical modelling on combined effects of global warming and water acidification on single aquatic population.

4. Mathematical modelling on combined effects of global warming and water acidification on interacting aquatic populations.

In chapter 1, the general introduction about the aquatic population dynamics under the effect of various anthropogenic stressors such as pollution, acidification, global warming etc. has been given. The literature review section brings into light, certain noteworthy works done by researchers in this field till date. In view of the same, the research gaps have been identified and the objectives of the study have been proposed. The important concepts, terms and mathematical preliminaries used throughout the study have also been described in this chapter. The chapter concludes with a summary of the chapters included in the thesis.
In chapter 2, the effect of increasing toxicity and acidity in water bodies on the aquatic population dynamics is studied. A non-linear mathematical model having variables as concentration of acid in water, concentration of toxicant in water, concentration of dissolved oxygen in water and density of aquatic population (like fish) has been proposed. Through stability analysis and numerical simulations, it has been shown that the rising water toxicity and acidity are detrimental to the growth and survival of the aquatic population. Sensitivity analysis is also carried out for the model, which shows that both dissolved oxygen and aquatic population are found to be sensitive and negatively dependent on the input rate of toxicant and input rate of acid in water. Threshold value for dissolved oxygen is calculated under the hypothetical numerical simulation values and the results obtained are

validated with the results of previously available experimental and mathematical studies in this field.

In chapter 3, the impacts of rising toxicants and acid components in water on the resource i.e. dissolved oxygen, the prey population and predator population in an aquatic ecosystem are studied by proposing a non-linear mathematical model. Stability analysis for the model is carried out. It is shown that the prey population decreases with rising toxicity and acidity level in water. Consequently, the predator population which is dependent on prey population for its food also exhibits a decline in its density with rising toxicity and acidity. Moreover, from the sensitivity analysis, it is further observed that dissolved oxygen and predator population are sensitive and negatively dependent on input rate of toxicant in water. Oscillatory behaviour is observed for prey and predator populations on increasing the assimilation rate above the value 1.28. The results obtained from the model analysis and numerical simulations are validated by comparing them with results of previously available studies.

In chapter 4, the effects of rising level of carbon emissions and the rising acidity on concentration of dissolved oxygen in water are studied. A non-linear mathematical model consisting of variables as concentration of carbon in water, pH level of water, density of algal population and concentration of dissolved oxygen in water is proposed and analyzed. Results of stability analysis and numerical simulations carried out for the model show that under the simultaneous effects of increased carbon emissions and acid in water, the oxygen level in water will decrease more rapidly than under the single effect of each factor. With increase in natural decay rate of algal bloom to $h = 8.893$ and above, the system bifurcates to a stable limit cycle periodic solution and Hopf bifurcations are observed. The results of our study are supported by study done by Chakraborty et al. 2017. Also, threshold values for input rate of carbon in water and input rate of dissolved oxygen in water have been calculated for the model.

In chapter 5, a mathematical model consisting of non-linear differential equations is formulated, to study the impact of global warming, increased carbon emissions and increased algal bloom growth on the level of dissolved oxygen in water. Local and global stability analysis is done for the model. Numerical simulations are

carried out using MATLAB. It is observed that with rise in global warming and carbon emissions, the dissolved oxygen concentration exhibits a decline. A threshold level for carbon input is proposed, above which the survival of species in an aquatic ecosystem may not be possible due to development of hypoxic conditions.
In chapter 6, a non-linear mathematical model is proposed to study the hazardous consequences of the growing plastic pollution on aquatic ecosystem and the impact of this menace on the dissolved oxygen in water, in the presence of already existing environment stressors such as global warming and eutrophication. The results of the model analysis suggest that interplay between the anthropogenic stressors i.e. plastic pollution, global warming and eutrophication is much more detrimental to aquatic ecosystem rather than the single effect, as these factors may lead to deficiency of dissolved oxygen pushing the system towards a state of hypoxia. Sensitivity analysis for the model is also carried out which shows that the water temperature increases with rising greenhouse gases and also shows that the increasing rates of eutrophication promote high algal growth in water which in turn results in decreased oxygen levels in water. It is suggested that certain methods to control the environment stressors have to be devised at the earliest, especially focusing on waste disposal and treatment before their inlet in the water bodies.

In chapter 7, a non-linear mathematical model is proposed to study the impact of inflating level of carbon emissions which is contributing towards global warming, and water acidification on the algal bloom population and aquatic populations like fishes which are dependent on dissolved oxygen for their survival. Stability analysis and numerical simulations performed using MATLAB for the proposed model, reveal that the unprecedented rise of carbon emissions, water temperature and water acidity can create a hypoxic situation, if not controlled timely which in turn will hamper the oxygen-dependent population species residing in the aquatic bodies. It is also observed that with the increase in rate of algal decomposition (h) to 0.952 and above, the system bifurcates to a stable limit cycle periodic solution and Hopf-bifurcations are observed.

In the end, the problems undertaken for investigation in this study have been justified by a bibliography given in the concluding part of the thesis.

ACKNOWLEDGEMENT

I express my heartfelt gratitude to my thesis supervisor, Dr. Preety Kalra, Assistant Professor, School of Chemical Engineering and Physical Sciences, Lovely Professional University, Punjab for her interest, excellent rapport, untiring co-operation, invaluable advice and encouragement throughout my Ph.D. program. Without her unfailing support and belief in me, this thesis would not have been possible. I am indeed feeling short of words to express my sense of gratitude towards her. Besides being a scholar par eminence, she is a person par excellence - a perfect embodiment of dedication, intelligence and humility. She pushed me farther than I thought I could go.

I acknowledge with pleasure the cooperation from the esteemed faculty of the University for their enthusiastic support and and encouragement throughout this research work.

Above all, I feel very much obliged to my father Mr. Narinder Mohan and my mother Mrs. Neeru Tangri for what I have received from them in the form of motivation, inspiration, love, encouragement and moral support. Without them, it would have really been impossible to carry out this task. They have supported me unconditionally and relentlessly over all these years.

22 July, 2020. Shreya

Contents

List of Tables

List of Figures

Chapter 1

General Introduction

1.1 Introduction

Aquatic ecosystem is a discrete unit having well-defined boundaries, energy sources, certain abiotic components and a group of interacting organisms which constantly interact among themselves as well as their surrounding environment leading to transfer of energy within the ecosystem. It is basically a water-based ecosystem. Aquatic ecosystem can be further categorized as Fresh water ecosystems and Marine ecosystems. Lake ecosystem and river ecosystem are examples of freshwater ecosystems. Marine ecosystems constitute about 97% of the water on Earth. These include the organisms which live in oceans or sea. These can be found in the depths of ocean floor, near the sea or ocean surface as well as on the ocean surface. Coral reefs, mangroves, estuaries, and deep-sea vent communities are examples of marine ecosystems. An aquatic ecosystem are home to various types of species which include aquatic plants (also referred to as hydrophytes) such as ferns and seaweeds, aquatic vertebrates like fishes, whales, cords, sharks etc., organisms such as shrimps, crayfish and other crustaceans, amphibians, reptiles, bacteria and other micro-organisms. Abiotic components such as sand, silt etc. also form a part of the aquatic ecosystem.

The scientific study of populations having marine habitat is called marine ecology which is basically a subset of marine biology and includes observations at the individual and community levels combined with the study of aquatic ecosystems. This includes the study of structure, efficiency of marine food webs, the functional, structural relationships within a species, among organisms of different species and takes into accounts their interactions with the physical and chemical environments as well.

Population can be explained as an assembly of identical community members which live together under a homogeneous environment. The marine ecosystems have a diverse collection of populations, some of which are given below:

- Benthic organisms which are the organisms that live at the bottom and are associated with activities like crawling and burrowing, for example, mollusks, small gastropods, crabs etc.
- Pelagic organisms i.e. the organisms swimming or drifting in water, for example, Blue whale, red tuna crabs etc.
- Plankton species, which are not able to swim against the ocean currents, e.g., dinoflagellates, jellyfish, algae etc.
- Nekton species which can able to against the ocean currents, for example, lobsters, scallops etc.

A series of continuous interactions and interrelations exist among the different populations present in an aquatic ecosystem as well as between the population and the abiotic environmental factors. The interactions can be of various types, some of them are illustrated below:

- Mutualism: It is an interspecific connection between two living beings in the aquatic system with advantage to both the partner individuals in interaction with each other. Amid this connection, populations of each associating species develop, survive, and reproduce at a larger rate within the sight of other interacting species.
- Competition: Where individuals of a species compete amongst one another or with individuals of a different species for various resources like nutrition, space etc. which in turn determines the diversity, profuseness, life cycles, distribution, and health of a species. In this interaction each species is affected negatively.
- Predation: An organism which eats another living being for their sustenance is called predator while the living being that is being eaten upon is named as prey.

This sort of association between the prey and predator is known as predation.
• Commensalism: It is an interspecific connection between two life forms in the ecosystem where one group of species benefits while the alternate species stays unaffected. In this affiliation, for the most part a commensal can acquire supplements from the host species for their living place, development, and movement whereas the host remains unaffected.
• Amensalism: Any relationship existing between organisms of varied species wherein one organism is destroyed or inhibited while the other organism is unaffected.
The environment of a species in an ecosystem also plays a determining role in the existence, growth, and survival of the species. It basically constitutes the physical properties which directly or indirectly influence an organism and may affect many natural processes like rate of reproduction, survival, or extinction of a particular species in a habitat. In an aquatic ecosystem, the environment is majorly consisting of water as the species reside and interact either inside or on the surface of water. The influencing environmental factors can be abiotic such as heat, pH of water, dissolved oxygen in water, dissolved carbon dioxide, nitrogen phosphates etc. or, the affecting parameters can be biotic in nature such as other organisms which live in and share the same habitat.
It is hard to exaggerate the role of marine biological communities (particularly plankton communities) in impacting life on earth. Marine phytoplankton provides a large portion of the total oxygen available by human and other living beings. The activities of plankton populations are also contributing to global climate change. In addition the ocean is a very important source of food for many nations. That makes the study of marine ecosystems a primary task. Another part of the issue concerns the issue of conserving nature and protecting biodiversity. The increasing anthropogenic impact on marine ecosystems (such as waste disposal, increased carbon emissions and intensive fishing) has driven many ocean and marine ecosystems to a dangerous state wherein many aquatic species are on the verge of extinction. Despite substantial progress over the last decades, more comprehensive studies are imperative.
The aquatic ecosystem influences human population in many vital ways. Potable

water, water for industrial, commercial, and agricultural use etc. is obtained from freshwater bodies. Marine ecosystems also act as a source for fertilizers, minerals, food, tourism avenues, transportation facilities etc. However, currently these ecosystems are facing a threat from various activities such eutrophication and acidification caused by discharge of agricultural, household, and industrial wastes in water bodies. Human acts such as overfishing and hunting of exotic species as well as increasing temperature of water due to global warming are also posing a threat to the sustainability and diversity of these ecosystems. A variety of different co-occurring stressors are likely to affect the ecology of deep sea ecosystems.

Globally, temperature and climatic conditions have exhibited notable changes in recent years and recent studies foresee even more shifts in climate patterns due to anthropogenic activities [1]. The anthropogenic activities are leading to a substantial inflation in the release of gases such as carbon dioxide in the earth's atmosphere. The oceans are known to play a crucial role in buffering the impacts of the global alterations due to human- driven activities by acting as the largest active carbon sink by absorbing the carbon emissions and heat generated in the atmosphere. However, the magnified carbon emissions, increasing temperature and inflated pollution rates of water are posing a threat to the functioning and sustainability of the marine ecosystems as well as to the survival and productiveness of the organisms and species in the ecosystems.

The variation of one of the most salient environmental factors i.e. Temperature is found to have many important ecological effects. The oxygen production is decreasing to accommodate the warming of oceans, which is leading to altered plankton-oxygen dynamics and may prove fatal to the aquatic populations [2].This shall also negatively affect the resource based Prey-predator system [3]. Along with the increase of temperature, the anthropogenic activities are contributing to an increase in pollution of water bodies due to the unchecked release of various kinds of wastes such as agricultural and household effluents in aquatic bodies leading to eutrophication and acidification of water. Global warming is found to further add to the eutrophication process in lakes. These activities also lead to an increase of nitrogen and phosphorus concentration in water which causes algae to grow rapidly at a rate which the ecosystem is incapable of handling. This all is having catastrophic consequences for biological species residing in water, a major effect being the decrease of dissolved oxygen in water. Continuous decrease of dissolved oxygen in water may lead to oxygen being present in quantity which is insufficient for the fishes and other aquatic life to survive in water. The food web and community structure are also being disturbed due to these changes [4, 5].

The increasing carbon dioxide concentration in environment, along with increasing the temperature of water, is also leading to lowering of pH of seawater, thus leading to oceanic acidification. The various anthropogenic stresses such as pollution and climate changes are also exerting pressures on the coral reefs which is leading to high mortality rates and mass bleaching of the coral reefs. This in turn is disturbing the existing biodiversity of oceans. The impacts further extend to coastal ecosystems due to increase of harmful algal blooms (HAB's). These algal blooms have been found to kill aquatic species such as fishes, contaminate sea food by poisoning and altering the aquatic ecosystems, coastal tourism, the fisheries, and human and other species health [6]. The changing climate dynamics especially an increase in carbon emissions shall also impact the overall economic growth in a negative way [8]. In research environments, modelling commonly serves purpose such as integrating knowledge or the quantitative testing hypotheses and for modelling, the system of interest needs to be described. In aquaculture and marine sciences, the system of interest is commonly a marine organism for example, phytoplankton or zooplankton and very often a collection of interacting species for example, a group of fishes, small fishes, and whales etc. It is found that few works with mathematical modelling has been proposed in this direction.

The study of marine ecosystems is an increasingly significant issue. Often, however, field experiments seem either very expensive, or even impossible. A marine ecosystem is a particularly complicated object from the point of a regular scientific investigation, due both to multiple number of interacting aquatic species and the complexity of the aquatic environment properties. That is one of the reasons why the role of mathematical modelling in marine ecology is very important.

In view of the above, in the proposed study mathematical modelling on the aquatic population under effect of toxicants like water pollutants, metals, nutrients such as nitrogen, phosphorus etc. , the phenomenon of global warming and the combined effect of toxicants and global warming will be carried out. The mathematical modelling in study of aquatic ecosystem shall be helpful in paving way and providing guidance for future research. This study shall prove beneficial to carry out a quantitative study of the damage caused to organisms, their growth and survival in presence of limiting factors such as pollutants and toxicants in water, reduction in dissolved oxygen, temperature of water, acidification and eutrophication of water bodies etc. The outcome of the proposed research work will help us to predict loss of ecological diversity and quality loss due to the adverse effects of toxic chemicals and temperature. The models proposed in the thesis shall also assess the effects of increasing carbon emissions resulting in the temperature increase of water on the growth dynamics of aquatic population and these will be used for designing and exploring various decision policies at agricultural, regional and industrial scales. System analysis and mathematical modelling supported analysis of a particular water ecosystem will also help the experimentalists and marine biologists in designing strategies to control yield and quality of marine bodies under reducing factors such as toxicants in the form of toxic chemicals.

1.2 Literature Review

The work carried out by initial researchers in this field was mainly of theoretical, empirical, and statistical type. Gamo et al. [12] studied the temporal and spatial variations in water characteristics of the Japan sea. Meyer et al. [8] were among the early researchers to review the theoretical models to explore the impacts of change in climate on freshwater ecosystems. They also identified certain improvements that need to be made in the models to further improve the understanding of climate alterations in future. Hulme [9] discussed the various threats of the climate change and explored various strategies, methodologies, and management strategies to tackle this problem. Research has shown that both abiotic and ocean-based biological changes would be considerably more complex under global climate change. Also, climate -induced changes are likely to be intensified by synergistic effects between pressures such as overfishing and the temperature rise [10]. Mackenzie et al. [11] described the impact of climate change on the fisheries management and the fish species of the Baltic sea using a regional – scale climate– ocean modelling considering the factors of increased temperature and salinity. Kundzewicz et al. [13] conducted a theoretical study of climate change in Anthropocene and concluded that the climate change is likely to cause decline in quality of freshwater, thus leading to its scarcity. The increasing temperatures also posed threat to pursuit of sustainable development of the affected areas. Sokolova and Lannig [14] conducted a review to understand the implications of the temperature rise due to global warming and pollution by discharge of trace metals in water bodies, on marine species. The scope for studying the effect of global warming on freshwater bodies was further broadened by Vadadi-Fulop et al. [15], who showed by theoretical ecological modelling that freshwater zooplankton exhibited shifts in their distribution, abundance, structure, size spectra and phenology to respond to the climate change. Their study further opened avenues for more in-depth study of climate change effects on freshwater populations. Collins et al. [16] conducted a theoretical study on the impact of the rising global warming on the El Niño–Southern Oscillation (ENSO) and the Tropical Pacific Ocean.

Apart from the above-mentioned theoretical studies, many statistical and empirical studies have also been conducted to study the effect of increasing temperatures on aquatic ecosystems. The climate change impact was statistically studied by Hoegh-Guldberg [17] who proved that climate change was a fundamental factor in causing aquatic ecological transformations and may lead to irreversible effects such as species distribution alteration, changed dynamics of food webs, less ocean productivity and greater probability of disease. Few researchers through their study concluded that the physio–chemical characteristics of deep water may undergo radical changes under the climate change. Evidences for these observations were found by empirical studies done in various water bodies such as study of Mediterranean Sea by Danovaro et al. [18] and the study of the Baltic Sea by Carstensen et al. [19]. Quere et al. [20] showed the weakening of Southern Ocean Carbon sink due to the climate change resulting from recent human activities. Numerical experiments conducted by Okunishi et al. [21] for pelagic fish ecosystem in the western North Pacific revealed that the under the global warming scenario, the growth of fish in the key spawning area was slightly slower than under the present climatic conditions. Through statistical work, they proved that carbon sink will be present as long as atmospheric carbon dioxide exists but fraction of carbon emissions that the ocean will be able to absorb shall decrease in capacity. Statistical studies by Kibler et al. [22] also revealed that due to changes in water temperature, the growth relationships of the aquatic species such as dinoflagellates will show a substantial shift in their distribution and abundance. As per the empirical study conducted by Deutsch et al. [23], climate shifts may lead to alteration of species ecologies by reducing the metabolic index of the upper oceans by 20% globally and forcing the metabolically viable habitats to contract pole ward. The relationship between the process of global warming and effect of increase of carbon dioxide in atmosphere was studied statistically by Specht et al. [24], in which it was demonstrated that, if the concentration of carbon dioxide is doubled, the temperature of Earth shall show an increase by 0.4 K. Gleckler et al. [25] also proved through their statistical work that due to anthropogenic warming, heat uptake by the oceans had doubled in the recent decades. This in turn led to warming of oceans and subsequent loss of dissolved oxygen in a marine ecosystem. The increased carbon dioxide concentration and the resulting rising acidity level of water threaten the growth and early-life survival rates of larval-fish populations and hence lead to perturbations in the ability of adult fish to adapt to surging carbon dioxide level [26]. Sweetman et al. [27] through their study based on statistical observations provided many vital effects of change of climate on the deep-sea benthic ecosystems. According to the study, the main environmental variables expected to be altered due to increasing carbon emissions were pH of water, dissolved oxygen in water, temperature of water and food supply of benthic organisms. The increase of carbon in atmosphere may lead to increase of ocean temperature by $1 \circ$C and cause decrease of the level of dissolved oxygen in water. This shall further impact the food availability for aquatic species, alter the rates of predation and competition, alter embryonic growth and survival rates of egg laying elasmobranches and lead to early maturation of fishes resulting in slow population rates and long generation times. It was concluded from their study that increase in carbon emissions shall characterize decrease of biodiversity and populations of flora and fauna in the oceanic seabed. Trolle et al. [28] analyzed in their experimental study that uncertainties of land-use, eco-hydrological models and climate models in potential aquatic ecosystem status predictions.

A few mathematical studies have attempted to explore the effect of global warming and rising water temperatures on the aquatic ecosystem. Dymnikov et al. [29] stated various strategies to construct mathematical models for modelling climatic changes and discussed main concepts regarding the mathematical aspects of climate theory. Hijmans and Graham [30] probed the feasibility of climate envelope models for predication of species distribution pattern under the climatic variations. Kellie-Smith and Cox [7] highlighted in their mathematical study that the changing climate dynamics, especially an increase in carbon emissions shall also impact the overall economic growth in a negative way. The mathematical study carried out by Misra et al. [31] concluded that the rising level of Chlorofluoro Carbon (CFC) is depleting the concentration of ozone in atmosphere and leading towards global warming. The study also recognized the effects of increasing global warming on survival level of two competing populations. To better understand the adverse effects of increasing carbon dioxide in atmosphere due to human activities, Shukla et al. [32] proposed a non-linear mathematical model having six dynamical variables which were concentration of atmospheric carbon dioxide, human population , ice sheets mass, mean surface temperature and sea level and area of land submerged in water. The model was analysed qualitatively and conditions for local and global equilibriums were evaluated through Lyapunov's method. It was shown that by controlling the carbon emissions in atmosphere, melting of ice glaciers could be minimized which would lead to stabilization of sea level, decrease of land submerging in water and consequently shall benefit the human population.

Another disastrous consequence of human – driven activities in Anthropocene was found to be rise of quantity of pollutants and toxicants in water bodies. Muyibi et al. [33] evaluated the consequences of economic advancement in Malaysia and the challenges faced in enforcing the regulatory policies for control of water pollution. Ahmed et al. [34] conducted a study on river Buriganga, Bangladesh and found that the heavy metals accumulated in the shellfish and tropical fishes could have carcinogenic health risks if consumed continuously and excessively by humans over a time period of 70 years. Halder and Islam [35] have discussed that the rising water pollution is having devastating impact on human health wherein the humans are getting exposed to various health problems such as respiratory diseases, anaemia, reproduction and childbirth problems, dengue, malaria, yellow fever etc. The continuous exposure of aquatic species to the toxic metals and its uptake by them poses many health risks to human population which consume these species, especially fish [36]. Hamilton et al. [37] conducted a data-based study on the adaptive capabilities of the fish in contact with the water pollutants, the effects on their fitness and critically reviewed the lethal impacts of chemical spills on the exposed wild fish population in water bodies. Zohra and Habib [38] deduced from their study on fish populations of the Mediterranean Sea that heavy metal contaminants and toxicants give rise to high risks towards the health of the fish population. Corcoll et al. [39] studied the effects of Copper pollution at environmental concentrations on marine microbial communities. Sadeq and Beckerman [40] highlighted the chronic impact of sublethal heavy metal concentrations on Cladocera Species and observed reduced growth and reproduction rate along with delayed maturity in the population under the effect of these heavy metals. Study conducted by Raja et al. [41] in the Adyar estuary of South India revealed that chromium toxicity caused mass mortality of fishes. Wang et al. [42] carried out an experimental study to bring forth the toxic effects of increased concentrations of Silver (Ag) and Zinc (Zn) on organisms in freshwater bodies and recommended optimal concentration of Silver and Zinc for protection of the freshwater ecosystems.

One of the most dreadful anthropogenic activity in the last 60 years adversely affecting the marine ecosystems worldwide is the rise in plastic production. The plastic which at one time was viewed as just another pollutant has now emerged as an omnipresent catastrophe and a major environmental threat worldwide. In the aquatic ecosystems, besides the entanglement and ingestion of macro debris by large vertebrates, the planktonic and invertebrate species ingest and accumulate the microplastics and are further transferred and moved along food chains [43]. Vegter et al. [44] emphasized the need to plastic pollution in order to safeguard the survival of marine wildlife and ensure the future survival of species in ocean and coastal habitats. Eerkes-Medrano et al. [45] reviewed the surfacing threats and identified knowledge gaps by investigating the presence of microplastics in freshwater systems and the effect of the plastic pollution on the aquatic organisms. The plastic nanoparticles which are transferred upwards through an aquatic food chain cause brain disorders and behavioural impairments in aquatic zooplankton especially fish [46].

Some mathematical works have attempted to stress the severity of the negative effect of the pollutants entering in the water bodies on the marine biota. He and Wang [47] mathematically analysed the behaviour over a long period of time and criterial for extinction or survival of a population in a closed environment contaminated with pollutants. The spatial dynamics for a system of nutrient-phytoplankton where the phytoplankton is assumed to be affected by the toxins is studied using a mathematical model by Chakraborty et al. [48]. Chakraborty and Das [49] proposed a model for a system of two phytoplankton and one zooplankton exhibiting a Holling type II functional response under the influence by toxicity. They demonstrated that in order to achieve a sustainable ecosystem, an ideal control strategy for toxic substances needs to be defined. Mathematical model proposed by Kumar et al. [50] analysed the effect of toxicants on the deformity in a biological population which could be applied to human population also. Bhatia et al. [51] described a stage-structured bio-economic fishery model under toxicants presence with harvesting having the control parameter as Taxation. An optimal harvesting policy was proposed in their study using Pontryagins maximum principle. Tiwari et al. [52] conducted a mathematical study on the impact or organic as well as inorganic pollutants on the fish population and highlighted that in order to ensure the survival and life of fish population, restrictions need to be imposed on release of pollutants in water bodies.

The rising carbon emissions and soaring amount of pollutants and toxicants entering aquatic bodies is accelerating ocean acidification. McNeil and Matear [53] showed from their empirical study that ocean acidification shall follow the increase in anthropogenic carbon emissions. The lowered pH will impact the marine biological species adversely; hence they raised the concern to stop the future acidification of water by reducing the carbon emissions to atmosphere through activities such as fossil fuel burning. Guinotte and Fabry [54] attempted to review the effects of rising acidification of oceans on marine organisms. Bijma et al. [55] proved by their theoretical study, that the deadly appearance of the three risk factors in oceans namely ocean warming, water acidity rise pushed the ecosystem towards deterioration. Cripps et al. [56] revealed through their study that the ocean acidification leads to decrease in growth rates and suppressed the reproductive scope in zooplankton. The rising stress of ocean and coastal water acidification was studied by Breitburg et al. [57] wherein they synthesized some discrete observations regarding the concurrence of ocean acidification along with other environment co-stressors like modifications in food webs, climatic changes, oxygen and productivity variations etc. Dixson et al. [58] and Jellison et al. [59] showed through their empirical study that the acidification of water was disrupting the ability of organisms like fishes and snails to detect predators. Ocean acidification has been found to substantially increase the toxicity response of two principle benthic species i.e. purple sea urchins (Paracentrotus lividus) and mussels (Mytilus edulis) to a global coastal contaminant (copper -0,1 μM) [60]. Nagelkerken et al. [61] predicted that the rise in ocean acidification could lead to loss of marine biodiversity and low productivity. Elevation in carbon dioxide emissions could also lead to modifications and alterations in the habitat of fish populations. Ocean acidification is also found to boost the accumulation of Cadmium in bivalve species which can be latent risk to sea food safety [62]. Qi et al. [63] showed by their statistical study that the western Arctic Ocean was being rapidly acidified due to various human activities like water transport and increase in carbon uptake by the oceans. Law et al. [64] have attempted to review the devastating effects of water acidification on the vulnerability of calcifying organisms focussing on aquatic ecosystems of New Zealand. The increasing carbon dioxide concentration, which is a major driver for acidification of oceans and climatic disturbances, coupled with desalination can majorly affect the micro planktonic food web [65]. Using a sample data, Mukherjee et al. [66] studied the physiological responses of the freshwater fish populations under the fluctuating acidity levels.

Recent researchers have also drawn attention towards the degradation of coral reefs because of ocean warming and increased pollutants and consequent ocean acidification. Ocean acidification is causing irreversible losses to the to coral reef community and decreasing the abundance and growth of crustose coralline algae [67]. Buddemeier et al. [68] attempted to calculate the long-term effects of the future temperature increase, ocean acidification and bleaching events on coral reefs using a simulation model. Pandolfi et al. [69] found that the coral reefs are degrading under the pressure of human-induced stressors such as climate change, overfishing and pollution and maintaining the normal ecological and biological functioning of these ecosystem is a massive global challenge. Munday et al. [70] highlighted that the rising ocean acidification shall contribute towards emergence of behavioural impairments in the reef fishes. Hughes et al. [71] have pointed out on the basis of their experimental and empirical study that after the ill-effects of the pollution, temperature increase was the second factor adding to stress on coral reefs. They also identified prevailing challenges of sustaining coral reefs and ensuring normal ecosystem functioning. Further a conceptual outline of framework was provided which gave an insight to the options to be incorporated for the conservation and restoration of coral ecosystems. The effect of ocean warming on coral reefs was further studied empirically by DeCarlo et al. [72] wherein it was concluded that an increase of 2$\circ$C ocean temperatures led to mass coral bleaching and mortality. These increased death rates of Coral reefs could have devastating consequences in future and would impact coastal economies in a negative way greatly. The ocean acidification shall lead to harmful influence on marine life such as causing bleaching, decreased productivity and lower diversity of species in Coral reefs ,which was proved through many statistical studies conducted by Anthony et al. [73], Enochs et al. [74] and by Sunday et al. [75].

The aggravating global warming, pollution, eutrophication, and ocean acidification is increasing the growth of Harmful Algal Bloom in water. Rabalais et al. [76] showed through empirical studies that the Harmful algal blooms are increasing manifold which can prove harmful for aquatic and water dependent populations. The increased eutrophication under global change is thus likely to cause many harmful impacts such as poor water quality, loss of habitat, biodiversity loss and boom in harmful algal blooms. Hallegraeff [77] predicted a rise in harmful algal bloom and secondary negative effects on the marine food webs because as a result of global climate mutations. Fu et al. [6] concluded from their study that the harmful algal growth which is increasing due to global climate change is detrimental to both the aquatic and human population. Glibert et al. [78] used a global modelling approach to study the impacts of harmful algal blooms to coastal ecosystems. Through a statistical model, they proved due to the sudden increase in frequency and magnitude of algal blooms due to increasing temperatures, detrimental effects on aquatic life have been seen and these warming conditions have caused contamination of seafood with toxins and disrupted the functioning of the ecological processes of the ecosystem. These findings received support by McCoy and Pfister [79] and Gobler et al. [80], who through their experimental study put forward the finding that intensification of harmful algal bloom due to global warming was leading to an increased human health threat and concern. Snickars et al. [81] determined the changes in distribution and availability of zoobenthos and benthic-feeding fish under the effects of climate changes, salinity level and eutrophication. The growth of algal bloom leads to decrease in the dissolved oxygen level of water because the decomposition process of algal blooms uses the dissolved oxygen and can create a hypoxic situation. The fish kill event witnessed in 2002 in the coastal waters of Bolinao, Pangasinan, Philippines was attributed to increased eutrophication and algal bloom growth which led to drop of dissolved oxygen level below 2.0 mg/L [82].

Pal et al. [83] proposed a mathematical model to show that phytoplankton-zooplankton persist in case the maximum ingestion rate becomes more than threshold value. They proved that under high nutrient concentration, algal bloom increased in growth. The growth of algal blooms in water due to nutrient discharge in form of agricultural and domestic wastes was deduced from mathematical study conducted by Shukla et al. [84]. Their model considered the combined interactions of algal population density, concentration of nutrients, detritus density and concentration of dissolved oxygen in the water. Through equilibria analysis it was found that with increase in eutrophication, the rate of algal blooms had increased. Shukla et al. [85] proposed a nonlinear mathematical model to study the simultaneous effect of eutrophication and water pollutants on the level of dissolved oxygen in water bodies and showed that under the individual effect of either of the two factors, the dissolved oxygen level was greater as compared to the dissolved oxygen when these two factors operate together in a water body. Misra et al. [86] proposed a mathematical model to mitigate the burgeoning algal bloom growth through creating awareness among the farmers to reduce agricultural run-off in surrounding water bodies such as lake and adopt is as a remedial measure to stop this aquatic catastrophe. Nie et al. [87] presented a resource competition model to study two algal species in the presence of uncurbed and excess rising atmospheric carbon dioxide concentration. Wolkowicz and Yuan [88] developed a mathematical model to study the effect of light on the nitrogen fixing and non-nitrogen fixing phytoplankton population. Jiang et al. [89] mathematically analysed a system of toxin producing phytoplankton along with zooplankton under the effect of harvesting with Holling III functional response. In the mathematical study conducted by Yu et al. [90], they considered a nutrient-plankton model along with toxin-producing phytoplankton and emphasized that the toxin-producing phytoplankton and fluctuations in the environment play an important role in ending algal blooms. Zhang et al. [91] described a mathematical model consisting of coupled system of partial and ordinary differential equations to study the interplay among pelagic algae, benthic algae and nutrient in a shallow aquatic ecosystem. Mandal et al. [92], in their mathematical study emphasized that in order to maintain the stability of a phytoplankton-zooplankton system, there is dire need to control the rate of input of environmental toxins like chemicals pesticides etc. into the water bodies. Warming waters, increasing ocean acidification and pollution was disorienting and creating chaos in growth and survival of marine species which was shown by statistical data analysis conducted by various researchers such as Guinotte and Fabry [54], Cripps et al. [56], Mearns et al. [93], Munday et al. [70], and Tembo [94]. Serafy and Harrell [95] documented some laboratory and field observations with regard to the behavioural responses of freshwater fish assemblages to high pH and dissolved oxygen levels.

One of the alarming consequences of the damage caused to marine ecosystems by the climate change was the decreasing content of oxygen in water due to the increasing temperature. This was pointed out in the statistical studies done by various researchers such as Joos et al. [96] and Stramma et al. [97]. Nurnberg [98] proposed the concept of the Hypoxic Factor for quantifying the dissolved oxygen concentration in lakes and reservoirs. A decrease of 1 to 7% in global oxygen concentration is predicted by the ocean models as a result of ocean warming leading to adverse effects on productivity and habitat for marine species [99]. Foley et al. [100] conducted an essential data study over a time span of 40 years (1968–2008) and highlighted the negative consequences on dissolved oxygen concentration in a lake in a long-time response to eutrophication and climatic changes. Decrease in dissolved oxygen concentration leading to hypoxia has been associated with transgenerational reproductive impairments in species such as fishes [101]. Modification in ocean ventilation rates and deoxygenation are vital ecological and biogeochemical implications of climate change [102]. The prediction of decline in oxygen content in oceans was also proved by Schmidtko et al. [103] in their empirical work on the available data of oceans. Through their work they proved that the global oxygen content has deteriorated in the past five decades which could in turn affect the marine habitats and populations, nutrient cycles, fisheries, and coastal economies. The models proposed also predicted a 25% more decline in oxygen content than the currently observed trend due to anthropogenic warming which may lead to harmful impacts on ocean dynamics.

Few researchers have undertaken mathematical studies in the past to understand the decreasing amount of dissolved oxygen in water under the effect of various factors such as increased temperature, toxicity, eutrophication, acidification of water etc. and subsequent effect of the phenomenon on the aquatic ecosystem. A mathematical study on effect of discharging pollutants such as industrial and household organic wastes in water bodies and consequent dissolved oxygen depletion was carried out by Misra et al. [104] by proposing a non-linear mathematical model incorporating the variables of pollutants, population and level of dissolved oxygen. It was concluded in their study that with acceleration in discharge rate of pollutants in water body, the equilibrium level of oxygen exhibits a decreasing trend. This can threaten the survival of various species living in water bodies. Survival of aquatic biotic species in polluted water was further studied mathematically by Shukla et al. [105]. The study was conducted on a food chain and modelled using the parameters of pollutant concentration, biological population, bacteria concentration, dissolved oxygen density of protozoa. Through stability analysis and numerical example, it was demonstrated that when the discharge of pollutants is made at very large rates, the dissolved oxygen content will decrease and threaten the survival of biological species living in water. The simultaneous effect of eutrophication and pollutants was studied by Shukla et al. [85] by proposing a mathematical model which considered six parameters. The variables taken were concentration of nutrients, pollutants, bacteria density, density of algae, detritus, and oxygen. Equilibrium and stability analysis for the model was conducted which showed that the combined simultaneous occurrence of water pollution and eutrophication decreases the dissolved oxygen more as compared to a single effect thus threatening the survival of oxygen dependent species in water. Khare et al. [106] observed from their mathematical study of impact of decreasing dissolved oxygen on the survival and extinction of the biotic species such as interacting zooplankton and phytoplankton. They showed that with the occurrence of deficiency of dissolved oxygen in water on account of eutrophication caused in Anthropocene, the density of phytoplankton and zooplankton was also depleted. Kalra and Shreya [107] formulated a mathematical study to examine the simultaneous effects of acidity and toxicity on the aquatic populations like fishes and concluded that rising toxicity and acidity lead to depriciation in oxygen level in water and hence hamper survival of aquatic population. The altering dynamics of oxygen depletion and its consequent effect on plankton population due to global warming was studied by Sekerci and Petrovskii [2]. They developed a mathematical model having variables as oxygen concentration and density of zooplankton and phytoplankton in water. Through steady state analysis and numerical simulations, they found out that a large amount of warming may lead to a stage resulting in absolute depletion of dissolved oxygen. Bharathi et al. [108] discussed a mathematical approach to evaluate the impacts of increasing toxicity and pollutants in the marine habitats. The increasing acidity of water and its subsequent effect on the phytoplankton and fish population was studied and criteria for extinction or survival of the phytoplatonic and fish population were obtained. The fact that fish population shall lead to extinction on account of decrease of oxygen due to anthropogenic activities was further supported by mathematical study of Misra and

Chaturvedi [109]. They proposed a novel mathematical model which studied the depletion of dissolved oxygen in water bodies and the fate (survival/extinction) of fish population with nutrient loading i.e. with input of phosphorus and nitrogen in water body due to anthropogenic activities. It was shown that population of fish shall tend to extinction, in case the concentration of dissolved oxygen was reduced below threshold level as specified in their study. Venturino et al. [110] gave a mathematical study which concluded that the industries and human population destabilize a water body located near a city, by overburdening it with pollutants and effluents which decrease the amount of oxygen in the water body.

1.3 Proposed objectives of the study

In view of the above therefore, in the proposed study mathematical modelling on the aquatic population under the effects of toxicants and global warming will be carried out. The objective of the research work includes the study of:

1. Mathematical modelling on effects of water pollutants and toxicants on single aquatic population.
2. Mathematical modelling on effects of water pollutants and toxicants on interacting aquatic populations.
3. Mathematical modelling on combined effects of global warming and water acidification on single aquatic population.
4. Mathematical modelling on combined effects of global warming and water acidification on interacting aquatic populations.

1.4 Main terms used in Thesis

1. **Population**: [111] A number of individuals of the same species living and breeding in a specific area.

2. **Predator**: [112, 113] An animal that captures and kills another animal (the Prey) in order to eat it. The predator attacks prey and reduces its growth. A predator that is at the top of the food chain is often called a top predator. Top predators are often Keystone Species: if their populations are healthy, it is a good indication that the ecosystem as a whole is in a healthy state, because the rest of the food chain must be in a healthy enough state to support it.

3. **Prey**: [113] An organism that is likely to be killed and eaten by a Predator.

4. **Food Chain**: [111] A series of organisms that pass energy and minerals from one to another as each provides food for the next. The first organism in the food chain is the producer and the rest are consumers.

5. **Food Web**: [111] A series of food chains that are linked together in an ecosystem.

6. **Interaction**: [111] A relationship between two or more biological organisms or species.

7. **Stability**: [111] The situation where the number of individuals in a population or the level of a resource quickly returns to its original value following a disturbance.

8. **Stress**: [111] A condition where an outside influence changes the composition or functioning of something.

9. **Toxicant**: [111] Referring to a substance that is poisonous or harmful to humans, animals or the environment.

10. **Pollute**: [111] To discharge harmful substances in unusually high concentrations into the environment.

11. **Eutrophication**: [111] The process by which water becomes full of phosphates and other mineral nutrients which encourage the growth of algae andkill other organisms.

12. **pH**: [111] pH gives the measurement of the acidity for a solution. It is calculated as the negative logarithm of the hydrogen ion concentration, measured on a scale from 0 to 14.

13. **Acidification**: [111] The process of becoming acidic or of making a substance more acidic.

14. **Bifurcation**: [114] "A bifurcation occurs when a small smooth change made to the parameter values (the bifurcation parameters) of a system causes a sudden "qualitative" or topological change in its behavior".

1.5 Mathematical Preliminaries

1.5.1 Autonomous and non-autonomous system [115]

"Let x(t) be vector valued function defined by

$$x(t) = \begin{pmatrix} x_1 \\ x_2 \\ x_3 \\ \vdots \\ \vdots \\ x_n(t) \end{pmatrix} = col(x_1(t), x_2(t) \ldots\ldots\ldots x_n(t))$$

and f be vector valued function given by

$$f(t,x) = \begin{pmatrix} f_1(t, x_1, x_2, \ldots x_n) \\ f_2(t, x_1, x_2, \ldots x_n) \\ \vdots \\ \vdots \\ f_n(t, x_1, x_2, \ldots x_n) \end{pmatrix} = col(f_1(t,x), f_2(t,x) \ldots\ldots\ldots f_n(t,x))$$

then the system

$$\frac{dx}{dt} = f(t,x) \tag{1.1}$$

with initial condition $x(t_0) = x_0$ is a non-autonomous system. A differential equation of the form

$$\frac{dx}{dt} = f(x) \tag{1.2}$$

with initial condition $x(t_0) = x_0$ in which right hand does not involve independent variable t, is said to be autonomous system."

1.5.2 Equilibrium point [115]

"Consider a system of first order differential equations of the form

$$\begin{aligned} x_1^{'} &= f_1(t, x_1, x_2, ...x_n) \\ x_2^{'} &= f_2(t, x_1, x_2, ...x_n) \\ &\vdots \\ x_n^{'} &= f_n(t, x_1, x_2, ...x_n) \end{aligned}$$

where $f_1, f_2, ...f_n$ are n given functions in some domain B of (n+1)-dimensional Euclidean space R^{n+1} and $x_1, x_2, ...x_n$ are n unknown functions. A set of n - function $\phi_1, \phi_2...\phi_n$ defined on I is said to be solution of equation (1.1) on I if for $t \in I$,
(i) $\phi_1^{'}(t), \phi_2^{'}(t)...\phi_n^{'}(t)$ exist.
(ii) The point $(t, \phi_1(t), \phi_2(t)...\phi_n(t))$ remain in B; and
(iii) $\phi_i^{'} = f_i(t, \phi_1(t), \phi_2(t)...\phi_n(t)), i = 1, 2...n$."

1.5.3 Solution of differential system [115]

"Consider a system

$$\frac{dx_i}{dt} = f_i(x_1, x_2, ..., x_n) \tag{1.3}$$

A point $x^* = (x_1^*, x_2^*, ...x_n^*)$, is called a positive equilibrium of equation (1.3) if
(i) $x^* > 0$,
(ii) $f_i(x_1^*, x_2^*, ...x_n^*)$=0 hold for all i=1,2,...n."

1.5.4 Definitions of Stability [115]

Definition 1.5.4.1. [115] "The solution x(t) of system (1.1) is said to be stable if, for each $\epsilon > 0$ there exist a $\delta = \delta(\epsilon) > 0$ such that for any solution $\bar{x}(t) = x(t, t_0, \bar{x_0})$ of system (1.1), the inequality $\| \bar{x} - x_0 \| < \delta$ implies $\| \bar{x}(t) - x_0(t) \| < \epsilon$ for all $t \geq t_0$."

Definition 1.5.4.2. [115] "The solution x(t) of (1.1) is said to be asymptotically stable if it is stable and if there exist a $\delta_0 > 0$ such that $\| \bar{x} - x_0 \| < \delta_0$ implies $\| \bar{x}(t) - x_0(t) \| \to 0$ as $t \to \infty$".

Definition 1.5.4.3. [115] "The solution x(t) of (1.1) is said to be unstable if it is not stable."

1.5.5 Hurwitz Theorem [115]

"Necessary and sufficient condition for the negativity of real parts of all the roots of polynomial $P(\lambda) = \lambda^n + a_1\lambda^{n-1} + a_2\lambda^{n-2} + ... + a_{n-1}\lambda + a_n$, with real coefficients the positivity of all the principle diagonals of the minors of the Hurwitz matrix

$$H_n = \begin{pmatrix} a_1 & 1 & 0 & 0 & 0 & 0 & 0 & ... & 0 \\ a_3 & a_2 & a_1 & 1 & 0 & 0 & 0 & ... & 0 \\ a_5 & a_4 & a_3 & a_2 & a_1 & 0 & 0 & ... & 0 \\ \vdots & \vdots & \vdots & \vdots & \vdots & \vdots & \vdots & ... & \vdots \\ 0 & 0 & 0 & 0 & 0 & 0 & 0 & ... & a_n \end{pmatrix}$$

Principal diagonals of H_n, for n=1,2,3,— are given by

$$D_1 = |a_1|, \quad D_2 = \begin{vmatrix} a_1 & 1 \\ a_3 & a_2 \end{vmatrix}, ..., D_n = det(H_n).$$

In the case of second, third and fourth degree polynomials, the Hurwitz conditions can be written as follows:
(i) For $P(\lambda) = \lambda^2 + a_1\lambda + a_2$, the Hurwitz condition are $a_1 > 0, a_2 > 0$.
(ii) For $P(\lambda) = \lambda^3 + a_1\lambda^2 + a_2\lambda + a_3$, the Hurwitz condition are
$a_1 > 0, a_2 > 0, a_3 > 0$ and $a_1a_2 - a_3 > 0$.

(iii) For $P(\lambda) = \lambda^4 + a_1\lambda^3 + a_2\lambda^2 + a_3\lambda + a_4$, the Hurwitz condition are $a_1 > 0, a_2 > 0, a_3 > 0, a_4 > 0$, and $a_1a_2a_3 - a_3^2 - a_1^2a_4 > 0$."

Theorem 1.5.1. *[115] "If all the characteristic roots of A have negative real parts, then every solution of*

$$\frac{dx}{dt} = Ax$$

, where $A = (a_{ij})$ is a constant matrix, is asymptotically stable."

Theorem 1.5.2. *[115] "If all the characteristic roots of A with multiplicity greater than one have negative real parts and all its roots with multiplicity one have non positive real parts, then all the solution of system $\frac{dx}{dt} = Ax$ are bounded and hence stable."*

1.5.6 Liapunov's Second Method of Stability [115]

"The following system of an autonomous differential equation is of the form

$$\frac{dx}{dt} = f(x) \tag{1.4}$$

where, $f \in C[R^n, R^n], x = (x_1, x_2, ..., x_n), f = (f_1, f_2, ..., f_n), x(t_0) = x_0, t \in [t_0, \infty)$. Assume that f is a smooth enough to ensure the existence and uniqueness of the solution of (1.4). Let $f(0) = 0$ and $f(x) \neq 0$ for $x \neq 0$ in some neighbourhood of the origin so that (1.4) admits the so called zero solution (x = 0) and the origin is an isolated critical point of (1.4).
Let Ω be an open set in R^n containing the origin. Suppose V (x) is a scalar continuous function (i.e., a real-valued continuous function in the variables $(x_1, x_2, ..., x_n)$ defined on Ω. For the sake of easy geometrical interpretation, we shall use the Euclidean norm,

$$\| x \|_e^2 = x_1^2 + x_2^2 + ... + x_n^2$$

in our discussion. For convenience, we shall drop the subscript e."

Definition 1.5.6.1. [115] "A scalar function V (x) is said to be positive definite on the set Ω if and only if V (0) = 0 and $V(x) > 0$ for $x \neq 0$ and $x \in \Omega$."

Definition 1.5.6.2. [115] "A scalar function V (x) is called positive semidefinite on the set Ω when V has the positive sign throughout Ω, except at points (include the origin) where it is zero."

Definition 1.5.6.3. [115] "A scalar function V (x) is negative definite (negative semi-definite) on the set Ω if and only if -V (x) is positive definite (positive semi-definite) on Ω."

1.5.7 Sylvester's Criterion [115]

"Let

$$V(x) = x^T Bx = \sum_{i,j=1}^{n} b_{ij} x_i x_j, \tag{1.5}$$

be a quadratic form with the symmetric matrix $B = (b_{ij})$ i.e. , $b_{ij} = b_{ji}$.
To test positive definiteness of V (x) in (1.5), we can apply the Sylvester's criterion which asserts that a necessary and sufficient condition for V (x) in (1.5) to be positive definite is that the determinants of all the successive principal minors of the symmetric matrix $B = (b_{ij})$ be positive, that is,

$$b_{11} > 0, \quad \begin{vmatrix} b_{11} & b_{12} \\ b_{21} & b_{22} \end{vmatrix}, ..., \begin{vmatrix} b_{11} & b_{12} & ... & b_{1n} \\ b_{21} & b_{22} & ... & b_{2n} \\ \vdots & \vdots & ... & \vdots \\ b_{n1} & b_{n2} & ... & b_{nn} \end{vmatrix} > 0.$$

The derivative of V with respect to (1.4) is the scalar product given by

$$V^*(x) = gradV(x).f(x),$$

$$V^*(x) = \frac{\partial V}{\partial x_1} f_1(x) + \frac{\partial V}{\partial x_2} f_2(x) + ... + \frac{\partial V}{\partial x_n} f_n(x). \tag{1.6}$$

It should be noted that if x = x(t) is any solution of (1.4), then by the chain rule and from (1.6), we can obtain

$$\frac{d}{dt} V(x(t)) = \frac{\partial V}{\partial x_1} x_1'(t) + \frac{\partial V}{\partial x_2} x_2'(t) + ... + \frac{\partial V}{\partial x_n} x_n'(t),$$

$$= \sum_{i=1}^{n} \frac{\partial V}{\partial x_i} f_i(x(t)) = V^*(x(t)).$$

Let S_ρ be the set $S_\rho = \{x \in R^n :\| x \|< \rho\}$ and let $R^+ = [0, \infty)$ and $J = [t_0, \infty), t_0 \geq 0$. Suppose $x(t) = x(t, t_0, x_0)$ is any solution of (1.4) with the initial value $x(t_0) = x_0$ such that $\| x \|< \rho$ for $x \in J$. Also since (1.4) is autonomous, we can further suppose, without any loss of generality, that $t_0 = 0$."

Theorem 1.5.3. *[115] "If there exists a positive definite scalar function $V(x)$ such that $V^*(x) \leq 0$ on S_ρ, then the zero solution of (1.4) is stable."*

Theorem 1.5.4. *[115] "If there exists a positive definite scalar function $V(x)$ such that $V^*(x)$ is negative definite on S_ρ, then the zero solution of (1.4) is asymptotically stable."*

Theorem 1.5.5. *[115] "If there exists a scalar function $V(x), V(0) = 0$, such that $V^*(x)$ is positive definite on S_ρ and if in every neighbourhood N of the origin, $N \subset S_\rho$, there is a point x_0, where $V(x_0) > 0$, then the zero solution of (1.4) is unstable."*

1.5.8 Comparison Principle [115]

"Consider the initial value problem

$$u' = g(t, u), \quad u(t_0) = u_0, \tag{1.7}$$

where $g \in C[\Omega, R], \Omega$ being on open set in R^2. Let $J_1 = [t_0, t_0 + a), a > 0$.
Let $g \in C[\Omega, R], \Omega$ being on open set in R^2, and let r(t) be the maximal solution of (1.7) on J_1. Also, let m(t) be a continuous function on J_1 such that $m(t_0) \leq u_0$ and $(t, m(t)) \in \Omega$ satisfying the differential inequality,

$$D_+ m(t) \leq g(t, m(t)), \quad t \in J_1 \tag{1.8}$$

Then, on the common interval of existence of m(t) and r(t), the inequality

$$m(t) \leq r(t) \tag{1.9}$$

holds."

1.5.9 Sensitivity Analysis

The sensitivity indices of state variables with respect to the parameters of the model, help in the measurement of relative variation in variables with respect to change in parameter values. These indices help to identify that how minor changes in the value of parameters bring about variations in the value of state variables. These indices therefore help in modelling process, designing of necessary control strategies, and gives an insight of the overall behaviour of the proposed mathematical model.
The normalized forward sensitivity index of a variable 'Z' depending on a parameter 'u' is given by the following expression [117]:

$$\gamma_u^Z = \frac{\partial Z}{\partial u} * \frac{u}{Z} \tag{1.10}$$

The results of sensitivity analysis prove to be more mathematically sound than the simple variation in the parameter values.

1.6 Summary of the thesis

In the proposed work, the study of the underlying system consisting of major inter-related components, viz. aquatic population, global warming, acidification, eutrophication, pollutants and toxicants is carried out. The system is analysed and studied by defining its borders, by distinguishing its major components, characterizing the change in them by mathematical equations and then interconnecting the representative equations in order to obtain a model of the original system. For the proposed study, deterministic and dynamic mathematical models are constructed using systems of ordinary differential equations in order to predict the changes in the attributes of the inter-related objects of the system. The population growth dynamics is modelled independently, taking into account the factors such as toxicity of water, rising temperature of water, pH of water, dissolved oxygen in water etc. and then these models are used to predict the effects of toxicant concentration, acidification and global warming on the process rates affecting the growth of an aquatic organism.

Once the model is governed by differential equations, these equations are solved assuming the initial positivity of all the state variables as initial conditions and by using mathematical techniques related to the system of non-linear differential equations. The system of differential equations constituting the models is analyzed using stability theory. The boundedness of all the solutions obtained and the processes involved is checked using comparison principles. The local stability is checked using Jacobian and Lyapunov's method and the global stability iss analysed using Lyapunov function. Also, numerical solutions of the models are obtained by using numerical techniques and MATLAB. For the models, the sensitivity analysis is also conducted in order to estimate the sensitivity of state variables with respect to model parameters. Further, for the verification and validation of the results/outcomes of the model, they are compared with the existing experimental results and the available data in research papers related to our field in order to verify that whether the model assembly really represents the functioning of the system or not.

In chapter 1, the general introduction about the aquatic population dynamics under the effect of various anthropogenic stressors such as pollution, acidification, global warming etc. has been given. The literature review section brings into light, certain noteworthy works done by researchers in this field till date. In view of the same, the research gaps have been identified and the objectives of the study have been proposed. The important concepts, terms and mathematical preliminaries used throughout the study have also been described in this chapter. The chapter concludes with a summary of the chapters included in the thesis.

In chapter 2, the effect of increasing toxicity and acidity in water bodies on the aquatic population dynamics is studied. A non-linear mathematical model having variables as concentration of acid in water, concentration of toxicant in water, concentration of dissolved oxygen in water and density of aquatic population (like fish) has been proposed. Through stability analysis and numerical simulations, it has been shown that the rising water toxicity and acidity are detrimental to the growth and survival of the aquatic population. Sensitivity analysis is also carried out for the model, which shows that both dissolved oxygen and aquatic population are found to be sensitive and negatively dependent on the input rate of toxicant and input rate of acid in water. Threshold value for dissolved oxygen is calculated under the hypothetical numerical simulation values and the results obtained are validated with the results of previously available experimental and mathematical studies in this field.

In chapter 3, the impacts of rising toxicants and acid components in water on the resource i.e. dissolved oxygen, the prey population and predator population in an aquatic ecosystem are studied by proposing a non-linear mathematical model. Stability analysis for the model is carried out. It is shown that the prey population decreases with rising toxicity and acidity level in water. Consequently, the predator population which is dependent on prey population for its food also exhibits a decline in its density with rising toxicity and acidity. Moreover, from the sensitivity analysis, it is further observed that dissolved oxygen and predator population are sensitive and negatively dependent on input rate of toxicant in water. Oscillatory behaviour is observed for prey and predator populations on increasing the assimilation rate above the value 1.28. The results obtained from the model analysis and numerical simulations are validated by comparing them with results of previously available studies.

In chapter 4, the effects of rising level of carbon emissions and the rising acidity on concentration of dissolved oxygen in water are studied. A non-linear mathematical model consisting of variables as concentration of carbon in water, pH level of water, density of algal population and concentration of dissolved oxygen in water is proposed and analyzed. Results of stability analysis and numerical simulations carried out for the model show that under the simultaneous effects of increased carbon emissions and acid in water, the oxygen level in water will decrease more rapidly than under the single effect of each factor. With increase in natural decay rate of algal bloom to $h = 8.893$ and above, the system bifurcates to a stable limit cycle periodic solution and Hopf bifurcations are observed. The results of our study are supported by study done by Chakraborty et al. 2017. Also, threshold values for input rate of carbon in water and input rate of dissolved oxygen in water have been calculated for the model.

In chapter 5, a mathematical model consisting of non-linear differential equations

is formulated, to study the impact of global warming, increased carbon emissions and increased algal bloom growth on the level of dissolved oxygen in water. Local and global stability analysis is done for the model. Numerical simulations are carried out using MATLAB. It is observed that with rise in global warming and carbon emissions, the dissolved oxygen concentration exhibits a decline. A threshold level for carbon input is proposed, above which the survival of species in an aquatic ecosystem may not be possible due to development of hypoxic conditions.
In chapter 6, a non-linear mathematical model is proposed to study the hazardous consequences of the growing plastic pollution on aquatic ecosystem and the impact of this menace on the dissolved oxygen in water, in the presence of already existing environment stressors such as global warming and eutrophication. The results of the model analysis suggest that interplay between the anthropogenic stressors i.e. plastic pollution, global warming and eutrophication is much more detrimental to aquatic ecosystem rather than the single effect, as these factors may lead to deficiency of dissolved oxygen pushing the system towards a state of hypoxia. Sensitivity analysis for the model is also carried out which shows that the water temperature increases with rising greenhouse gases and also shows that the increasing rates of eutrophication promote high algal growth in water which in turn results in decreased oxygen levels in water. It is suggested that certain methods to control the environment stressors have to be devised at the earliest, especially focusing on waste disposal and treatment before their inlet in the water bodies.

In chapter 7, a non-linear mathematical model is proposed to study the impact of inflating level of carbon emissions which is contributing towards global warming, and water acidification on the algal bloom population and aquatic populations like fishes which are dependent on dissolved oxygen for their survival. Stability analysis and numerical simulations performed using MATLAB for the proposed model, reveal that the unprecedented rise of carbon emissions, water temperature and water acidity can create a hypoxic situation, if not controlled timely which in turn will hamper the oxygen-dependent population species residing in the aquatic bodies. It is also observed that with the increase in rate of algal decomposition (h) to 0.952 and above, the system bifurcates to a stable limit cycle periodic solution

and Hopf-bifurcations are observed.
In the end, the problems undertaken for investigation in this study have been justified by a bibliography given in the concluding part of the thesis.

Chapter 2

Study of Effects of Toxicants and Acidity on Oxygen-Dependent Aquatic Population: A Mathematical Model

2.1 Introduction

The aquatic ecosystem influences human population in varied vital ways. Potable water, water for industrial, commercial and agricultural use etc. are obtained from fresh water bodies. Marine ecosystems also act as a source of fertilizers, minerals, food, tourism avenues, transportation facilities etc. However, currently these ecosystems are under constant threat from various activities such as eutrophication and acidification caused by intractable discharge of agricultural, household wastes in water bodies. Industrial and metal pollution is threatening the existence of aquatic communities [39, 40, 42]. The toxicity level of water is increasing manifold due to rising pollutants. The increasing carbon dioxide concentration in environment is leading to lowering of pH of water, thus leading to water acidification [53]. As the environment of an aquatic species plays a determining role in the existence, growth and survival of the species, hence the population dynamics of species in water is also altered by growing toxicity and acidity. Increasing water acidification and pollution is responsible for disorienting and creating chaos in growth and survival of aquatic species [34, 56, 36, 37, 66, 94, 38]. Experimental and mathematical studies have also supported that the resource and fish populations are sensitive to the acidification and water pollution [108]. Increasing water toxicity has been found to cause mass fish mortality [41]. These effects are also leading to decrease of dissolved oxygen (DO) in water, which is one of the primary resources for survival of aquatic population [86, 110]. Decrease in dissolved oxygen (DO) level leads to decrease in water quality [35], death and reproductive impairments in fishes [101]. Increased rates of eutrophication and pollution also lead to steep increase in algal blooms which further limit the level of dissolved oxygen in water [48, 118, 6]. A few mathematical models exist which have studied the effect of toxicity and pollutants on dissolved oxygen and subsequent effects on the phytoplankton and fish population [106, 105, 84, 85]. Several mathematical studies [47, 104, 52] have highlighted that the toxicant discharge rate must be controlled in order to avoid the situations like hypoxia. The studies also show that the fish population shall lead to extinction on account of decrease of dissolved oxygen caused by anthropogenic activities [109]. The mathematical studies conducted till now have focussed on individual effects of increasing pollution, toxicant or acidity of water on aquatic population. However, the combined effect of acidity and toxicants on the target population has not been considered in the available studies. To focus on the combined effect of all these damaging factors especially on primary favourable resource i.e. dissolved oxygen in water and consequently on residing aquatic population like fishes, a non-linear mathematical model is being proposed.

In this model, it is assumed that the toxicity of water is increasing from discharge of metals, organic pollutants, inorganic pollutants, etc. into water bodies whereas the rise in acidity can be attributed to two phenomena. One reason is the direct discharge of industrial wastes, acids, chemicals in water and the second cause being the addition of carbon-rich pollutants in water. By carrying out analytical and numerical analysis for the model, the conditions for survival of aquatic population under the stress of toxicity and acidity are derived.

2.2 Mathematical Model

In this model, the aquatic population dynamics is studied by presuming that the water toxicity and acidity is rising due to anthropogenic activities. It is assumed that the acidity of water is increasing by two ways, one by direct input of acid components in water and the second through the carbon present in the pollutants. The latter results in formation of carbonic acid because the carbon reacts with the dissolved oxygen in water, thus increasing acidity of water. The rising acidity has grave consequences for aquatic populations. The incoming pollutants also increase the toxicity level of water. This results in decrease of dissolved oxygen in water which is assumed as the prime resource for survival of aquatic population. Depletion of dissolved oxygen , thus, has critical negative effect on survival and growth of aquatic population.

In view of the above, let A($\mu g L^{-1}$) and S($\mu g L^{-1}$) represent the concentration of acid and toxicant in water, P($mg L^{-1}$) represent the density of aquatic population like fish and let $D_0(mg L^{-1})$ denote the concentration of favourable resources i.e. dissolved oxygen in water. The above mentioned notations are incorporated for formulation of the model containing the system of non-linear differential equations given as:

$$\frac{dA}{dt} = p - b_1 A + k_1 A S, \tag{2.1}$$

$$\frac{dS}{dt} = q - \alpha S - k_1 A S, \tag{2.2}$$

$$\frac{dP}{dt} = \left(\frac{\beta_{11} D_0}{\beta_{12} + P} - d_1 A \right) P - mP - \delta_1 P^2, \tag{2.3}$$

$$\frac{dD_0}{dt} = r - n_1 D_0 - n_2 S D_0 - \frac{\beta_{11} D_0 P}{\beta_{12} + P}, \tag{2.4}$$

where the initial conditions are given by:

$$A(0) > 0, S(0) > 0, P(0) > 0, D_0(0) > 0.$$

The system parameters can be defined as follows:

p is the input rate of acid in water through various sources such as industrial wastes, acid rain etc. b_1 is the rate at which the acid is washed out of the water bodies in a natural way. The pollutants being uptaken by the water bodies due to anthropogenic activities are potentially rich in carbon, leading to the increase of acidity of water. This is represented by the term k_1AS through a bilinear interaction where k_1 represents the rate of increase in water acidity due to increased toxicant amount in water. q is the rate at which the toxicants and pollutants are introduced in the aquatic ecosystem. α represents the depletion rate of the toxicants and pollutants due to natural processes of toxicants draining out of the water bodies, sedimentation or intake of these pollutants by various populations thriving in the water bodies. β_{11} is the rate of consumption of favourable resource i.e. dissolved oxygen by the aquatic population and β_{12} is the half saturation constant. The increasing water acidity has a negative consequences on growth of the aquatic population denoted by the term d_1AP where the rate of depletion of population on account of increased acidity is represented by the parameter d_1. m represents the death rate of the population and the self-restricting rates of growth of population is given by δ_1. The input rate of favourable resource i.e. dissolved oxygen is given by r. n_1 is the natural depletion rate of dissolved oxygen. The rising toxicity and high rate of eutrophication cause an increase in the algal bloom growth. The decomposition of the increased organic matter in water uses the dissolved oxygen which leads to scarcity of the oxygen in water. The utilisation of oxygen in the decomposition process is given by the term n_2SD_0 ; where the term n_2 represents the decomposition rate of the algal biomass and the organic pollutants in water. All the parameters $p, k, b_1, \alpha, \beta_{11}, \beta_{12}, d_1, n_1, n_2$ and δ_1 are assumed to be positive constants.

In the following sections, we shall carry out the mathematical analysis of the model given by eqs. (2.1) $-$ (2.4).

2.3 Dynamical Behaviour of Model

2.3.1 Boundedeness of Solutions :

Now, we shall show that the solutions of the mathematical model given by eqs. $(2.1) - (2.4)$ are bounded in the positive orthant R_4^+. The following lemma establishes the boundedness of solutions.

Lemma 2.3.1. *All solutions of the model given by Eqs.* $(2.1)-(2.4)$ *shall lie in the region* F_r *where:* $F_r = \left\{(A, S, P, D_0)\epsilon R_4^+ : 0 \leq A + S \leq W_{1u}, 0 \leq D_0 + P \leq W_{2u}\right\}$ *for all* $t \to \infty$ *with positive initial values* $A(0), S(0), P(0), D_0(0)$ *where* $W_{1u} = \frac{p+q}{\gamma}; \gamma = min(b_1, \alpha)$ *and* $W_{2u} = \frac{r}{\gamma'}; \gamma' = min(n_1, m)$.

Proof. Consider the following function $W_1(t)$ given by :

$$W_1(t) = A(t) + S(t).$$

From eqs.$(2.1) - (2.2)$ and taking $\gamma = \min\ (b_1, \alpha)$ we obtain,

$$\frac{dW_1(t)}{dt} \leq p + q - \gamma W_1(t).$$

Then, following the usual comparison theorem we obtain:

$$\limsup_{t\to\infty}(W_1, t) \leq \frac{p+q}{\gamma},$$

and hence,

$$A(t) + S(t) \leq \frac{p+q}{\gamma} = W_{1u}(t).$$

Let us now consider another function $W_2(t)$ given as:

$$W_2(t) = P(t) + D_0(t).$$

From eqs. $(2.3) - (2.4)$ and taking $\gamma' = min(n_1, m)$ we obtain

$$\frac{dW_2(t)}{dt} \leq r - \gamma' W_2(t).$$

Then, following the usual comparison theorem we obtain:

$$\lim_{t\to\infty}\sup(W_2, t) \leq \frac{r}{\gamma'},$$

and hence,

$$P(t) + D_0(t) \leq \frac{r}{\gamma'} = W_{2u}(t).$$

This leads to the completion of the proof of lemma 2.3.1. □

2.3.2 Positivity of solutions

Since the model given by eqs. (2.1) − (2.4) studies the dynamical behaviour of aquatic population under the effect of increasing acidity and toxicity, hence it becomes imperative to prove that the solutions exhibit positivity for all times. Since the persistence of solutions is implied by positivity, hence the positivity of solutions is shown by the following lemma.

Lemma 2.3.2. *The solution of the model given by eqs.* (2.1) − (2.4), $(A(t), S(t), P(t), D_0(t))$, *with initial conditions,* $A(0) > 0, S(0) > 0, P(0) > 0,$ $D_0 > 0$, *exhibits positivity for all time* $t > 0$.

Proof. From eq. (2.1) we get,

$$\frac{dA}{dt} = p - b_1A + k_1AS,$$

$$\frac{dA}{dt} \geq -b_1A,$$

$$A \geq h_1e^{-b_1t},$$

where h_1 is an integration constant.
Hence, $A > 0$ as $t \to \infty$.
Similarly, from eq. (2.2), we get,

$$\frac{dS}{dt} \geq -(\alpha + k_1W_{1u})S,$$

$$S \geq h_2 e^{-(\alpha + k_1 W_{1u})t},$$

where h_2 is an integration constant.
Hence, $S > 0$ as $t \to \infty$.
From eq. (2.3), we get,

$$\frac{dP}{dt} \geq -(d_1 W_{1u} + m + \delta_1 W_{2u})P,$$
$$P \geq h_3 e^{-(d_1 W_{1u} + m + \delta_1 W_{2u})t},$$

where h_3 is an integration constant.
Hence, $P > 0$ as $t \to \infty$.
Similarly, from eq. (2.4), we obtain,

$$\frac{dD_0}{dt} \geq -(n_1 + n_2 W_{1u} + \beta_{11} W_{2u})D_0,$$

$$D_0 \geq h_4 e^{-(n_1 + n_2 W_{1u} + \beta_{11} W_{2u})t},$$

where h_4 is an integration constant.
Hence, $D_0 > 0$ as $t \to \infty$.
This leads to completion of the proof of lemma 2.3.2. □

2.3.3 Possible equilibrium points and existence conditions

Now, we find the equilibrium points for the given model defined by set of equations (2.1) – (2.4). The model has the following three equilibrium points:
1. Population vanishing equilibrium point $\hat{E}(\hat{A}, \hat{S}, 0, \hat{D}_0)$ where $\hat{P} = 0$ i.e. when the toxicant and acid in the system increases to such a high level such that the population tends towards extinction.
From eq. (2.1) we have,

$$\hat{A} = \frac{p}{b_1 - k_1 \hat{S}}. \tag{2.5}$$

$$\hat{A} > 0 \quad if \quad b_1 - k_1 \hat{S} > 0. \tag{2.6}$$

$$\hat{D}_0 = \frac{r}{n_1 + n_2 \hat{S}}. \tag{2.7}$$

Since $\hat{S} > 0$, $\hat{D}_0 > 0$.
$\hat{S}$ is given as the positive root of the following quadratic equation ,

$$\alpha k_1 \hat{S}^2 - \hat{S}(qk_1 + \alpha b_1 + k_1 p) + qb_1 = 0.$$

2. Interior Equilibrium Point $E^*(A^*, S^*, P^*, D_0^*)$: The values of A^*, S^*, P^*, D_0^* are given as:
From eq. (2.1) we have,

$$A^* = \frac{p}{b_1 - k_1 S^*}. \tag{2.8}$$

$$A^* > 0 \quad if \quad b_1 - k_1 S^* > 0. \tag{2.9}$$

$$D_0^* = \frac{r(\beta_{12} + P^*)}{(n_1 + n_2 S^*)(\beta_{12} + P^*) + \beta_{11} P^*}. \tag{2.10}$$

Since $P^* > 0$ and $S^* > 0$, hence $D_0^* > 0$.
S^* is given as the positive root of the following quadratic equation ,

$$\alpha k_1 S^{*2} - S^*(qk_1 + \alpha b_1 + k_1 p) + qb_1 = 0. \tag{2.11}$$

P^* is given as the positive root of the following cubic equation,

$$\begin{aligned} &P^{*3}(\delta_1(n_1 + n_2 S^*) + \beta_{11}\delta_1) + P^{*2}(2\delta_1 n_1 \beta_{12} + 2\delta_1 n_2 \beta_{12} S^* + d_1 n_1 A^* \\ &+ d_1 n_2 A^* S^* + mn_1 + mn_2 S^* + \beta_{11}(\delta_1 \beta_{12} + d_1 A^* + m) + P^*(\delta_1 \beta_{12}^2 n_1 \\ &+ \delta_1 \beta_{12}^2 n_2 S^* + 2(d_1 A^* \beta_{12} n_1 + \beta_{12} n_2 d_1 A^* S^* + mn_1 \beta_{12} + mn_2 \beta_{12} S^*) \\ &+ \beta_{11}(\beta_{12} d_1 A^* + m\beta_{12}) - \beta_{11} r) + (\beta_{12}^2 n_1 d_1 A^* + mn_1 \beta_{12}^2 + \\ &n_2 d_1 \beta_{12}^2 A^* S^* + mn_2 \beta_{12}^2 S^* - \beta_{11}\beta_{12} r) = 0. \end{aligned} \tag{2.12}$$

The equation (2.12) will have at least one positive root if,

$$\beta_{12}^2 n_1 d_1 A^* + mn_1 \beta_{12}^2 + n_2 d_1 \beta_{12}^2 A^* S^* + mn_2 \beta_{12}^2 S^* < \beta_{11}\beta_{12} r \tag{2.13}$$

3. Acid vanishing equilibrium Point $\breve{E}(0, \breve{S}, \breve{P}, \breve{D}_0)$ i.e. $\breve{A} = 0$.
The values of variables $\breve{S}, \breve{P}, \breve{D}_0$ are given as:

$$\breve{S} = \frac{q}{\alpha}. \tag{2.14}$$

From eq. (2.3) we get,

$$\breve{D}_0 = \frac{r(\beta_{12} + \breve{P})}{(n_1 + n_2\breve{S})(\beta_{12} + \breve{P}) + \beta_{11}\breve{P}}. \tag{2.15}$$

Since $\breve{P} > 0$ and $\breve{S} > 0$, hence $\breve{D}_0 > 0$.
$\breve{P}$ is given as the positive root of the following cubic equation,

$$\begin{aligned}&\breve{P}^3(\delta_1(n_1 + n_2\breve{S}) + \beta_{11}\delta_1) + \breve{P}^2(2\delta_1 n_1\beta_{12} + 2\delta_1 n_2\beta_{12}\breve{S} + mn_1 + mn_2\breve{S}\\&+\beta_{11}(\delta_1\beta_{12} + m) + \breve{P}(\delta_1\beta_{1}^{2}{}_{2}n_1 + \delta_1\beta_{1}^{2}{}_{2}n_2\breve{S} + 2(mn_1\beta_{12} + mn_2\beta_{12}\breve{S})\\&+\beta_{11}\beta_{12}m - \beta_{11}r) + (mn_1\beta_{1}^{2}{}_{2} + mn_2\beta_{1}^{2}{}_{2}\breve{S} - \beta_{11}\beta_{12}r) = 0.\end{aligned} \tag{2.16}$$

The equation (2.16) will have at least one positive root if,

$$\delta_1\beta_{1}^{2}{}_{2}n_1 + \delta_1\beta_{1}^{2}{}_{2}n_2\breve{S} + 2(mn_1\beta_{12} + mn_2\beta_{12}\breve{S}) + \beta_{11}\beta_{12}m < \beta_{11}r \tag{2.17}$$

Remark: The toxicant (S) in the system can not be taken as zero, as the external input of toxicant cannot be completely nullified. Due to the multiple sources by which the toxicant enters the system such as discharge of household, agricultural or industrial wastes etc. in water, a certain amount of toxicant is always present in the water bodies.
In the next section, the dynamical behaviour of the model shall be studied about these equilibrium points in terms of local and global stability.

2.3.4 Local Stability

1. **For population vanishing equilibrium point $\hat{E}(\hat{A}, \hat{S}, 0, \hat{D}_0)$:** The variational matrix for system of eqs. (2.1) – (2.4) at population vanishing equilibrium point $\hat{E}$ is given by ,

$$\hat{M} = \begin{pmatrix} -b_1 + k_1\hat{S} & k_1\hat{A} & 0 & 0 \\ -k_1\hat{S} & -\alpha - k_1\hat{A} & 0 & 0 \\ 0 & 0 & \left(\frac{\beta_{11}}{\beta_{12}}\hat{D}_0 - d_1\hat{A} - m\right) & 0 \\ 0 & -n_2\hat{D}_0 & -\frac{\beta_{11}\hat{D}_0}{\beta_{12}} & \frac{-r}{\hat{D}_0} \end{pmatrix}$$

The characteristic equation corresponding to variational matrix $\hat{M}$ is

$$(\lambda + \frac{r}{\hat{D}_0})(\lambda - \frac{\beta_{11}}{\beta_{12}}\hat{D}_0 + d_1\hat{A} + m)(\lambda^2 + \lambda(b_1 + \alpha + k_1\hat{A} \\ -k_1\hat{S}) + (\alpha b_1 - \alpha k_1\hat{S} + k_1 b_1\hat{A})) = 0. \tag{2.18}$$

The eigen values corresponding to characteristic equation of matrix $\hat{M}$ are given as:

$$\lambda_1 = -\frac{r}{\hat{D}_0} \ , \quad \lambda_2 = \frac{\beta_{11}}{\beta_{12}}\hat{D}_0 - d_1\hat{A} - m \tag{2.19}$$

λ_3 and λ_4 are obtained by solving the following quadratic equation:

$$\lambda^2 + \lambda(b_1 + \alpha + k_1\hat{A} - k_1\hat{S}) + (\alpha b_1 - \alpha k_1\hat{S} + k_1 b_1\hat{A}) = 0. \tag{2.20}$$

Using Routh's criteria, λ_3 and λ_4 will have non-positive real parts if,

$$b_1 + \alpha + k_1\hat{A} > k_1\hat{S}, \tag{2.21}$$

$$d_1\hat{A} + m > \frac{\beta_{11}}{\beta_{12}}\hat{D}_0, \tag{2.22}$$

and

$$\alpha b_1 + k_1 b_1\hat{A} > \alpha k_1\hat{S}. \tag{2.23}$$

2. **For acid vanishing equilibrium point:** $\breve{E}(0, \breve{S}, \breve{P}, \breve{D}_0)$: The variational matrix at acid vanishing equilibrium point $\breve{E}$ is given by,

$$\breve{M} = \begin{pmatrix} Z_1 & 0 & 0 & 0 \\ -k_1\breve{S} & -Z_2 & 0 & 0 \\ -d_1\breve{P} & 0 & Z_3 & Z_4 \\ 0 & -n_2\breve{D}_0 & Z_5 & -Z_6 \end{pmatrix}$$

where

$$Z_1 = -b_1 + k_1\breve{S}, \quad Z_2 = \alpha, \quad Z_3 = \frac{-\beta_{11}\breve{D}_0\breve{P}}{(\beta_{12}+\breve{P})^2} - \delta_1\breve{P},$$

$$Z_4 = \frac{\beta_{11}\breve{P}}{\beta_{12}+\breve{P}}, \quad Z_5 = \frac{-\beta_{11}\beta_{12}\breve{D}_0}{(\beta_{12}+\breve{P})^2}, \quad Z_6 = \frac{r}{\breve{D}_0}.$$

The characteristic equation corresponding to variational matrix $\breve{M}$ is given as :

$$(Z_1 - \lambda)(-Z_2 - \lambda)(\lambda^2 + \lambda(Z_6 - Z_3) - (Z_3Z_6 + Z_4Z_5)) = 0. \tag{2.24}$$

The conditions for the equilibrium state $\breve{E}$ to be asymptotically stable are given by Routh-Hurwitz criteria as:

$$b_1 > k_1\breve{S},$$

$$Z_6 - Z_3 > 0,$$

$$-Z_3Z_6 - Z_4Z_5 > 0,$$

i.e.

$$b_1 > k_1\breve{S}, \tag{2.25}$$

$$\frac{r}{\breve{D}_0} + \frac{\beta_{11}\breve{D}_0\breve{P}}{(\beta_{12}+\breve{P})^2} + \delta_1\breve{P} > 0, \tag{2.26}$$

$$\left(\frac{\beta_{11}\breve{D}_0\breve{P}}{(\beta_{12}+\breve{P})^2} + \delta_1\breve{P}\right)\left(\frac{r}{\breve{D}_0}\right) + \left(\frac{\beta_{11}\breve{P}}{\beta_{12}+\breve{P}}\right)\left(\frac{\beta_{11}\beta_{12}\breve{D}_0}{(\beta_{12}+\breve{P})^2}\right) > 0, \tag{2.27}$$

3. **For interior equilibrium** $E^*(A^*, S^*, P^*, D_0^*)$**:** The variational matrix corresponding to interior equilibrium E^* is given by :

$$M^* = \begin{pmatrix} Z_1 & k_1A^* & 0 & 0 \\ -k_1S^* & -Z_2 & 0 & 0 \\ -d_1P^* & 0 & Z_3 & Z_4 \\ 0 & -n_2D_0^* & Z_5 & -Z_6 \end{pmatrix}$$

where

$$Z_1 = -b_1 + k_1S^*, \quad Z_2 = \alpha + k_1A^*, \quad Z_3 = \frac{-\beta_{11}D_0^*P^*}{(\beta_{12}+P^*)^2} - \delta_1P^*,$$

$$Z_4 = \frac{\beta_{11} P^*}{\beta_{12} + P^*}, \quad Z_5 = \frac{-\beta_{11}\beta_{12} D_0^*}{(\beta_{12} + P^*)^2}, \quad Z_6 = \frac{r}{D_0^*}.$$

The characteristic equation corresponding to variational matrix M^* is given as :

$$\left\{\lambda^2 + \lambda(Z_6 - Z_3) - (Z_3 Z_6 + Z_4 Z_5)\right\}\{\lambda^2 + \lambda(Z_2 - Z_1) - Z_1 Z_2 + k_1^2 A^* S^*\} = 0 \tag{2.28}$$

By Routh Hurwitz criteria, the conditions for the equilibrium state E^* to be asymptotically stable are obtained as :

$$Z_6 - Z_3 > 0,$$

$$-Z_3 Z_6 - Z_4 Z_5 > 0,$$

$$Z_2 - Z_1 > 0,$$

$$k_1^2 A^* S^* > Z_1 Z_2.$$

Thus, the conditions for the equilibrium state E^* to be stable are :

$$\frac{r}{D_0^*} + \frac{\beta_{11} D_0^* P^*}{(\beta_{12} + P^*)^2} + \delta_1 P^* > 0, \tag{2.29}$$

$$\left(\frac{\beta_{11} D_0^* P^*}{(\beta_{12} + P^*)^2} + \delta_1 P^*\right)\left(\frac{r}{D_0^*}\right) + \left(\frac{\beta_{11} P^*}{\beta_{12} + P^*}\right)\left(\frac{\beta_{11}\beta_{12} D_0^*}{(\beta_{12} + P^*)^2}\right) > 0, \tag{2.30}$$

$$k_1 A^* + \alpha + b_1 > k_1 S^*, \tag{2.31}$$

$$b_1 \alpha + b_1 k_1 A^* > k_1 \alpha S^*. \tag{2.32}$$

2.3.5 Global Stability

In this section, we shall establish the global stability of the model given by eqs. (2.1) − (2.4). The following two theorems shall show the global stability:

Theorem 2.3.1. *The box F_r is compact and positive invariant set in the space (A, S, P, D_0).*

Proof. Consider the system of equations given by (2.1) – (2.4). We consider a box F_r in the phase space $ASPD_0$ with one vertex at a point $\bar{\chi} = (\bar{A}, \bar{S}, \bar{P}, \bar{D_0})$ and the other vertex at the origin. The point $\bar{\chi}$ lies outside the box F_r with $\bar{A} > A_u$,$\bar{S} > S_u$,$\bar{P} > P_u$,$\bar{D_0} > D_{0u}$.

In order to prove the theorem, we shall first compute the upper bound for P. From eq.(2.3) we get,

$$\frac{dP}{dt} \leq \beta_{11} W_{2u} P - \delta_1 P^2,$$

$$\frac{dP}{P(G - \delta_1 P)} \leq dt,$$

where

$$G = \beta_{11} W_{2u},$$

and then by usual comparison theorem we get,

$$\limsup_{t\to\infty} P(t) \leq \frac{G}{\delta_1} = P_u. \tag{2.33}$$

Now, let

$$\frac{d\bar{w}}{dt} = \left(\frac{dA}{dt}, \frac{dS}{dt}, \frac{dP}{dt}, \frac{dD_0}{dt} \right).$$

We shall compute the angle of the flow with each face of the box F_r not lying in the coordinate planes. Let v_1, v_2, v_3 and v_4 be the outward unit normal vectors to the planes $w_1 : A = \bar{A}, w_2 : S = \bar{S}, w_3 : P = \bar{P}, w_4 : D_0 = \bar{D}_0$ in reference to the box F_r.

Then from eq. (3) we get,

$$v_3 \frac{d\bar{\chi}}{dt}|_{w_3} = \left(\frac{\beta_{11} D_0}{\beta_{12} + \bar{P}} - d_1 A - m \right) \bar{P} - \delta_1 \bar{P}^2,$$

$$v_3 \frac{d\bar{\chi}}{dt}|_{w_3} \leq \left(\beta_{11} W_{2u} - \delta_1 \bar{P} \right) \bar{P} - m\bar{P}.$$

Since

$$\bar{P} > \frac{1}{\delta_1} \left(\beta_{11} W_{2u} \right)$$

Table 2.1: Different initial values for variables A^*, S^*, P^*, D_0^* of the model.

Variable	1^{st} initial value	2^{nd} initial value	3^{rd} initial value	4^{th} initial value
A	0.3	7	2	0.1
S	0.6	10	5	10
P	0.5	6	10	9
D_0	0.8	17	22	0.5

therefore,

$$v_3 \frac{d\bar{\chi}}{dt}|_{w_3} \leq -m\bar{P},$$

hence

$$v_3 \frac{d\bar{\chi}}{dt}|_{w_3} \leq 0.$$

Similarly it can be proved that,

$$v_1 \frac{d\bar{\chi}}{dt}|_{w_1} \leq 0, v_2 \frac{d\bar{\chi}}{dt}|_{w_2} \leq 0, v_4 \frac{d\bar{\chi}}{dt}|_{w_4} \leq 0.$$

The above theorem makes it clear that the trajectories of the system given by (2.1) – (2.4) will not cross F_r once they enter inside F_r. The interior equilibrium E^* is also observed to lie inside the F_r.

In the next theorem, we shall prove that E^* is the only global attractor inside F_r. □

Theorem 2.3.2. *The following inequalities should hold for the interior equilibrium E^* to be globally asymptotically stable:*

$$(b_1 - k_1 S)(\alpha + k_1 A) > (k_1 S^* - k_1 A^*)^2,$$

$$(b_1 - k_1 S)\left(\frac{\beta_{11} D_0^*}{(\beta_{12} + P)(\beta_{12} + P^*)} + \delta_1\right) > d_1^2, ,$$

$$(\alpha + k_1 A)\left(\frac{\beta_{11}P^*}{\beta_{12}+P^*} + n_2 S^* + n_1\right) > (n_2 D_0^*)^2,$$

$$\left(\frac{\beta_{11}D_0^*}{(\beta_{12}+P)(\beta_{12}+P^*)} + \delta_1\right)\left(\frac{\beta_{11}P^*}{\beta_{12}+P^*} + n_2 S^* + n_1\right) >$$
$$\left(\frac{\beta_{11}\beta_{12}D_0}{(\beta_{12}+P)(\beta_{12}+P^*)} - \frac{\beta_{11}}{\beta_{12}+P}\right)^2.$$

Proof. For showing the global stability of the equilibrium state E^*, assume the following positive definite function:

$$Y = \frac{1}{2}(A - A^*)^2 + \frac{1}{2}(S - S^*)^2 + \left(P - P^* - P^* ln\frac{P}{P^*}\right) + \frac{1}{2}(D_0 - D_0^*)^2 \quad (2.34)$$

Differentiating the above equation w.r.t. 't' we get,

$$\begin{aligned}\frac{dY}{dt} = &(-b_1 + k_1 S)(A - A^*)^2 - \left(\frac{\beta_{11}D_0^*}{(\beta_{12}+P)(\beta_{12}+P^*)} + \delta_1\right)(P - P^*)^2\\ &-(\alpha + k_1 A)(S - S^*)^2 - \left(\frac{\beta_{11}P^*}{\beta_{12}+P^*} + n_2 S^* + n_1\right)(D_0 - D_0^*)^2\\ &-d_1(A - A^*)(P - P^*) + (k_1 A^* - k_1 S^*)(S - S^*)(A - A^*)\\ &+\left(\frac{\beta_{11}}{\beta_{12}+P} - \frac{\beta_{11}\beta_{12}D_0}{(\beta_{12}+P)(\beta_{12}+P^*)}\right)(P - P^*)(D_0 - D_0^*)\\ &-n_2 D_0^*(S - S^*)(D_0 - D_0^*),\end{aligned}$$

$$\begin{aligned}\frac{dY}{dt} = &-[(b_1 - k_1 S)(A - A^*)^2 + \left(\frac{\beta_{11}D_0^*}{(\beta_{12}+P)(\beta_{12}+P^*)} + \delta_1\right)(P - P^*)^2\\ &+(\alpha + k_1 A)(S - S^*)^2 + \left(\frac{\beta_{11}P^*}{\beta_{12}+P^*} + n_2 S^* + n_1\right)(D_0 - D_0^*)^2\\ &+d_1(A - A^*)(P - P^*) + (k_1 S^* - k_1 A^*)(S - S^*)(A - A^*) +\\ &\left(\frac{\beta_{11}\beta_{12}D_0}{(\beta_{12}+P)(\beta_{12}+P^*)} - \frac{\beta_{11}}{\beta_{12}+P}\right)(P - P^*)(D_0 - D_0^*)\\ &+n_2 D_0^*(S - S^*)(D_0 - D_0^*)],\end{aligned}$$

$$\frac{dY}{dt} = -[a_{11}(A-A^*)^2 + a_{22}(S-S^*)^2 + a_{33}(P-P^*)^2 + a_{44}(D_0-D_0^*)^2 \\ +a_{12}(A-A^*)(S-S^*) + a_{13}(A-A^*)(P-P^*) + \\ a_{24}(S-S^*)(D_0-D_0^*) + a_{34}(P-P^*)(D_0-D_0^*)]$$

where

$$a_{11} = (b_1 - k_1 S), \quad a_{22} = (\alpha + k_1 A), \quad a_{12} = k_1 S^* - k_1 A^*,$$
$$a_{33} = \frac{\beta_{11} D_0^*}{(\beta_{12}+P)(\beta_{12}+P^*)} + \delta_1, \quad a_{44} = \frac{\beta_{11} P^*}{\beta_{12}+P^*} + n_2 S^* + n_1,$$
$$a_{13} = d_1, \quad a_{24} = n_2 D_0^*, \quad a_{34} = \frac{\beta_{11}\beta_{12} D_0}{(\beta_{12}+P)(\beta_{12}+P^*)} - \frac{\beta_{11}}{\beta_{12}+P}.$$

Sufficient conditions for $\frac{dY}{dt}$ to be negative definite obtained by Sylvester's criteria are:

$$a_{11}a_{22} > a_{12}^2, \quad a_{11}a_{33} > a_{13}^2, \quad a_{22}a_{44} > a_{24}^2, \quad a_{33}a_{44} > a_{34}^2, \tag{2.35}$$

i.e.

$$(b_1 - k_1 S)(\alpha + k_1 A) > (k_1 S^* - k_1 A^*)^2, \tag{2.36}$$

$$(b_1 - k_1 S)\left(\frac{\beta_{11} D_0^*}{(\beta_{12}+P)(\beta_{12}+P^*)} + \delta_1\right) > d_1^2, \tag{2.37}$$

$$(\alpha + k_1 A)\left(\frac{\beta_{11} P^*}{\beta_{12}+P^*} + n_2 S^* + n_1\right) > (n_2 D_0^*)^2, \tag{2.38}$$

$$\left(\frac{\beta_{11} D_0^*}{(\beta_{12}+P)(\beta_{12}+P^*)} + \delta_1^2\right)\left(\frac{\beta_{11} P^*}{\beta_{12}+P^*} + n_2 S^* + n_1\right) > \\ \left(\frac{\beta_{11}\beta_{12} D_0}{(\beta_{12}+P)(\beta_{12}+P^*)} - \frac{\beta_{11}}{\beta_{12}+P}\right)^2. \tag{2.39}$$

□

Table 2.2: Sensitivity Indices(γ) of A^*, S^*, P^*, D_0^* at E^* to parameters Z_p.

Parameters(Z_p)	$\gamma_{Z_p}^{A^*}$	$\gamma_{Z_p}^{S^*}$	$\gamma_{Z_p}^{D_0^*}$	$\gamma_{Z_p}^{P^*}$
p	0.869	-0.22	-0.3	-0.459
b_1	-1.38	0.351	0.478	0.732
k_1	0.384	-0.351	-0.043	-0.066
q	0.512	0.864	-0.527	-0.808
α	-0.382	-0.643	0.393	0.602
β_{11}	0	0	-0.729	0.413
β_{12}	0	0	0.043	-0.522
r	0	0	0.357	0.546
n_1	0	0	-0.045	-0.07
n_2	0	0	-0.359	-0.551
d_1	0	0	0.456	-0.666
m	0	0	0.07	0
δ_1	0	0	0.037	0

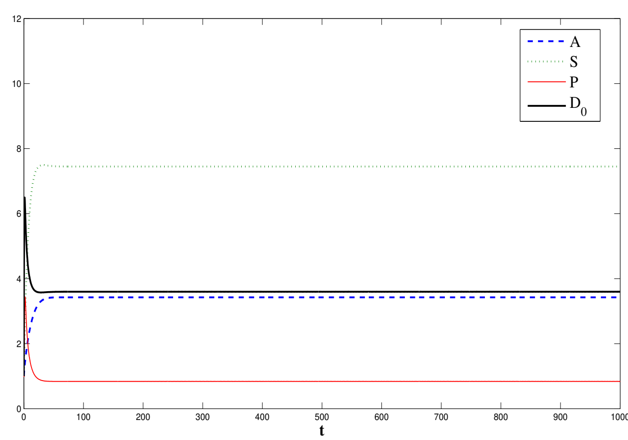

Figure 2.1: Trajectories of the model with respect to time showing the stability behaviour of interior equilibrium point E^*.

2.4 Numerical Simulation and Sensitivity Analysis

In order to support the analytical results derived for the system of equations given by (2.1) – (2.4) numerical simulation is carried out in this section.

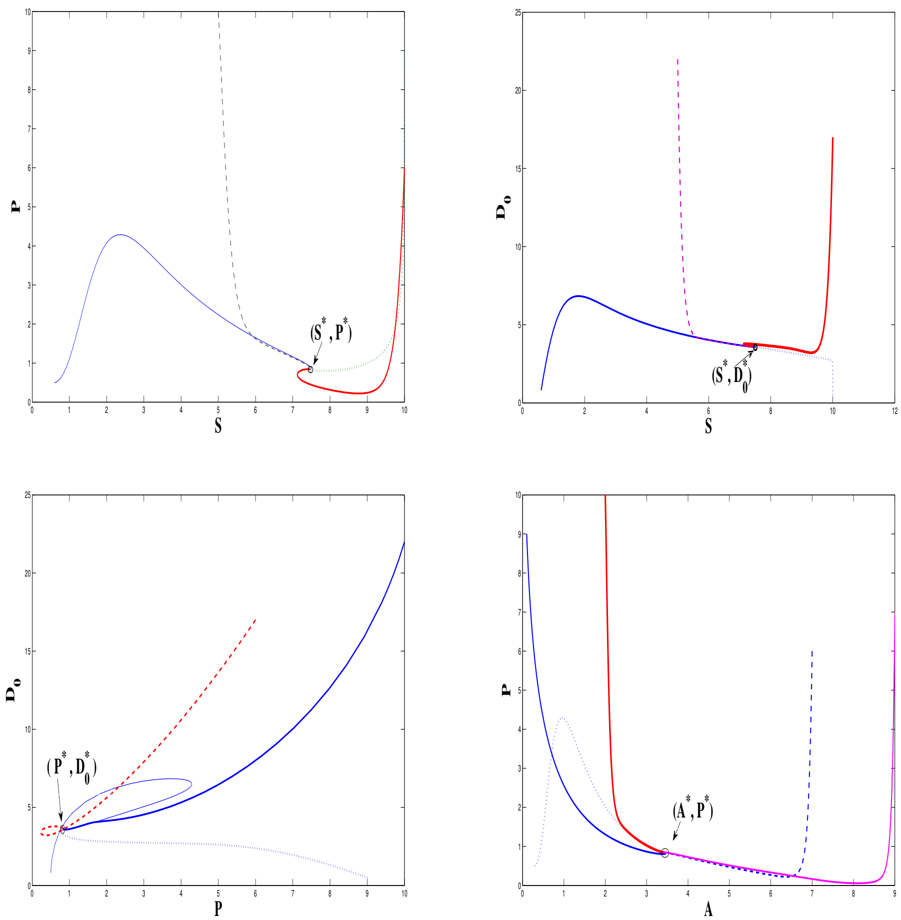

Figure 2.2: Phase plane graphs at different values of initial conditions as given in Table 1 showing the global stability behaviour.

Let us consider the below mentioned values of the model parameters:

p= 0.43 $\mu g L^{-1} day^{-1}, b_1 = 0.2 day^{-1}, q = 1.0 \mu g L^{-1} day^{-1}, \alpha = 0.1 day^{-1}$,

k$_1 = 0.01 L \mu g^{-1} day^{-1}, \beta_{11} = 1.02 day^{-1}, \beta_{12} = 0.524 mg L^{-1}$,

d$_1 = 0.7 L \mu g^{-1} day^{-1}, m = 0.19 day^{-1}, \delta_1 = 0.12 L mg^{-1} day^{-1}$,

r= 12.56 mgL$^{-1} day^{-1}, n_1 = 0.33 day^{-1}, n_2 = 0.34 L \mu g^{-1} day^{-1}$. (2.40)

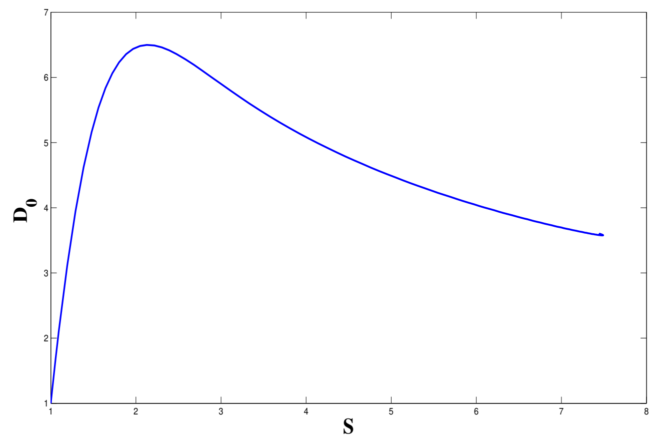

Figure 2.3: Phase space graph for concentration of dissolved oxygen (D_0) and toxicant concentration (S).

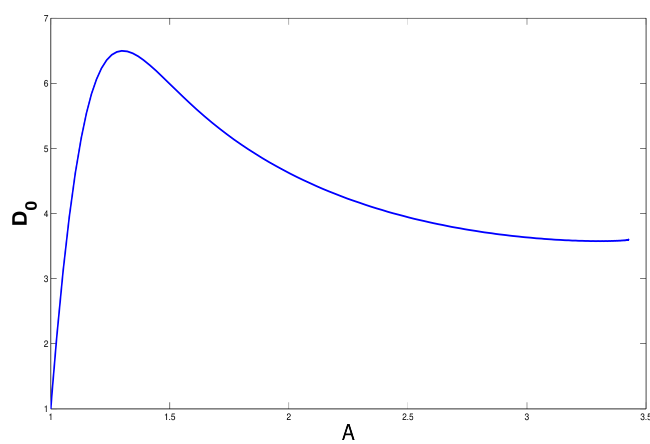

Figure 2.4: Phase space graph for concentration of dissolved oxygen (D_0) and acid concentration(A).

For these set of parametric values, the equilibrium values corresponding to interior equilibrium point E^* are A^*= 3.4258, S^*=7.4483, P^*= 0.8406, D_0^*=3.5984.
For the above mentioned set of parametric values, the feasibility and stability conditions as given by eqs. $(2.9, 2.13, 2.29 - 2.32, 2.36 - 2.39)$ are satisfied for the

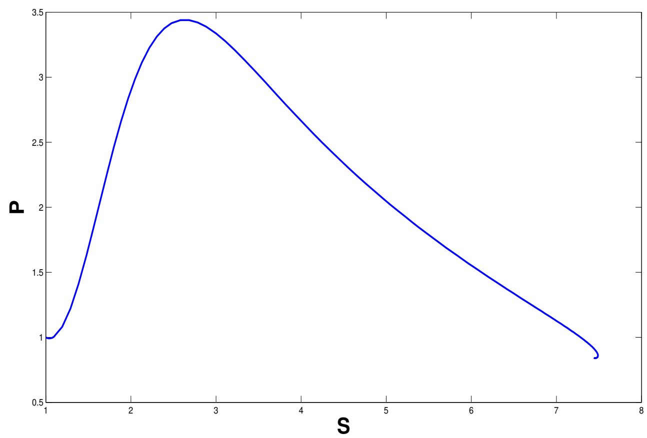

Figure 2.5: Phase space graph for density of aquatic population (P) and toxicant concentration (S).

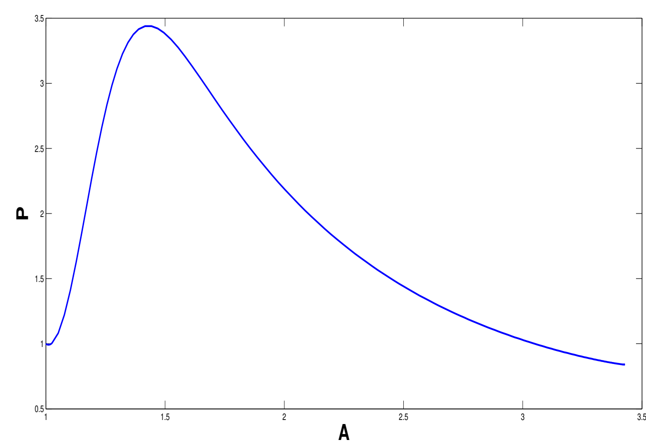

Figure 2.6: Phase space graph for density of aquatic population (P) and acid concentration(A).

interior equilibrium point E^*. The interior equilibrium point E^* is found to be asymptotically stable for these values as shown by fig. 2.1. Further, the numerical simulations are performed for illustration of the global stability of the interior equilibrium E^* for varying initial conditions as given in Table 2.1. The results

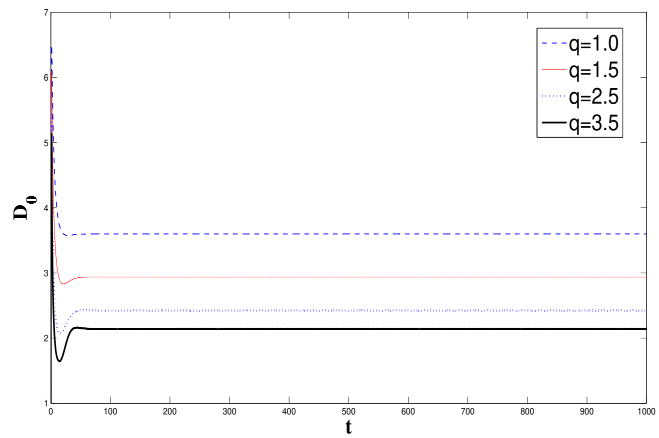

Figure 2.7: Graph between dissolved oxygen (D_0) and time t with increasing values of q.

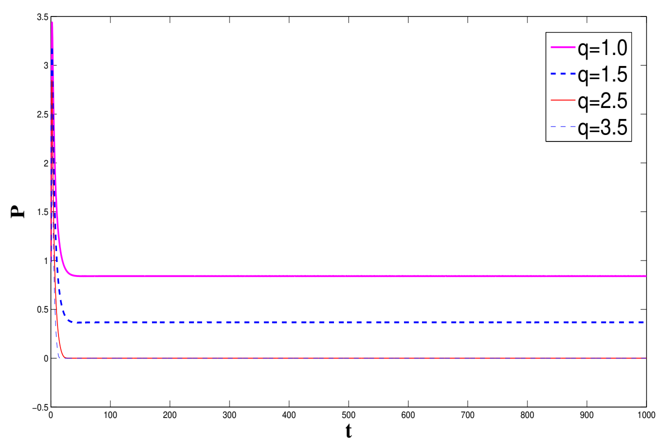

Figure 2.8: Graph between population (P) and time t with increasing values of q.

are exhibited in the phase plane graphs for variables S-P, S-D_0 , P-D_0 and A-P given by fig. 2.2. It is shown that all trajectories initiating from varying initial conditions reach to the equilibrium value at E^* with increasing time.

The results of sensitivity analysis prove to be more mathematically sound than the

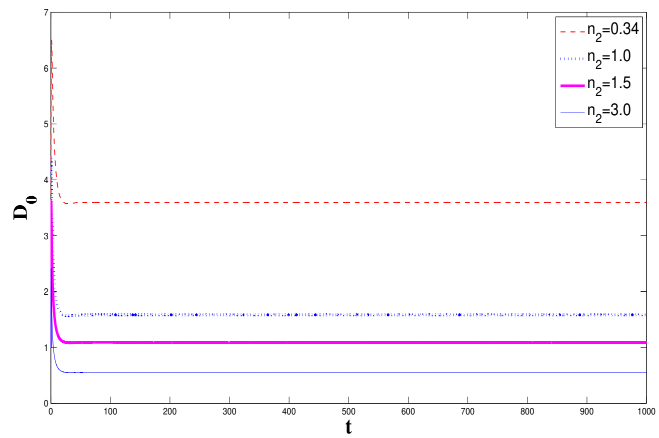

Figure 2.9: Graph between dissolved oxygen (D_0) and time t with different values of n_2.

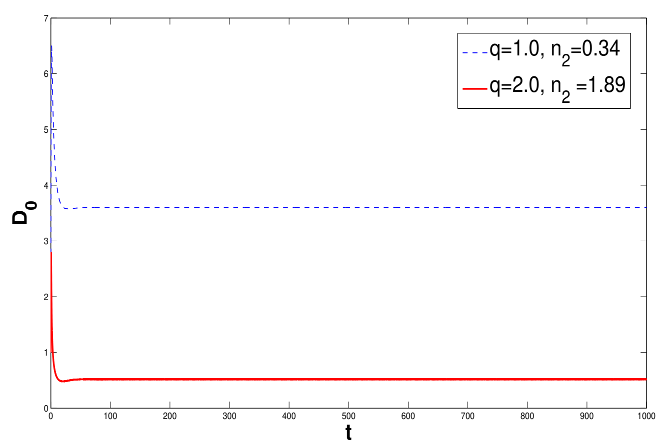

Figure 2.10: Graph between dissolved oxygen (D_0) and time t under increased values of q and n_2

simple variation in the parameter values. Hence, to examine the effect of all the model parameters such as $p, k, b_1, \alpha, \beta_{11}, \beta_{12}, d_1, n_1, n_2$ and δ_1 on the concentration of dissolved oxygen (D_0) and the survival of target population (P), the sensitivity analysis has been carried out at the interior equilibrium point E^*. The sensitivity

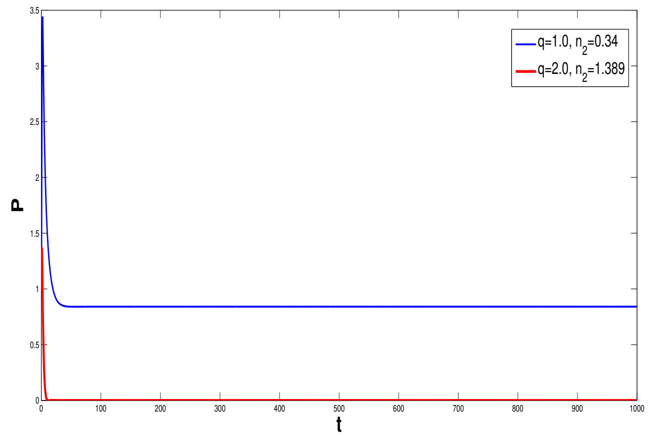

Figure 2.11: Graph between Population (P) and time t under increased values of q and n_2

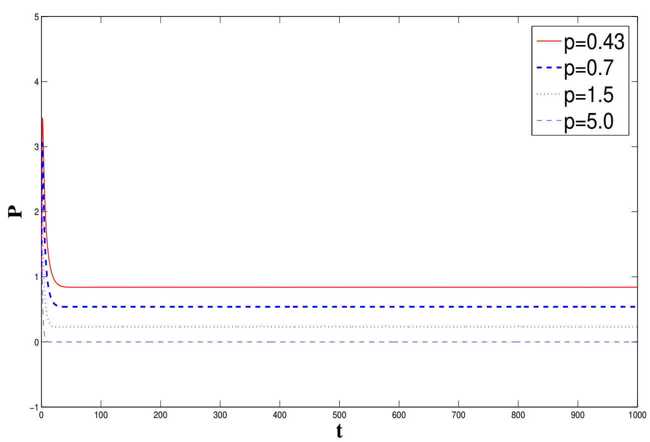

Figure 2.12: Graph between population (P) and time t with increasing values of p.

indices help in the measurement of relative variation in variables with respect to change in parameter values. These indices identify the parameters having more effect on population and dissolved oxygen level in water, and therefore will help in designing of necessary control strategies. The normalized forward sensitivity index

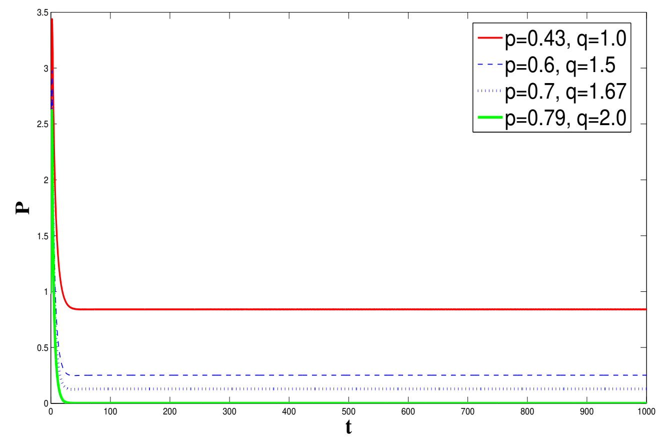

Figure 2.13: Graph between population (P) and time t under combined increase of p and q.

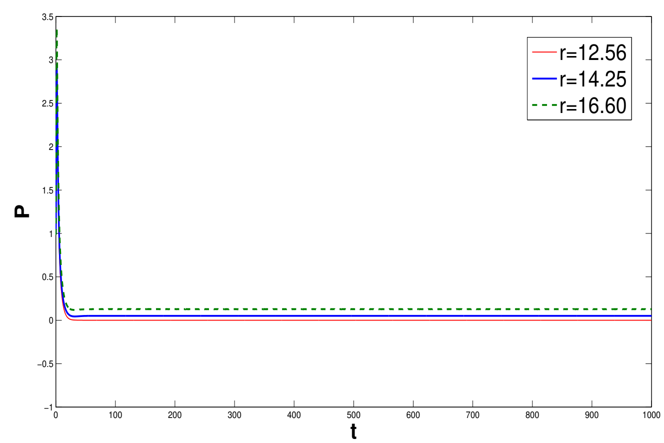

Figure 2.14: Graph between aquatic population (P) and time t under increasing values of r.

of a variable 'Z' depending on a parameter 'u' is given by the following expression [117]:

$$\gamma_u^Z = \frac{\partial Z}{\partial u} * \frac{u}{Z}$$

The sensitivity indices of each variable with the parameters of the model given by eqs. $(2.1) - (2.4)$ are calculated using the above formula. Table 2.2 gives the sensitivity indices at the interior equilibrium point E^* by using the baseline parameter values as given by eq.(2.40).

2.5 Conclusion

The mathematical model proposed in this chapter studies the combined effect of increasing toxicity, pollutants and acidity of water on dissolved oxygen (DO) and on oxygen-dependent aquatic population (P). The interior equilibrium E^* is found to be asymptotically stable as shown in fig.2.1 which is satisfying the conditions given by eqs. $(2.9, 2.13, 2.29 - 2.32, 2.36 - 2.39)$. From the stability analysis, it is observed that the dissolved oxygen and aquatic population exhibit a decrease with the rise in toxicity and acidity of water as shown in figs. 2.3, 2.4, 2.5 and 2.6. By the sensitivity analysis of the model at interior equilibrium point E^*, both dissolved oxygen and aquatic population are found to be sensitive and negatively dependent on the input rate of toxicant (q) and input rate of acid (p). It is observed that as the value of input rate of toxicants (q) in water increases from 1.0 to 3.5 , the level of dissolved oxygen declines as shown in fig. 2.7. It is further observed that the density of aquatic population also decreases with the increasing toxicant input (q) in water as shown in fig. 2.8. As the amount of organic pollutants in water and eutrophication rate rises, more oxygen is consumed in the decomposition of organic matter, which reduces its amount in water. This is shown numerically in fig. 2.9 from which it is observed that when the decomposition rate of organic matter in water (n_2) increases from 0.34 to 3.0, the concentration of dissolved oxygen decreases. These results are also supported by the study carried out by Sirota et al. [119].

In our study , it is found that in the absence of any input of toxicant and acid in water, the value of dissolved oxygen level is 9.7531 mgL^{-1}. But, when the value of input rate of toxicant (q) is increased to 2.0 and value of decomposition rate (n_2) is increased to 1.89, the dissolved oxygen level falls to 0.5190 mgL^{-1} as shown in fig. 2.10 , thus leading to a condition of hypoxia. The results obtained in our study have been validated by comparing them with the results obtained in the study done by Chakraborty et al. [118]. They proved that the rising agricultural pollution leads to increase in algal bloom, consequently causing decrease in the dissolved oxygen (DO) level due to consumption in their decomposition process. In the absence of any agricultural pollution the dissolved oxygen level obtained was 9.5 mgL^{-1} which is comparable to the dissolved oxygen level obtained in our study in absence of any toxicant or acid input. Chakraborty et al. [118] also obtained similar results to our study where they found that with the introduction of agricultural pollution in water, the dissolved oxygen level falls to 0.5 mgL^{-1} which is insufficient for survival of aquatic population. Moreover, the results of our study are supported by the case study carried out by San Diego-McGlone et al. [82] which showed that the fish kill event that occurred in 2002 in the coastal waters of Bolino, Phillipines was due to the stress of eutrophication which led to fall in level of dissolved oxygen to a level less than 2.0 mgL^{-1} in water. However, since we are considering the combined effect of eutrophication, pollution and acidification, the dissolved oxygen level obtained in our study is 0.5 mgL^{-1} which is quite low than the value 2.0 mgL^{-1} . This reinforces the observation that the combined effect of toxicant and acid leads to a more rapid decrease in the dissolved oxygen level as compared to the individual effect. Besides, as the dissolved oxygen (DO) is a primary resource required for growth and survival of aquatic population, hence hypoxic condition leads to extinction of populations in water. This effect is shown in fig. 2.11 which shows that the increase in toxicant input (q) and decomposition rate (n_2), leads to decrease of population to zero level due to decline in dissolved oxygen level (DO).

Furthermore, for increasing values of input rate of acid in water (p) from 0.43 to 5.0, the population level decreases as shown in fig. 2.12. This is supported by the study conducted by Bharathi et al.[108] . Initially, it is observed that the fish population is resistant to changing acid levels as shown in fig. 2.6. This is because the eggs and larvae are more vulnerable to the acidic conditions. So, the fish population begins to decline only over some time. These findings are also supported by the experimental study done by Baumann et al. [26].

Moreover, if only the single effect of toxicity is considered, it is found that the aquatic population tends towards extinction when the value of input rate of toxicants (q) is increased to 2.5. Under the individual effect of acidity, the population tends to zero when the value of input rate of acid (p) is increased to 5.0. However, under the combined effect of both acidity and toxicity , the population tends towards zero for parameter values q=2.0 and p=0.79 as shown in fig. 2.13. This establishes that the aquatic population decreases more rapidly under the combined stress of toxicity and acidity as compared to the single effect of acidity or toxicant. It is further observed that at the parameter values q=2.0 and p=0.79 , if the value of input rate of dissolved oxygen (r) is increased from 12.56 to 14.25, the population rises from zero level and again starts existing in the system as shown in fig. 2.14. Henceforth, for the aquatic population to exist, either the value of input rate of dissolved oxygen (r) should be increased and maintained at a higher value than the threshold value (r=14.25) or the toxicant input rates (q) and acid input rate (p) should be maintained less than q=2.0 and p=0.79. Therefore, it is concluded that in order to maintain a level of dissolved oxygen suitable for growth and survival of aquatic population, the release of acid and toxicants in water on account of anthropogenic activities needs to be reduced.

Chapter 3

Impact of water toxicity and acidity on dynamics of prey-predator aquatic populations: a mathematical model

3.1 Introduction

One of the most alerting environmental concerns of recent times is the contamination of water bodies caused by various anthropogenic activities such as uncontrolled discharge of household wastes, agricultural and industrial effluents into the water bodies. Due to intractable release of pollutants directly into water bodies, the toxicity and acidity level of water is rising rapidly. The increasing acidity of water can also be attributed to the carbon components released by pollutants present in water bodies as well as the inflating level of carbon dioxide in the atmosphere [53]. The acidifying water bodies are also leading to exacerbation of coral reef cover [120]. The loss in coral cover is harmful to the macro invertebrate species in the coral reefs [121]. The aquatic organisms exposed directly or indirectly to toxic and acidic environment face several stresses which alter and threaten their growth and survival in water [66, 36, 94, 122, 34, 56, 38]. The increasing chemicals and metal wastes also have prominent negative effects on the aquatic species [39, 40, 42]. The human population, which is dependent on the aquatic ecosystem for food, minerals, fertilizers etc. is also facing grave consequences owing to the undermining effects of increasing water toxicity and acidity. The top predators in an aquatic food chain become exposed to the toxicants by feeding on the prey affected by the toxicants [123]. Increased water acidity and metal contamination can also cause disturbances in the trophic structure of aquatic species, loss in biodiversity and decrease in density of fish stock in the water bodies [124, 125]. Several mathematical and experimental studies have also proved that the fish population have high sensitivity to toxicant and pollutant [108] and exhibit high mortality rates when exposed to them [41]. The presence of toxicants and pollutants in water not only has negative consequences for the aquatic species but also for their resource i.e. oxygen as they decrease the dissolved oxygen level in water [110]. The increased acidification and eutrophication lead to a rise in toxic algal bloom in water. This further reduces oxygen level in water due to consumption of dissolved oxygen in the decomposition process of these algal blooms [118, 6]. Drop in the concentration of dissolved oxygen in water also causes disruption in the pelagic food web [126]. Various biological phenomena have been studied by using mathematical modelling as an efficient tool [31]. Khare et al. [106] conducted a mathematical study to evaluate the negative effects of decreasing dissolved oxygen on interacting planktonic population. A few mathematical studies have also studied the effect of toxicant on prey-predator aquatic population [49, 127, 128]. Several mathematical studies have also highlighted the harmful role of increasing acidity on aquatic communities [129]. These studies show that the aquatic populations and their interactions are highly sensitive to the toxicant and acid level in water. However, the focus of the mathematical studies carried out till now is on the individual role of pollution, toxicant or acidity in an aquatic ecosystem. But, the effects of these factors have not been taken into account together in the available studies. In order to study the effects of toxicant and acid taken together on prey-predator aquatic populations, in this chapter, a non-linear mathematical model is proposed. In this model, it is presumed that the water toxicity is increasing from various processes such as eutrophication, release of industrial pollutants, household wastes etc. directly into the water bodies. The acidity of water is rising via two processes, one is direct discharge of chemicals and acids in water bodies and the second being the release of carbon from the pollutants present in the water bodies. The carbon reacts with the dissolved oxygen present in water and forms carbonic acid, thus, acidifying the water bodies. The rise in water acidity and toxicity cause a decline in the concentration of resource i.e. dissolved oxygen in water. This further has negative influences on the prey and predator populations residing in water.

3.2 Mathematical Model

In the proposed mathematical model, the population dynamics of a prey-predator in an aquatic environment is studied under the effect of increasing water toxicity and acidity. It is assumed that the incoming pollutants cause a rise in toxicity level of water. The carbon components present in the pollutants reacts with the dissolved oxygen and form carbonic acid. Also, the industrial and agricultural pollution lead to direct input of acid components into the water bodies. Thus, the water acidity increases by two phenomena, one is the direct discharge of acidic components and the second one being through the released pollutants in water. These phenomena lead to decrease in dissolved oxygen level in water, thus, threatening the survival of the aquatic species. It is further assumed that the predator population is solely dependent on prey population for its growth and survival through feeding on prey.

In view of the above, let A denote the acid concentration in water and T represent the concentration of toxicant in water. Let D_0 represent the concentration of dissolved oxygen in water. N denotes the density of aquatic prey population like small fishes and let P represent the density of predator population directly dependent on prey for food, like sharks, perch etc. With the above mentioned notations, a mathematical model consisting a set of non-linear differential equations is formulated given as:

$$\frac{dA}{dt} = p_0 - \beta A + kAT, \tag{3.1}$$

$$\frac{dT}{dt} = q_0 - a_0T - kAT, \tag{3.2}$$

$$\frac{dD_0}{dt} = r - n_{11}D_0 - n_{12}D_0T - \gamma ND_0, \tag{3.3}$$

$$\frac{dN}{dt} = \frac{hN}{1+A} + \gamma ND_0 - \frac{\alpha_{11}NP}{g+N} - \delta_1N^2, \tag{3.4}$$

$$\frac{dP}{dt} = \frac{\alpha_{12}NP}{g+N} - a_1P, \tag{3.5}$$

where the initial conditions for variables are given as:

$$A(0) > 0, T(0) > 0, D_0(0) > 0, N(0) > 0, P(0) > 0.$$

The system parameters are given as follows:
p_0 represents the rate of input of acid components in water via industrial effluents, acid rain etc. Rate of washing out of acid out of water bodies through natural processes is given by β. The bilinear interaction represented by the term kAT depicts the reaction of carbon present in the toxicants and pollutants with the dissolved oxygen in water leading to formation of carbonic acid. k represents the rate of increase of water acidity on account of formation of carbonic acid. The rate of input of toxicants and pollutants into the water bodies is represented by q_0. a_0 gives the depletion rate of the pollutants and toxicants from the water bodies due to natural washing out, decomposition and intake by aquatic populations etc. r represents the input rate of dissolved oxygen in water and n_{11} gives its natural depletion rate in water. The increase in acidity and toxicity of water gives rise to inflated algal bloom growth. These algal blooms use the dissolved oxygen in their decomposition process , thus depleting its level in water. The rate at which the dissolved oxygen decreases due the algal decomposition is represented by n_{12}. The rate of uptake of dissolved oxygen by the prey population in water is given by γ. h represents the natural growth rate of the prey population. α_{11} represents the consumption rate of prey population by predator population. g is the extent to which the prey population is protected by the environment. δ_1 represents the intraspecific competition between the prey population. α_{12} represents the assimilation rate of predator and a_1 gives the natural mortality rate of the predator population. All the parameters $p_0, \beta, k, q_0, a_0, r, n_{11}, n_{12}, \gamma, h, \alpha_{11}, \delta_1, g, \alpha_{12}$ and a_1

are assumed to be positive constants.

The mathematical analysis of the model given by equations (3.1) − (3.5) shall be carried out in the subsequent sections.

3.3 Boundedness and Dynamical Behaviour of Model

In this section, we shall establish the boundedness of solutions of the mathematical model given by equations (3.1) − (3.5). The following lemma shows that the solutions are bounded in R_5^+.

Lemma 3.3.1. *All solutions of the system given by equations* (3.1)−(3.5) *with positive initial conditions will lie in the region* V_r *where:* $V_r = \{(A, T, D_0, N, P)\epsilon R_5^+ : 0 \leq A + T \leq M_{11u}, 0 \leq N + D_0 + \frac{\alpha_{11}P}{\alpha_{12}} \leq M_{12u}, T_l \leq T \leq T_u, 0 \leq D_0 \leq D_{0u}, 0 \leq N \leq N_u\}$ *for all* $t \to \infty$ *for positive initial values* $A(0), T(0), D_0(0), N(0), P(0)$ *where* $M_{11u} = \frac{p_0+q_0}{w_2}$ *;* $w_2 = min(\beta, a_0)$ *;* $M_{12u} = \frac{r+N_u(h+\mu)}{\mu}$ *;* $n_{11} > \mu$ *;* $\frac{\alpha_{11}a_1}{\alpha_{12}} > \mu$*;* $T_u = \frac{q_0}{a_0}$ *;* $T_l = \frac{q_0}{a_0+kM_{11u}}$*;* $D_{0u} = \frac{r}{n_{11}}$ *and* $N_u = \frac{h+\gamma D_{0u}}{\delta_1}$.

Proof. From equation (3.2) we obtain,

$$\frac{dT(t)}{dt} \leq q_0 - a_0 T.$$

Then, following the usual comparison theorem we obtain:

$$\limsup_{t\to\infty}(T, t) \leq \frac{q_0}{a_0},$$

and hence,

$$T(t) \leq \frac{q_0}{a_0} = T_u(t).$$

Similarly from equation (3.3) following the usual comparison theorem, we get,

$$\limsup_{t\to\infty}(D_0, t) \leq \frac{r}{n_{11}},$$

and,

$$D_0(t) \leq \frac{r}{n_{11}} = D_{0u}(t),$$

and from equation (3.4), following the usual comparison theorem, we obtain,

$$\limsup_{t\to\infty}(N,t) \leq \frac{h+\gamma D_{0u}}{\delta_1},$$

hence,

$$N(t) \leq \frac{h+\gamma D_{0u}}{\delta_1} = N_u(t).$$

Let us consider a function $M_{11}(t)$ given as ,

$$M_{11}(t) = A(t) + T(t).$$

Taking $w_2 = \min\,(\beta, a_0)$ and from equations (3.1) and (3.2) we obtain,

$$\frac{dM_{11}(t)}{dt} \leq p_0 + q_0 - w_2 M_{11}(t).$$

Then, by the usual comparison theorem we have:

$$\limsup_{t\to\infty}(M_{11},t) \leq \frac{p_0+q_0}{w_2}.$$

Hence,

$$A(t) + T(t) \leq \frac{p_0+q_0}{w_2} = M_{11u}(t).$$

Again, from equation (3.2) we get,

$$\frac{dT(t)}{dt} \geq q_0 - a_0 T - kM_{11u}T,$$

and by usual comparison theorem we get,

$$\liminf_{t\to\infty}(T,t) \geq \frac{q_0}{a_0 + kM_{11u}}.$$

Therefore,

$$T(t) \geq \frac{q_0}{a_0 + kM_{11u}} = T_l(t).$$

Now, consider a function $M_{12}(t)$ given as,

$$M_{12}(t) = N(t) + D_0(t) + \frac{\alpha_{11}P(t)}{\alpha_{12}}.$$

From equations (3.3), (3.4) and (3.5) we get,

$$\frac{dM_{12}(t)}{dt} \leq r - n_{11}D_0 + hN_u - \frac{\alpha_{11}a_1P}{\alpha_{12}},$$

For a positive constant μ and assuming $n_{11} > \mu$; $\frac{\alpha_{11}a_1}{\alpha_{12}} > \mu$ we get,

$$\frac{dM_{12}}{dt} + \mu M_{12} \leq r + (h+\mu)N_u$$

. Then by the usual comparison theorem we have:

$$\limsup_{t\to\infty}(M_{12}, t) \leq \frac{r + (h+\mu)N_u}{\mu} = M_{12u}(t).$$

Hence we get,

$$N(t) + D_0(t) + \frac{\alpha_{11}P(t)}{\alpha_{12}} \leq \frac{r + (h+\mu)N_u}{\mu}.$$

□

Positivity of solutions : Since the positivity of solutions of the the model given by equations $(3.1) - (3.5)$ implies persistance, hence it is important to prove the solutions of the model studying the dynamical behaviour of aquatic prey-predator population under the effect of increasing acidity and toxicants, exhibit positivity for all times . The positivity of solutions shall be shown by the following lemma.

Lemma 3.3.2. *The solutions of the model given by equations* $(3.1) - (3.5)$, $(A(t), T(t), D_0(t), N(t), P(t))$, *with initial conditions,* $A(0) > 0, T(0) > 0$, $D_0(0) > 0, N(0) > 0, P(0) > 0$, *remain positive for all times* $t > 0$.

Proof. From equation (3.1) we get,

$$\frac{dA}{dt} \geq -\beta A,$$

$$A \geq g_1 e^{-\beta t},$$

where g_1 is an integration constant.
Hence, $A > 0$ as $t \to \infty$.
Similarly, from equation (3.2), we get

$$\frac{dT}{dt} \geq -(a_0 + kM_{11u})T,$$

$$T \geq g_2 e^{-(a_0+kM_{11u})t},$$

where g_2 is an integration constant.
Hence, $T > 0$ as $t \to \infty$.
From equation (3.3), we get

$$\frac{dD_0}{dt} \geq -(n_{11} + n_{12}M_{11u} + \gamma M_{12u})D_0,$$
$$D_0 \geq g_3 e^{-(n_{11}+n_{12}M_{11u}+\gamma M_{12u})t},$$

where g_3 is an integration constant.
Hence, $D_0 > 0$ as $t \to \infty$.
Similarly, from equation (3.4), we obtain

$$\frac{dN}{dt} \geq -(\alpha_{11}M_{12u} + \delta_1 N_u)N,$$

$$N \geq g_4 e^{-(\alpha_{11}M_{12u}+\delta_1 N_u)t},$$

where g_4 is an integration constant.
Hence, $N > 0$ as $t \to \infty$.
From equation (3.5), we obtain

$$\frac{dP}{dt} \geq -a_1 P,$$

$$P \geq g_5 e^{-a_1 t},$$

where g_5 is an integration constant.
Hence, $P > 0$ as $t \to \infty$.
This leads to completion of the proof of the lemma 3.3.2. □

3.3.1 Possible equilibrium points and existence conditions

In this section, for the model defined by set of equations (3.1) – (3.5) , we find the possible equilibrium points. The model has the following four equilibrium points:
1. Prey and predator population vanishing equilibrium point
$\hat{E}(\hat{A}, \hat{T}, \hat{D}_0, 0, 0)$ where $\hat{N} = 0$ and $\hat{P} = 0$ i.e. when the toxicant and acid level

in the water increases to such a high amount such that the prey and predator populations tends towards extinction.

$$\hat{A} = \frac{p_0}{\beta - k\hat{T}}. \tag{3.6}$$

$$\hat{A} > 0 \quad if \quad \beta - k\hat{T} > 0. \tag{3.7}$$

$$\hat{D}_0 = \frac{r}{n_{11} + n_{12}\hat{T}}. \tag{3.8}$$

Since $\hat{T} > 0$, $\hat{D}_0 > 0$.
$\hat{T}$ is given as the positive root of the following quadratic equation ,

$$a_0 k\hat{T}^2 - \hat{T}(q_0 k + a_0\beta + kp_0) + q_0\beta = 0.$$

2. Predator vanishing equilibrium point $\tilde{E}(\tilde{A}, \tilde{T}, \tilde{D_0}, \tilde{N}, 0)$
i.e. $\tilde{P} = 0$.

$$\tilde{A} = \frac{p_0}{\beta - k\tilde{T}}. \tag{3.9}$$

$$\tilde{A} > 0 \quad if \quad \beta - k\tilde{T} > 0. \tag{3.10}$$

$$\tilde{N} = \frac{1}{\delta_1}\left(\frac{h}{1+\tilde{A}} + \gamma\tilde{D_0}\right). \tag{3.11}$$

$\tilde{T}$ is given as the positive root of the following quadratic equation ,

$$a_0 k\tilde{T}^2 - \tilde{T}(q_0 k + a_0\beta + kp_0) + q_0\beta = 0.$$

$\tilde{D_0}$ is given as the positive root of the following quadratic equation ,

$$\tilde{D_0}^2 + \frac{\tilde{D_0}}{\gamma^2(1+\tilde{A})}((n_{11} + n_{12}\tilde{D_0})(1+\tilde{A})\delta_1 + \gamma h) - \frac{r\delta_1}{\gamma^2} = 0.$$

3. Interior equilibrium point $E^*(A^*, T^*, D_0^*, N^*, P^*)$: The values of $A^*, T^*, D_0^*, N^*, P^*$ are given as:
From equation (3.1) we have,

$$A^* = \frac{p_0}{\beta - kT^*}. \tag{3.12}$$

$$A^* > 0 \quad if \quad \beta - kT^* > 0. \tag{3.13}$$

$$N^* = \frac{a_1 g}{\alpha_{12} - a_1}. \tag{3.14}$$

$$N^* > 0 \quad if \quad \alpha_{12} - a_1 > 0. \tag{3.15}$$

$$D_0^* = \frac{r}{n_{11} + n_{12}T^* + \gamma N^*}. \tag{3.16}$$

Since $N^* > 0$ and $T^* > 0$, hence $D_0^* > 0$.
T^* is given as the positive root of the following quadratic equation ,

$$a_0 k T^{*2} - T^*(q_0 k + a_0 \beta + k p_0) + q_0 \beta = 0. \tag{3.17}$$

$$P^* = \frac{g + N^*}{\alpha_{11}} \left(\frac{h}{1 + A^*} + \gamma D_0^* - \delta_1 N^* \right). \tag{3.18}$$

$$P^* > 0 \quad if \quad \frac{h}{1 + A^*} + \gamma D_0^* - \delta_1 N^* > 0. \tag{3.19}$$

4. Acid vanishing equilibrium point $\breve{E}(0, \breve{T}, \breve{D}_0, \breve{N}, \breve{P})$ i.e. $\breve{A} = 0$.
The values of variables $\breve{T}, \breve{D}_0, \breve{N}, \breve{P}$ are given as:

$$\breve{T} = \frac{q_0}{a_0}. \tag{3.20}$$

From equation (3.5) we get,

$$\breve{N} = \frac{a_1 g}{\alpha_{12} - a_1}. \tag{3.21}$$

$\breve{N} > 0$ only if,

$$\alpha_{12} - a_1 > 0. \tag{3.22}$$

From equation (3.3) we get,

$$\breve{D}_0 = \frac{r}{n_{11} + n_{12}\breve{T} + \gamma \breve{N}}. \tag{3.23}$$

Since $\breve{N} > 0$ and $\breve{T} > 0$, hence $\breve{D}_0 > 0$.
From equation (3.4), $\breve{P}$ is given as ,

$$\breve{P} = \frac{g + \breve{N}}{\alpha_{11}} \left(h + \gamma \breve{D}_0 - \delta_1 \breve{N} \right). \tag{3.24}$$

$\breve{P} > 0$ only if,

$$h + \gamma \breve{D}_0 - \delta_1 \breve{N} > 0. \tag{3.25}$$

Remark: The toxicant (T) enters the water bodies through various multiple sources such as agricultural, household and industrial wastes discharge. Hence, the amount of toxicant entering in the system in the system can not be nullified completely and consequently T cannot be taken as zero.

The dynamical behaviour of the model given by equations (3.1) − (3.5) in terms of local and global stability for these possible equilibrium points shall be studied in the next section.

3.3.2 Local Stability

(a) **For prey and predator population vanishing equilibrium point** $\hat{E}(\hat{A}, \hat{T}, \hat{D}_0, 0, 0)$ **:** The characteristic equation corresponding to variational matrix about prey and predator population vanishing equilibrium point $\hat{E}$ is given as:

$$(-a_1 - \lambda)(-n_{11} - n_{12}\hat{T} - \lambda)((-\beta + k\hat{T} - \lambda)(-a_0 - k\hat{A} - \lambda) + k^2\hat{A}\hat{T})\left(\frac{h}{1+\hat{A}} + \gamma\hat{D}_0 - \lambda\right) = 0. \tag{3.26}$$

The eigen values corresponding to the above characteristic equation are given as:

$$\lambda_1 = -a_1, \quad \lambda_2 = -n_{11} - n_{12}\hat{T}, \quad \lambda_3 = \frac{h}{1+\hat{A}} + \gamma\hat{D}_0, \tag{3.27}$$

λ_4 and λ_5 are obtained by solving the following quadratic equation:

$$(-\beta + k\hat{T} - \lambda)(-a_0 - k\hat{A} - \lambda) + k^2\hat{A}\hat{T} = 0. \tag{3.28}$$

As the eigen value $\lambda_3 = \frac{h}{1+\hat{A}} + \gamma\hat{D}_0$ is positive, hence the equilibrium point $\hat{E}(\hat{A}, \hat{T}, \hat{D}_0, 0, 0)$ is unstable.

(b) **For predator population vanishing equilibrium point** $\tilde{E}(\tilde{A}, \tilde{T}, \tilde{D_0}, \tilde{N}, 0)$ **:** The characteristic equation associated with the variational matrix about predator population vanishing equilibrium point $\tilde{E}$ is given by:

$$(\tilde{Z_5} - \lambda)(\lambda^2 + (\tilde{Z_2} - \tilde{Z_1})\lambda - \tilde{Z_1}\tilde{Z_2} + k^2\tilde{A}\tilde{T})(\lambda^2 + (\tilde{Z_3} - \tilde{Z_4})\lambda - \tilde{Z_3}\tilde{Z_4} + \gamma^2\tilde{D_0}\tilde{N}) = 0, \quad (3.29)$$

where $\tilde{Z_1} = -\beta + k\tilde{T}$; $\tilde{Z_2} = a_0 + k\tilde{A}$; $\tilde{Z_3} = n_{11} + n_{12}\tilde{T} + \gamma\tilde{N}$; $\tilde{Z_4} = \frac{h}{1+\tilde{A}} + \gamma\tilde{D_0} - 2\delta_1\tilde{N}$; $\tilde{Z_5} = \frac{\alpha_{12}\tilde{N}}{g+\tilde{N}} - a_1$; $\tilde{Z_6} = \frac{-h\tilde{N}}{(1+\tilde{A})^2}$; $\tilde{Z_7} = \frac{-\alpha_{11}\tilde{N}}{g+\tilde{N}}$.
The eigen values corresponding to the above characteristic equation are given as:

$$\lambda_1 = \tilde{Z_5}, \quad (3.30)$$

λ_2 and λ_3 are obtained by solving the following quadratic equation:

$$\lambda^2 + (\tilde{Z_2} - \tilde{Z_1})\lambda - \tilde{Z_1}\tilde{Z_2} + k^2\tilde{A}\tilde{T} = 0. \quad (3.31)$$

λ_4 and λ_5 are obtained by solving the following quadratic equation:

$$\lambda^2 + (\tilde{Z_3} - \tilde{Z_4})\lambda - \tilde{Z_3}\tilde{Z_4} + \gamma^2\tilde{D_0}\tilde{N} = 0. \quad (3.32)$$

Using Routh-Hurwitz criteria, the boundary equilibrium state $\tilde{E}$ will be asymptotically stable subject to satisfying the following conditions,

$$\tilde{Z_2} > \tilde{Z_1}, \quad (3.33)$$

$$k^2\tilde{A}\tilde{T} > \tilde{Z_1}\tilde{Z_2}, \quad (3.34)$$

$$\tilde{Z_3} > \tilde{Z_4}, \quad (3.35)$$

$$\gamma^2\tilde{D_0}\tilde{N} > \tilde{Z_3}\tilde{Z_4}, \quad (3.36)$$

$$a_1 > \frac{\alpha_{12}\tilde{N}}{g+\tilde{N}}, \quad (3.37)$$

$$k\tilde{T} > \beta_1, \quad (3.38)$$

and

$$\frac{h}{1+\tilde{A}} + \gamma\tilde{D_0} > 2\delta_1\tilde{N}. \quad (3.39)$$

(c) **For interior equilibrium point** $E^*(A^*, T^*, D_0^*, N^*, P^*)$ **:**
The characteristic equation associated with the variational matrix about interior equilibrium point E^* is given by:

$$[\lambda^2 + (Z_2^* - Z_1^*)\lambda - Z_1^* Z_2^* + k^2 A^* T^*][\lambda^3 - \lambda^2(-Z_3^* + Z_4^*) - \lambda(Z_3^* Z_4^* + Z_7^* Z_8^* - \gamma^2 D_0^* N^*) - (Z_3^* Z_7^* Z_8^*)] = 0 \quad (3.40)$$

where $Z_1^* = -\beta + kT^*;;$ $Z_2^* = a_0 + kA^*;$ $Z_3^* = n_{11} + n_{12}T^* + \gamma N^*;$
$Z_4^* = \frac{h}{1+A^*} + \gamma D_0^* - 2\delta_1 N^* - \frac{\alpha_{11} g P^*}{(g+N^*)^2};$ $Z_6^* = \frac{-hN^*}{(1+A^*)^2};$
$Z_7^* = \frac{-\alpha_{11} N^*}{g+N^*};$ $Z_8^* = \frac{\alpha_{12} g P^*}{(g+N^*)^2}.$

Using Routh Hurwitz criteria, the interior equilibrium state E^* will be asymptotically stable subject to satisfying the following conditions,

$$Z_2^* > Z_1^*, \quad (3.41)$$

$$k^2 A^* T^* > Z_1^* Z_2^*, \quad (3.42)$$

$$Z_3^* > Z_4^*, \quad (3.43)$$

$$\gamma^2 D_0^* N^* > Z_3^* Z_4^* + Z_7^* Z_8^*, \quad (3.44)$$

$$(-Z_3^* + Z_4^*)(Z_3^* Z_4^* + Z_7^* Z_8^* - \gamma^2 D_0^* N^*) + Z_3^* Z_7^* Z_8^* > 0, \quad (3.45)$$

$$kT^* > \beta_1 \quad (3.46)$$

and

$$\frac{h}{1+A^*} + \gamma D_0^* > 2\delta_1 N^* + \frac{\alpha_{11} g P^*}{(g+N^*)^2}. \quad (3.47)$$

(d) **For acid vanishing equilibrium point** $\breve{E}(0, \breve{T}, \breve{D}_0, \breve{N}, \breve{P})$ **:** The characteristic equation corresponding to the variational matrix about acid vanishing equilibrium point $\breve{E}$ is given by:

$$(\breve{Z}_1 - \lambda)(-\breve{Z}_2 - \lambda)[\lambda^3 - \lambda^2(-\breve{Z}_3 + \breve{Z}_4) - \lambda(\breve{Z}_3 \breve{Z}_4 + \breve{Z}_7 \breve{Z}_8 - \gamma^2 \breve{D}_0 \breve{N}) - \breve{Z}_3 \breve{Z}_7 \breve{Z}_8] = 0 \quad (3.48)$$

where $\breve{Z}_1 = -\beta + k\breve{T};$ $\breve{Z}_2 = a_0;$ $\breve{Z}_3 = n_{11} + n_{12}\breve{T} + \gamma \breve{N};$
$\breve{Z}_4 = h + \gamma \breve{D}_0 - 2\delta_1 \breve{N} - \frac{\alpha_{11} g \breve{P}}{(g+\breve{N})^2};$ $\breve{Z}_6 = -h\breve{N};$ $\breve{Z}_7 = \frac{-\alpha_{11}\breve{N}}{g+\breve{N}};$

$\breve{Z}_8 = \frac{\alpha_{12} g \breve{P}}{(g+\breve{N})^2}$.
The eigen values corresponding to the above characteristic equation are given as:

$$\lambda_1 = \breve{Z}_1, \quad \lambda_2 = -a_0, \tag{3.49}$$

Using Routh's criteria, the eigen values λ_3, λ_4 and λ_5 will have non-positive real parts subject to satisfying the following conditions,

$$\breve{Z}_3 > \breve{Z}_4, \tag{3.50}$$

$$\gamma^2 \breve{D}_0 \breve{N} > \breve{Z}_3 \breve{Z}_4 + \breve{Z}_7 \breve{Z}_8, \tag{3.51}$$

$$(-\breve{Z}_3 + \breve{Z}_4)(\breve{Z}_3 \breve{Z}_4 + \breve{Z}_7 \breve{Z}_8 - \gamma^2 \breve{D}_0 \breve{N}) + \breve{Z}_3 \breve{Z}_7 \breve{Z}_8 > 0, \tag{3.52}$$

$$k\breve{T} < \beta_1, \tag{3.53}$$

and

$$h + \gamma \breve{D}_0 > 2\delta_1 \breve{N} + \frac{\alpha_{11} g \breve{P}}{(g+\breve{N})^2}. \tag{3.54}$$

3.3.3 Global Stability

In this section, the global stability of the mathematical model given by equations (3.1) – (3.5) shall be established. The following theorems shall establish the global stability:

Theorem 3.3.1. *The box given by V_r is a positive invariant and compact set in the space (A, T, D_0, N, P).*

Proof. Let us consider the system of equations given by (3.1) – (3.5). Consider a box V_r in the phase space ATD_0NP with one vertex at the origin and the other vertex at a point $\bar{\omega} = (\bar{A}, \bar{T}, \bar{D_0}, \bar{N}, \bar{P})$. The point $\bar{\omega}$ is considered outside the box V_r with $\bar{A} > A_u$,$\bar{T} > T_u$, $\bar{D_0} > D_{0u}$, $\bar{N} > N_u$, $\bar{P} > P_u$.
Now we shall compute the angle of the flow with each face of the box V_r not lying in the coordinate planes. Let ν_1, ν_2, ν_3, ν_4 and ν_5 be the outward unit normal vectors to the planes $\chi_1 : A = \bar{A}, \chi_2 : T = \bar{T}, \chi_3 :$

$D_0 = \bar{D_0}, \chi_4 : N = \bar{N}, \chi_5 : P = \bar{P}$ in reference to the box V_r.
Then from equation (3.3) we get,

$$\nu_3 \frac{d\bar{\omega}}{dt}|_{\chi_3} \leq r - n_{11}\bar{D_0} - n_{12}T_l\bar{D_0},$$

since

$$\bar{D_0} > \frac{r}{n_{11}},$$

$$\nu_3 \frac{d\bar{\omega}}{dt}|_{\chi_3} \leq -n_{12}T_l\bar{D_0},$$

hence

$$\nu_3 \frac{d\bar{\omega}}{dt}|_{\chi_3} \leq 0.$$

Similarly , we can prove

$$\nu_1 \frac{d\bar{\omega}}{dt}|_{\chi_1} \leq 0, \nu_2 \frac{d\bar{\omega}}{dt}|_{\chi_2} \leq 0, \nu_4 \frac{d\bar{\omega}}{dt}|_{\chi_4} \leq 0, \nu_5 \frac{d\bar{\omega}}{dt}|_{\chi_5} \leq 0.$$

□

From the above theorem it is clear that the trajectories of the system of equations given by (3.1) – (3.5) do not not cross V_r once they enter inside the box V_r. The interior equilibrium E^* is also observed to lie inside the V_r.
In the next theorem, we will prove that the only global attractor inside V_r is E^*.

Theorem 3.3.2. *For the interior equilibrium point E^* to be globally asymptotically stable, the following inequalities should hold for E^*.*

$$(\beta - kT)(a_0 + kA) > (kT^* - kA^*)^2,$$

$$(a_0 + kA)(n_{11} + \gamma N + n_{12}T) > (n_{12}D_0^*)^2,$$

$$2(n_{11} + \gamma N + n_{12}T)\left(\frac{-\alpha_{11}P^*}{(g+N)(g+N^*)} + \delta_1\right) > 3(\gamma D_0^* - \gamma)^2,$$

$$4\left(\frac{-\alpha_{11}P^*}{(g+N)(g+N^*)} + \delta_1\right)\left(a_1 - \frac{\alpha_{12}N}{g+N}\right) >$$

$$3\left(\frac{\alpha_{11}}{g+N}-\frac{\alpha_{12}gP^*}{(g+N)(g+N^*)}\right)^2,$$

$$2(\beta-kT)\left(\frac{-\alpha_{11}P^*}{(g+N)(g+N^*)}+\delta_1\right)>3\left(\frac{h}{(1+A)(1+A^*)}\right)^2.$$

Proof. For establishing the global stability of the equilibrium state E^*, we shall assume the following positive definite function:

$$Z=\frac{1}{2}(A-A^*)^2+\frac{1}{2}(T-T^*)^2+\frac{1}{2}(D_0-D_0^*)^2+\left(N-N^*-N^*ln\frac{N}{N^*}\right)+\frac{1}{2}(P-P^*)^2. \tag{3.55}$$

Differentiating the above equation w.r.t. 't' we get,

$$\frac{dZ}{dt}=-[a_{11}(A-A^*)^2+a_{22}(T-T^*)^2+a_{33}(D_0-D_0^*)^2+a_{44}(N-N^*)^2+a_{55}(P-P^*)^2+a_{12}(A-A^*)(T-T^*)+a_{23}(T-T^*)(D_0-D_0^*)+a_{34}(N-N^*)(D_0-D_0^*)+a_{45}(P-P^*)(N-N^*)+a_{14}(A-A^*)(N-N^*)],$$

where

$$a_{11}=\beta-kT,\quad a_{22}=a_0+kA,\quad a_{12}=kT^*-kA^*,$$

$$a_{23}=n_{12}D_0^*,\quad a_{33}=n_{11}+\gamma N+n_{12}T,$$

$$a_{44}=\delta_1-\frac{\alpha_{11}P^*}{(g+N)(g+N^*)},\ a_{55}=a_1-\frac{\alpha_{12}N}{g+N},$$

$$a_{34}=\gamma D_0^*-\gamma,\quad a_{45}=\frac{\alpha_{11}}{g+N}-\frac{\alpha_{12}gP^*}{(g+N)(g+N^*)},$$

$$a_{14}=\frac{h}{(1+A)(1+A^*)}$$

.

Sufficient conditions for $\frac{dZ}{dt}$ to be negative definite obtained by Sylvester's criteria are:

$$a_{11}a_{22}>a_{12}^2,\quad a_{22}a_{33}>a_{23}^2,\quad 2a_{33}a_{44}>3a_{34}^2,$$
$$4a_{44}a_{55}>3a_{45}^2,\quad 2a_{11}a_{44}>3a_{14}^2, \tag{3.56}$$

i.e.

$$(\beta - kT)(a_0 + kA) > (kT^* - kA^*)^2, \tag{3.57}$$

$$(a_0 + kA)(n_{11} + \gamma N + n_{12}T) > (n_{12}D_0^*)^2, \tag{3.58}$$

$$2(n_{11} + \gamma N + n_{12}T)\left(\frac{-\alpha_{11}P^*}{(g+N)(g+N^*)} + \delta_1\right) > 3(\gamma D_0^* - \gamma)^2, \tag{3.59}$$

$$4\left(\frac{-\alpha_{11}P^*}{(g+N)(g+N^*)} + \delta_1\right)\left(a_1 - \frac{\alpha_{12}N}{g+N}\right) > 3\left(\frac{\alpha_{11}}{g+N} - \frac{\alpha_{12}gP^*}{(g+N)(g+N^*)}\right)^2,$$

$$2(\beta - kT)\left(\frac{-\alpha_{11}P^*}{(g+N)(g+N^*)} + \delta_1\right) > 3\left(\frac{h}{(1+A)(1+A^*)}\right)^2. \tag{3.60}$$

□

3.4 Numerical Simulation and Sensitivity Analysis

To substantiate the analytical results obtained for the system of equations given by (3.1) – (3.5), numerical simulations have been supplemented in this section. The set of parametric values considered are given below:

$$\begin{gathered} p_0 = 0.43\mu gL^{-1}day^{-1}, \beta = 0.2day^{-1}, q_0 = 1.0\mu gL^{-1}day^{-1}, \\ a_0 = 0.1day^{-1}, r = 70mgL^{-1}day^{-1}, k = 0.01L\mu g^{-1}day^{-1}, \\ n_{11} = 1.0day^{-1}, n_{12} = 1.0L\mu g^{-1}day^{-1}, \gamma = 0.995Lmg^{-1}day^{-1}, \\ h = 1.0\mu gL^{-1}day^{-1}, g = 1.0mgL^{-1}, \alpha_{11} = 1.00025day^{-1}, \\ \delta_1 = 1.1Lmg^{-1}day^{-1}, \alpha_{12} = 1.001day^{-1}, a_1 = 0.825day^{-1}. \end{gathered} \tag{3.61}$$

For the above mentioned parametric values, the equilibrium values corresponding to interior equilibrium E^* are given as:

$$A^* = 3.4258\mu g L^{-1}, T^* = 7.4483\mu g L^{-1}, D_0^* = 5.3383 mg L^{-1},$$
$$N^* = 4.6881 mg L^{-1}, P^* = 2.1687 mg L^{-1}. \quad (3.62)$$

For these values of the model parameters, the conditions of feasibility, boundedness and stability corresponding to interior equilibrium point E^* are satisfied. Also, for the mentioned parametric values , interior equilibrium E^* is found to exhibit asymptotic stability as shown in fig. 3.1. The numerical simulations also show that the interior equilibrium point E^* is globally stable. These results are shown by the phase plane graphs given by fig. 3.2 , which show that with increasing time, the trajectories starting from varied initial conditions as given by table 3.1, finally converge to the equilibrium value at E^*.
Further, for the model given by equations (3.1) – (3.5) sensitivity analysis has been carried out. Sensitivity analysis results provide a more mathematically sound study of the effect of the model parameters given by equation(3.61) on the resource i.e. dissolved oxygen (D_0), prey population (N) and predator population (P). The sensitivity indices have been calculated to examine the relative variation in the variables A^*, T^*, D_0^*, N^* and P^* with respect to change in the values of parameters $p_0, \beta, q_0, a_0, k, r, n_{11}, n_{12}, \gamma, h, \alpha_{11}, g, \delta_1, \alpha_{12}$ and a_1, so that the parameters having more profound effect on the model variables can be identified and accordingly necessary control strategies can be developed.
The normalized forward sensitivity index of a variable Z with dependent on parameter "v" is given by the expression given below [117]:

$$\gamma_v^Z = \frac{\partial Z}{\partial v} * \frac{v}{Z}$$

The sensitivity indices of each variable at equilibrium point E^* with respect to model parameters given by equation (3.61) are given in table 3.2.

Table 3.1: Varying values of initial conditions for $A^*, T^*, D_0^*, N^*, P^*$.

Variable	1^{st} intial value	2^{nd} intial value	3^{rd} intial value	4^{th} intial value	5^{th} intial value
A	1	1	2	1	2
T	1	1.5	1.5	1.5	5
D_0	1	1	4	1	10
N	1	10	4	10	1
P	1	2.5	3.5	1.5	2

Table 3.2: Sensitivity Indices(γ) of $A^*, T^*, D_0^*, N^*, P^*$ at E^* to parameters Z_p.

Parameters(Z_p)	$\gamma_{Z_p}^{A^*}$	$\gamma_{Z_p}^{T^*}$	$\gamma_{Z_p}^{D_0^*}$	$\gamma_{Z_p}^{N^*}$	$\gamma_{Z_p}^{P^*}$
p_0	0.869	-0.222	0.126	0	1.354
β	-1.384	0.353	-0.201	0	-2.157
k	0.384	-0.353	0.201	0	2.6155
q_0	0.515	0.868	-0.494	0	-7.1022
a_0	-0.384	-0.647	0.367	0	5.293
r	0	0	0.999	0	13.927
n_{11}	0	0	-0.0763	0	-1.0617
n_{12}	0	0	-0.568	0	-7.9081
γ	0	0	-0.356	0	-4.953
h	0	0	0	0	0.592
α_{11}	0	0	0	0	-0.998
g	0	0	-0.355	0.999	-17.477
δ_1	0	0	0	0	-13.522
α_{12}	0	0	2.027	-5.701	100.622
a_1	0	0	-2.026	5.698	-100.578

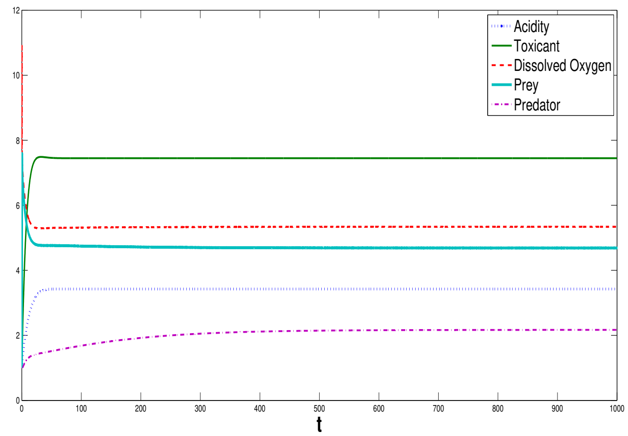

Figure 3.1: Trajectories plotted with respect to time showing the stability of interior equilibrium point E^*.

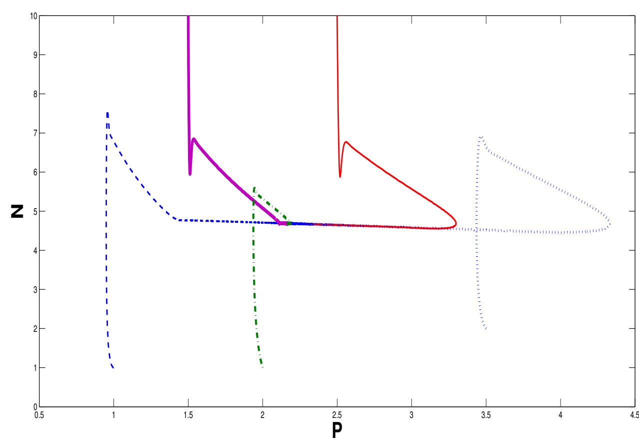

Figure 3.2: Phase plane graph for N-P at different initial values given in Table 3.1 demonstrating the global stability behaviour.

3.5 Conclusion

The mathematical model given by equations (3.1) $-$ (3.5) studies the impact of rising toxicants and acid components in water on the resource i.e. dissolved oxygen (D_0), prey population (N) and predator population

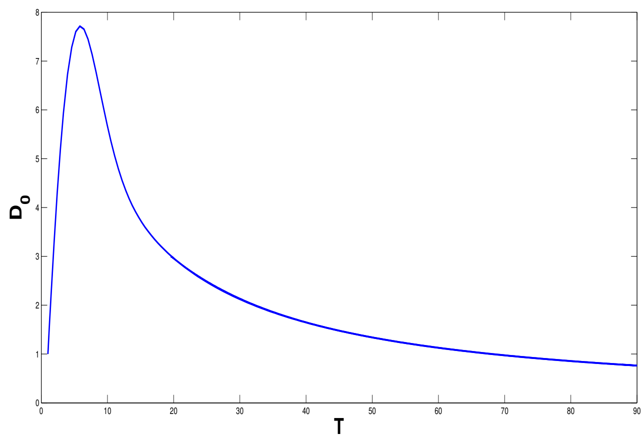

Figure 3.3: Phase space graph for toxicant concentration (T) and concentration of dissolved oxygen (D_0).

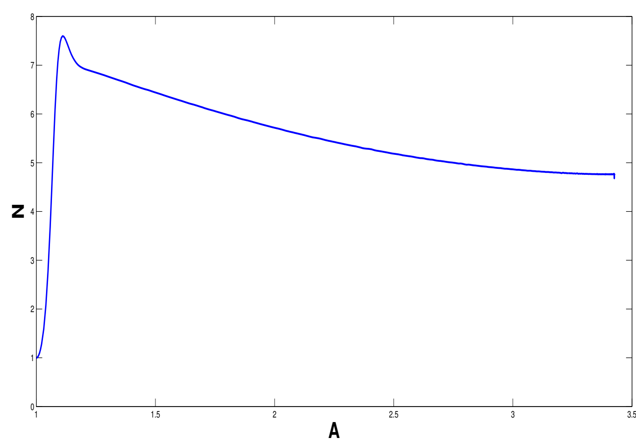

Figure 3.4: Phase space graph for acid concentration (A) and density of prey population (N).

(P) in an aquatic ecosystem. From the stability analysis it is observed that the acid vanishing point $\breve{E}$ is linearly asymptotically stable only when the interior equilibrium point E^* and boundary equilibrium point $\tilde{E}$ are unstable and vice-versa. The same is supported by equations $(3.38, 3.46, 3.53)$. Further, it is observed that the interior equilibrium

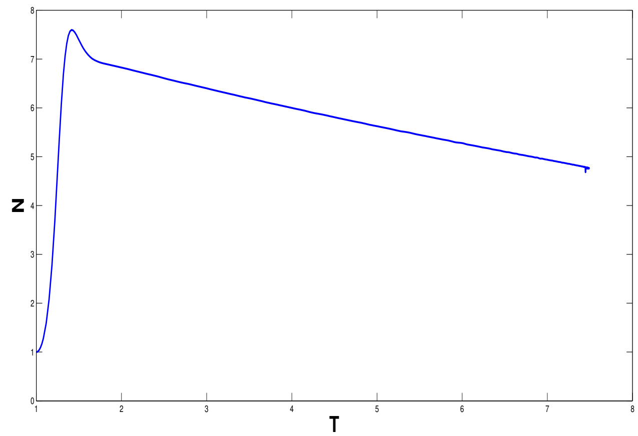

Figure 3.5: Phase space graph for toxicant concentration (T) and density of prey population (N).

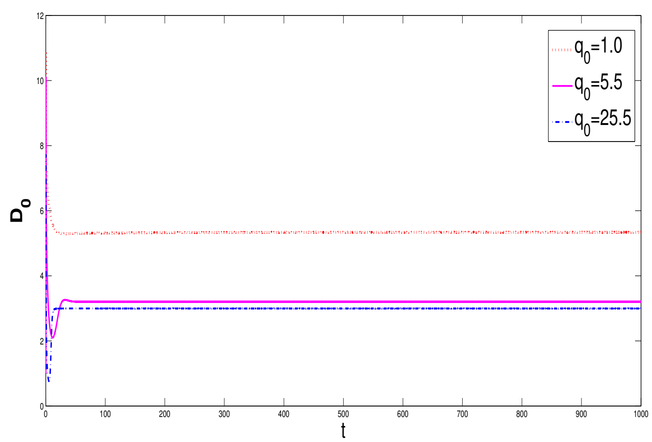

Figure 3.6: Graph between dissolved oxygen concentration(D_0) and time t with increasing values of q_0.

point E^* is asymptotically stable as shown in fig. 3.1 and the stability conditions given by equations $(3.12)-(3.19), (3.41)-(3.47), (3.57-3.60)$ are satisfied. Also, when the interior equilibrium point is stable, the boundary equilibrium point $\breve{E}$ shall be unstable as supported by equations $(3.46, 3.53)$. Further, it may be noted that the resource i.e. dis-

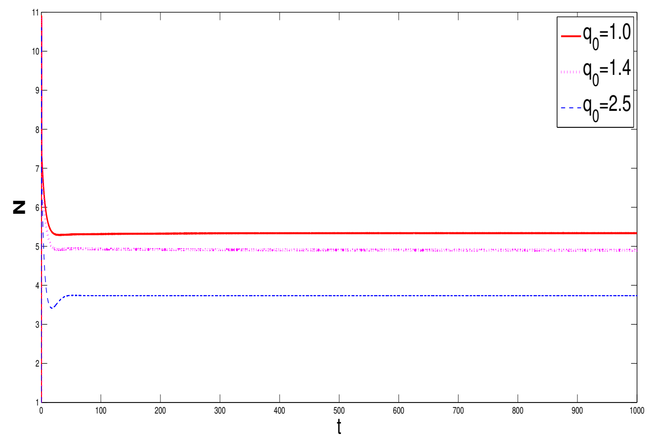

Figure 3.7: Graph between density of prey population(N) and time t with increasing values of q_0.

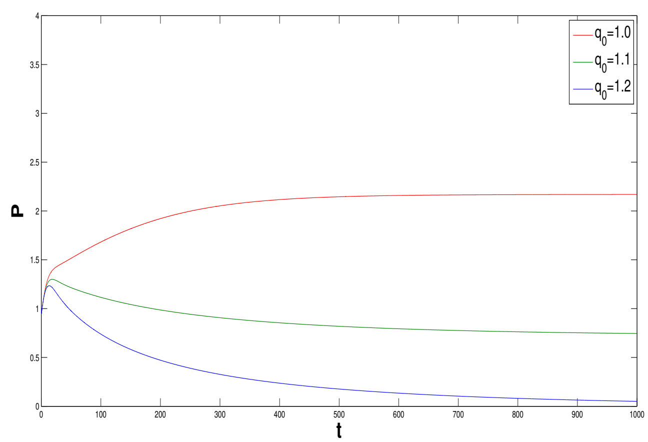

Figure 3.8: Graph between density of predator population(P) and time t with increasing values of q_0.

solved oxygen concentration decreases with increasing water toxicity as shown by fig. 3.3 and supported by equation 3.16. Also, the prey population (N) decreases with rising toxicity and acidity level in water as shown by figs. 3.4 and 3.5. Consequently, the predator population which is dependent on prey population for its food also exhibits a decline

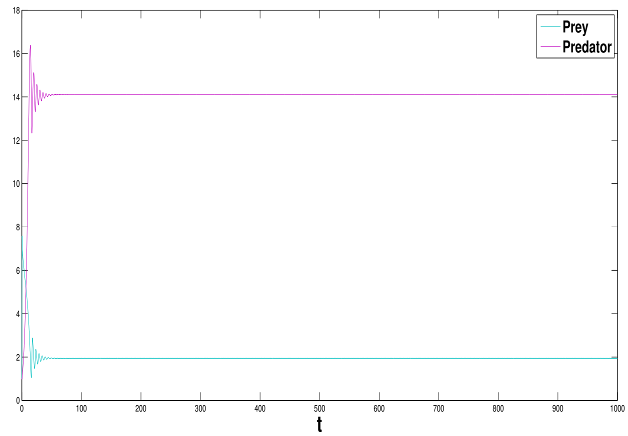

Figure 3.9: Time series graph showing stable limit cycles for prey population(N) and predator population(P) with rise in value of α_{12} to 1.25.

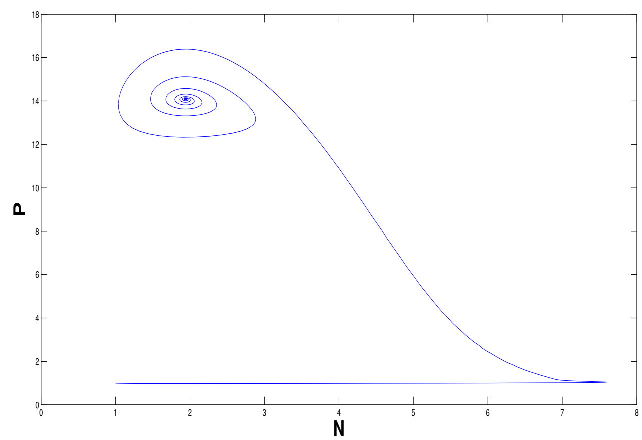

Figure 3.10: Phase plane graph showing stable limit cycles for prey population(N) and predator population(P) with rise in value of α_{12} to 1.25.

in its density with rising toxicity and acidity as supported by equation 3.18. Also, it is shown by fig. 3.6 that the dissolved oxygen concentration (D_0) shall decline on account of rise in value of toxicant input rate (q_0). Further, it may be noted that as the value of toxicant input rate (q_0) increases, it leads to decrease in density of prey population as

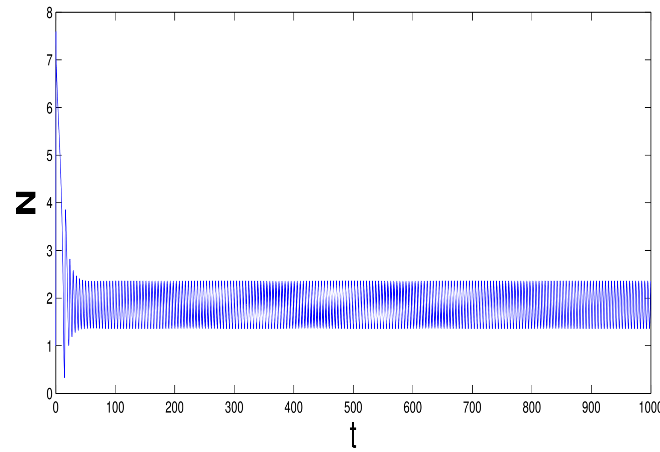

Figure 3.11: Graph showing oscillations for prey population(N) with rise in value of α_{12} to 1.28.

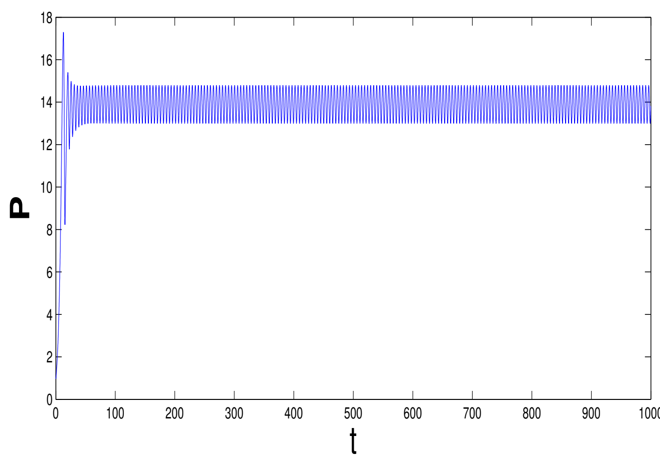

Figure 3.12: Graph showing oscillations for predator population(P) with rise in value of α_{12} to 1.28.

shown in fig. 3.7. Similarly, as illustrated by fig. 3.8, with increase in the toxicant input level(q_0) in water, the predator population tends towards extinction. Moreover, from the sensitivity analysis, it is further observed that dissolved oxygen (D_0) and predator population (P) are sensitive and negatively dependent on input rate of toxicant (q_0) in

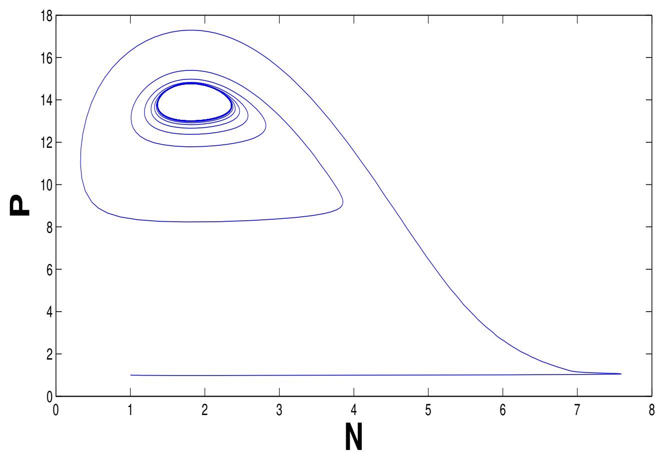

Figure 3.13: Graph showing oscillations for predator population(P) and prey population(N) with rise in value of α_{12} to 1.28.

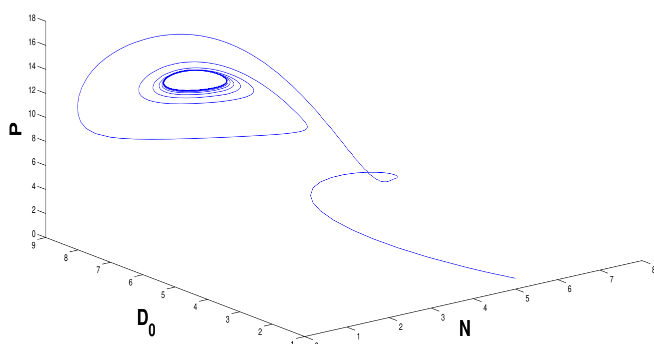

Figure 3.14: Graph showing oscillations for P, N and D_0 with rise in value of α_{12} to 1.28.

water. Also, the prey and predator populations are highly sensitive to assimilation rate of predator (α_{12}). For values of α_{12} equal to or greater than 1.23 but less than 1.28, stable limit cycles are observed. Figs. 3.9 and 3.10 show the stable limit cycles observed for prey and predator populations for value of α_{12} equal to 1.25. It may also be noted that

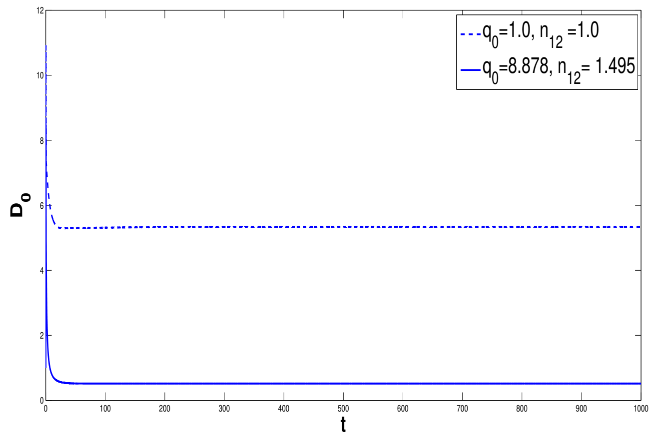

Figure 3.15: Graph between concentration of dissolved oxygen(D_0) and time t for rise in value of q_0 and n_{12}.

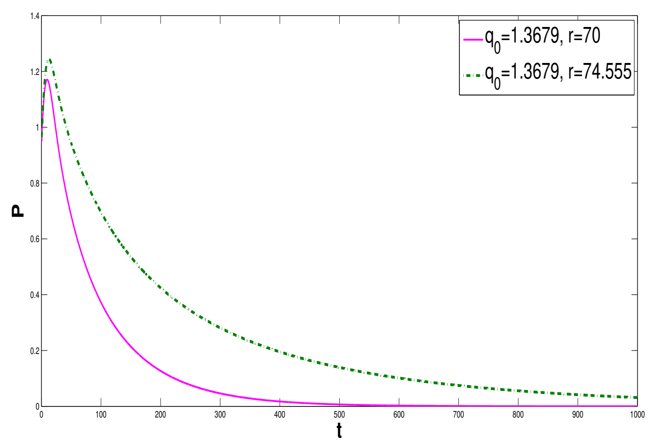

Figure 3.16: Graph between predator population (P) and time t for rise in value of r.

on increasing value of α_{12} to 1.28, the stable co-existing behaviour is changed to co-existing oscillatory behaviour. The oscillatory behaviour observed for prey and predator populations is shown in figs. 3.11-3.14. Furthermore, as the amount of agricultural and organic pollutants rise in water, the algal bloom in water increases and more oxygen is con-

sumed in its decomposition process. From our study, it is inferred that in the absence of any toxicant or acid input in water, the dissolved oxygen level is 12.3567 mgL^{-1} which lies in the required optimal range [118]. However, under these conditions, when the toxicant input (q_0) is increased from 1.0 to 8.878 and the oxygen utilisation rate in the decomposition process (n_{12}) is increased to 1.495, the concentration of dissolved oxygen falls to 0.5182 as shown in fig. 3.15, thus creating a hypoxic condition which threatens the survival of aquatic species. The results of our study are validated by the results of the study carried out by Chakraborty et al. [118]. They found that with rising agricultural pollutants, the algal bloom growth increases which leads to consumption of dissolved oxygen in its decomposition process. Due to this, the concentration of dissolved oxygen falls to 0.5 mgL^{-1} which is comparable to the results of our study. Moreover, the case study carried out by San-Diego-Mc Glone et al. [82] also support the results of our study. They showed that under the stress of eutrophication, the dissolved oxygen level in coastal waters of Bolino, Philippines fell to 2.0 mgL^{-1} which caused fish kills in year 2002. However, since we are considering the effects of pollutants, eutrophication and acidification together , the level of dissolved oxygen obtained in our study is $0.5182 mgL^{-1}$ which is considerably low than $2.0 mgL^{-1}$.
It is further established that at the value of toxicant input rate $q_0 = 1.3679$, the predator population tends towards zero a shown in fig. 3.16. It is also observed that at the parameter values q_0=1.3679, if the value of r i.e. input rate of dissolved oxygen is increased from r=70.00 to 74.555, the predator population again starts rising from zero level as shown in fig. 3.16. Thus, for the predator populations to exist , either the toxicant input rate q_0 should be maintained less than 1.3679 or the dissolved oxygen input rate(r) should always be maintained above threshold value of r= 74.555. Thus, it is concluded from our study that to sustain the prey-predator aquatic populations while maintaining a healthy level of dissolved oxygen in water, the release of toxic and acid

components in water needs to be mitigated and control strategies needs to be developed for the same in future.

Chapter 4

Impact of Carbon Emissions and Increased Acidity on Aquatic Population: A Mathematical Model

4.1 Introduction

The aquatic ecosystem is essential for the existence and survival of human population. It serves basic needs of human population such as potable water, water for agricultural and commercial use etc. Currently, the water bodies are facing the pressure of contamination caused by various anthropogenic activities. The increasing carbon emissions are leading to pollution and global warming. Temperature and climatic conditions have exhibited notable changes due to global warming in past years and recent studies foresee even more shifts in climate patterns due to continuous increase of carbon emissions in environment [17, 25] . Global warming causes a rise in temperature of water and this is found to have negative ecological effects on the aquatic population [1, 27]. To accommodate the warming of oceans, the oxygen production in water is decreasing which is proving fatal to the aquatic populations [103]. The uptake of carbon dioxide by water bodies has also increased in last 50 years [142]. The carbon reacts with oxygen in water and forms carbonic acid. Hence, the increasing carbon dioxide concentration in water is leading to lowering of pH of water, thus acidifying the water bodies. The unchecked release of various kinds of wastes such as industrial effluents in aquatic bodies further contribute to acidification of water [134]. Various studies show that the increased carbon emissions and acidity of water obstruct the growth and survival of aquatic species [54, 56]. Increasing water acidity also induces the growth of harmful algal blooms in water [126]. Further, the rising carbon emissions which cause global warming lead to the growth of algal blooms in water [78, 80]. The decomposition of these algal blooms uses the dissolved oxygen (DO) in water which decreases its level further in water. Since, oxygen is a vital resource for the aquatic population hence its depletion negatively affects the aquatic population. These algal blooms have been found to kill aquatic species such as fishes and alter the aquatic ecosystems [6]. Few mathematical works are available which show the negative effect of increasing algal blooms on the aquatic ecosystem [118] and determine that that the resource and fish populations are sensitive to the acidification and pollution of water [108]. However, the mathematical studies available till now have focused on the individual effect of pollutants, acidity, or temperature on the aquatic population. To study the combined effect of increasing acidity and carbon input on the aquatic population like fishes, a mathematical model having parameters as carbon concentration in water, pH of water, density of algal bloom population and concentration of dissolved oxygen in water is proposed and analyzed. It is assumed that the carbon concentration in water is increasing due to the input of carbon-rich pollutants in water as well as carbon emissions in atmosphere. This leads to lowering of pH of water. The rising temperature of water is decreasing the dissolved oxygen level in water bodies. Further, it is assumed that the increase in carbon concentration and warming temperatures also increase the growth of algal bloom in water which lead to subsequent decrease in dissolved oxygen in water. The analytical results are supported by numerical simulations done using MATLAB.

4.2 Mathematical Model

In this model, it is presumed that the pH of water is decreasing due to two reasons. One is due to increasing carbon content in water. The carbon reacts with the dissolved oxygen (DO) in water and forms carbonic acid, thus leading to water acidification. Second cause is the direct discharge of acid components and chemicals in water bodies. The inflating carbon emissions also lead to rise in temperature of water. As a result, the solubility of oxygen in water decreases due to low absorption in warmed waters. Further, it is assumed that due to increase in carbon and acid components in water along with rising water temperature, the algal population also increases. The dissolved oxygen is used in the decomposition process of algal bloom, thus depleting the concentration of dissolved oxygen in water. In view of the above, let C represent the concentration of carbon in water, pH represents pH level of water, A_l represent the density of algal population and D_0 represent the concentration of favourable resource i.e. dissolved oxygen in water. Incorporating the stated variables, the model containing the following system of non-linear differential equations is formulated.

$$\frac{dC}{dt} = C_E - \frac{1}{\tau_c}(C - C_0) - \gamma_1 D_0 C, \tag{4.1}$$

$$\frac{d(pH)}{dt} = \frac{pH_0}{1+C} - g(pH), \tag{4.2}$$

$$\frac{dA_l}{dt} = \frac{\alpha_1 A_l(1 + aC - b(pH))}{\beta_0 + A_l} + d_1 A_l D_0 - hA_l, \tag{4.3}$$

$$\frac{dD_0}{dt} = q - m_1 D_0 - n_1 d_1 D_0 A_l - \gamma_1 D_0 C, \tag{4.4}$$

where $C(0) > 0, pH(0) > 0, A_l(0) \geq 0, D_0(0) \geq 0$, and $C \geq C_0$.
The model parameters can be defined as:

C_E represents the input rate of carbon in water. τ_c represents the latent time period of carbon in water. C_0 gives the threshold level of carbon in water. The carbon in water reacts with dissolved oxygen and forms carbonic acid. This reaction is represented by the term $\gamma_1 D_0 C$ where γ_1 gives the rate of reaction of dissolved oxygen with carbon. The threshold level of pH of water is given by pH_0 and g is the natural lowering rate of pH in water. α_1 represents the rate of natural growth of algal population. a represents the growth of algal blooms on account of increasing carbon concentration in water and b gives the rate of growth of algal blooms on account of decreasing pH. β_0 is the half saturation constant. Algal blooms use dissolved oxygen for respiration at night which is represented by bilinear interaction $d_1 D_0 A_l$, where d_1 gives the rate of utilization of oxygen in respiration process. h is the natural decay rate of algal bloom. Input rate of dissolved oxygen is given by q. m_1 is natural depletion rate of dissolved oxygen. n_1 gives the consumption rate of dissolved oxygen in the decomposition of algal blooms.
All the parameters stated above are assumed to be positive constants.

4.3 Dynamical Behaviour of the model

4.3.1 Boundedness of Solutions

Lemma 4.3.1. *All solutions of the mathematical model given by eqs. (4.1)-(4.4) shall lie in the region B_r where $B_r = (C, pH, A_l, D_0) \in R_4^+ : 0 < C < C_u, 0 < pH < pH_u,\ 0 < A_l < A_{lu}, 0 < D_0 < D_{0u}$ for all $t \to \infty$ with positive initial values $C(0), pH(0), A_l(0), D_0(0)$, where*

$$C_u = \tau_c C_E + C_0, \quad D_{0u} = \frac{q}{m_1}, \quad pH_u = \frac{pH_0}{g}, \quad A_{lu} = \frac{\alpha_1(1 + aC_u)}{h - d_1 D_{0u}}.$$

Proof. From equation (4.1) we get,

$$\frac{dC}{dt} \leq \tau_c C_E + C_0 - C.$$

Then, following the usual comparison theorem we obtain,

$$\limsup_{t\to\infty}(C,t) \le \tau_c C_E + C_0 = C_u.$$

Now, from eq (4.2), we get,

$$\frac{d(pH)}{dt} \le pH_0 - g(pH).$$

Then, following the usual comparison theorem we obtain,

$$\limsup_{t\to\infty}(pH,t) \le \frac{pH_0}{g} = pH_u.$$

Similarly from eq. (4.3) we get,

$$\limsup_{t\to\infty}(A_l,t) \le \frac{\alpha_1(1+aC_u)}{h-d_1D_{0u}} = A_{lu}.$$

and from eq. (4.4), we get,

$$\limsup_{t\to\infty}(D_0,t) \le \frac{q}{m_1} = D_{0u}.$$

□

4.3.2 Positivity of solutions

Since the persistence of solutions is implied by positivity, hence the positivity of solutions is shown by the following lemma.

Lemma 4.3.2. *The solutions of the model given by eqs. (4.1)-(4.4) i.e.* $(C(t), pH(t), A_l(t), D_0t))$*, having initial conditions,* $C(0) > 0, pH(0) > 0, A_l(0) > 0, D_0(0) > 0$ *, show positivity for all times* $t > 0$*.*

Proof. From eq. (4.1), we obtain,

$$\frac{dC}{dt} \ge -\left(\frac{1}{\tau_c} + \gamma_1 D_{0u}\right) C,$$

which implies,

$$C \ge f_1 e^{-\left(\frac{1}{\tau_c}+\gamma_1 D_{0u}\right)t},$$

where f_1 is integration constant. Hence we get, $C > 0$ as $t \to \infty$. From eq. (4.2)), we get,

$$pH \geq f_2 e^{-gt}$$

, where f_2 denotes an integration constant. Therefore, we get, $pH > 0$ as $t \to \infty$. Similarly, from eq. (4.3), we get,

$$A_l \geq f_3 e^{-(h+b(pH)_u)t},$$

where f_2 denotes an integration constant. This implies that $A_l > 0$ as $t \to \infty$. From eq. (4.4), we obtain,

$$D_0 \geq f_4 e^{-(m_1+n_1d_1A_{lu}+\gamma_1C_u)t},$$

where f_4 is integration constant. Hence, $D_0 > 0$ as $t \to \infty$. This completes the proof of lemma 4.3.2. □

4.3.3 Possible equilibrium points and existence conditions

Now, we shall study the equilibrium points corresponding to the model defined by eqs. (4.1)-(4.4). The model has following three equilibrium points:

1. Carbon Vanishing Equilibrium Point: $\breve{E}(0, p\breve{H}, \breve{A}_l, \breve{D}_0)$ where $\breve{C} = 0$.

$$p\breve{H} = \frac{pH_0}{g}, \tag{4.5}$$

$$\breve{D}_0 = \frac{q}{m_1 + n_1d_1\breve{A}_l}. \tag{4.6}$$

$\breve{A}_l$ is given as the positive root of the following quadratic equation,

$$n_1d_1\breve{A}_l^2 + \breve{A}_l(m_1h + h\beta_0n_1d_1 + \alpha_1bn_1d_1p\breve{H} - d_1q - \alpha_1n_1d_1) - (\beta_0(qd_1 - m_1h) + \alpha_1m_1(1 - bp\breve{H})) = 0. \tag{4.7}$$

By Descarte's rule of signs, the above equation will have at least one non-negative root if,

$$\beta_0qd_1 + \alpha_1m_1 > m_1h\beta_0 + \alpha_1bm_1p\breve{H} \tag{4.8}$$

2. Algal Population Vanishing Equilibrium Point:
$\hat{E}(\hat{C}, p\hat{H}, 0, \hat{D}_0)$ where $\hat{A}_l = 0$.

$$p\hat{H} = \frac{pH_0}{g(1+\hat{C})}, \tag{4.9}$$

$$\hat{D}_0 = \frac{q}{m_1 + \gamma_1 \hat{C}}. \tag{4.10}$$

$\hat{C}$ is given as the positive root of the following quadratic equation,

$$\gamma_1 \hat{C}^2 + \hat{C}(m_1 + \gamma_1 \tau_c q + \gamma_1 C_0 - \gamma_1 \tau_c C_E) - (C_0 m_1 + \tau_c C_E m_1) = 0. \tag{4.11}$$

The above equation (4.11) shall have a positive root, following Descarte's rule of signs, hence, the algal population vanishing equilibrium point shall be asymptotically stable.

3. Interior Equilibrium Point:$E^*(C^*, pH^*, A_l^*, D_0^*)$.

$$pH^* = \frac{pH_0}{g(1+C^*)}, \tag{4.12}$$

$$D_0^* = \frac{\tau_c C_E - (C^* - C_0)}{\tau_c \gamma_1 C^*}, \tag{4.13}$$

$$A_l^* = \frac{q - \gamma_1 D_0^* C^* - m_1 D_0^*}{n_1 d_1 D_0^*}. \tag{4.14}$$

Hence, $D_0^* > 0$ if,

$$\tau_c C_E > (C^* - C_0), \tag{4.15}$$

and $A_l^* > 0$ if,

$$q - \gamma_1 D_0^* C^* - m_1 D_0^* > 0. \tag{4.16}$$

C^* is is given as the positive root of the following equation,

$$\begin{aligned}
&C^{*4}(M_3M_4M_5 + d_1\gamma_1 + \gamma_1 hM_3) - C^{*3}[M_3M_4(M_8 + M_2M_5) + \\
&M_4M_7 + \gamma_1 M_2(2d_1 + hM_3) - \{M_3M_4(\alpha_1 + M_5) + d_1(\gamma_1 + qM_3 + \\
&m_1) + hM_3(qM_3 + m_1 + \gamma_1)\}] - C^{*2}[M_3M_4(M_8 + \alpha_1 M_2 + M_2M_5 + \\
&M_0M_6) + M_4M_7 + \gamma_1 M_2(2d_1 + hM_3) + d_1M_2(qM_3 + 2m_1) + \\
&hm_1M_2M_3 - \{M_4(M_2M_3M_8 + \alpha_1 M_3 + 2M_2M_7) + d_1(qM_3 + m_1 + \\
&\gamma_1 M_2^2) + hM_3(qM_3 + m_1)\}] - C^*[M_2M_3(\alpha_1 M_4 + qd_1 + hm_1) + \\
&M_2(M_2M_7M_4 + 2m_1d_1) - \{M_2M_3M_4(M_8 + M_0M_6) + 2M_2M_4M_7 + \\
&d_1M_2^2(\gamma_1 + m_1)\}] - M_2^2(M_4M_7 - m_1d_1) = 0, \quad (4.17)
\end{aligned}$$

where,

$$M_0 = \frac{pH_0}{g}, \quad M_2 = \tau_c C_E + C_0, \quad M_3 = \tau_c\gamma_1, \quad M_4 = n_1 d_1,$$

$$M_5 = \alpha_1 a, \quad M_6 = \alpha_1 b, \quad M_7 = d_1\beta_0, \quad M_8 = h\beta_0.$$

By Descarte's rule of signs, the above equation (4.17) will have at least one positive root if,

$$M_4M_7 > m_1 d_1 \quad (4.18)$$

4.4 Local Stability Analysis

1. Local Stability of Carbon Vanishing Equilibrium Point: $\breve{E}(0, p\breve{H}, \breve{A}_l, \breve{D}_0)$:

The characteristic equation corresponding to variational matrix about equilibrium point $\breve{E}$ is given by:

$$\left(\frac{1}{\tau_c} + \gamma_1\breve{D}_0 - \lambda\right)(-g - \lambda)(\lambda^2 + (\breve{Z}_4 - \breve{Z}_3)\lambda - \breve{Z}_3\breve{Z}_4 + n_1 d_1^2 \breve{A}_l\breve{D}_0) = 0, \quad (4.19)$$

where,

$$\breve{Z}_3 = \frac{-\alpha_1(1 - bp\breve{H})\breve{A}_l}{(\beta_0 + \breve{A}_l)^2}, \quad \breve{Z}_4 = m_1 + n_1 d_1\breve{A}_l.$$

By Routh's criteria, $\breve{E}$ shall be asymptotically stable only if,

$$\breve{Z}_4 - \breve{Z}_3 > 0, \tag{4.20}$$

and

$$n_1 d_1^2 \breve{A}_l \breve{D}_0 > \breve{Z}_3 \breve{Z}_4. \tag{4.21}$$

2. Local Stability of Algal Population Vanishing Equilibrium Point: $\hat{E}(\hat{C}, p\hat{H}, 0, \hat{D}_0)$:

The characteristic equation corresponding to variational matrix about the equilibrium point $\hat{E}$ is given by:

$$\left(\lambda - \left(\frac{\alpha_1(1 + a\hat{C} - bp\hat{H})}{\beta_0} + d_1\hat{D}_0 - h\right)\right)(\lambda + g)$$
$$\left(\lambda^2 + \left(\frac{1}{\tau_c} + \gamma_1\hat{D}_0 + m_1 + \gamma_1\hat{C}\right)\lambda + \frac{1}{\tau_c}(m_1 + \gamma_1\hat{C}) + \gamma_1\hat{D}_0 m_1\right) = 0. \tag{4.22}$$

Following the Routh's criteria, the boundary equilibrium point E is asymptotically stable if,

$$h\beta_0 + \alpha_1 bp\hat{H} > \alpha_1(1 + a\hat{C}) + \beta_0 d_1\hat{D}_0. \tag{4.23}$$

3. Local Stability Interior Equilibrium Point:$E^*(C^*, pH^*, A_l^*, D_0^*)$:

The characteristic equation corresponding to variational matrix about equilibrium point $E^*$is given by:

$$\lambda^4 + \lambda^3(Z_1 + Z_6 + Z_5 + g) + \lambda^2(n_1 d_1^2 D_0^* A_l^* + Z_1 Z_6 + (Z_5 + g)(Z_1 + Z_6) + Z_5 g - \gamma_1^2 D_0^* C^*) + \lambda(n_1 d_1^2 D_0^* A_l^*(Z_1 + g) + Z_5 g(Z_1 + Z_6) - \gamma_1 D_0^* C^*(\gamma_1(Z_5 + g + n_1 d_1 Z_3) + Z_1 Z_6(Z_5 + g)) + [g Z_1 Z_5 Z_6 - \gamma_1 C^* D_0^*\{Z_5 g\gamma_1 + n_1 d_1(Z_3 g + Z_2 Z_4)\} + n_1 d_1^2 Z_1 g D_0^* A_l^*] = 0, \tag{4.24}$$

where,

$$Z_1 = \frac{1}{\tau_c} + \gamma_1 D_0^*, \quad Z_2 = \frac{-pH_0}{(1 + C^*)^2}, \quad Z_3 = \frac{\alpha_1 a A_l^*}{\beta_0 + A_l^*}, \quad Z_4 = \frac{-\alpha_1 b A_l^*}{\beta_0 + A_l^*},$$

$$Z_5 = \frac{\alpha_1(1 + aC^* - b(pH^*))A_l^*}{(\beta_0 + A_l^*)^2}, \quad Z_6 = m_1 + n_1 d_1 A_l^* + \gamma_1 C^*.$$

By Routh's criteria, the interior equilibrium point shall be asymptotically stable only if the following conditions are satisfied:

$$n_1 d_1^2 D_0^* A_l^* + Z_1 Z_6 + (Z_5 + g)(Z_1 + Z_6) + Z_5 g > \gamma_1^2 D_0^* C^*, \tag{4.25}$$

$$n_1 d_1^2 D_0^* A_l^* (Z_1 + g) + Z_5 g(Z_1 + Z_6) + Z_1 Z_6 (Z_5 + g) > \gamma_1 D_0^* C^* (\gamma_1 (Z_5 + g) + n_1 d_1 Z_3), \tag{4.26}$$

$$g Z_1 Z_5 Z_6 + n_1 d_1^2 Z_1 g D_0^* A_l^* > \gamma_1 C^* D_0^* \{Z_5 g \gamma_1 + n_1 d_1 (Z_3 g + Z_2 Z_4)\}. \tag{4.27}$$

4.5 Global Stability

In this section, the following two theorems shall establish the global stability of the model given by equations (4.1)-(4.4):

Theorem 4.5.1. *The box B_r in the space (C, pH, A_l, D_0) is a compact and positive invariant set.*

Proof. Consider a box B_r in the space (C, pH, A_l, D_0). One vertex of the box is considered to be at origin and other at point $\varpi = (\tilde{C}, p\tilde{H}, \tilde{A}_l, \tilde{D}_0)$. The point ϖ shall lie outside the box B_r with $\tilde{C} > C_u, p\tilde{H} > pH_u, \tilde{A}_l > A_{lu}, \tilde{D}_0 > D_{0u}$.
Let us now consider the equations given by (4.1)-(4.4).
Now let,

$$\frac{d\nu}{dt} = \left(\frac{dC}{dt}, \frac{d(pH)}{dt}, \frac{dA_l}{dt}, \frac{dD_0}{dt}\right).$$

Now, let us compute the angle which the flow makes with each face of the box B_r not lying in the coordinate planes. Let σ_1,σ_2,σ_3,σ_4 be the outward unit normal vectors to the planes: $\phi_1 : C = \tilde{C}, \phi_2 : pH =$

$p\tilde{H}, \phi_3 : A_l = \tilde{A}_l, \phi_4 : D_0 = \tilde{D}_0$ for the box B_r. From equation (4.1) we obtain,

$$\sigma_1 \frac{d\nu}{dt}|\phi_1 = \left(C_E + \frac{C_0}{\tau_c}\right) - \frac{\tilde{C}}{\tau_c} - \gamma_1 D_0 \tilde{C},$$

$$\sigma_1 \frac{d\nu}{dt}|\phi_1 \leq \left(C_E + \frac{C_0}{\tau_c}\right) - \frac{C_u}{\tau_c} - \gamma_1 D_0 \tilde{C},$$

$$\sigma_1 \frac{d\nu}{dt}|\phi_1 \leq -\gamma_1 D_0 \tilde{C},$$

Hence,

$$\sigma_1 \frac{d\nu}{dt}|\phi_1 \leq 0.$$

Similarly,

$$\sigma_2 \frac{d\nu}{dt}|\phi_2 \leq 0 \quad \sigma_3 \frac{d\nu}{dt}|\phi_3 \leq 0, \quad \sigma_4 \frac{d\nu}{dt}|\phi_4 \leq 0.$$

Thus, it is proved that the trajectories of the system given by (4.1) - (4.4) will not cross B_r once they enter inside B_r. This completes the proof of theorem 4.5.1. □

Theorem 4.5.2. *The interior equilibrium E^* shall be globally asymptotically stable if the following five inequalities are satisfied:*

$$2\left(\frac{1}{\tau_c} + \gamma_1 D_0\right)(m_1 + n_1 d_1 A_l + \gamma_1 C^*) > 3(\gamma_1(C^* + D_0))^2,$$

$$4\left(\frac{1}{\tau_c} + \gamma_1 D_0\right)\left(\frac{\alpha_1(1 + aC^* - bpH^*)}{(\beta_0 + A_l)(\beta_0 + A_l^*)}\right) > 9\left(\frac{a\alpha_1}{\beta_0 + A_l}\right)^2,$$

$$2\left(\frac{\alpha_1(1 + aC^* - bpH^*)}{(\beta_0 + A_l)(\beta_0 + A_l^*)}\right)\left(\frac{g}{(1 + C)(1 + C^*)}\right) > 3\left(\frac{b\alpha_1}{\beta_0 + A_l}\right)^2,$$

$$2\left(\frac{\alpha_1(1 + aC^* - bpH^*)}{(\beta_0 + A_l)(\beta_0 + A_l^*)}\right)(m_1 + n_1 d_1 A_l + \gamma_1 C^*) > 3(n_1 d_1 D_0^* - d_1)^2,$$

$$2\left(\frac{1}{\tau_c} + \gamma_1 D_0\right) g > 3\left(\frac{pH_0}{(1 + C)(1 + C^*)}\right)^2.$$

Proof. Let us consider the following positive definite function:

$$Z = \frac{1}{2}(C - C^*)^2 + \frac{1}{2}(pH - pH^*)^2 + \left(A_l - A_l^* - A_l^* ln\frac{A_l}{A_l^*}\right) + \frac{1}{2}(D_0 - D_0^*)^2. \tag{4.28}$$

Differentiating the above equation w.r.t.'t' we get,

$$\frac{dZ}{dt} = -[b_{11}(C-C^*)^2+b_{22}(pH-pH^*)^2+b_{33}(A_l-A_l^*)^2+b_{44}(D_0-D_0^*)^2+$$
$$b_{14}(C-C^*)(D_0-D_0^*)+b_{12}(C-C^*)(pH-pH^*)+b_{13}(C-C^*)(A_l-A_l^*)$$
$$+b_{23}(pH-pH^*)(A_l-A_l^*)+b_{34}(A_l-A_l^*)(D_0-D_0^*)], \quad (4.29)$$

where $b_{11} = \frac{1}{\tau_c} + \gamma_1 D_0, \quad b_{22} = g, \quad b_{33} = \frac{\alpha_1(1+aC^*-bpH^*)}{(\beta_0+A_l)(\beta_0+A_l^*)}$
$b_{44} = m_1 + n_1 d_1 A_l + \gamma_1 C^*, b_{14} = \gamma_1(C^* + D_0),$
$b_{12} = \frac{pH_0}{(1+C)(1+C^*)}, \quad b_{13} = -\frac{a\alpha_1}{\beta_0+A_l}, \quad b_{23} = \frac{b\alpha_1}{\beta_0+A_l}, \quad b_{34} = n_1 d_1 D_0^* - d_1.$
By Sylvester's criteria, sufficient conditions for $\frac{dZ}{dt}$ to be negative definite are:

$$2b_{11}b_{44} > 3b_{14}^2, \quad 2b_{11}b_{22} > 3b_{12}^2, \quad 4b_{11}b_{33} > 9b_{13}^2,$$
$$2b_{22}b_{33} > 3b_{23}^2, \quad 2b_{33}b_{44} > 3b_{34}^2,$$

i.e.

$$2\left(\frac{1}{\tau_c} + \gamma_1 D_0\right)(m_1 + n_1 d_1 A_l + \gamma_1 C^*) > 3(\gamma_1(C^* + D_0))^2, \quad (4.30)$$

$$4\left(\frac{1}{\tau_c} + \gamma_1 D_0\right)\left(\frac{\alpha_1(1+aC^*-bpH^*)}{(\beta_0+A_l)(\beta_0+A_l^*)}\right) > 9\left(\frac{a\alpha_1}{\beta_0+A_l}\right)^2, \quad (4.31)$$

$$2\left(\frac{\alpha_1(1+aC^*-bpH^*)}{(\beta_0+A_l)(\beta_0+A_l^*)}\right)\left(\frac{g}{(1+C)(1+C^*)}\right) > 3\left(\frac{b\alpha_1}{\beta_0+A_l}\right)^2, \quad (4.32)$$

$$2\left(\frac{\alpha_1(1+aC^*-bpH^*)}{(\beta_0+A_l)(\beta_0+A_l^*)}\right)(m_1 + n_1 d_1 A_l + \gamma_1 C^*) > 3(n_1 d_1 D_0^* - d_1)^2, \quad (4.33)$$

$$2\left(\frac{1}{\tau_c} + \gamma_1 D_0\right) g > 3\left(\frac{pH_0}{(1+C)(1+C^*)}\right)^2. \quad (4.34)$$

This leads to completion of proof of theorem 4.5.2. □

4.6 Numerical Simulation and Discussion

The analytical results for the model equations given by (4.1)-(4.4) are supported by performing numerical simulations. Consider the following

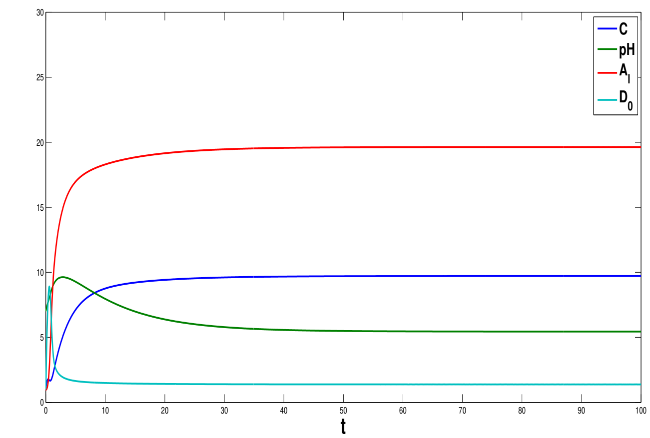

Figure 4.1: Trajectories of model w.r.t. time t showing stability behaviour of interior equilibrium E^*.

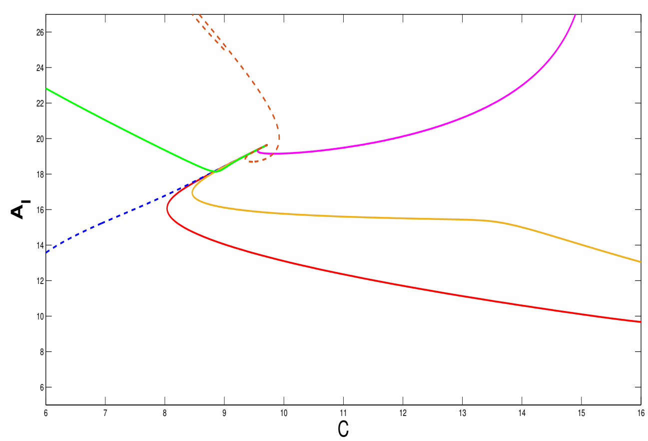

Figure 4.2: Phase plane graph for C and A_l for different initial values to show global stability behavior.

set of parameters for the interior equilibrium point $E^*(C^*, pH^*, A_l^*, D_0^*)$,

$$C_E = 4.7, C_0 = 6.6, \gamma_1 = 0.345, pH_0 = 7.0, g = 0.12, \alpha_1 = 0.412,$$
$$a = 0.85, b = 0.57, \beta_0 = 1.5, d_1 = 0.43, h = 0.715, q = 26.9,$$
$$m_1 = 0.3, n_1 = 1.87, \tau_c = 50. \quad (4.35)$$

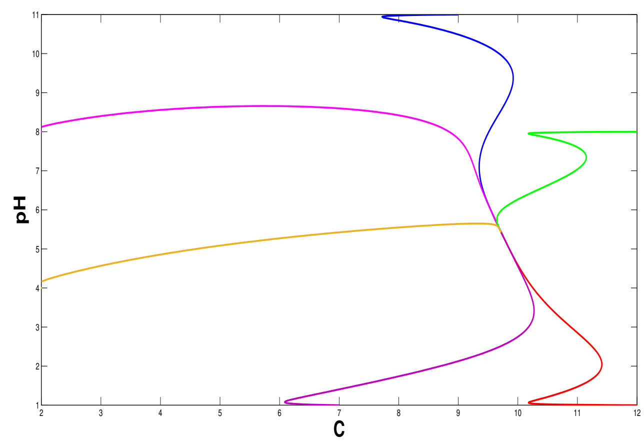

Figure 4.3: Phase plane graph for C and pH for different initial values to show global stability behavior.

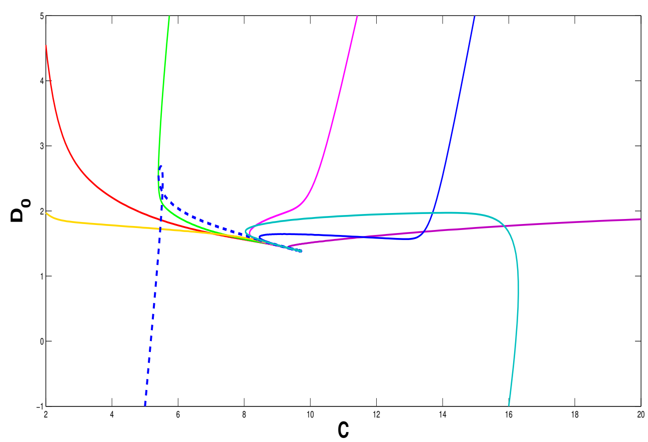

Figure 4.4: Phase plane graph for C and D_0 for different initial values to show global stability behavior.

For the above set of parametric values, the values of interior equilibrium $E^*(C^*, pH^*, A_l^*, D_0^*)$ are found to be E^* (9.7145, 5.4444, 19.6337, 1.3848). The interior equilibrium $E^*(C^*, pH^*, A_l^*, D_0^*)$ is found to be asymptotically stable as shown in fig. 4.1 and is satisfying the feasibility and stability conditions given by eqs. (4.15)-(4.16), (4.18), (4.25)-(4.27),

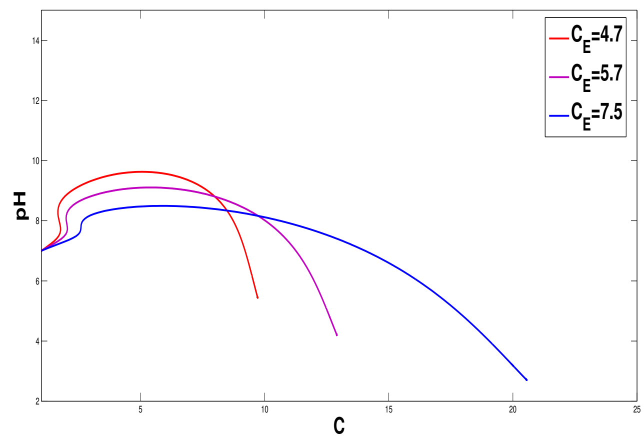

Figure 4.5: Graph of pH with C for different values of C_E

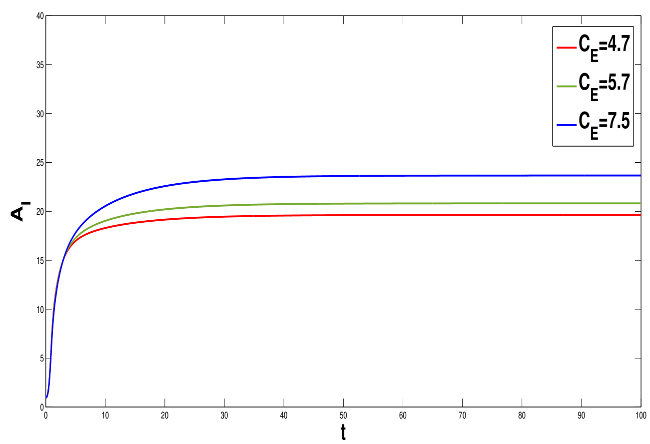

Figure 4.6: Graph of A_l with time t for different values of C_E

(4.30)-(4.34). It is also observed that E^* is globally stable for different initial values as shown in figs. 4.2, 4.3 and 4.4. With regard to the carbon vanishing equilibrium point $\breve{E}(0, p\breve{H}, \breve{A}_l, \breve{D}_0)$, for the parameter values satisfying eqs. (4.8), (4.20)-(4.21), the values of $\breve{E}(0, p\breve{H}, \breve{A}_l, \breve{D}_0)$ are found to be (0, 7.000, 18.463, 5.6188). With regard to the algal population vanishing equilibrium point $\hat{E}(\hat{C}, p\hat{H}, 0, \hat{D}_0)$, for the parameter

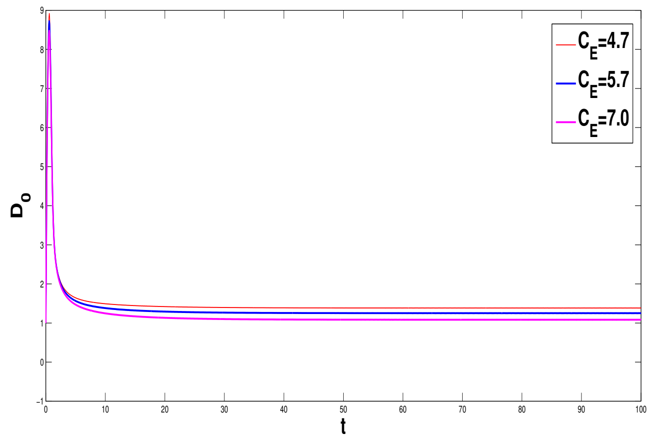

Figure 4.7: Graph of D_0 with time t for different values of C_E

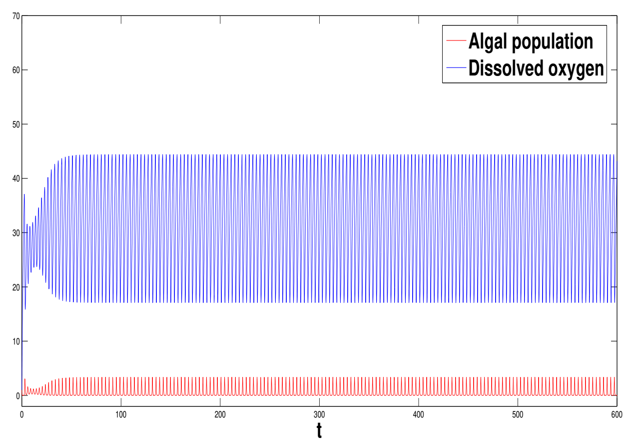

Figure 4.8: Graph showing limit cycles for A_l and D_0 for increase in parameter h.

values satisfying eq. (4.23), the values of $\hat{E}(\hat{C}, p\hat{H}, 0, \hat{D}_0)$ are found to be (10.2285, 5.1972, 0, 2.7433). From the stability analysis of interior equilibrium point E^*, it is observed that with the increase of rate of carbon input C_E in water, the pH level of water decreases as shown in fig. 4.5. Also, as the rate of carbon input C_E, increases from 0.715 to 7.5, the concentration of algal bloom increases as shown in fig. 4.6. Fur-

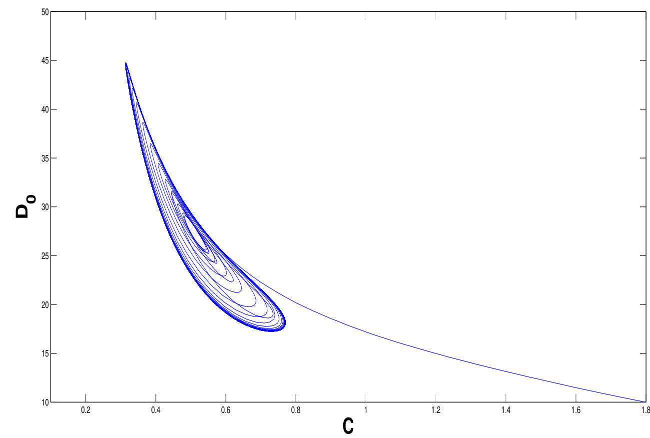

Figure 4.9: Graph showing limit cycles in $C - D_0$ plane for increase in h.

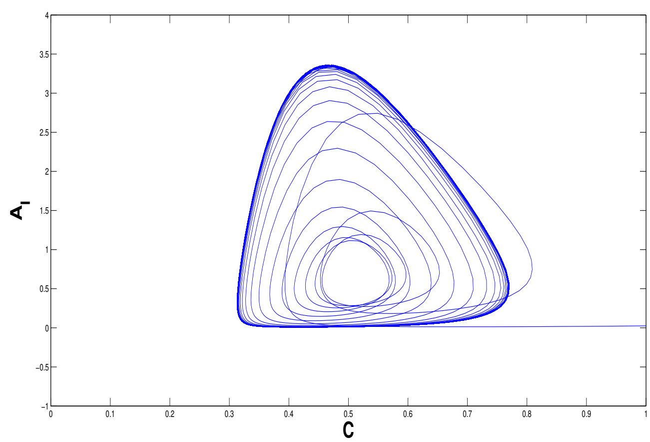

Figure 4.10: Graph showing limit cycles in $C - A_l$ plane for increase in h.

ther, with increased carbon input rate C_E in water, along with acidity and algal bloom growth, the temperature of water also increases due to elevated levels of global warming. Hence, dissolved oxygen decreases as shown in fig. 4.7. This is because of decreased oxygen solubility in warmer waters and more oxygen consumption in the reaction with carbon as well as its utilisation in the decomposition process of increased

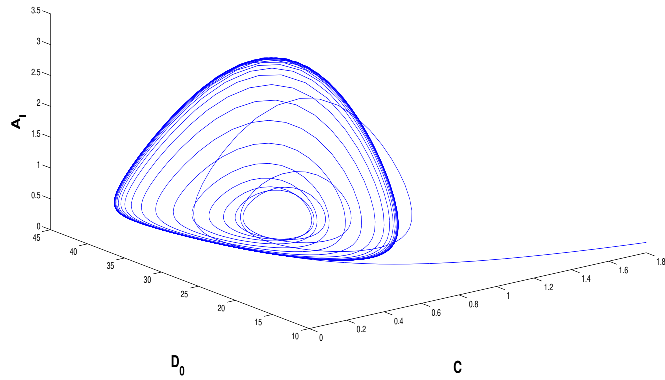

Figure 4.11: Graph of $D_0 - C - A_l$ for increase in h.

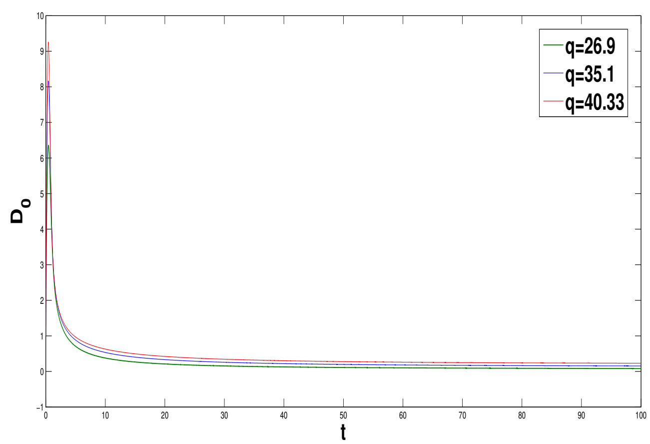

Figure 4.12: Graph of D_0 with time t for increasing value of q at C_E=22.0.

algal blooms. This is supported by study done by Sirota et al. [119]. Further, in the study conducted by Chakraborty et al. [118], under the single effect of agricultural pollution, the algal population existed at equilibrium value =19.62 and the corresponding oxygen concentration value was calculated to be 2.62. However, in our study, at the algal population existing at level =19.6337, the value of dissolved oxygen concentration is 1.3848 as given by eq. (4.35). The comparison of results with the study done by Chakraborty et al. [118] supports that under the combined effects of increased carbon emissions and acid in water, the oxygen level in water will decrease more rapidly than under the single effect of each factor. Moreover, since dissolved oxygen (DO) is an important resource for aquatic population to survive, hence its depletion may even lead to extinction of the aquatic population. It is also observed that as the value of natural decay rate of algal bloom (h) is increased from 0.715 to 8.893, while keeping the other model parameters same as given in eq. (4.35), the stable solutions of dissolved oxygen and algal population are transformed into oscillatory solutions as shown in fig.4.8. Thus, it is inferred that with increase in natural decay rate of algal bloom to h= 8.893 and above, the system bifurcates to a stable limit cycle periodic solution and Hopf bifurcations are observed as shown in figs. 4.9, 4.10, 4.11. It is also observed that if the rate of carbon input C_E is increased from 4.7 to 22.0, keeping all the other parameters same, then the dissolved oxygen tends towards a zero level. However, at this stage if the oxygen input rate q is increased to 35.1, then the dissolved oxygen starts increasing from zero level as shown in fig. 4.12. Henceforth, it is shown that for the dissolved oxygen to exist in the system, either the rate of carbon input C_E should be maintained below 22.0 or the input rate of dissolved oxygen should be increased from its threshold level i.e. q=35.1. Thus, it is concluded that the cumulative effect of factors like increasing acidity, global warming, decomposition of algal blooms, and direct discharge of carbon-rich pollutants in water have dire consequences for the oxygen-dependent aquatic population and hamper their growth and survival rate. Thus, it is imperative that for the existence of the aquatic population dependent on dissolved oxygen for their survival, the rate of carbon emissions should be controlled. Further, the discharge of input of acid and industrial wastes in water needs to be monitored and reduced. Otherwise, with the rising algal blooms and consequent decrease of dissolved oxygen in water, a situation of hypoxia can arise, which will ultimately lead to hazardous consequences such as growth impairments in aquatic population and fish kills[80, 94].

Chapter 5

Decline in Dissolved Oxygen Due to Increasing Temperature and Algal Blooms: Mathematical Model

5.1 Introduction

In recent times, the human activities are leading to a steep rise in the pollution and the carbon dioxide level in the environment. The marine environment is exposed to toxins, toxic chemicals, industrial wastes, etc. by their direct input in water. The presence of pollutants in water results in habitat degradation of aquatic species [47]. Increased fossil fuel burning, industrial pollutants etc. are some of the factors which lead to rise of carbon emissions in the environment [130]. The increased atmospheric carbon dioxide level contributes to global warming [131]. This increases the water temperature in different bodies of fresh water and marine water. Climate change also has a direct influence on an ecosystem's structure and functions. The way materials and energy flow in an environment is heavily influenced by climate change [132]. Under global warming, the species' metabolic rates are also changed [133].

Additional carbon dioxide level can further result in weak acidification of the water body [53] . Poor acidification in the marine environment has the potential to harm reproduction abilities in macrophytes in water and cause alterations in phytoplankton communities [134] . The rising acidity, contamination and rising water temperatures lead to an increased growth of algal blooms in the water bodies [135], [136]. Climate change is also found to have a significant impact on the frequency and abundance of algal blooms affecting the growth and habitat of the algal blooms. The growing algal blooms have negative affect on ecosystem functioning [78]. They also disturb the aquatic biodiversity and food chains [126]. It is seen that, due to pollutants present in the water bodies, not only the species are affected but the resource i.e. dissolved oxygen is also decreased. The oxygen levels in water fall with rise in algal growth [137]. Ocean warming caused by global climate change results in deoxygenation with negative consequences for ocean productivity and marine habitat. Ocean models predict declines of 1 to 7 percent over the next century in the global ocean oxygen stocks, with declines extending into the future for a thousand years or more [99]. The decline in dissolved oxygen due to global warming can lead to condition of hypoxia which may lead to death of various aquatic species dependent on oxygen for their survival. Increased acidity and global warming also lead to the loss of coral reefs ' biodiversity, which poses a threat to their dependent populations [138], [139]. Thus , due to the growing acidity and hypoxic conditions , aquatic species face difficulty in their growth and survival [140]. Various mathematical and experimental studies are available which support the decrease of dissolved oxygen due to global warming [141]. Also, certain mathematical studies study the effect of pollutants and acidification on aquatic ecosystem individually [118], [47], [109], [84]. But, a combined study which studies the effects of global warming and carbon emissions together in one mathematical model is not yet available.

In our study, we have formulated a mathematical model of non-linear differential equations to study the impact of global warming, increased carbon emissions and increased algal bloom growth on the level of dissolved oxygen in water. Threshold levels for maximum amount of carbon input the aquatic ecosystem can handle has been calculated, above which the carbon input increase can lead to condition of hypoxia having dreadful effects on aquatic populations like fishes. Also, threshold level of oxygen input has also been calculated required to sustain the aquatic life under increased carbon dioxide concentration and global warming. It has been found that under the effects of global warming and carbon dioxide increase in the atmosphere, the dissolved oxygen decreases which can have very harmful effects on the aquatic ecosystem.

5.2 Mathematical Model

It is assumed in the proposed mathematical model that due to increase of carbon dioxide concentration in the environment, the atmospheric temperature is increasing which is leading to warming of waters. Also, the water acidity is increasing due to the increasing carbon concentration. These factors are leading to increase in growth of algal blooms in the water bodies. The increasing algal blooms and water temperature further cause decline in the concentration of dissolved oxygen in water. Under these assumptions, let $\tau(t)$ be the average surface temperature, R(t) be the concentration of atmospheric carbon dioxide, $A_g(t)$ be the density of algal blooms and O(t) be the dissolved oxygen concentration in water.
The model is formulated as given below:

$$\frac{d\tau}{dt} = \phi(R - R_0) - \delta(\tau - \tau_0) \tag{5.1}$$

$$\frac{dR}{dt} = Q - \alpha R - \frac{hRA_g}{1 + aR} \tag{5.2}$$

$$\frac{dA_g}{dt} = \frac{hRA_g}{1 + aR} - \beta A_g \tag{5.3}$$

$$\frac{dO}{dt} = I - dA_gO - nO - d_3O\tau \tag{5.4}$$

with initial conditions $\tau(0) \geq 0, R(0) \geq 0, A_g(0) \geq 0, O(0) \geq 0, \tau \geq \tau_0, R \geq R_0$.

The model parameters are as given below:

ϕ is the growth rate coefficient corresponding to average surface temperature, δ is the coefficient of depletion of average surface temperature. R_0 is the level of carbon dioxide in absence of pollution and human activities. τ_0 is the average surface temperature in absence of rising carbon dioxide levels. Q is the rate of increase of carbon dioxide due to human activities. α is the natural depletion rate of carbon concentration. h gives the growth rate of algal blooms due to increasing carbon concentration in water and rising water acidity and a represents the proportionality constant. β is the natural death rate of algal blooms. I is the input rate of oxygen in water. d gives the depletion rate of dissolved oxygen due to decomposition process of algal blooms in water. n is the natural depletion rate of oxygen and d_3 gives the rate of decrease of dissolved oxygen concentration due to low solubility of oxygen in water due to global warming.

All model parameters are assumed to be positive constants.

5.3 Dynamical Behaviour

In order to carry out the analysis of the model given by equations (5.1)-(5.4), the dynamical behaviour of the mathematical model shall be studied in this section.

5.3.1 Boundedness and Positivity

In order to show the boundedness of the solutions of the model given by equations (5.1)-(5.4), the following lemma shall be proved.

Lemma 5.3.1. *All the solutions of the system of equations given by*

(5.1)-(5.4) lie in the region

$$\varpi_1 = \Big\{(\tau, R, A_g, O) \in R_+^4 : 0 \leq \tau_0 \leq \tau \leq \tau_M, 0 \leq R_0 \leq R \leq R_M,$$

$0 < O < O_M, 0 < R + A_g + O \leq W_{1M}$,*as* $t \to \infty$*, for all positive initial values* $(\tau(0), R(0), A_g(0), O(0)) \in R_+^4$*, where,*$\tau_M = \frac{\phi R_M + \delta\tau_0}{\delta}$*,* $R_M = \frac{Q}{\alpha}, O_M = \frac{I}{n}, W_{1M} = \frac{Q+I}{b_{11}}$*, where* $b_{11} = min(\alpha, \beta, n)$*.*

Proof. From equation (5.2) we get,

$$\frac{dR}{dt} \leq Q - \alpha R$$

then by usual comparison theorem, as $t \to \infty$,

$$\limsup_{t\to\infty}(R, t) \leq \frac{Q}{\alpha} = R_M$$

From equation (5.1) we get,

$$\frac{d\tau}{dt} + \delta\tau \leq \phi R_M + \delta\tau_0$$

By comparison theorem we get as $t \to \infty$,

$$\limsup_{t\to\infty}(\tau, t) \leq \frac{\phi R_M + \delta\tau_0}{\delta} = \tau_M$$

From equations (5.2)-(5.4),

$$\frac{d(R + A_g + O)}{dt} \leq Q + I - \alpha R - \beta A_g - nO$$

then by comparison theorem we get as $t \to \infty$,

$$\limsup_{t\to\infty}(R + A_g + O, t) \leq \frac{Q + I}{b_{11}} = W_{1M}$$

where b_{11}=min(α, β, n). From equation (5.4) we get,

$$\frac{dO}{dt} \leq I - nO.$$

By comparison theorem we get as $t \to \infty$,

$$\limsup_{t\to\infty}(O, t) \leq \frac{I}{n} = O_M.$$

□

In order to show the positivity of the solutions of the model given by equations (5.1)-(5.4), the following lemma shall be proved.

Lemma 5.3.2. *The solutions of the model given by equations (5.1)-(5.4),* $(\tau(t), R(t), A_g(t), O(t))$ *are positive for* $t > 0$*, for initial values:* $\tau(0) > 0, R(0) > 0, A_g(0) > 0, O(0) > 0$.

Proof. From equation (5.1),

$$\frac{d\tau}{dt} \geq -\delta\tau$$

$$\tau \geq k_1 e^{-\delta t}$$

where k_1 is an integration constant.
Thus, we have $\tau > 0$ for $t \to \infty$. From equation (5.2),

$$\frac{dR}{dt} \geq -(\alpha + hW_{1M})R$$

$$R \geq k_2 e^{-(\alpha + hW_{1M})t}$$

where k_2 is an integration constant.
Thus, we have $R > 0$ for $t \to \infty$. From equation (5.3),

$$\frac{dA_g}{dt} \geq -\beta A_g$$

$$A_g \geq k_3 e^{-\beta t}$$

where k_3 is an integration constant.
Thus, we have $A_g > 0$ for $t \to \infty$. From equation (5.4),

$$\frac{dO}{dt} \geq -(dW_{1M} + n + d_3\tau_M)O$$

$$O \geq k_4 e^{-(dW_{1M} + n + d_3\tau_M)t}$$

where k_4 is an integration constant.
Thus, we have $O > 0$ for $t \to \infty$. □

5.3.2 Equilibrium points

In this section, the feasible equilibria of the system given by equations (5.1)-(5.4) shall be calculated.

1. Boundary equilibrium $E_1(\hat{\tau}, 0, 0, \hat{O})$, where $\hat{R} = 0, \hat{A}_g = 0$ i.e. the carbon dioxide emissions and the algal population is taken as zero.

$$\hat{\tau} = \frac{\delta\tau_0 - \phi R_0}{\delta} \tag{5.5}$$

$$\hat{\tau} > 0 \;\; if \;\; \delta\tau_0 - \phi R_0 > 0 \tag{5.6}$$

$$\hat{O} = \frac{I}{n + d_3\hat{\tau}} \tag{5.7}$$

Since $\hat{\tau} > 0$, hence $\hat{O} > 0$.

2. Interior equilibrium $E_2(\tau^*, R^*, A_g^*, O^*)$, where ,

$$R^* = \frac{\beta}{h - a\beta} \tag{5.8}$$

$$R^* > 0 \quad if \quad h > a\beta \tag{5.9}$$

$$\tau^* = \frac{\phi(R^* - R_0) + \delta\tau_0}{\delta} \tag{5.10}$$

$$\tau^* > 0 \quad as \quad R^* \geq R_0$$

$$A_g^* = \frac{(Q - \alpha R^*)(1 + aR^*)}{hR^*} \tag{5.11}$$

$$A_g^* > 0 \quad if \quad Q > \alpha R^* \tag{5.12}$$

$$O^* = \frac{I}{dA_g^* + n + d_3\tau^*} \tag{5.13}$$

As $\tau^* > 0$, hence $O^* > 0$.

5.3.3 Local Stability

In this section we shall carry out the local stability analysis for the model given by equations (5.1)-(5.4).

i. **Local Stability of Boundary Equilibrium Point E_1:** For the variational matrix associated with the boundary equilibrium E_1 , the characteristic equation is given by

$$(-\frac{I}{\hat{O}} - \lambda)(-\delta - \lambda)(-\alpha - \lambda)(-\beta - \lambda) = 0 \tag{5.14}$$

$$\lambda_1 = -\frac{I}{\hat{O}},\ \ \lambda_2 = -\delta,\ \ \lambda_3 = -\alpha,\ \ \lambda_4 = -\beta \tag{5.15}$$

The nature of roots of the equation (5.14) shows that the equilibrium point E_1 is asymptotically stable.

ii. **Local Stability of Interior Equilibrium Point E_2:** For the variational matrix associated with the interior equilibrium E_2, the characteristic equation is given by

$$(-\frac{I}{O^*} - \lambda)(-\delta - \lambda)(\lambda^2 - Z_1\lambda + Z_2 Z_3) = 0 \tag{5.16}$$

where

$$Z_1 = -\alpha - hA_g^* + \frac{haA_g^* R^*}{(1 + aR^*)^2},\ \ Z_2 = \frac{hR^*}{1 + aR^*},$$

$$Z_3 = \frac{hA_g^*}{1 + aR^*} - \frac{haA_g^* R^*}{(1 + aR^*)^2}.$$

We get,

$$\lambda_1 = -\frac{I}{O^*},\ \ \lambda_2 = -\delta \tag{5.17}$$

Using Routh's criteria, the equilibrium point E_2 is stable only if the following is satisfied,

$$\alpha + hA_g^* > \frac{haA_g^* R^*}{(1 + aR^*)^2} \tag{5.18}$$

$$\frac{aR^*}{1 + aR^*} < 1 \tag{5.19}$$

5.3.4 Global Stability

In this section, for the model given by equations (5.1)-(5.4), we shall study the global stability behaviour about the interior equilibrium E_2 .

Theorem 5.3.1. *The box ϖ_1 in the space (τ, R, A_g, O) is compact and positive invariant.*

Proof. Consider a box ϖ_1 in space $\tau, R, A_g, O)$. One vertex of the box is considered to be at origin and the other vertex at $V = (\tau', R', A'_g, O')$. Also, consider $\tau' > \tau, R' > R, A'_g > A_g$ and $O' > O$. For calculating the angle of flow that is made with each face of ϖ_1 not lying in coordinate planes, let ρ_1, ρ_2, ρ_3 and ρ_4 be the outward unit normal vectors to planes $G_1 : \tau = \tau', G_2 : R = R', G_3 : A_g = A'_g$ and $G_4 : O = O'$.
We get from equation (5.4),

$$\rho_{44}\frac{dV}{dt}|G_4 \leq I - nO' - d_3O'\tau_0,$$

since $O' > \frac{I}{n}$,

$$\rho_4\frac{dV}{dt}|G_4 \leq -d_3O'\tau_0,$$

hence

$$\rho_4\frac{dV}{dt}|G_4 \leq 0.$$

Similarly,

$$\rho_1\frac{dV}{dt}|G_1 \leq 0, \quad \rho_2\frac{dV}{dt}|G_2 \leq 0, \quad \rho_3\frac{dV}{dt}|G_3 \leq 0.$$

Hence,ϖ_1 is the region of attraction for model given by equations (5.1)-(5.4).

□

Theorem 5.3.2. *The following inequalities should hold for the model given by the system of equations (5.1)-(5.4) to be globally stable.*

$$\delta\left(\alpha + \frac{hA^*_g}{(1 + aR^*)(1 + aR)}\right) > \phi^2,$$

$$\left(\alpha + \frac{hA_g^*}{(1+aR^*)(1+aR)}\right)\left(\beta - \frac{hR}{1+aR}\right) >$$
$$\left(\frac{hR}{1+aR} - \frac{hA_g^*}{(1+aR^*)(1+aR)}\right)^2,$$
$$\left(\beta - \frac{hR}{1+aR}\right)(dA_g + n + d_3\tau) > (dO^*)^2,$$
$$\delta(dA_g + n + d_3\tau) > (d_3O^*)^2.$$

Proof. Consider a positive definite function,

$$Z = \frac{1}{2}(\tau - \tau^*)^2 + \frac{1}{2}(R - R^*)^2 + \frac{1}{2}(A_g - A_g^*)^2 + \frac{1}{2}(O - O^*)^2.$$

Differentiating w.r.t. t we get,

$$\frac{dZ}{dt} = -[b_{11}(\tau - \tau^*)^2 + b_{22}(R - R^*)^2 + b_{33}(A_g - A_g^*)^2 + b_{44}(O - O^*)^2 + b_{12}(\tau - \tau^*)(R - R^*) + b_{14}(\tau - \tau^*)(O - O^*) + b_{23}(R - R^*)(A_g - A_g^*) + b_{34}(A_g - A_g^*)(O - O^*)] \quad (5.20)$$

where, $b_{11} = \delta,\ b_{22} = \alpha + \frac{hA_g^*}{(1+aR^*)(1+aR)},\ b_{33} = \beta - \frac{hR}{1+aR},\ b_{14} = d_3O^*,$ $b_{34} = dO^*, b_{44} = dA_g + n + d_3\tau,\ b_{12} = -\phi,\ b_{23} = \frac{hR}{1+aR} - \frac{hA_g^*}{(1+aR^*)(1+aR)}.$
Using Sylvester's criteria we get,

$$b_{11}b_{22} > b_{12}^2,\ b_{22}b_{33} > b_{23}^2,\ b_{33}b_{44} > b_{34}^2,\ b_{11}b_{44} > b_{14}^2.$$

Hence,the system of equations (5.1)-(5.4) shall be globally stable if the following are satisfied,

$$\delta\left(\alpha + \frac{hA_g^*}{(1+aR^*)(1+aR)}\right) > \phi^2, \quad (5.21)$$

$$\left(\alpha + \frac{hA_g^*}{(1+aR^*)(1+aR)}\right)\left(\beta - \frac{hR}{1+aR}\right) > \left(\frac{hR}{1+aR} - \frac{hA_g^*}{(1+aR^*)(1+aR)}\right)^2, \quad (5.22)$$

$$\left(\beta - \frac{hR}{1+aR}\right)(dA_g + n + d_3\tau) > (dO^*)^2, \tag{5.23}$$

$$\delta(dA_g + n + d_3\tau) > (d_3O^*)^2. \tag{5.24}$$

□

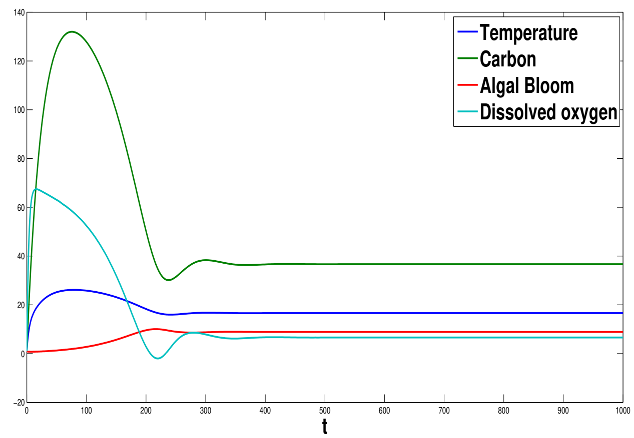

Figure 5.1: Local stability behaviour at Interior equilibrium

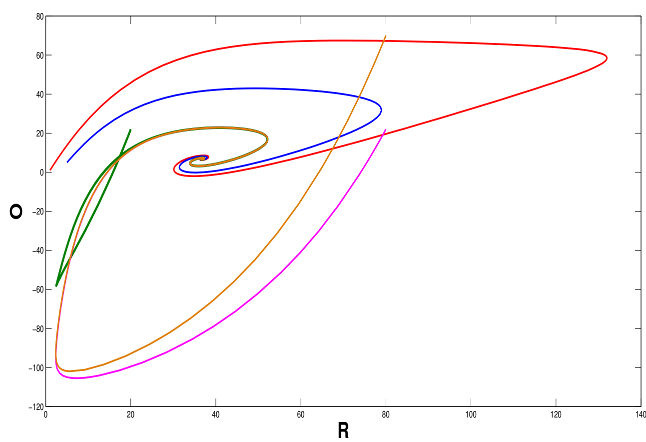

Figure 5.2: Global stability behaviour at interior equilibrium point

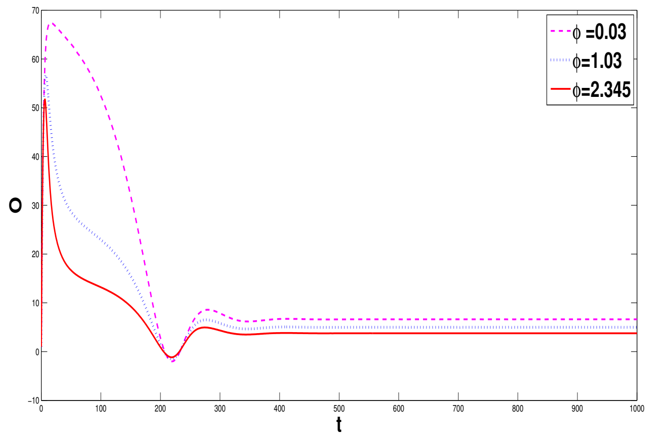

Figure 5.3: Decrease in dissolved oxygen with increasing global warming

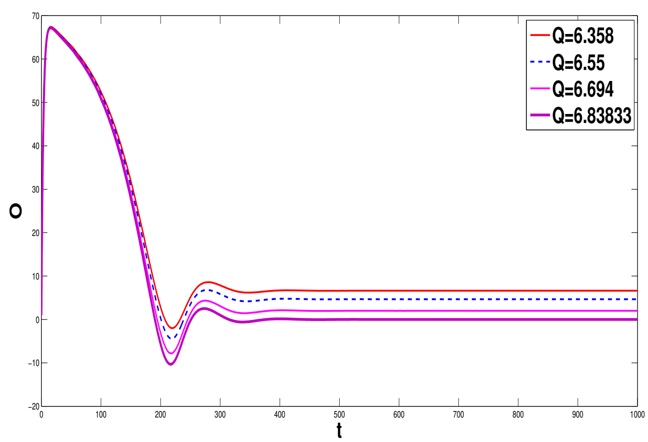

Figure 5.4: Decrease in dissolved oxygen with increasing carbon dioxide

5.4 Numerical Example

For the equations given in (5.1)-(5.4), we shall consider the values of parameters as given below:

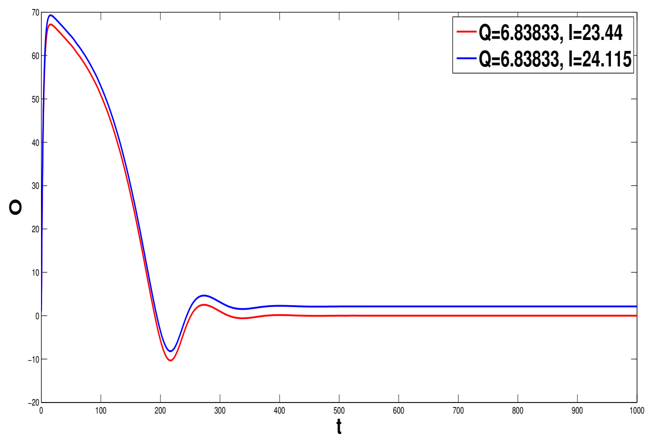

Figure 5.5: Graph for threshold value of dissolved oxygen

$$\phi = 0.03, \delta = 0.3, R_0 = 5.5, \tau_0 = 13.5, \alpha = 0.04,\ h = 0.4, a = 0.7,$$
$$\beta = 0.55, I = 23.44, d = 0.6, n = 0.3, Q = 6.358, d_3 = 0.001. \quad (5.25)$$

With these values of parameters given by equation (5.25), the following values of variables at interior equilibrium point $E_2(\tau^*, R^*, A_g^*, O^*)$ are obtained,
$\tau^* = 16.6167,\ R^* = 36.6667,\ A_g^* = 8.8933,\ O^* = 6.6193.$
For the above mentioned set of values of parameters given by equation (5.25), the conditions of stability given by equations (5.18)-(5.19), (5.21) - (5.24) are satisfied. Therefore, the interior equilibrium E_2 is stable. The same is supported by figure 5.1. Also, the dissolved oxygen equilibrium value is similar to the threshold level of dissolved oxygen concentration in fresh water bodies [98].

5.5 Conclusion

From the stability analysis of the model given by equations (5.1)-(5.4), it is concluded that the feasibility and stability conditions at interior equilibrium E_2 given by (5.9),(5.12), (5.18) - (5.19), (5.21) - (5.24) are satisfied for the values of parameters given by equation (5.25). E_2 is found to be locally stable as shown in figure 5.1. Also, the interior equilibrium point is globally stable as shown in figure 5.2. The dissolved oxygen concentration decreases with rise in global warming as shown in figure 5.3. This is also supported by equation(5.13). With the increase in carbon dioxide concentration, the dissolved oxygen level decreases as supported by equation(5.13) and shown in figure 5.4. It is also observed that if the value of carbon input increases more than Q=6.694, value of dissolved oxygen drops below 2.00. Thus, a condition of hypoxia arises which can be detrimental for the aquatic population. Also, at value of carbon input Q=6.83833, the dissolved oxygen level decreases to zero which can lead to fish kills. Hence, we get a threshold level for carbon input, above which the survival of species in an aquatic ecosystem is not possible. It is also shown that Q=6.83833, if the value of dissolved oxygen input is maintained above I= 24.115, the dissolved oxygen level again starts to increase. This is shown in figure 5.5. Thus, for the survival of aquatic species under the carbon input(Q) greater than 6.83833, the dissolved oxygen input in water has to be maintained above I=24.115. Thus, it is concluded from our study that the rising global warming and carbon dioxide levels in atmosphere greatly decrease the dissolved oxygen level in water, thus, harming the aquatic ecosystem.

Chapter 6

Mathematical Study on Simultaneous Effects of Rising Plastic Waste, Global Warming and Eutrophication on Aquatic Ecosystem

6.1 Introduction

As the whole world battles the unprecedented times due to pandemic COVID-19 which has caused disruptions in the lives of people worldwide, its impending repercussions on the environment and the aquatic ecosystem is also causing a flurry of concern among the environmentalists. The outspread of COVID-19 has skyrocketed the demand of gloves, face masks, personal protective equipment, body bags, plastic face shield etc., most of which are designed from single-use plastic. As these supplies are essential to battle the health crisis, increasing their production is seen as the focus of all the governments worldwide. However, no proper strategies and procedural guidelines for their recycling and disposal are being developed. As a result, it is expected that inadvertent disposal of these plastic items by people could add to the already existing environmental hazard of plastic pollution, an issue which has been left to simmer on the backburner for past long time. Since plastic items are becoming an indispensable and addictive part of human lifestyle, the pollution caused by it as landfills and accumulation in water bodies is also surging day-by-day having dire consequences for the environment. A report from the Ellen MacArthur Foundation developed with the World Economic Forum as a partner [143], has estimated that by year 2050, the amount of plastics in the oceans shall outweigh the fish populations. The swelling plastic waste is having precarious out-turns for the residing populations in the aquatic bodies [144]. The plastic particles are entering the aquatic food webs due to their consumption by the aquatic biota which is hampering the growth patterns, reproduction and life cycles of these species [145, 146, 147]. The burden of plastic pollution is also intensifying the already existing problem of global warming. The heat uptake by the oceans has shown a two times increase in the heat uptake[25]. The rising temperatures are causing loss to biodiversity of ecosystems and the organisms [148, 27]. Upon degradation, plastic releases gases such as methane and ethylene which further increases global warming [149, 150]. If the rate of production of plastics continues in the same way, then by 2050, Global Greenhouse Gases emissions due to plastic would touch a figure of 15 percent of the global carbon budget, [151] which shall further contribute towards global warming.

Though lockdowns imposed to combat the spread of COVID-19, have temporarily cut-down on the carbon emissions but experts believe this should not be taken as the slowing of climate change [152]. Along with this, the human-induced activities due to rapid industrialization and urbanization which were contributing towards the soaring carbon emissions in atmosphere will further give way to atmospheric temperature increase once the health crisis ends and the situation resumes towards normal [153]. A recent data released by the United States National Oceanic and Atmospheric Association (NOAA) [154] exhibits that global carbon dioxide levels are sharply rising.

The uptake of carbon dioxide by the ocean and land carbon sinks has increased manifold in the last 50 years [142]. Further the carbon dioxide when absorbed by the water bodies, reacts with the dissolved oxygen, forms carbonic acid [94], and increases the acidity level of water which is expected to be more severe in the coming times [155] which is bound to have devastating effects on the species [134, 156]. The acidity of water is also increased by eutrophication process [157, 158, 159], which is caused by the input of rich nutrients into the water bodies, mostly as agricultural run-off [118]. The acidic waters can prove harmful for the health and development of residing populations and their biodiversity [56, 75]. The eutrophic waters and the increased acidity levels further promote the growth of Harmful Algal Blooms in water [6]. Warming waters have also led to expansion of algal growth in oceans [80]. These algal blooms, when present in large concentrations, prove detrimental to the survival of aquatic species because their decomposition process utilises the dissolved oxygen in the water body and leads to oxygen scarcity which may lead to hypoxia, or in worst cases, anoxia also [82]. The plastic particles also hinder with the photosynthesis process of the algal population and pose problems for their growth [160, 161]. Thus, mortality rate of algal bloom is increased due to plastic, thus having a direct negative impact on the concentration of dissolved oxygen due to its consumption in the algal decomposition. Furthermore, due to the climatic changes, the water temperature is also witnessing a rise and it has been found that warmer waters are beneficial for the growth of algal bloom and are weaker in holding dissolved oxygen. Thus, the global warming is catastrophically steering the aquatic ecosystems towards low dissolved oxygen concentrations.

The global content of oxygen has decreased over the past five decades and a decline of one percent to seven percent in the global oxygen inventory is predicted by the ocean models [103]. Dissolved oxygen is a predominant resource for the existence of the aquatic species. Climate changes, acidification, eutrophication, and hypoxia play an interactive role to reduce the viability and growth of aquatic organisms such as certain fishes especially affecting their early-life stages [26, 1] and adversely affect the ecosystem [78, 17, 102, 81]. These phenomena are also leading to loss of life, biodiversity, and habitat for various aquatic species. In some cases, it can cause the collapse of the food webs, which play a key role in benthic community structuring [126].

Several researchers have attempted to study the effect of pollution, eutrophication and global warming on the populations by developing mathematical studies [162, 31, 86, 2, 163, 92, 164]. Bharathi A.T. et al. [108] have studied the combined impacts of acid and metal concentration in water on the survival of resource-based aquatic population under nutrient recycling. Shukla et. al. [32] gave a mathematical model to study the effect of growing anthropogenic carbon emissions and resulting temperature increase on the level of sea water and cautioned that the sea level rise due to melting of ice sheets in globally-warmed environment shall cause survival problems for the human population. Sekerci and Petrovskii [141] , in their mathematical study reinforced the fact that the global warming causes decrease in the dissolved oxygen level by obstructing the process of algal photosynthesis. Shukla et al. [84] proposed a mathematical model to study the reduction in dissolved oxygen caused by growth of algal bloom population in water wherein the algal growth rate is governed by the Holling type-II functional response of the nutrient concentration in water. However, Misra A.K. [165] enhanced this mathematical model in his study and replaced the Holling-type -II functional response by a more suited Holling-type-III functional response for depicting the interaction between algal population and the nutrients. Several other researchers have also used Holling-type-III functional response in their studies to analyse the interactions between various species [157]. H However, in all the available mathematical studies, mostly the individual effect of the environment stressors is studied but the effect of simultaneous occurrence of all the salient environmental stresses such as plastic pollution, global warming, eutrophication and

their cumulative consequences for the dissolved oxygen concentration have still not been explored.
In view of the same, in this chapter, we propose a mathematical study to analyse the effects of the simultaneous occurrence of pollution, plastic wastes, acidification, algal bloom growth and global warming on the concentration of dissolved oxygen in water. The model variables and parameters are explained in the next section.

6.2 Mathematical Model-I

In our mathematical model-I, it is assumed that rising greenhouse gases in the atmosphere and the accumulating plastic wastes in water bodies are leading to global warming which is increasing the water temperature. In addition to this the carbon emissions and eutrophication are increasing the acidity of water. Warmer, acidic, and eutrophic waters, in turn, promote the growth of algal bloom population in water. These all factors, especially warming waters and inflating algal population density, when operate together in an aquatic ecosystem, lead to decline in the concentration of dissolved oxygen in water. Reduction in dissolved oxygen further leads to condition of hypoxia, which can be harmful for survival of aquatic biota.
In view of the assumptions, let P_l denote the concentration of plastic waste in water body and G denote the concentration of greenhouse gases in the atmosphere. Let n represents the concentration of nutrients entering the water body leading to eutrophication and algal bloom growth. a represents the density of algal population. T represents the average surface temperature and O denotes the concentration of dissolved oxygen in water. The algal-nutrient concentration is assumed to be governed by a Holling type-III functional response.
Certain considerations comprising the model propsoed are given as following:
1. The term I_{11} represents the increase in greenhouse gases due to

degradation process of plastics [149, 150].
2. Growth rate of algal bloom which is assumed to be a resultant of rise of nutrient concentration in water is represented by $\frac{\theta_{11}\beta_{11}n^2a}{\mu_0^2+n^2}$. This interaction is assumed to follow a Holling type-III functional response [165].
3. $\mu_{11}(G-G_0)$ represents the growth of temperature due to increase in greenhouse gases concentrations in atmosphere.
4. The term $K_r\gamma_1^{\left(\frac{T-T_r}{10}\right)}O$ represents the rate of degradation of plastic which lowers the dissolved oxygen concentration in water through direct and indirect effects [166].
5. The term $\alpha_4 aO$ represents the consumption of dissolved oxygen in the decomposition process of algal population, which may lead to hypoxic conditions under aggravated risen algal concentrations [82].
Incorporating the variables and assumptions stated above the **mathematical model-I** consisting of differential equations is formulated as given below:

$$\frac{dP_l}{dt} = Q_1 - \alpha_1 P_l \tag{6.1}$$

$$\frac{dG}{dt} = I_1 - \alpha_2 G \tag{6.2}$$

$$\frac{dn}{dt} = q_0 - \alpha_{10}n - \frac{\beta_{11}n^2a}{\mu_0^2+n^2} \tag{6.3}$$

$$\frac{da}{dt} = \frac{\theta_{11}\beta_{11}n^2a}{\mu_0^2+n^2} - \psi_1 a - \psi_2 a^2 \tag{6.4}$$

$$\frac{dT}{dt} = \mu_{11}(G-G_0) - \mu_{12}(T-T_0) \tag{6.5}$$

$$\frac{dO}{dt} = R - K_r\gamma_1^{\left(\frac{T-T_r}{10}\right)}O + \alpha_5 a - \psi_3 O \tag{6.6}$$

where $I_1 = I_{10} + I_{11}P_l, \psi_1 = \psi_0 + \theta_{12}P_l$ and $\psi_3 = \alpha_3 + \alpha_4 a$
with initial conditions as given below:
$P_l(0) \geq 0, G(0) > 0, n(0) > 0, a(0) \geq 0, T \geq 0, O \geq 0, T \geq T_0,\ G \geq G_0$ and $T \geq T_r$.
The description of the parameters of the mathematical model are given in Table 6.1.
All parameters are assumed to be positive constants.

6.3 Model Analysis

In this section, we study the various stationary solutions (equilibria) of the mathematical model-I and examine the system given by equations (6.1)-(6.6) for boundedness and positivity of the solutions.

6.3.1 Boundedness and Positivity of Solutions

Theorem 6.3.1. *All the solutions of the mathematical model-I denoted by equations (6.1)-(6.6) are lying in the region given by* $\varpi = \{(P_l, G, n, a, T, O) \in R_+^6 :\ 0 < P_l < P_{lu}, 0 < G < G_u, 0 < n < n_u, 0 < a < a_u, T_l < T < T_u, T_l > 0, 0 < O < O_u\}$ *for positive initial values* $(P_l(0), G(0), n(0), a(0), T(0), O(0)) \in R_+^6$ *as* $t \to \infty$. *where* $P_{lu} = \frac{Q_1}{\alpha_1}, G_u = \frac{I_{10}+I_{11}P_{lu}}{\alpha_2}, n_u = \frac{q_0}{\alpha_{10}}, a_u = \frac{\theta_{11}\beta_{11}}{\psi_2}, T_u = \frac{\mu_{11}G_u+\mu_{12}T_0}{\mu_{12}}, T_l = \frac{\mu_{11}(G-G_0)}{\mu_{12}}$,
$O_u = \frac{R+\alpha_5 a_u}{\alpha_3}$.

Proof. From equation (6.1) we get,

$$\limsup_{t\to\infty}(P_l, t) \leq \frac{Q_1}{\alpha_1} = P_{lu}.$$

From equation (6.2) we have,

$$\limsup_{t\to\infty}(G, t) \leq \frac{I_{10} + I_{11}P_{lu}}{\alpha_2} = G_u.$$

Table 6.1: Description of Model Parameters.

Parameter	Description
Q_1	Input rate of plastic in water body
α_1	Decay and sedimentation rate of plastic
I_{10}	Emission rate of greenhouse gases due to anthropogenic activities
I_{11}	Increase in greenhouse gases due to degradation of plastic particles
α_2	Natural depletion rate of greenhouse gases
q_0	Rate of inflow of nutrients due to agricultural run-off or domestic drainage
α_{10}	Rate of natural loss of nutrients
β_{11}	Proportionality constant
μ_0	Half-saturation constant
θ_{11}	Fractional proportionality constant
θ_{12}	Rate of decrease of algal growth due to reduced photosynthesis by plastics
ψ_0	Natural mortality rate of algal population
ψ_2	Depletion rate of algal population due to crowding
μ_{11}	Rate of increase of water temperature due to rise in greenhouse gases
μ_{12}	Coefficient of surface heat transfer
G_0	Threshold value for greenhouse gases above which temperature will rise due to global warming
T_0	Temperature of environment
R	Input rate of oxygen in water
K_r	Constant of reaction rate under specific temperature T_r
γ_1	Coefficient demonstrating rate of reaction increase if temperature rises by 10 degrees Celsius
T_r	Reference Temperature
α_5	Rate of increase in oxygen concentration due to algal photosynthesis
α_4	Proportionality constant
α_3	Coefficient for rate of natural loss of oxygen

Equation (6.3) gives the following,

$$\lim_{t\to\infty}\sup(n,t) \leq \frac{q_0}{\alpha_{10}} = n_u.$$

Similarly from equation (6.4),(6.5) and (6.6) the following expressions are obtained respectively,

$$\lim_{t\to\infty}\inf(T,t) \geq \frac{\mu_{11}(G-G_0)}{\mu_{12}} = T_l,$$

$$\lim_{t\to\infty}\sup(a,t) \leq \frac{\theta_{11}\beta_{11}}{\psi_2} = a_u,$$

$$\lim_{t\to\infty}\sup(T,t) \leq \frac{\mu_{11}G_u + \mu_{12}T_0}{\mu_{12}} = T_u,$$

$$\lim_{t\to\infty}\sup(O,t) \leq \frac{R+\alpha_5 a_u}{\alpha_3} = O_u.$$

This completes the proof of the theorem 6.3.1. □

Theorem 6.3.2. *All the solutions of the system of equations denoted by equations (6.1)-(6.6) exhibit positivity for all time $t \geq 0$ for positive initial conditions.*

Proof. We have from equation (6.1),

$$\frac{dP_l}{dt} \geq -\alpha_1 P_l,$$

$$P_l \geq h_1 e^{-\alpha_1 t},$$

where h_1 denotes the integration constant. Hence, $P_l \geq 0$ for all time $t \geq 0$. Similarly from equations (6.2),(6.3),(6.4),(6.5) and (6.6), the following can be deduced,

$$G \geq h_2 e^{-\alpha_2 t},$$

$$n \geq h_3 e^{-(\alpha_{10}+\beta_{11}n_u a_u)t},$$

$$a \geq h_4 e^{-(\theta_{12}P_{lu}+\psi_0+\psi_2 a_u)t}$$

$$T \geq \frac{-\mu_{11}G_0}{\mu_{12}} + \left(T(0) + \frac{\mu_{11}G_0}{\mu_{12}}\right)e^{-\mu_{12}t},$$

$$O \geq h_5 e^{-\left(K_r \gamma_1^{\left(\frac{T_u - T_r}{10}\right)} + \alpha_4 a_u + \alpha_3\right)t},$$

where h_2, h_3, h_4 and h_5 are integration constants.
Hence, we get $G \geq 0, n \geq 0, a \geq 0, T \geq 0$ and $O \geq 0$, for all times $t > 0$, which leads to the completion of the proof of theorem 6.3.2. □

6.3.2 Equilibrium points

The system given by equations (6.1)-(6.6) has the below given three equilibrium points:

1. Algal Vanishing Boundary Equilibrium Point
$\hat{E}(\hat{P}_l, \hat{G}, \hat{n}, 0, \hat{T}, \hat{O})$:
From the system given by equations (6.1)-(6.6) we get,

$$\hat{P}_l = \frac{Q_1}{\alpha_1}, \tag{6.7}$$

$$\hat{G} = \frac{I_{10} + I_{11}\hat{P}_l}{\alpha_2}, \tag{6.8}$$

$$\hat{T} = \frac{\mu_{11}(\hat{G} - G_0) + \mu_{12}T_0}{\mu_{12}}, \tag{6.9}$$

$$\hat{n} = \frac{q_0}{\alpha_{10}}, \tag{6.10}$$

$$\hat{O} = \frac{R}{K_r \gamma_1^{\left(\frac{\hat{T} - T_r}{10}\right)} + \alpha_3}. \tag{6.11}$$

2. Plastic Vanishing Boundary Equilibrium Point
$\tilde{E}(0, \tilde{G}, \tilde{n}, \tilde{a}, \tilde{T}, \tilde{O})$:
From the system given by equations (6.1)-(6.6) we get,

$$\tilde{G} = \frac{I_{10}}{\alpha_2}, \tag{6.12}$$

$$\tilde{T} = \frac{\mu_{11}(\tilde{G} - G_0) + \mu_{12}T_0}{\mu_{12}}, \tag{6.13}$$

$$\tilde{n} = \frac{q_0}{\alpha_{10}} - \left(\frac{\psi_0 \tilde{a} + \psi_2 \tilde{a}^2}{\alpha_{10}\theta_{11}}\right), \tag{6.14}$$

$\tilde{n} > 0$ if,

$$\frac{q_0}{\alpha_{10}} > \left(\frac{\psi_0\tilde{a} + \psi_2\tilde{a}^2}{\alpha_{10}\theta_{11}}\right), \tag{6.15}$$

$$\tilde{O} = \frac{R + \alpha_5\tilde{a}}{K_r\gamma_1^{\left(\frac{\tilde{T}-T_r}{10}\right)} + \alpha_3 + \alpha_4\tilde{a}}. \tag{6.16}$$

$\tilde{a}$ is given by the positive root of the equation:

$$B_1\tilde{a}^5 + B_2\tilde{a}^4 + B_3\tilde{a}^3 + B_4\tilde{a}^2 + B_5\tilde{a} + B_6 = 0, \tag{6.17}$$

where

$$B_1 = \psi_2^3, \quad B_2 = 3\psi_0\psi_2^2 - \theta_{11}\beta_{11}\psi_2^2,$$

$$B_3 = 3\psi_0^2\psi_2 - 2\theta_{11}q\psi_2^2 - 2\psi_0\psi_2\theta_{11}\beta_{11},$$

$$B_4 = \psi_0^3 - 4\theta_{11}q\psi_0\psi_2 - \psi_0^2\theta_{11}\beta_{11} + 2\theta_{11}^2\beta_{11}q\psi_2,$$

$$B_5 = \mu_0^2\alpha_{10}^2\theta_{11}^2\psi_2 + \theta_{11}^2q^2\psi_2 + 2\theta_{11}^2\beta_{11}q\psi_0 - 2\theta_{11}q\psi_0^2,$$

$$B_6 = \psi_0\mu_0^2\alpha_{10}^2\theta_{11}^2 + \psi_0\theta_{11}^2q^2 - \theta_{11}^3\beta_{11}q^2.$$

The equation (6.17) has at least one positive root if the following condition is satisfied:

$$3\psi_0 < \beta_{11}\theta_{11}. \tag{6.18}$$

3. Interior Equilibrium Point $E^*(P_l^*, G^*, n^*, a^*, T^*, O^*)$:
From the system given by equations (6.1)-(6.6) we get,

$$P_l^* = \frac{Q}{\alpha_1}, \tag{6.19}$$

$$G^* = \frac{I_{10} + I_{11}P_l^*}{\alpha_2}, \tag{6.20}$$

$$T^* = \frac{\mu_{11}(G^* - G_0) + \mu_{12}T_0}{\mu_{12}}, \tag{6.21}$$

$$n^* = \frac{q_0}{\alpha_{10}} - \left(\frac{\psi_1 a^* + \psi_2 a^{*2}}{\alpha_{10}\theta_{11}}\right), \tag{6.22}$$

$n^* > 0$ if,

$$\frac{q_0}{\alpha_{10}} > \left(\frac{\psi_1 a^* + \psi_2 a^{*2}}{\alpha_{10}\theta_{11}}\right), \tag{6.23}$$

$$O^* = \frac{R + \alpha_5 a^*}{K_r \gamma_1^{\left(\frac{T^* - T_r}{10}\right)} + \alpha_3 + \alpha_4 a^*}. \tag{6.24}$$

a^* is given as the positive root of the following equation:

$$A_1 a^{*5} + A_2 a^{*4} + A_3 a^{*3} + A_4 a^{*2} + A_5 a^* + A_6 = 0, \tag{6.25}$$

where

$$A_1 = \psi_2^3, \quad A_2 = 3\psi_1\psi_2^2 - \theta_{11}\beta_{11}\psi_2^2,$$

$$A_3 = 3\psi_1^2\psi_2 - 2\theta_{11}q\psi_2^2 - 2\psi_1\psi_2\theta_{11}\beta_{11},$$

$$A_4 = \psi_1^3 - 4\theta_{11}q\psi_1\psi_2 - \psi_1^2\theta_{11}\beta_{11} + 2\theta_{11}^2\beta_{11}q\psi_2,$$

$$A_5 = \mu_0^2\alpha_{10}^2\theta_{11}^2\psi_2 + \theta_{11}^2 q^2\psi_2 + 2\theta_{11}^2\beta_{11}q\psi_1 - 2\theta_{11}q\psi_1^2,$$

$$A_6 = \psi_1\mu_0^2\alpha_{10}^2\theta_{11}^2 + \psi_1\theta_{11}^2 q^2 - \theta_{11}^3\beta_{11}q^2.$$

The equation (6.25) has at least one positive root if the following condition is satisfied:

$$3\psi_1 < \beta_{11}\theta_{11}. \tag{6.26}$$

6.4 Stability Analysis of the Model

Consider the system of equations as given below:

$$\frac{dx}{dt} = \breve{f}(t, x) \tag{6.27}$$

$$\frac{dy}{dt} = \breve{g}(y) \tag{6.28}$$

where$\breve{f}$ and $\breve{g}$ are locally Lipschitz functions and continous in variable 'x' in R^n with the solutions existing for all time $t \geq 0$.The equation (6.28) shall be asymptotically autonomous with limit equation (6.27), if for all 'x' in R^n, $\breve{f}(t, x) \to \breve{g}(x)$ uniformly as $t \to \infty$.

Lemma 6.4.1. *[167, 168]: "Let e be a locally asymptotically stable equilibrium of (6.28) and ω be the ω-limit set of a forward bounded solution x(t) of (6.27). If ω contains a point y_0 such that the solutions of (6.28), with $y(0) = y_0$ converges to e as $t \to \infty$, then $\omega = \{e\}$ i.e. $x(t) \to e$ as $t \to \infty$"*

Corollary 6.4.1.1. *[168]: "If the solutions of the system (6.28) are bounded and the equilibrium e of the limit system (6.28) is globally asymptotically stable then any solution x(t) of the system (6.28) satisfies* $x(t) \to e$ *as* $t \to \infty$ *."*

Since $P_l^* \leq \limsup_{t\to\infty} P_l, G^* \leq \limsup_{t\to\infty} G$ and $T^* \leq \limsup_{t\to\infty} T$, therefore upon solving the system of equations (6.1)-(6.6) for P_l, G and T, the system given by (6.1)-(6.6) shall be reduced to an equivalent autonomous system given below:

Mathematical Model-II

$$\frac{dn}{dt} = q_0 - \alpha_{10} n - \frac{\beta_{11} n^2 a}{\mu_0^2 + n^2}, \tag{6.29}$$

$$\frac{da}{dt} = \frac{\theta_{11}\beta_{11} n^2 a}{\mu_0^2 + n^2} - \theta_{12} P_l^* a - \psi_0 a - \psi_2 a^2, \tag{6.30}$$

$$\frac{dO}{dt} = R - K_r \gamma_1^{\left(\frac{T^* - T_r}{10}\right)} O + \alpha_5 a - \alpha_3 O - \alpha_4 a O. \tag{6.31}$$

6.4.1 Equilibrium Points of Mathematical Model - II and their existence conditions

The equilibrium points corresponding to the mathematical model given by equations (6.29)-(6.31) are solved and given below:

1. Algal Vanishing Equilibrium Point$\check{E}(\check{n}, 0, \check{O})$: From equations (6.29)-(6.31) we get,

$$\check{n} = \frac{q_0}{\alpha_{10}}, \tag{6.32}$$

$$\check{O} = \frac{R}{K_r \gamma_1^{\left(\frac{T^* - T_r}{10}\right)} + \alpha_3}. \tag{6.33}$$

2. Interior Equilibrium Point$E^{**}(n^{**}, a^{**}, O^{**})$: From equations (6.29)-(6.31) we get,

$$n^{**} = \frac{q_0}{\alpha_{10}} - \left(\frac{\psi_1^* a^{**} + \psi_2 a^{**2}}{\alpha_{10}\theta_{11}}\right), \tag{6.34}$$

$n^{**} > 0$ if,

$$\frac{q_0}{\alpha_{10}} > \left(\frac{\psi_1^* a^{**} + \psi_2 a^{**2}}{\alpha_{10}\theta_{11}}\right), \tag{6.35}$$

$$O^{**} = \frac{R + \alpha_5 a^{**}}{K_r \gamma_1^{\left(\frac{T^* - T_r}{10}\right)} + \alpha_3 + \alpha_4 a^{**}}. \tag{6.36}$$

a^{**} is given as the positive root of the following equation:

$$C_1 a^{**5} + C_2 a^{**4} + C_3 a^{**3} + C_4 a^{**2} + C_5 a^{**} + C_6 = 0, \tag{6.37}$$

where

$$C_1 = \psi_2^3, \quad C_2 = 3\psi_1^*\psi_2^2 - \theta_{11}\beta_{11}\psi_2^2,$$

$$C_3 = 3\psi_1^{*2}\psi_2 - 2\theta_{11} q \psi_2^2 - 2\psi_1^*\psi_2\theta_{11}\beta_{11},$$

$$C_4 = \psi_1^{*3} - 4\theta_{11} q \psi_1^* \psi_2 - \psi_1^{*2}\theta_{11}\beta_{11} + 2\theta_{11}^2\beta_{11} q \psi_2,$$

$$C_5 = \mu_0^2 \alpha_{10}^2 \theta_{11}^2 \psi_2 + \theta_{11}^2 q^2 \psi_2 + 2\theta_{11}^2 \beta_{11} q \psi_1^* - 2\theta_{11} q \psi_1^{*2},$$

$$C_6 = \psi_1^* \mu_0^2 \alpha_{10}^2 \theta_{11}^2 + \psi_1^* \theta_{11}^2 q^2 - \theta_{11}^3 \beta_{11} q^2.$$

where $\psi_1^* = \psi_0 + \theta_{12} P_l^*$.

The equation 6.37 has at least one positive root if the following condition is satisfied:

$$3\psi_1^* < \beta_{11}\theta_{11}. \tag{6.38}$$

Lemma 6.4.2. *The solutions of the mathematical model-II given by equations (6.29)-(6.31) shall lie in the reqion* Σ *given as,* $\Sigma = \{(n, a, O) \in R_+^3 : 0 < n < n_u, 0 < a < a_u, 0 < O < O_u\}$ *for* $t \to \infty$ *with positive initial values* $(n(0), a(0), O(0)) \in R_+^3$ *where* $n_u = \frac{q_0}{\alpha_{10}}, a_u = \frac{\theta_{11}\beta_{11}}{\psi_2}, O_u = \frac{R + \alpha_5 a_u}{\alpha_3}$.

Proof. The proof of this lemma shall follow the similar steps as followed in the theorem 6.3.1 for proving the boundedness of mathematical model-I. □

6.4.2 Dynamical behaviour of the mathematical model-II

Theorem 6.4.1. *The Algal vanishing equilibrium point $\check{E}$ corresponding to mathematical model-II given by equations (6.29)-(6.31) shall be asymptotically stable if* $\frac{\theta_{11}\beta_{11}\check{n}^2}{\mu_0^2+\check{n}^2} > \theta_{12}P_l^* + \psi_0$.

Proof. The characteristic equation corresponding to the Jacobian Matrix at $\check{E}$ is given as:

$$(\lambda+\alpha_{10})(\lambda^2+(\check{Z}_5+\check{Z}_8)\lambda+\check{Z}_5\check{Z}_8)=0, \tag{6.39}$$

where

$$\check{Z}_5 = K_r\gamma_1^{\left(\frac{T^*-T_r}{10}\right)}+\alpha_3, \qquad \check{Z}_8 = \frac{\theta_{11}\beta_{11}\check{n}^2}{\mu_0+\check{n}^2} - \theta_{12}P_l^* - \psi_0.$$

Following the Routh-Hurwitz criteria, $\check{E}$shall be asymptotically stable if:

$$\check{Z}_8 > 0$$

i.e.

$$\frac{\theta_{11}\beta_{11}\check{n}^2}{\mu_0^2+\check{n}^2} > \theta_{12}P_l^* + \psi_0. \tag{6.40}$$

□

Theorem 6.4.2. *The Interior equilibrium point E^{**} corresponding to mathematical model-II given by equations (6.29)-(6.31) is always stable if the conditions for existence for E^{**} hold true.*

Proof. The characteristic equation corresponding to the Jacobian Matrix at E^{**} is given as:

$$(\lambda+Z_5^{**})(\lambda^2+(Z_1^{**}+\psi_2a^{**})\lambda+Z_1^{**}\psi_2a^{**}+Z_2^{**}Z_3^{**})=0, \tag{6.41}$$

where

$$Z_1^{**} = \alpha_{10} + \frac{2\mu_0^2\beta_{11}n^{**}a^{**}}{(\mu_0^2+n^{**2})^2}, Z_2^{**} = \frac{\beta_{11}n^{**2}}{\mu_0^2+n^{**2}},$$

$$Z_3^{**} = \frac{2\theta_{11}\mu_0^2\beta_{11}n^{**}a^{**}}{(\mu_0^2 + n^{**2})^2}, Z_5^{**} = K_r\gamma_1^{\left(\frac{T^*-T_r}{10}\right)} + \alpha_3 + \alpha_4 a^{**}$$

From the Routh-Hurwitz criteria we deduce that the equation (6.41) will have negative roots or roots with negative real part under the condition of existence for E^{**}, which proves the theorem 6.4.2. □

6.4.3 Global Stability for the mathematical model-II

Theorem 6.4.3. *The Interior equilibrium point E^{**} corresponding to mathematical model-II given by equations (6.29)-(6.31) shall be globally asymptotically stable if the following conditions hold true:*

$$2\left(\alpha_{10} + \mu_0^2\beta_{11}\left(\frac{(an + a^{**}n^{**})}{(\mu_0^2 + n^2)(\mu_0^2 + n^{**2})}\right)\right)(\psi_2 m_1 + \theta_{12}P_l^* m_1) > \left(\frac{\beta_{11}n^{**2}(\mu_0^2 - n^2)}{(\mu_0^2 + n^2)(\mu_0^2 + n^{**2})}\right)^2$$

and

$$2\left(\psi_2 m_1 + \theta_{12}P_l^* m_1\right)\left(K_r\gamma_1^{\left(\frac{T^*-T_r}{10}\right)} + \alpha_3 + \alpha_4 a^{**}\right) > \left(\alpha_4 O - \alpha_5\right)^2$$

where

$$p_{11} = \alpha_{10} + \mu_0^2\beta_{11}\frac{(an + a^{**}n^{**})}{(\mu_0^2 + n^2)(\mu_0^2 + n^{**2})}, \quad p_{22} = \psi_2 m_1 + \theta_{12}P_l^* m_1,$$

$$p_{33} = K_r\gamma_1^{\left(\frac{T^*-T_r}{10}\right)} + \alpha_3 + \alpha_4 a^{**}, \quad p_{12} = \frac{\beta_{11}n^{**2}(\mu_0^2 - n^2)}{(\mu_0^2 + n^2)(\mu_0^2 + n^{**2})},$$

$$p_{23} = \alpha_4 O - \alpha_5.$$

Proof. Consider a positive definite function,

$$W(n, a, O) = \frac{1}{2}(n - n^{**})^2 + m_1\left(a - a^{**} - a^{**}ln\frac{a}{a^{**}}\right) + \frac{1}{2}(O - O^{**})^2), \quad (6.42)$$

where $m_1 = \frac{n^{**}}{\theta_{11}}$. Differentiating equation (6.42) w.r.t. t we obtain,

$$\frac{dW}{dt} = -[p_{11}(n-n^{**})^2 + p_{22}(a-a^{**})^2 + p_{33}(O-O^{**})^2 + p_{12}(a-a^{**})(n-n^{**}) + p_{23}(a-a^{**})(O-O^{**})],$$

where

$$p_{11} = \alpha_{10} + \mu_0^2\beta_{11}\frac{(an + a^{**}n^{**})}{(\mu_0^2+n^2)(\mu_0^2+n^{**2})}, p_{22} = \psi_2 m_1 + \theta_{12}P_l^* m_1,$$

$$p_{33} = K_r\gamma_1^{\left(\frac{T^*-T_r}{10}\right)} + \alpha_3 + \alpha_4 a^{**}, p_{12} = \frac{\beta_{11}n^{**2}(\mu_0^2-n^2)}{(\mu_0^2+n^2)(\mu_0^2+n^{**2})},$$

$$p_{23} = \alpha_4 O - \alpha_5.$$

Using Sylvester's Criteria, E^{**} shall be globally asymptotically stable if,

$$2p_{11}p_{22} > p_{12}^2, 2p_{22}p_{33} > p_{23}^2,$$

i.e.

$$\left(\alpha_{10} + \mu_0^2\beta_{11}\left(\frac{(an+a^{**}n^{**})}{(\mu_0^2+n^2)(\mu_0^2+n^{**2})}\right)\right)(\psi_2 m_1 + \theta_{12}P_l^* m_1) > \left(\frac{\beta_{11}n^{**2}(\mu_0^2-n^2)}{(\mu_0^2+n^2)(\mu_0^2+n^{**2})}\right)^2 \quad (6.43)$$

$$2\left(\psi_2 m_1 + \theta_{12}P_l^* m_1\right)\left(K_r\gamma_1^{\left(\frac{T^*-T_r}{10}\right)} + \alpha_3 + \alpha_4 a^{**}\right) > (\alpha_4 O - \alpha_5)^2 \quad (6.44)$$

□

6.5 Numerical Simulation and Sensitivity Analysis

In this section, the numerical simulations are performed to support the analytical results obtained for the model represented by equations (6.1)-

Table 6.2: Sensitivity Indices(γ) of $P_l^*, G^*, n^*, a^*, T^*, O^*$ at E^* with respect to the parameters denoted by Z_p.

Parameters(Z_p)	$\gamma_{Z_p}^{P_l^*}$	$\gamma_{Z_p}^{G^*}$	$\gamma_{Z_p}^{n^*}$	$\gamma_{Z_p}^{a^*}$	$\gamma_{Z_p}^{T^*}$	$\gamma_{Z_p}^{O^*}$
Q_1	1	0.1844	0.0596	-0.0389	0.2482	-0.0125
α_1	-1	-0.1844	-0.0596	0.0389	-0.2482	0.0125
I_{10}	0	0.8147	0	0	1.090	-0.1381
I_{11}	0	0.1844	0	0	0.2482	-0.03126
α_2	0	-0.999	0	0	-1.3458	0.16948
q_0	0	0	3.222	3.7466	0	-1.8024
α_{10}	0	0	-0.9672	-0.0075	0	-0.00005
β_{11}	0	0	0.1972	1.1303	0	-0.5437
μ_0	0	0	0.0428	-0.0148	0	0.0072
θ_{11}	0	0	-1.8162	1.1871	0	-0.5711
θ_{12}	0	0	0.0596	-0.0389	0	0.01875
ψ_0	0	0	0.3136	-0.2049	0	0.09861
ψ_2	0	0	1.4428	-0.9432	0	0.4537
μ_{11}	0	0	0	0	0.525	-0.0661
G_0	0	0	0	0	-0.821	0.1033
μ_{12}	0	0	0	0	-0.525	0.0661
T_0	0	0	0	0	0.4748	-0.0598
R	0	0	0	0	0	0.0654
K_r	0	0	0	0	0	-0.1417
γ_1	0	0	0	0	0	-0.1052
T_r	0	0	0	0	0	0.9397
α_3	0	0	0	0	0	-0.0323
α_4	0	0	0	0	0	-0.8258
α_5	0	0	0	0	0	0.3447

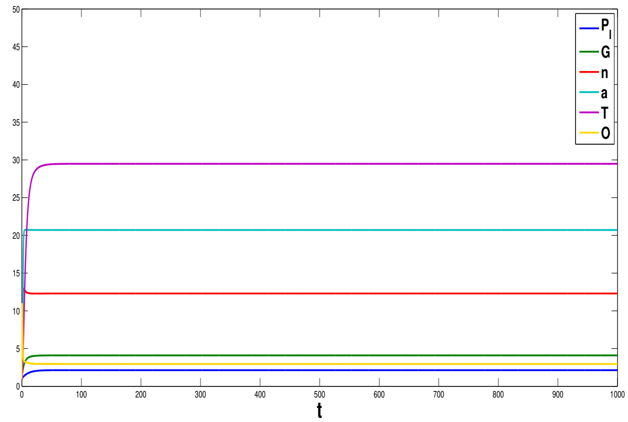

Figure 6.1: Model Trajectories exhibiting the stability behaviour at interior equilibrium point.

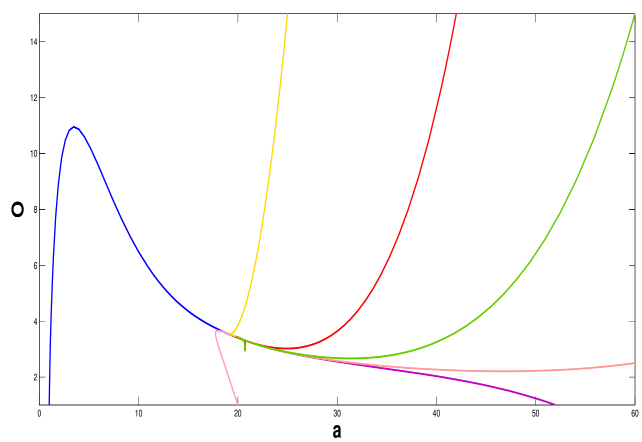

Figure 6.2: Phase Plane Graph between O and a exhibiting global stability for varying initial conditions

(6.6). We consider the below mentioned parameter values for our model:

$$Q_1 = 0.214, \alpha_1 = 0.1, I_{10} = 1.003, I_{11} = 0.106, \alpha_2 = 0.3, q_0 = 9.447,$$
$$\alpha_{10} = 0.3, \beta_{11} = 0.28, \mu_0 = 1.0, \theta_{11} = 9.105, \theta_{12} = 0.04, \psi_0 = 0.45,$$
$$\psi_2 = 0.1, \mu_{11} = 3.8717, G_0 = 2.5, \mu_{12} = 0.4, T_0 = 14.0, R = 24.0,$$
$$K_r = 1.049, \gamma_1 = 2.0, T_r = 22.0, \alpha_3 = 0.4, \alpha_4 = 0.495, \alpha_5 = 0.61. \quad (6.45)$$

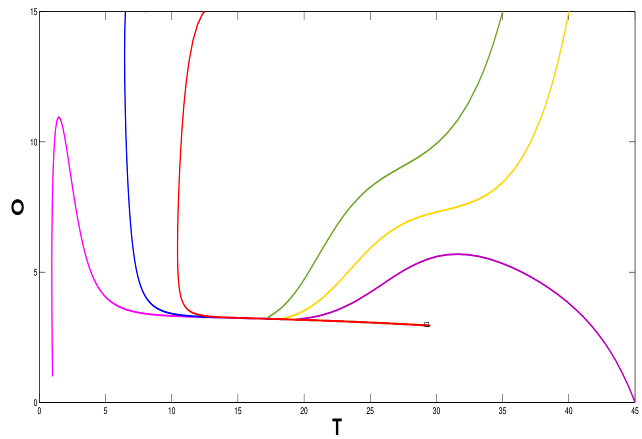

Figure 6.3: Phase Plane Graph between O and T exhibiting global stability for varying initial conditions

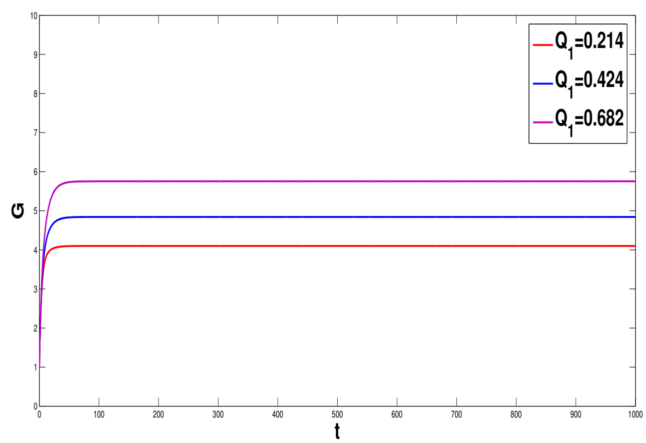

Figure 6.4: Graph exhibiting rise in greenhouse gases concentration for increasing plastic input

The value of the model variables obtained for the above given set of parameter values are : P_l^*=2.140, G^*=4.0995, n^*=12.2929, a^*=20.7044, T^*=29.4816 and O^*=2.9520.

For the values of model parameters given by equation (6.45), the con-

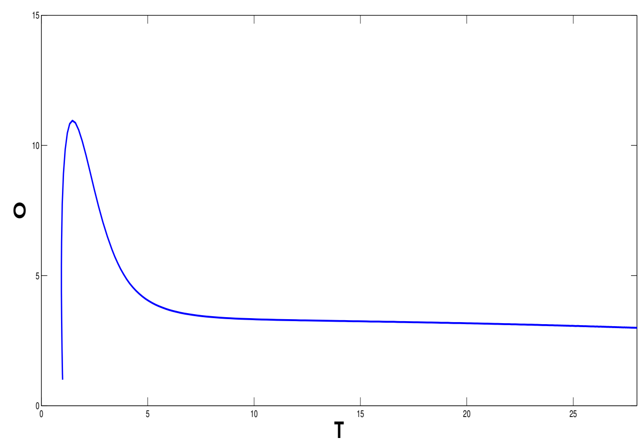

Figure 6.5: Phase space graph between O and T

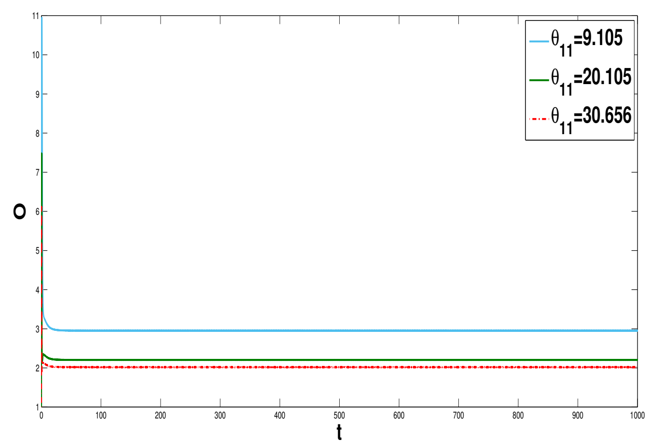

Figure 6.6: Graph between dissolved oxygen and time for increase in growth rate of algal population

ditions for feasibility and stability derived analytically for the interior equilibrium point corresponding to mathematical model-II, given by equations (6.35), (6.38), (6.43) and (6.44) are found to be satisfied. Also, the stability of interior equilibrium point for the model-I given by equations (6.1)-(6.6) is shown by figure 6.1. Further, we performed

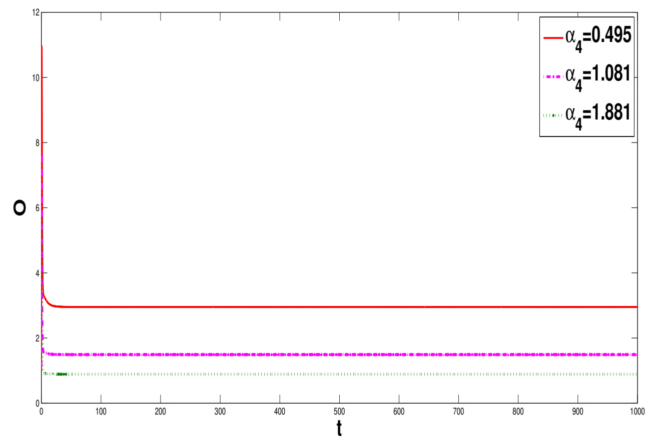

Figure 6.7: Graph between dissolved oxygen and time for increase rate of utilisation rate of dissolved oxygen in algal decomposition

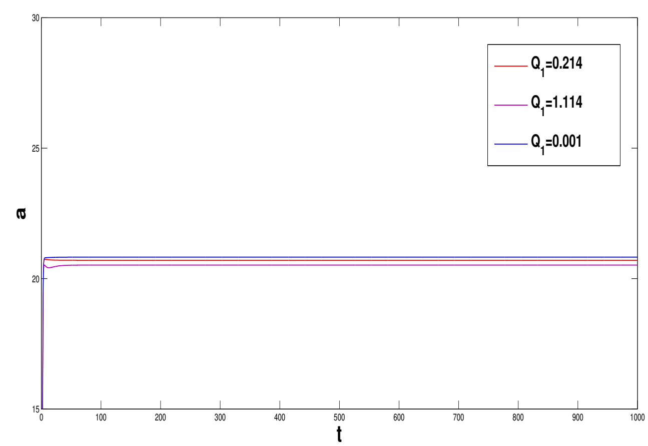

Figure 6.8: Behaviour of algal population for increasing plastic input

numerical simulations to establish the global stability behaviour of the model given by equations (6.1)-(6.6) under variable initial conditions which is shown by phase-plane graphs given by figures 6.2 and 6.3 . It is demonstrated that all the trajectories which start from different initial conditions converge to the equilibrium value with increase in time.

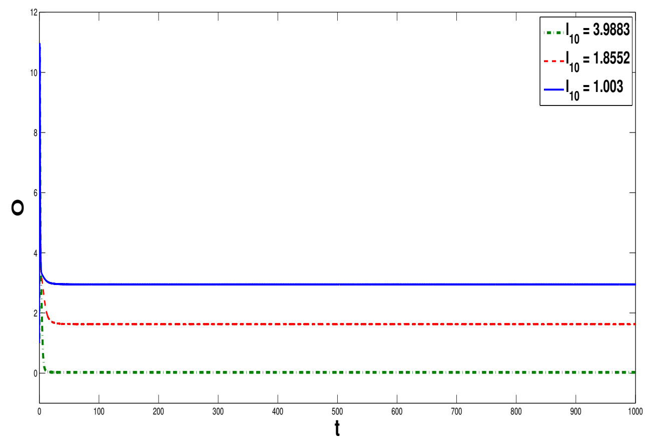

Figure 6.9: Threshold level for dissolved oxygen under the effect of rising greenhouse gases concentration

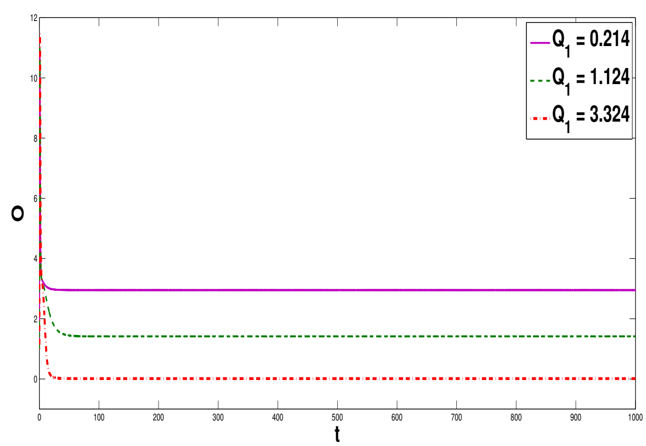

Figure 6.10: Threshold level for dissolved oxygen under the effect of rising plastic waste concentration

Further, to study the relative variation in the model variables P_l^*, G, n^*, a^*, T^* and O^* with respect to the model parameters given by the equation (6.45), sensitivity analysis has been performed using the below given formula for calculating normalized forward sensitivity index

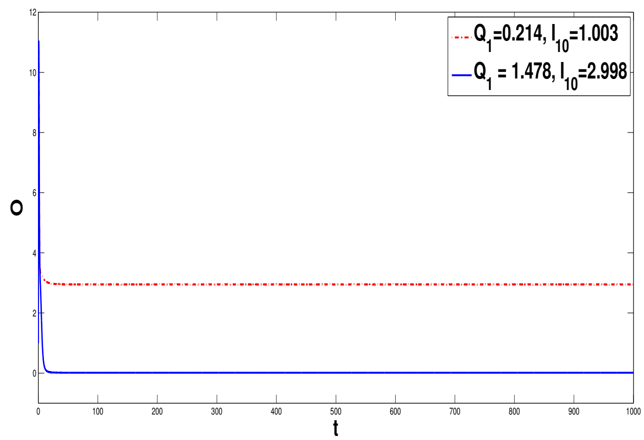

Figure 6.11: Threshold level for dissolved oxygen under the simultaneous effect of rising greenhouse gases and plastic waste concentration

for variable 'Z' depending on a parameter 'w' [117]:

$$\gamma_w^Z = \frac{\partial Z}{\partial w} * \frac{w}{Z}$$

. The sensitivity indices calculated for the model variables P_l^*, G, n^*, a^*, T^* and O^* with respect to the model parameters given by the equation (6.45) are given in Table 6.2. These sensitivity indices give a fair idea for the parameters whose variation has a more influential value on the model variables and can be extremely helpful in design of control strategies to minimise the anthropogenic pollution.

6.6 Conclusion

Plastics have become indispensably omnipresent in our lives, right from being a part of our basic necessities like food wrappers, water bottles, packaging materials etc. to armouring the frontline workers against the deadly COVID-19 in the form of masks, gloves, PPE kits, face shields etc. But, the absence of its proper disposal is creating a havoc for the environment, especially for the aquatic ecosystem. This phenomenon coupled with various kinds of pollutants entering water and climatic alterations, is adversely impacting the growth rate and the survival of aquatic organisms. In our study, the results of the analysis carried out for the mathematical model given by (6.1)-(6.6) bring into foreground the interplay between various anthropogenic stressors such as accumulating plastic waste in aquatic bodies, rising carbon emissions, global warming, eutrophication, climate change etc. and their subsequent effects on the aquatic ecosystem especially on the oxygen-dependent populations residing in the water bodies like fishes.

From the analytical study of system dynamics, it is observed that the interior equilibrium point for model-II, satisfies existence conditions and is locally and globally asymptotically stable as shown by equations (6.35), (6.38), (6.43) , (6.44) and supported by figures 6.1, 6.2 and 6.3.

It is observed that the rising plastic waste is becoming a contributor towards the increasing concentration of greenhouse gases in the atmosphere as shown in figure 6.4 which is in turn causing an increase in the temperature leading to global warming as shown by equation (6.21). Moreover, the positive sensitivity index of Temperature (T) with respect to plastic input rate Q_1 and the high positive sensitivity index of Temperature (T) with respect to greenhouse gases emission rate I_{10} also support that rising greenhouse gases on account of human activities and plastic pollution lead to climate changes induced by global warming. It is further noted that the dissolved oxygen exhibits a decrease with time under the influence of global warming as shown by figure 6.5. The eutrophication process also leads to highly promoting the growth of algal population as seen by the high positive sensitivity index of Algal population (a) with respect to parameter q_0. It is further shown by figure 6.6, that with increase in growth rate of algal population (θ_{11}) owing to eutrophication, the concentration of dissolved oxygen shall decline, as with rise in algal population more dissolved oxygen is utilised for its decomposition process. This is also supported by the large negative sensitivity indices of Dissolved oxygen(O) with respect to nutrient

inflow rate (q_0) and Dissolved oxygen(O) with respect to oxygen utilisation rate in algal decomposition (α_4). The latter phenomenon is shown by figure 6.7, which shows that with increase in the utilisation rate of oxygen in the algal decomposition process (α_4), the concentration of dissolved oxygen in water shall reduce over time. These results are also supported by the study done by Shukla et al. [84]. Notably, the growing plastic pollution hinders with the algal photosynthesis which raises difficulty in the survival of algal population. This is shown by figure 6.8. Moreover, this also leads to deterioration of dissolved oxygen level in water as with rise in algal mortality rate, more dissolved oxygen shall be consumed in its decomposition process [141].
Further, it is observed that the dissolved oxygen approaches a zero value when the emission rate of greenhouse gases due to anthropogenic activities (I_{10}) reaches a value equal to or more than 3.9883 as shown in figure 6.9. Similarly, for increase in input rate of plastic waste in water body (Q_1) exceeding 3.324, the dissolved oxygen approaches a zero value as shown by figure 6.10. However, under the simultaneous effects of both rise greenhouse gases and plastic waste accumulation in a water body, the dissolved oxygen approaches zero much faster for much lower values, I_{10}=2.998 and Q_1=1.478 as demonstrated by figure 6.11. Thus, this supports the fact that the simultaneous effects of both the anthropogenic stressors i.e. plastic pollution and global warming is much more detrimental to aquatic ecosystem rather than the single effect, as the deficiency of dissolved oxygen in water can lead to the system approaching a state of hypoxia which will be harmful for existence and survival of aquatic organisms [26, 1].

We are at the crossroads of two divergent paths in the situation of this pandemic COVID-19. First one being the expedient approach that places us squarely on track for a foreseeable future in which more plastic is available in the ocean than fish. The other is a sustainable living and working paradigm which will support us for a long time to come. We have to quickly devise methods to control the environment stressors at the earliest, especially focusing on waste disposal and treatment before their inlet in the water bodies. Only then, we shall be able to aim for a sustainable future. The analytical study of our model, supported by numerical simulations, supports this fact and provides a structured framework to examine the impacts of the combined factors of plastic pollution, global warming and eutrophication, on oxygen-dependent aquatic species, in the light of the future risks posed by the recent health crisis of COVID-19 pandemic outbreak world over.

Chapter 7

Modelling on Rising Carbon Emissions and Water Acidity to Assess Their Impacts on Algal Bloom Growth and Oxygen-Dependent Population

7.1 Introduction

The ecosystem is eminently dependent on the complex interrelations and interactions between its species and environment. Alterations in the environment, whether direct or indirect, play a significant role in shaping of the ecological communities in an ecosystem. In recent times, the aquatic ecosystem is becoming highly vulnerable to the hazardous consequences of modern-age developmental activities being carried out by the human population. Human activities are resulting in contamination and quality degradation of the water bodies and altering the physical, biological, and chemical processes in the aquatic ecosystem. One of the major deleterious threats posed to the health ecosystem biodiversity is anthropogenic climate change [148]. The untapped rise of anthropogenic carbon emissions is a major cause contributing to global warming affecting many ecological communities [169]. Drastic changes have been witnessed in the climate and temperature conditions in the past years [25]. Certain recently conducted studies point towards more serious climatic disruptions in the aquatic environments in future [17, 169]. Global warming and associated rise in water temperature is found to affect freshwater resources and have severe consequences for the populations residing in water bodies [27, 1, 13]. Global Warming causes reduced oxygen solubility in warmer waters and leads to oxygen scarcity in water bodies [102]. Moreover, global warming leads to disturbances in the process of phytoplankton photosynthesis. A sufficiently significant rise in water temperature is likely to force the environment towards oxygen dearth, leading to condition of hypoxia or even anoxia [141]. In ecosystems like Arctic, warming can also affect the predation activities of species like wolf spiders in a disproportionate manner [170]. Increasing carbon dioxide concentration in water has also been found to negatively impact the early life stage growth and survival rate in the fish population [26]. Between 1750 and 2011 human activities caused the carbon dioxide atmospheric level to rise by approximately 40 per cent [171]. In the last 50 years, the absorption of carbon dioxide by water bodies has also shown an increase [142]. Many juvenile reef fishes are also found to exhibit abnormalities in their behaviours at CO_2 seeps [70]. Another grave consequence of increased carbon emissions is the rise in acidity of water. When carbon dioxide enters the water bodies, it forms carbonic acid through the following equilibrium reaction:

$$CO_2 + H_2O \Leftrightarrow H_2CO_3 \Leftrightarrow H^+ + HCO_3^- \Leftrightarrow H^+ + CO_3^{2-}$$

The pH level of water exhibits a decrease when more amount of carbonic acid is formed resulting in higher release of H+ ions in water. Caldeira and Wickett [155] have predicted a decline in seawater pH of 0.4 units by 2100 and another drop of 0.7 by the year 2300. It has also been found that the rising carbon emissions and coupled acidity rise have many harmful effects on the residing population hampering their growth processes and survival rates in aquatic ecosystem [56, 54, 156]. Along with this, unrestrained release of industrial pollutants further contributes in making the water bodies more acidic [134]. The increasing eutrophication, which is a resultant of unmanaged agricultural activities, is another factor which has emerged as a contributor in lowering the pH of water bodies by increasing the acidity [159]. The rising eutrophication and acidity also promote the growth of algal bloom in water bodies. This leads to high respiration rates producing more carbon dioxide in water bodies causing a further drop in pH value [126, 157, 158]. Apart from the rising acidity level of water, global warming also induces the growth of algal bloom water bodies [78, 80]. Rise in algal population density, is accompanied by decline in the concentration of the dissolved oxygen, as the decomposition process consumes the oxygen, thus depleting its level in water bodies [157]. The rising algal blooms are also deteriorating the biodiversity and, in some cases, leading to death of aquatic species as well because of scarcity of the most vital resource required for their survival i.e. dissolved oxygen in water [6]. According to some studies, the escalation in acidification of water bodies is severely and negatively impacting the species biodiversity in coral reefs as the corals and some plankton are facing difficulty in maintenance of their external carbon skeletons as decreasing in water pH causes reduction in calcium carbonate saturation [172, 75].

Few mathematical studies are available which study the individual impacts of the rising acidity, carbon emissions and pollution of water bodies on the resource populations [108, 162, 164], and the effect of rising algal bloom growth in water bodies [86, 84, 118]. Certain mathematical studies have also focussed on the harmful effects of growing global warming on environment and subsequently on dependent populations [32, 31]. These individuals studied conclude that the individual effects of these factors can be very harmful for the ecosystem and dependent species. However, a mathematical study which encompasses all these factors together, and its impact on the aquatic population is still unavailable.

In view of the above, in this chapter we propose a mathematical model considering the variables as carbon concentration in water, pH of water, algal bloom concentration, dissolved oxygen concentration and density of population dependent on dissolved oxygen for its survival. It is assumed that the carbon input in water through industrial, agricultural and domestic pollution leads to a rise in acidity and global warming. These in turn, lead to rise in algal bloom growth in the water bodies. As a consequence, the dissolved oxygen concentration in water is reduced and which is hazardous to the survival of the population which is dependent on oxygen intake. The model is analysed by analytical method for stability analysis and the results have been supported by numerical simulations performed using MATLAB.

7.2 Mathematical Model

In the mathematical modelling process, it is assumed that the rising carbon emissions in the atmosphere are leading to two major complications for aquatic environment, one being the increasing water acidity due to formation of carbonic acid and other being the warming water temperature on account of global warming. These processes further catalyse the growth of algal bloom in the water bodies. Further it is presumed, that the increased algal population utilises more dissolved oxygen for its decomposition process. This decline in dissolved oxygen is in turn assumed to negatively impact the oxygen-dependent aquatic biota. In view of the above given assumptions, let C denote the concentration of carbon in water, pH represents the pH level of the water, A_g gives the density of algal population in water, D represents the concentration of dissolved oxygen in water and P represent the density of aquatic population like fish dependent on intake of oxygen for its survival. Embodiment of these variables leads to formulation of the following mathematical model comprising of non-linear differential equations:

$$\frac{dC}{dt} = E - \frac{1}{\tau_l}(C - C_0) - a_1 DC, \tag{7.1}$$

$$\frac{d(pH)}{dt} = \frac{pH_0}{1 + C} - \gamma_1(pH), \tag{7.2}$$

$$\frac{dA_g}{dt} = \frac{\beta_1 A_g(1 + \alpha_1 C - \alpha_2(pH))}{\beta_2 + A_g} + \gamma_2 A_g D - hA_g, \tag{7.3}$$

$$\frac{dD}{dt} = R - \psi_0 D - \psi_1 A_g D - a_1 DC - \frac{n_1 PD}{v_1 + D}, \tag{7.4}$$

$$\frac{dP}{dt} = \frac{n_2 PD^2}{v_2^2 + D^2} - \theta_1 P - \theta_2 P^2, \tag{7.5}$$

where $C(0) > 0, pH(0) > 0, A_g(0) \geq 0, D(0) \geq 0,\ P(0) \geq 0 and C \geq C_0$. The model parameters, assumed to be positive constants, are explained as given below:

E denotes the rate of input of carbon dioxide in water body via various mode of anthropogenic pollution, τ_l gives the latent time period corresponding to carbon dioxide in the water body, C_0 represents the threshold level of carbon dioxide in water. a_1 represents the rate of formation of carbonic acid in water due to reaction of carbon dioxide with the dissolved oxygen and this reaction is represented by the term a_1DC. pH_0 denotes the normal pH of water at which the aquatic organisms show optimum growth. γ_1 is the natural rate of decrease of pH caused due to increase in water flow, acid rain and other water turbulences. The natural growth rate of algal population is represented by β_1. The rising carbon concentration enhances algal growth in water with rate given by α_1. α_2 gives the rate of increase in algal population on account of lowering pH i.e. increasing water acidity. β_2 is half saturation constant. Rate of utilisation of dissolved oxygen in algal respiration process is denoted by γ_2. The natural decay rate of algal population is given by h. The input rate of oxygen in water is denoted by R. ψ_0 is natural depletion rate of oxygen in water. The dissolved oxygen is depleted due to algal decomposition and rate of this depletion is given by ψ_1. n_1 gives the rate of depletion of oxygen due to its consumption in respiration and growth of the oxygen-dependent population. n_2 gives the growth rate of oxygen dependent population. v_1 and v_2 are half-saturation constants. θ_1 is the natural mortality rate of the population and θ_2 gives rate of intraspecific competition for the aquatic species.

7.3 Model Analysis

In this section, we study the equilibrium points for the model defined by the equations (7.1)-(7.5) and discuss the boundedness and positivity of the solutions.

7.3.1 Boundedness and Positivity of Model Solutions

Theorem 7.3.1. *All the solutions of the mathematical model represented by equations (7.1)-(7.5) lie in the region given by* $\varpi = \{(C, pH, A_g, D, P) \in R^5_+ : 0 < C < C_u, 0 < pH < pH_u,$ $0 < A_g < A_{gu}, 0 < D < D_u, 0 < P < P_u\}$ *for positive initial values* $(C(0), pH(0), A_g(0), D(0), P(0)) \in R^5_+$ *as* $t \to \infty$ *in case the condition* $\beta_1 + \gamma_2 D_u > h$ *holds, where* $C_u = \tau_l E + C_0, pH_u = \frac{pH_0}{\gamma_1}, A_{gu} = \frac{\beta_1 \alpha_1 C_u}{\beta_1 + \gamma_2 D_u - h}, D_u = \frac{R}{\psi_0}, P_u = \frac{n_2}{\theta_2}$.

Proof. From equation (7.1) we get,

$$\frac{dC}{dt} \leq E + \frac{1}{\tau_l} C_0 - \frac{1}{\tau_l} C,$$

using comparison theorem we obtain,

$$\lim_{t \to \infty} \sup(C, t) \leq \tau_l E + C_0 = C_u,$$

From equation (7.2) we have,

$$\frac{d(pH)}{dt} \leq pH_0 - \gamma_1 pH,$$

by comparison theorem, we get,

$$\lim_{t\to\infty}\sup(pH,t) \leq \frac{pH_0}{\gamma_1} = pH_u,$$

From equation (7.4) we obtain,

$$\lim_{t\to\infty}\sup(D,t) \leq \frac{R}{\psi_0} = D_u,$$

From equation (7.3), using comparison theorem we have,

$$\lim_{t\to\infty}\sup(A_g,t) \leq \frac{\beta_1\alpha_1 C_u}{\beta_1+\gamma_2 D_u - h} = A_{gu},$$

provided the following inequality holds good,

$$\beta_1 + \gamma_2 D_u > h \tag{7.6}$$

Similarly, from equation (7.5) and comparison theorem we have,

$$\frac{dP}{dt} \leq n_2 P - \theta_2 P^2,$$

hence,

$$\lim_{t\to\infty}\sup(P,t) \leq \frac{n_2}{\theta_2} = P_u$$

This proves the theorem 7.3.1. □

Theorem 7.3.2. *For positive initial conditions, all the solutions of the model represented by equations* (7.1)−(7.5) *remain positive for all times* $t \geq 0$.

Proof. We have from equation (7.1),

$$\frac{dC}{dt} \geq -\frac{1}{\tau_l}C - a_1 D_u C,$$

which implies,

$$C \geq u_1 e^{-\left(\frac{1}{\tau_l}+a_1 D_u\right)t}$$

where u_1 denotes the integration constant.

Hence, $C \geq 0$ for all times $t \geq 0$.

Similarly from equation (7.2) we have,

$$\frac{d(pH)}{dt} \geq -\gamma_1 pH,$$

which implies,

$$pH \geq u_2 e^{-\gamma_1 t},$$

where u_2 is an integration constant.
Therefore, $pH \geq 0$ for all times $t \geq 0$.
From equation (7.3), we get,

$$\frac{dA_g}{dt} \geq -(\beta_1 \alpha_2 (pH)_u + h) A_g,$$

thus implying,

$$A_g \geq u_3 e^{-(\beta_1 \alpha_2 (pH)_u + h)t}.$$

where u_3 is an integration constant.
Hence, $A_g \geq 0$ for all times $t \geq 0$.
Moreover, from equation (7.4) we deduce,

$$\frac{dD}{dt} \geq -(\psi_0 + \psi_1 A_{gu} + a_1 C_u + n_1 P_u) D,$$

which implies,

$$D \geq u_4 e^{-(\psi_0 + \psi_1 A_{gu} + a_1 C_u + n_1 P_u)t}$$

where u_4 is an integration constant.
Therefore, $D \geq 0$ for all times $t \geq 0$.
Equation (7.5) gives that,

$$\frac{dP}{dt} \geq -(\theta_1 + \theta_2 P_u) P$$

implying

$$P \geq u_5 e^{-(\theta_1 + \theta_2 P_u)t}$$

where u_5 is an integration constant.
Hence,$P \geq 0$ for all times $t \geq 0$.
This completes the proof of theorem 7.3.2. □

7.3.2 Equilibria of the Model

1. Algal Vanishing Equilibrium Point $\breve{E}(\breve{C}, p\breve{H}, 0, \breve{D}, \breve{P})$**:**
From equation (7.1) we obtain,

$$\breve{C} = \frac{\tau_l E + C_0}{a_1 \tau_l \breve{D} + 1}. \tag{7.7}$$

From equation (7.2) we have,

$$p\breve{H} = \frac{1}{\gamma_1}\left(\frac{pH_0}{1 + \breve{C}}\right). \tag{7.8}$$

Similarly from equation (7.5) we get,

$$\breve{P} = \frac{1}{\theta_2}\left(\frac{n_2 \breve{D}^2}{v_2^2 + \breve{D}^2} - \theta_1\right) \tag{7.9}$$

$\breve{P} > 0$ if,

$$\frac{n_2 \breve{D}^2}{v_2^2 + \breve{D}^2} - \theta_1 > 0. \tag{7.10}$$

Also, from equation (7.4) we get, $\breve{D}$ is given as the positive root of the following equation,

$$\begin{aligned}
&\breve{D}^5(\psi_0\theta_2 a_1\tau_l) + \breve{D}^4(\psi_0 a_1\tau_l\theta_2 v_1 - \theta_2 R a_1\tau_l + \psi_0\theta_2 + \theta_2 a_1\tau_l E + \theta_2 a_1 C_0 \\
&- n_1 a_1\tau_l\theta_1) + \breve{D}^3(\psi_0 a_1\tau_l\theta_2 v_2^2 - R a_1\tau_l\theta_2 v_1 + \psi_0\theta_2 v_1 + a_1\tau_l E\theta_2 v_1 + \\
&a_1 C_0\theta_2 v_1 - R\theta_2 + n_1 n_2 a_1\tau_l - n_1\theta_1) + \breve{D}^2(\psi_0\theta_2 v_1 v_2^2 a_1\tau_l - \theta_2 v_2^2 R a_1\tau_l + \psi_0\theta_2 v_2^2 + \\
&a_1\theta_2 v_2^2\tau_l E - R\theta_2 v_2 + a_1 C_0\theta_2 v_2^2 - R\theta_2 v_1 - a_1\tau_l n_1\theta_1 v_2^2 + n_1 n_2) + \breve{D}(\psi_0\theta_2 v_1 v_2^2 \\
&- R a_1\tau_l\theta_2 v_1 v_2^2 + a_1\theta_2 v_1 v_2^2\tau_l E + a_1 C_0\theta_2 v_1 v_2^2 - n_1\theta_1 v_2^2) - R\theta_2 v_1 v_2^2 = 0.
\end{aligned} \tag{7.11}$$

By Descarte's rule of signs, the equation (7.11) shall have at least one positive root.

2. Population Vanishing Equilibrium Point $\hat{E}(\hat{C}, p\hat{H}, \hat{A}_g, \hat{D}, 0)$**:**
From equation (7.1) we get,

$$\hat{D} = \frac{\tau_l E - \hat{C} + C_0}{a_1 \tau_l \hat{C}}. \tag{7.12}$$

From equation (7.2) we obtain,

$$\hat{pH} = \frac{pH_0}{\gamma_1(1+\hat{C})}. \tag{7.13}$$

From equation (7.4) we have,

$$\hat{A}_g = \frac{R - \psi_0\hat{D} - a_1\hat{D}\hat{C}}{\psi_1\hat{D}}. \tag{7.14}$$

$\hat{A}_g > 0$, if

$$R - \psi_0\hat{D} - a_1\hat{D}\hat{C} > 0. \tag{7.15}$$

From equation (7.3) we get,

$$\begin{aligned}&\hat{C}^4(a_1\gamma_2+\psi_1 M_3M_5+ha_1M_3)+\hat{C}^3[M_3\psi_1(\beta_1+M_5)+\gamma_2(\psi_0+RM_3+a_1)\\&+hM_3(RM_3+\psi_0+a_1)-\psi_1M_3(M_8+M_2M_5)-a_1M_2(2\gamma_2+hM_3)-\psi_1M_7)]\\&+\hat{C}^2[\psi_1(M_2M_3M_8+2M_2M_7+\beta_1M_3)+\gamma_2(RM_3+a_1M_2^2+\psi_0)+hM_3(\psi_0+\\&RM_3)-M_3\psi_1(M_2M_5+M_8+M_0M_6+\beta_1M_2)-\psi_1M_7-\psi_0M_2(hM_3+\gamma_2)-\\&a_1hM_2M_3-M_2\gamma_2(RM_3+2\psi_0)]+\hat{C}[M_2M_3\psi_1(M_0M_6+M_8)+2\psi_1M_2M_7+\\&\gamma_2M_2^2(\psi_0+a_1)-M_2M_3(R\gamma_2+\psi_0h+\beta_1\psi_1)-M_2(2\psi_0\gamma_2+\psi_1M_2M_7)]+\\&M_2^2(\psi_0\gamma_2-\psi_1M_7)=0, \end{aligned}\tag{7.16}$$

where

$$M_0 = \frac{pH_0}{\gamma_1}, \qquad M_2 = \tau_l E + C_0, \qquad M_3 = \tau_l a_1, \quad M_5 = \beta_1\alpha_1,$$

$$M_6 = \beta_1\alpha_2, \qquad M_7 = \gamma_2\beta_2, \qquad M_8 = h\beta_2.$$

According to Descarte's rule, equation (7.16) shall have a positive root, if the following condition holds true,

$$\psi_1\beta_2 > \psi_0. \tag{7.17}$$

3. Interior Equilibrium Point $E^*(C^*, pH^*, A_g^*, D^*, P^*)$**:**
From equation (7.1) we have,

$$C^* = \frac{\tau_l E + C_0}{1 + a_1\tau_l D^*}. \tag{7.18}$$

From equation (7.2) we get,

$$pH^* = \frac{pH_0}{\gamma_1(1+C^*)}. \tag{7.19}$$

Equation (7.5) gives,

$$P^* = \frac{n_2 D^{*2} - \theta_1 v_2^2 - \theta_1 D^{*2}}{\theta_2 v_2^2 + \theta_2 D^{*2}}. \tag{7.20}$$

$P^* > 0$ if,

$$n_2 D^{*2} - \theta_1 v_2^2 - \theta_1 D^{*2} > 0, \tag{7.21}$$

From equation (7.3) we have,

$$A_g^* = \frac{1}{\gamma_2 - D^*}\left(\beta_1 + \frac{A_2}{1+A_3 D^*} - \left(\frac{A_4 + A_3 A_4 D^*}{A_5 + \gamma_1 A_3 D^*}\right) + \beta_2\gamma_2 D^* - h\beta_2\right), \tag{7.22}$$

where,

$$A_1 = \tau_l E + C_0, \quad A_2 = \beta_1\alpha_1 A_1, \quad A_3 = a_1\tau_l,$$
$$A_4 = \beta_1\alpha_2 pH_0, \quad A_5 = \gamma_1(1+A_1)$$

$A_g^* > 0$ if,

$$\left(\beta_1 + \frac{A_2}{1+A_3 D^*} - \left(\frac{A_4 + A_3 A_4 D^*}{A_5 + \gamma_1 A_3 D^*}\right) + \beta_2\gamma_2 D^* - h\beta_2\right) > 0, \tag{7.23}$$

Let $A_6 = \psi_1\beta_2\gamma_2, \quad A_7 = \gamma_1 A_3, \quad M_0 = \psi_0 A_3 A_7,$
$M_1 = \psi_0 A_3 A_5 + \psi_0 A_7 - \psi_0\gamma_2 A_3 A_7 - R A_3 A_7 - A_3 A_6 A_7 + a_1 A_1 A_7,$
$M_2 = \psi_0 A_5 - \psi_0\gamma_2 A_3 A_5 - R A_3 A_5 - A_3 A_5 A_6 + a_1 A_1 A_5 - \psi_0\gamma_2 A_7 - R A_7 - A_6 A_7 + A_3 A_7\gamma_2 R - \psi_1\beta_1 A_3 A_7 + h\beta_2 A_3 A_7 - \gamma_2 a_1 A_1 A_7 + \psi_1 A_3^2 A_4,$
$M_3 = \gamma_2 R A_3 A_5 - \psi_0\gamma_2 A_5 - \psi_1\beta_1 A_3 A_5 + h\beta_2 A_3 A_5 - \gamma_2 a_1 A_1 A_5 - R A_5 - A_5 A_6 + R\gamma_2 A_7 - \psi_1\beta_1 A_7 + h\beta_2 A_7 - \psi_1 A_2 A_7 + 2\psi_1 A_3 A_4,$
$M_4 = R\gamma_2 A_5 - \psi_1\beta_1 A_5 + h\beta_2 A_5 - \psi_1 A_2 A_5 + \psi_1 A_4.$

Then, from equation (7.4) we obtain,

$$D^{*7}(\theta_2 M_0) + D^{*6}(\theta_2 v_1 M_0 + \theta_2 M_1 + n_1 n_2^2 A_3 A_7 - \theta_1 n_1 A_3 A_7) + D^{*5}(\theta_2 v_1 M_1 + \theta_2 v_2^2 M_0 + \theta_2 M_2 + n_1 n_2^2 A_3 A_5 + n_1 n_2^2 A_7 - \theta_1 n_1 A_3 A_5 - \theta_1 n_1 A_7 - n_1 n_2^2 \gamma_1 A_3 A_7 + \theta_1 n_1 \gamma_2 A_3 A_7) + D^{*4}(\theta_2 v_1 v_2^2 M_0 + \theta_2 v_1 M_2 + \theta_2 v_2^2 M_1 + \theta_2 M_3 - n_1 n_2^2 \gamma_2 A_3 A_5 + n_1 n_2^2 A_5 - n_1 n_2^2 \gamma_2 A_7 + \theta_1 v_2^2 n_1 \gamma_2 A_7 - \theta_1 v_2^2 n_1 A_3 A_7 - \theta_1 n_1 A_5 + \theta_1 n_1 \gamma_2 A_3 A_5 + \theta_1 n_1 \gamma_2 A_7) + D^{*3}(\theta_2 v_1 v_2^2 M_1 + \theta_2 v_1 M_3 + \theta_2 v_2^2 M_2 + \theta_2 M_4 - n_1 n_2^2 \gamma_2 A_5 - \theta_1 v_2^2 n_1 A_3 A_5 - \theta_1 v_2^2 n_1 A_7 + \theta_1 v_2^2 n_1 \gamma_2 A_3 A_7 + \theta_1 n_1 \gamma_2 A_5) + D^{*2}(\theta_2 v_1 v_2^2 M_2 + \theta_2 v_1 M_4 + \theta_2 v_2^2 M_3 - \theta_1 v_2^2 n_1 A_5 + \theta_1 v_2^2 n_1 \gamma_2 A_3 A_5) + D^{*}(\theta_2 v_1 V_2^2 M_3 + \theta_2 v_2^2 M_4) + \theta_2 M_4 v_1 v_2^2 + \theta_1 v_2^2 n_1 \gamma_2 A_5 = 0. \quad (7.24)$$

Following Descarte's Rule, the equation (7.24) shall have at least one positive root if at least any one of the below given conditions i.e. any of the equations given by (7.25) - (7.29) holds true,

$$\theta_2 v_1 M_0 + \theta_2 M_1 + n_1 n_2^2 A_3 A_7 < \theta_1 n_1 A_3 A_7, \quad (7.25)$$

$$\theta_2 v_1 M_1 + \theta_2 v_2^2 M_0 + \theta_2 M_2 + n_1 n_2^2 A_3 A_5 + n_1 n_2^2 A_7 + \theta_1 n_1 \gamma_2 A_3 A_7 < \theta_1 n_1 A_3 A_5 + \theta_1 n_1 A_7 + n_1 n_2^2 \gamma_1 A_3 A_7, \quad (7.26)$$

$$\theta_2 v_1 v_2^2 M_0 + \theta_2 v_1 M_2 + \theta_2 v_2^2 M_1 + \theta_2 M_3 + n_1 n_2^2 A_5 + \theta_1 v_2^2 n_1 \gamma_2 A_7 + \theta_1 n_1 \gamma_2 A_3 A_5 + \theta_1 n_1 \gamma_2 A_7 < n_1 n_2^2 \gamma_2 A_3 A_5 + n_1 n_2^2 \gamma_2 A_7 + \theta_1 n_1 A_5 + \theta_1 v_2^2 n_1 A_3 A_7, \quad (7.27)$$

$$\theta_2 v_1 v_2^2 M_1 + \theta_2 v_1 M_3 + \theta_2 v_2^2 M_2 + \theta_2 M_4 + \theta_1 v_2^2 n_1 \gamma_2 A_3 A_7 + \theta_1 n_1 \gamma_2 A_5 < n_1 n_2^2 \gamma_2 A_5 + \theta_1 v_2^2 n_1 A_3 A_5 + \theta_1 v_2^2 n_1 A_7, \quad (7.28)$$

$$\theta_2 v_1 v_2^2 M_2 + \theta_2 v_1 M_4 + \theta_2 v_2^2 M_3 + \theta_1 v_2^2 n_1 \gamma_2 A_3 A_5 < \theta_1 v_2^2 n_1 A_5. \quad (7.29)$$

7.4 Stability Analysis of the Mathematical Model

In this section we shall study the local stability and global stability behaviour for the equilbria of the mathematical model defined by equations(7.1)-(7.5).

7.4.1 Local Stability Analysis:

1. For Algal Vanishing Equilibrium Point $\breve{E}(\breve{C}, p\breve{H}, 0, \breve{D}, \breve{P})$:

For local stability analysis of the algal vanishing equilibrium point $\breve{E}$, we assume the following,

Suppose, $\breve{Z}_1 = \frac{1}{\tau_l} + a_1\breve{D}$, $\breve{Z}_2 = \frac{-pH_0}{(1+\breve{C})^2}$, $\breve{Z}_3 = \frac{\beta_1(1+\alpha_1\breve{C}-\alpha_2 p\breve{H})}{\beta_2} + \gamma_2\breve{D} - h$,
$\breve{Z}_4 = \frac{R}{\breve{D}} - \frac{n_1\breve{P}\breve{D}}{(v_1+\breve{D})^2}$, $\breve{Z}_5 = \frac{-n_1\breve{D}}{v_1+\breve{D}}$, $\breve{Z}_6 = \frac{2n_2\breve{D}\breve{P}}{v_2^2+\breve{D}^2} - \frac{2n_2\breve{P}\breve{D}^3}{(v_2^2+\breve{D}^2)^2}$, $\breve{Z}_7 = \theta_2\breve{P}$.

The characteristic equation corresponding to the Jacobian matrix at the algal vanishing equilibrium point $\breve{E}$ is given below,

$$(\breve{Z}_3 - \lambda)(\lambda^4 + \breve{A}_1\lambda^3 + \breve{A}_2\lambda^2 + \breve{A}_3\lambda + \breve{A}_4) = 0, \tag{7.30}$$

where

$$\breve{A}_1 = \breve{Z}_4 + \breve{Z}_7 + \breve{Z}_1 + \gamma_1,$$

$$\breve{A}_2 = \breve{Z}_1\gamma_1 + (\breve{Z}_1 + \gamma_1)(\breve{Z}_4 + \breve{Z}_7) + \breve{Z}_4\breve{Z}_7 - \breve{Z}_5\breve{Z}_6 - a_1^2\breve{C}\breve{D}$$

$$\breve{A}_3 = (\breve{Z}_1 + \gamma_1)(\breve{Z}_4\breve{Z}_7 - \breve{Z}_5\breve{Z}_6) + \breve{Z}_1\gamma_1(\breve{Z}_4 + \breve{Z}_7) - a_1^2\gamma_1\breve{C}\breve{D} - a_1^2\breve{Z}_7\breve{C}\breve{D},$$

$$\breve{A}_4 = \breve{Z}_1\gamma_1(\breve{Z}_4\breve{Z}_7 - \breve{Z}_5\breve{Z}_6) - a_1^2\breve{Z}_7\gamma_1\breve{C}\breve{D}.$$

Following the Routh-Hurwitz Criteria, the population vanishing equilibrium point will be locally asymptotically stable if the following conditions hold good,

$$\frac{\beta_1(1+\alpha_1\breve{C}-\alpha_2 p\breve{H})}{\beta_2} + \gamma_2\breve{D} - h < 0, \tag{7.31}$$

$$\breve{A}_1 > 0, \quad \breve{A}_2 > 0, \quad \breve{A}_3 > 0, \quad \breve{A}_4 > 0, \tag{7.32}$$

$$\breve{A}_1\breve{A}_2\breve{A}_3 - \breve{A}_3^{\,2} - \breve{A}_1^{\,2}\breve{A}_4 > 0. \tag{7.33}$$

2. For Population Vanishing Equilibrium Point $\hat{E}(\hat{C}, p\hat{H}, \hat{A}_g, \hat{D}, 0)$:

For local stability analysis of the population vanishing equilibrium point $\hat{E}$, we assume the following,

' Let $\hat{Z}_1 = \frac{1}{\tau_l} + a_1\hat{D}$, $\hat{Z}_2 = \frac{pH_0}{(1+\hat{C})^2}$, $\hat{Z}_3 = \frac{\beta_1\hat{A}_g\alpha_1}{\beta_2+\hat{A}_g}$, $\hat{Z}_4 = \frac{\beta_1\alpha_2\hat{A}_g}{\beta_2+\hat{A}_g}$,
$\hat{Z}_5 = \frac{\beta_1\hat{A}_g(1+\alpha_1\hat{C}-\alpha_2 p\hat{H})}{(\beta_2+\hat{A}_g)^2}$, $\hat{Z}_6 = \frac{R}{\hat{D}}$, $\hat{Z}_7 = \frac{n_1\hat{D}}{v_1+\hat{D}}$, $\hat{Z}_8 = \frac{n_2\hat{D}^2}{v_2+\hat{D}^2} - \theta_1$

The characteristic equation corresponding to the Jacobian matrix at the population vanishing equilibrium point $\hat{E}$ is given below,

$$(-\hat{Z}_8-\lambda)\Big[\lambda^4+\lambda^3(\hat{Z}_1+(\hat{Z}_5+\hat{Z}_6)+\gamma_1)+\lambda^2(\hat{Z}_1(\hat{Z}_5+\hat{Z}_6)+\gamma_1(\hat{Z}_5+\hat{Z}_6)+ \hat{Z}_5\hat{Z}_6+\psi_1\gamma_2\hat{A}_g\hat{D}+\gamma_1\hat{Z}_1-a_1^2\hat{C}\hat{D})+\lambda(\hat{Z}_1\hat{Z}_5\hat{Z}_6+\psi_1\gamma_2\hat{A}_g\hat{D}\hat{Z}_1+\hat{Z}_5\hat{Z}_6\gamma_1 +\psi_1\hat{A}_g\gamma_1\gamma_2\hat{D}+(\hat{Z}_5+\hat{Z}_6)\gamma_1\hat{Z}_1-a_1^2\hat{C}\hat{D}\gamma_1-a_1\psi_1\hat{Z}_3\hat{C}\hat{D}-a_1^2\hat{C}\hat{D}\hat{Z}_5)+ \gamma_1\hat{Z}_1\hat{Z}_5\hat{Z}_6+\gamma_1\hat{Z}_1\psi_1\gamma_2\hat{A}_g\hat{D}-\hat{Z}_3\psi_1a_1\gamma_1\hat{C}\hat{D}-a_1^2\gamma_1\hat{Z}_5\hat{C}\hat{D}-a_1\psi_1\hat{Z}_2\hat{Z}_4\hat{C}\hat{D}. \quad (7.34)$$

Following the Routh-Hurwitz Criteria, the population vanishing equilibrium point will be locally asymptotically stable if the following conditions hold good,

$$\frac{n_2\hat{D}^2}{v_2+\hat{D}^2}>\theta_1, \quad (7.35)$$

$$\hat{Z}_1(\hat{Z}_5+\hat{Z}_6)+\gamma_1(\hat{Z}_5+\hat{Z}_6)+\hat{Z}_5\hat{Z}_6+\psi_1\gamma_2\hat{A}_g\hat{D}+\gamma_1\hat{Z}_1-a_1^2\hat{C}\hat{D}>0, \quad (7.36)$$

$$\hat{Z}_1\hat{Z}_5\hat{Z}_6+\psi_1\gamma_2\hat{A}_g\hat{D}\hat{Z}_1+\hat{Z}_5\hat{Z}_6\gamma_1+\psi_1\hat{A}_g\gamma_1\gamma_2\hat{D}+(\hat{Z}_5+\hat{Z}_6)\gamma_1\hat{Z}_1-a_1^2\hat{C}\hat{D}\gamma_1 -a_1\psi_1\hat{Z}_3\hat{C}\hat{D}-a_1^2\hat{C}\hat{D}\hat{Z}_5>0, \quad (7.37)$$

$$\gamma_1\hat{Z}_1\hat{Z}_5\hat{Z}_6+\gamma_1\hat{Z}_1\psi_1\gamma_2\hat{A}_g\hat{D}-\hat{Z}_3\psi_1a_1\gamma_1\hat{C}\hat{D}-a_1^2\gamma_1\hat{Z}_5\hat{C}\hat{D}-a_1\psi_1\hat{Z}_2\hat{Z}_4\hat{C}\hat{D}>0, \quad (7.38)$$

$$(\hat{Z}_1+(\hat{Z}_5+\hat{Z}_6)+\gamma_1)(\hat{Z}_1(\hat{Z}_5+\hat{Z}_6)+\gamma_1(\hat{Z}_5+\hat{Z}_6)+\hat{Z}_5\hat{Z}_6+\psi_1\gamma_2\hat{A}_g\hat{D}+\gamma_1\hat{Z}_1 -a_1^2\hat{C}\hat{D})(\hat{Z}_1\hat{Z}_5\hat{Z}_6+\psi_1\gamma_2\hat{A}_g\hat{D}\hat{Z}_1+\hat{Z}_5\hat{Z}_6\gamma_1+\psi_1\hat{A}_g\gamma_1\gamma_2\hat{D}+(\hat{Z}_5+\hat{Z}_6)\gamma_1\hat{Z}_1- a_1^2\hat{C}\hat{D}\gamma_1-a_1\psi_1\hat{Z}_3\hat{C}\hat{D}-a_1^2\hat{C}\hat{D}\hat{Z}_5)-(\hat{Z}_1\hat{Z}_5\hat{Z}_6+\psi_1\gamma_2\hat{A}_g\hat{D}\hat{Z}_1+\psi_1\hat{A}_g\gamma_1\gamma_2\hat{D}+ \hat{Z}_5\hat{Z}_6\gamma_1+(\hat{Z}_5+\hat{Z}_6)\gamma_1\hat{Z}_1-a_1^2\hat{C}\hat{D}\gamma_1-a_1\psi_1\hat{Z}_3\hat{C}\hat{D}-a_1^2\hat{C}\hat{D}\hat{Z}_5)^2-(\hat{Z}_1+(\hat{Z}_5+\hat{Z}_6)+\gamma_1)^2 (\gamma_1\hat{Z}_1\hat{Z}_5\hat{Z}_6+\gamma_1\hat{Z}_1\psi_1\gamma_2\hat{A}_g\hat{D}-\hat{Z}_3\psi_1a_1\gamma_1\hat{C}\hat{D}-a_1^2\gamma_1\hat{Z}_5\hat{C}\hat{D}-a_1\psi_1\hat{Z}_2\hat{Z}_4\hat{C}\hat{D})>0. \quad (7.39)$$

Theorem 7.4.1. *The interior equilibrium point E^* shall be locally asymptotically stable provided that the below given inequalities are satisfied:*

$$4(\frac{1}{\tau_l}+a_1D)\left(\psi_0+a_1C+A_g\psi_1+\frac{n_1v_1P}{(v_1+D)(v_1+D^*)}\right)>9(a_1C^*+a_1D^*)^2,$$

$$2(\frac{1}{\tau_l}+a_1D)\gamma_1>3\left(\frac{pH_0}{(1+C^*)(1+C)^2}\right)^2,$$

$$4(\frac{1}{\tau_l}+a_1D)\left(\frac{h-\gamma_2 D}{A_g^*}-\frac{\beta_1\beta_2(1+\alpha_1C-\alpha_2pH)}{A_g^*(A_g+\beta_2)(A_g^*+\beta_2)}\right)>9\left(\frac{\alpha_1\beta_1}{A_g^*+\beta_2}\right)^2,$$

$$2\gamma_1\left(\frac{h-\gamma_2 D}{A_g^*}-\frac{\beta_1\beta_2(1+\alpha_1C-\alpha_2pH)}{A_g^*(A_g+\beta_2)(A_g^*+\beta_2)}\right)>3\left(\frac{\alpha_2\beta_1}{A_g^*+\beta_2}\right)^2,$$

$$4\left(\frac{h-\gamma_2 D}{A_g^*}-\frac{\beta_1\beta_2(1+\alpha_1C-\alpha_2pH)}{A_g^*(A_g+\beta_2)(A_g^*+\beta_2)}\right)(\psi_0+a_1C+A_g\psi_1+$$

$$\frac{n_1v_1P}{(v_1+D)(v_1+D^*)})>9(\psi_1D^*-\gamma_2)^2,$$

$$4\left(\psi_0+a_1C+A_g\psi_1+\frac{n_1v_1P}{(v_1+D)(v_1+D^*)}\right)\left(\frac{\theta_2P}{P^*}\right)>$$

$$3\left(\frac{n_1D^*}{v_1+D^*}-\frac{n_2v_2^2DP}{P^*(v_2^2+D^2)(v_2^2+D^{*2})}\right)^2.$$

Proof. In order to study the local stability of interior equilibrium point E^* by Lyapunov's direct menthod, we linearise the system given by equations (7.1)-(7.5) about E^* by using the transformations as given below:

$$C=C^*+z_1;\quad pH=pH^*+z_2;\quad A_g=A_g^*+z_3;\quad D=D^*+z_4;\quad P=P^*+z_5.$$

Consider the following positive definite function:

$$\zeta=\frac{1}{2}z_1^2+\frac{1}{2}z_2^2+\frac{1}{2A_g^*}z_3^2+\frac{1}{2}z_4^2+\frac{1}{2P^*}z_5^2 \tag{7.40}$$

Differentiating ζ with respect to time t along the solutions corresponding to the linearized system of equations (7.1)-(7.5) we get,

$$\frac{d\zeta}{dt}=-[a_{11}z_1^2+a_{22}z_2^2+a_{33}z_3^2+a_{44}z_4^2+a_{55}z_5^2+a_{14}z_1z_4+a_{12}z_1z_2+ a_{13}z_1z_3+a_{23}z_2z_3+a_{34}z_3z_4+a_{45}z_4z_5], \tag{7.41}$$

where $a_{11}=\frac{1}{\tau_l}+a_1D$, $a_{22}=\gamma_1$, $a_{33}=\frac{h-\gamma_2D}{A_g^*}-\frac{\beta_1\beta_2(1+\alpha_1C-\alpha_2pH)}{A_g^*(A_g+\beta_2)(A_g^*+\beta_2)}$
$a_{44}=\psi_0+a_1C+A_g\psi_1+\frac{n_1v_1P}{(v_1+D)(v_1+D^*)}$, $a_{55}=\frac{\theta_2P}{P^*}$, $a_{14}=a_1C^*+a_1D^*$,
$a_{12}=\frac{pH_0}{(1+C^*)(1+C)^2}$, $a_{13}=-\frac{\alpha_1\beta_1}{A_g^*+\beta_2}$, $a_{23}=\frac{\alpha_2\beta_1}{A_g^*+\beta_2}$, $a_{34}=\psi_1D^*-\gamma_2$,
$a_{45}=\frac{n_1D^*}{v_1+D^*}-\frac{n_2v_2^2DP}{P^*(v_2^2+D^2)(v_2^2+D^{*2})}$.

According to Sylvestor Criteria, $\frac{d\zeta}{dt}$ shall be negative definite, and thus E^* will be locally asymptotically stable only if the below given inequalities hold true,

$$4a_{11}a_{44} > 9a_{14}^2, \quad 2a_{11}a_{22} > 3a_{12}^2, \quad 4a_{11}a_{33} > 9a_{13}^2, \quad 2a_{22}a_{33} > 3a_{23}^2,$$

$$4a_{33}a_{44} > 9a_{34}^2, \quad 4a_{44}a_{55} > 3a_{45}^2,$$

i.e.

$$4(\frac{1}{\tau_l}+a_1D)\left(\psi_0 + a_1C + A_g\psi_1 + \frac{n_1v_1P}{(v_1+D)(v_1+D^*)}\right) > 9(a_1C^*+a_1D^*)^2, \quad (7.42)$$

$$2(\frac{1}{\tau_l}+a_1D)\gamma_1 > 3\left(\frac{pH_0}{(1+C^*)(1+C)^2}\right)^2, \quad (7.43)$$

$$4(\frac{1}{\tau_l}+a_1D)\left(\frac{h-\gamma_2D}{A_g^*} - \frac{\beta_1\beta_2(1+\alpha_1C-\alpha_2pH)}{A_g^*(A_g+\beta_2)(A_g^*+\beta_2)}\right) > 9\left(\frac{\alpha_1\beta_1}{A_g^*+\beta_2}\right)^2, \quad (7.44)$$

$$2\gamma_1\left(\frac{h-\gamma_2D}{A_g^*} - \frac{\beta_1\beta_2(1+\alpha_1C-\alpha_2pH)}{A_g^*(A_g+\beta_2)(A_g^*+\beta_2)}\right) > 3\left(\frac{\alpha_2\beta_1}{A_g^*+\beta_2}\right)^2, \quad (7.45)$$

$$4\left(\frac{h-\gamma_2D}{A_g^*} - \frac{\beta_1\beta_2(1+\alpha_1C-\alpha_2pH)}{A_g^*(A_g+\beta_2)(A_g^*+\beta_2)}\right)(\psi_0+a_1C+A_g\psi_1+ \frac{n_1v_1P}{(v_1+D)(v_1+D^*)}) > 9(\psi_1D^*-\gamma_2)^2, \quad (7.46)$$

$$4\left(\psi_0 + a_1C + A_g\psi_1 + \frac{n_1v_1P}{(v_1+D)(v_1+D^*)}\right)\left(\frac{\theta_2P}{P^*}\right) > 3\left(\frac{n_1D^*}{v_1+D^*} - \frac{n_2v_2^2DP}{P^*(v_2^2+D^2)(v_2^2+D^{*2})}\right)^2. \quad (7.47)$$

This leads to the completion of theorem 7.4.1. □

7.4.2 Global Stability

Theorem 7.4.2. *The set* $\varpi = \{(C, pH, A_g, D, P) \in R_+^5 : 0 < C < C_u,$ $0 < pH < pH_u, 0 < A_g < A_{gu}, 0 < D < D_u, 0 < P < P_u$ *where* $C_u = \tau_l E + C_0, pH_u = \frac{pH_0}{\gamma_1}, A_{gu} = \frac{\beta_1\alpha_1C_u}{\beta_1+\gamma_2D_u-h}, D_u = \frac{R}{\psi_0}, P_u = \frac{n_2}{\theta_2}$. *is a positively invariant set for positive initial values* $(C(0), pH(0), A_g(0), D(0), P(0)) \in R_+^5$. *The set* ϖ *is the region of attraction for the system of equations represented by equations(7.1)-(7.5).*

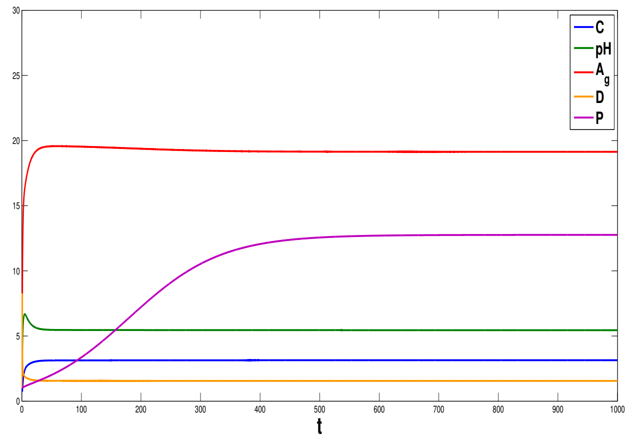

Figure 7.1: Time series graph of model trajectories exhibiting stability of interior equilibrium point.

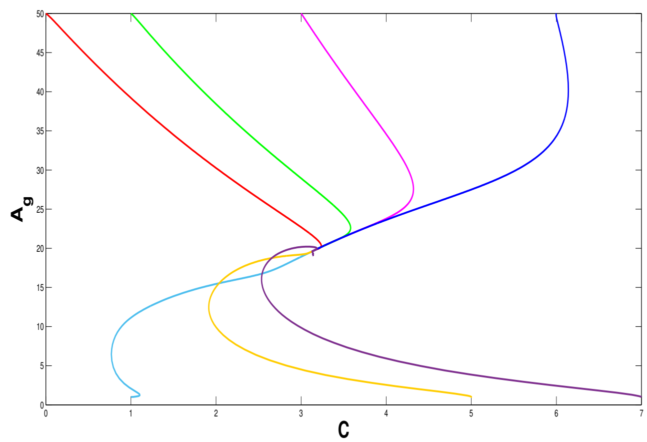

Figure 7.2: Phase Plane Graph between C and A_g exhibiting global stability for varying initial conditions

Proof. For the system of equations represented by equations(7.1)-(7.5), in phase space $CpHA_gDP$, let us consider a box ϖ with one of its vertex lying at the origin and an other vertex lying at a point $\sigma = (\bar{C}, p\bar{H}, \bar{A}_g, \bar{D}, \bar{P})$ where σ is a point located outside the box ϖ and $\bar{C} > C_u, p\bar{H} > pH_u, \bar{A}_g > A_{gu}, \bar{D} > D_u$ and $\bar{P} > P_u$.

For each face of the box ϖ, which does not lie in the coordinate planes, we shall

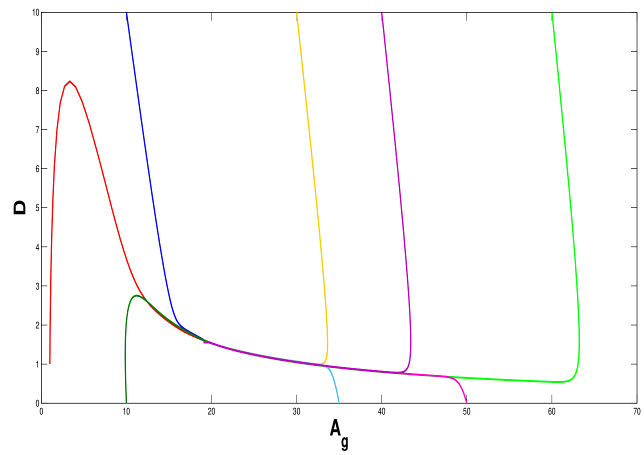

Figure 7.3: Phase Plane Graph between A_g and exhibiting global stability for varying initial conditions

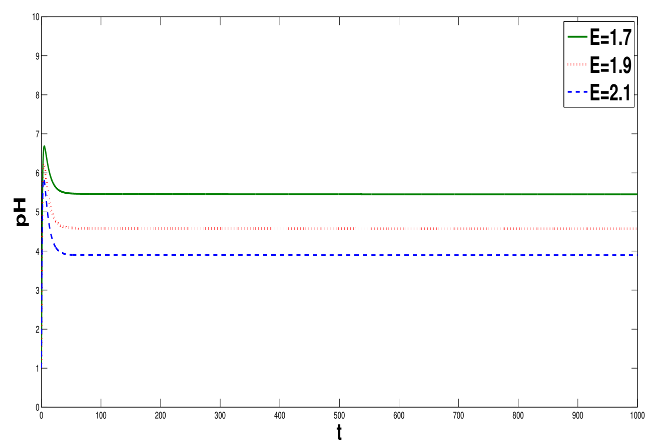

Figure 7.4: Equilibrium level of pH for increase in value of E

calculate angle of flow. For the planes denoted by $\pi_1 : C = \bar{C}, \pi_2 : pH = p\bar{H}, \pi_3 : A_g = \bar{A}_g, \pi_4 : D = \bar{D}, \pi_5 : P = \bar{P}$, let $\chi_1, \chi_2, \chi_3, \chi_4$ and χ_5 be the outward normal unit vectors, in reference to ϖ.
From equation (7.5) we have,

$$\chi_5 \frac{d\sigma}{dt}|\pi_5 \leq n_2\bar{P} - \theta_1\bar{P} - \theta_2\bar{P}^2$$

. We have $\bar{P} > P_u = \frac{n_2}{\theta_2}$,

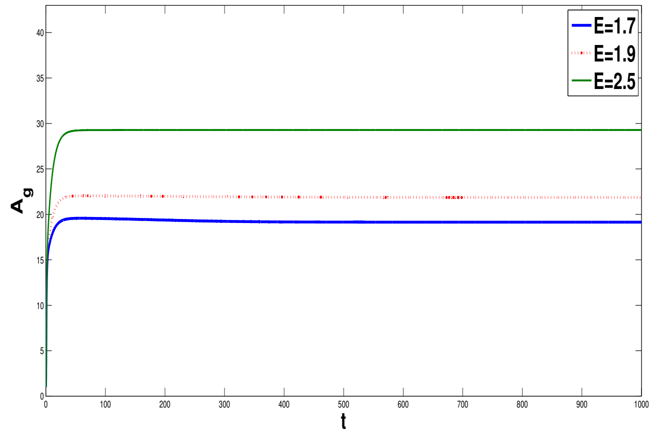

Figure 7.5: Equilibrium density of algal population (A_g) for increase in value of E

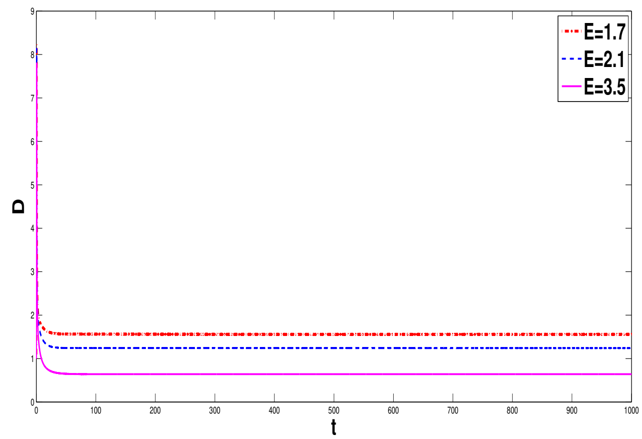

Figure 7.6: Equilibrium concentration of dissolved oxygen(D) for increase in value of E

hence, we get,

$$\chi_5 \frac{d\sigma}{dt}|\pi_5 \leq 0$$

. Similarly, we can also prove that,

$$\chi_1 \frac{d\sigma}{dt}|\pi_1 \leq 0, \chi_2 \frac{d\sigma}{dt}|\pi_2 \leq 0, \chi_3 \frac{d\sigma}{dt}|\pi_3 \leq 0, \chi_4 \frac{d\sigma}{dt}|\pi_4 \leq 0$$

Hence, we prove that the set ϖ is the region of attraction for the system of equa-

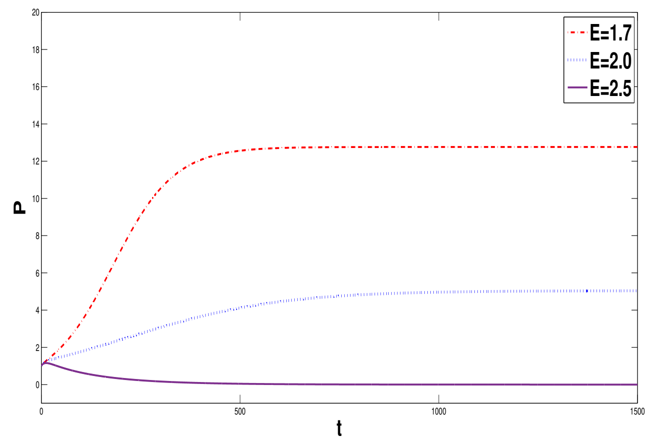

Figure 7.7: Equilibrium density of population (P) for increase in value of E

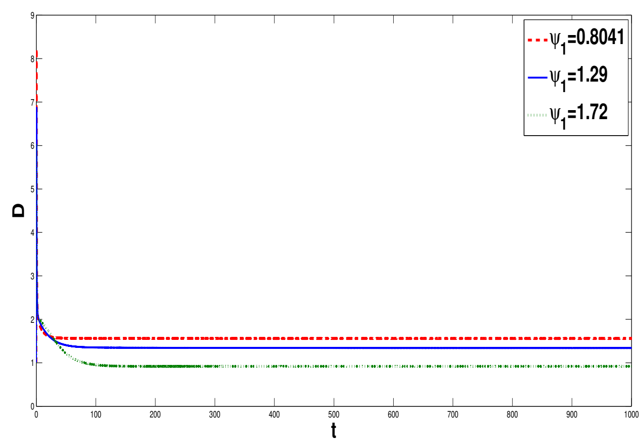

Figure 7.8: Equilibrium density of Dissolved oxygen for increase in value of ψ_1.

tions represented by equations(7.1)-(7.5). In the next theorem, we prove that E^* is the only global attractor inside ϖ. □

Theorem 7.4.3. *The interior equilibrium point E^* shall be globally asymptotically stable provided that the below given inequalities are satisfied:*

$$4(\frac{1}{\tau_l} + a_1 D)\left(\psi_0 + a_1 C + A_g\psi_1 + \frac{n_1 v_1 P}{(v_1 + D)(v_1 + D^*)}\right) > 9(a_1 C^* + a_1 D^*)^2,$$

$$2(\frac{1}{\tau_l} + a_1 D)\gamma_1 > 3\left(\frac{pH_0}{(1+C^*)(1+C)}^2\right)^2,$$

$$4(\frac{1}{\tau_l} + a_1 D)\left(\frac{\beta_1(1+\alpha_1 C^* - \alpha_2 pH^*)}{(A_g+\beta_2)(A_g^*+\beta_2)}\right) > 9\left(\frac{\alpha_1\beta_1}{A_g+\beta_2}\right)^2,$$

$$2\gamma_1\left(\frac{\beta_1(1+\alpha_1 C^* - \alpha_2 pH^*)}{(A_g+\beta_2)(A_g^*+\beta_2)}\right) > 3\left(\frac{\alpha_2\beta_1}{A_g+\beta_2}\right)^2,$$

$$4\left(\frac{\beta_1(1+\alpha_1 C^* - \alpha_2 pH^*)}{(A_g+\beta_2)(A_g^*+\beta_2)}\right)(\psi_0 + a_1 C + A_g\psi_1 +$$

$$\frac{n_1 v_1 P}{(v_1+D)(v_1+D^*)}) > 9(\psi_1 D^* - \gamma_2)^2,$$

$$4\left(\psi_0 + a_1 C + A_g\psi_1 + \frac{n_1 v_1 P}{(v_1+D)(v_1+D^*)}\right)(\theta_2) >$$

$$3\left(\frac{n_1 D^*}{v_1+D^*} - \frac{n_2 v_2^2 D}{(v_2^2+D^2)(v_2^2+D^{*2})}\right)^2.$$

Proof. In order to study the global stability of interior equilibrium point E^* we consider the following positive definite function:

$$\phi = \frac{1}{2}(C-C^*)^2 + \frac{1}{2}(pH-pH^*)^2 + \left(A_g - A_g^* - A_g^* ln\frac{A_g}{A_g^*}\right)$$
$$+ \frac{1}{2}(D-D^*)^2 + \left(P - P^* - P^* ln\frac{P}{P^*}\right) \quad (7.48)$$

Differentiating ϕ with respect to time t we get,

$$\frac{d\phi}{dt} = -[b_{11}(C-C^*)^2 + b_{22}(pH-pH^*)^2 + b_{33}(A_g-A_g^*)^2 + b_{44}(D-D^*)^2$$
$$+ b_{55}(P-P^*)^2 + b_{14}(C-C^*)(D-D^*) + b_{12}(C-C^*)(pH-pH^*)$$
$$+ b_{13}(C-C^*)(A_g-A_g^*) + b_{23}(pH-pH^*)(A_g-A_g^*) +$$
$$b_{34}(A_g-A_g^*)(D-D^*) + b_{45}(D-D^*)(P-P^*)], \quad (7.49)$$

where $b_{11} = \frac{1}{\tau_l} + a_1 D$, $b_{22} = \gamma_1$, $b_{33} = \frac{\beta_1(1+\alpha_1 C^* - \alpha_2 pH^*)}{(A_g+\beta_2)(A_g^*+\beta_2)}$
$b_{44} = \psi_0 + a_1 C + A_g\psi_1 + \frac{n_1 v_1 P}{(v_1+D)(v_1+D^*)}$, $b_{55} = \theta_2$ $b_{14} = a_1 C^* + a_1 D^*$,
$b_{12} = \frac{pH_0}{(1+C^*)(1+C)}$, $b_{13} = -\frac{\alpha_1\beta_1}{A_g+\beta_2}$, $b_{23} = \frac{\alpha_2\beta_1}{A_g+\beta_2}$, $a_{34} = \psi_1 D^* - \gamma_2$,
$b_{45} = \frac{n_1 D^*}{v_1+D^*} - \frac{n_2 v_2^2 D}{(v_2^2+D^2)(v_2^2+D^{*2})}$.

According to Sylvestor Criteria, $\frac{d\phi}{dt}$ shall be negative definite, and thus E^* will be globally asymptotically stable only if the below given inequalities hold true,

$$4b_{11}b_{44} > 9b_{14}^2, \quad 2b_{11}b_{22} > 3b_{12}^2, \quad 4b_{11}b_{33} > 9b_{13}^2, \quad 2b_{22}b_{33} > 3b_{23}^2,$$
$$4b_{33}b_{44} > 9b_{34}^2, \quad 4b_{44}b_{55} > 3b_{45}^2,$$

i.e.

$$4(\frac{1}{\tau_l}+a_1D)\left(\psi_0 + a_1C + A_g\psi_1 + \frac{n_1v_1P}{(v_1+D)(v_1+D^*)}\right) > 9(a_1C^*+a_1D^*)^2, \quad (7.50)$$

$$2(\frac{1}{\tau_l}+a_1D)\gamma_1 > 3\left(\frac{pH_0}{(1+C^*)(1+C)}^2\right)^2, \quad (7.51)$$

$$4(\frac{1}{\tau_l}+a_1D)\left(\frac{\beta_1(1+\alpha_1C^*-\alpha_2pH^*)}{(A_g+\beta_2)(A_g^*+\beta_2)}\right) > 9\left(\frac{\alpha_1\beta_1}{A_g+\beta_2}\right)^2, \quad (7.52)$$

$$2\gamma_1\left(\frac{\beta_1(1+\alpha_1C^*-\alpha_2pH^*)}{(A_g+\beta_2)(A_g^*+\beta_2)}\right) > 3\left(\frac{\alpha_2\beta_1}{A_g+\beta_2}\right)^2, \quad (7.53)$$

$$4\left(\frac{\beta_1(1+\alpha_1C^*-\alpha_2pH^*)}{(A_g+\beta_2)(A_g^*+\beta_2)}\right)(\psi_0 + a_1C + A_g\psi_1 + \frac{n_1v_1P}{(v_1+D)(v_1+D^*)}) > 9(\psi_1D^*-\gamma_2)^2, \quad (7.54)$$

$$4\left(\psi_0 + a_1C + A_g\psi_1 + \frac{n_1v_1P}{(v_1+D)(v_1+D^*)}\right)(\theta_2) > 3\left(\frac{n_1D^*}{v_1+D^*} - \frac{n_2v_2^2D}{(v_2^2+D^2)(v_2^2+D^{*2})}\right)^2. \quad (7.55)$$

This leads to the completion of theorem 7.4.3. □

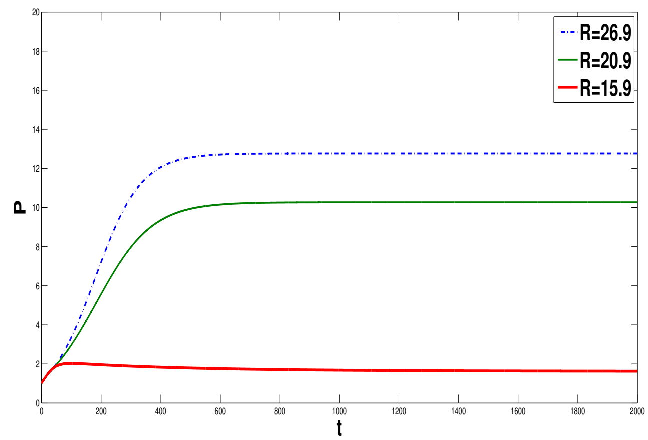

Figure 7.9: Equilibrium density of population (P) for decrease in value of R

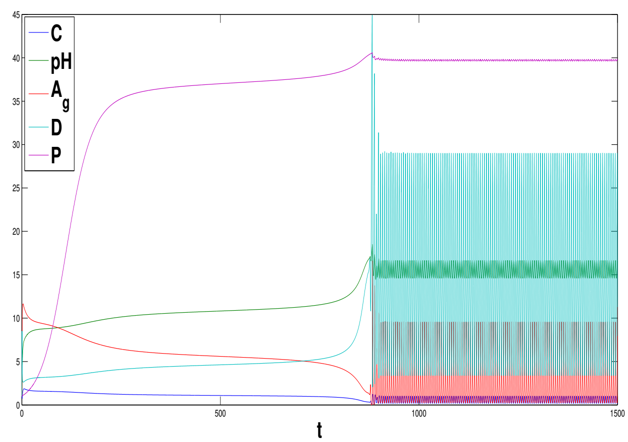

Figure 7.10: Trajectories for mathematical model showing the existence of limit cycles at h=0.952

7.5 Numerical Simulation and Discussion

In this section, we perform the numerical simulations so that the analytical results obtained for the mathematical model represented by equations (7.1)-(7.5) are supported. We consider the below mentioned values for the parameters considered in

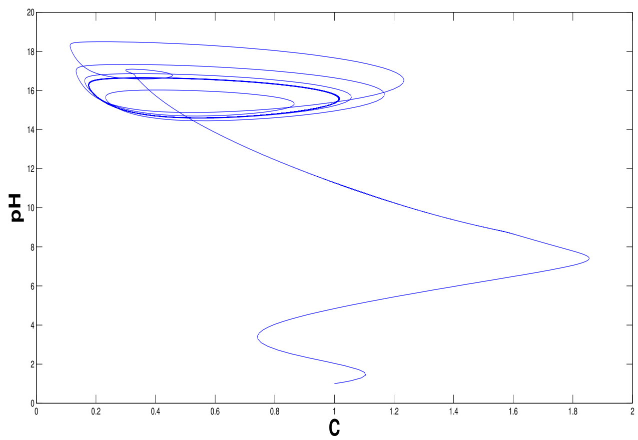

Figure 7.11: Phase potrait between C and pH showing the existence of limit cycles for h=0.952

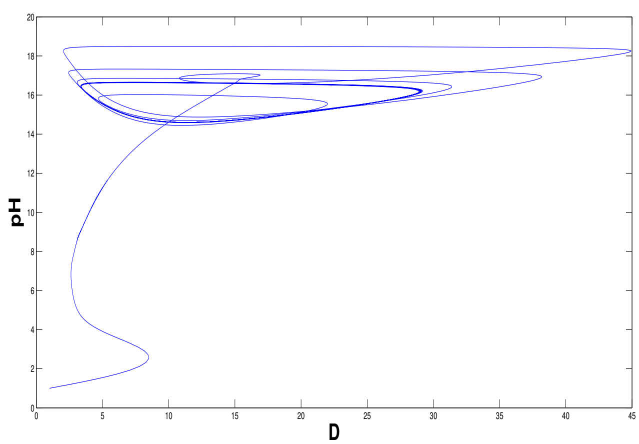

Figure 7.12: Phase potrait between D and pH showing the existence of limit cycles for h=0.952

our model:

$$E = 1.7, \tau_l = 50, C_0 = 2.6, a_1 = 0.345, pH_0 = 7.0, n_1 = 0.0985, \gamma_1 = 0.31,$$
$$\beta_1 = 1.608, \alpha_1 = 0.85, \alpha_2 = 0.57, \beta_2 = 1.0, \gamma_2 = 0.43, h = 0.715, R = 26.9$$
$$\psi_0 = 0.3, \psi_1 = 0.8041, v_1 = 1.0, n_2 = 0.0985, v_2 = 1.0, \theta_1 = 0.057, \theta_2 = 0.001. \tag{7.56}$$

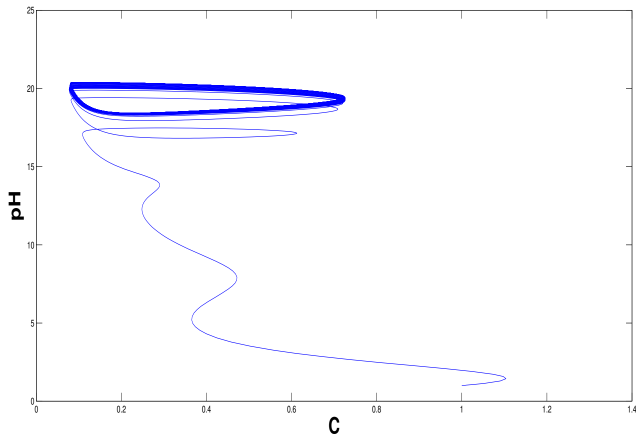

Figure 7.13: Phase potrait between C and pH showing the existence of limit cycles for h=3.956

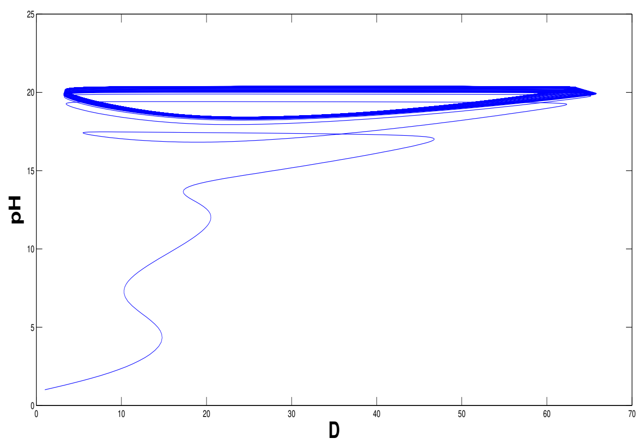

Figure 7.14: Phase potrait between D and pH showing the existence of limit cycles for h=3.956

The equilibrium values obtained for the variables considered in our model for the above stated set of parameter values given by equation (7.56) are :

$$C^* = 3.1424, pH^* = 5.4511, A_g^* = 19.1382, D^* = 1.5587, P^* = 12.7626. \quad (7.57)$$

For the parametric values and equilibrium values corresponding to the model given

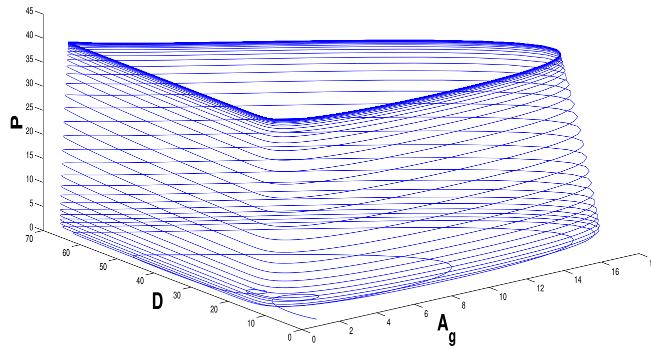

Figure 7.15: Phase potrait between A_g, D and P showing the existence of limit cycles for h=3.956

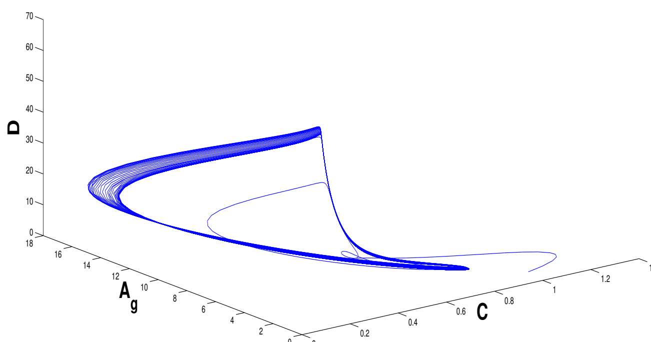

Figure 7.16: Phase potrait between C, A_g and D showing the existence of limit cycles for h=3.956

by equations (7.56) and (7.57),it is found that the conditions for existence given by equations(7.18)-(7.29) are satisfied.
It is further noticed from the numerical simulations that the conditions for boundedness, positivity and stability corresponding to the interior equilibrium point E^* given by equations (7.6), (7.42)-(7.47), (7.50)-(7.55) are satisfied. Hence, we can

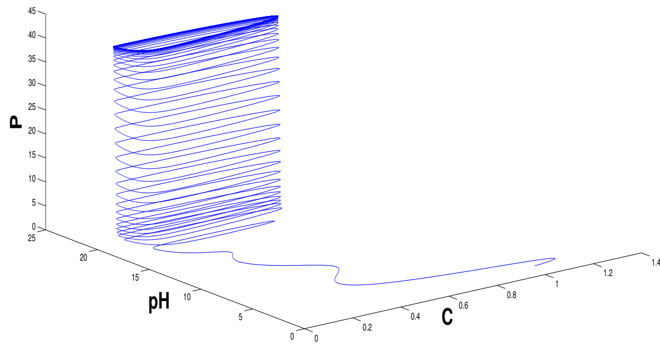

Figure 7.17: Phase potrait between C, pH and P showing the existence of limit cycles for h=3.956

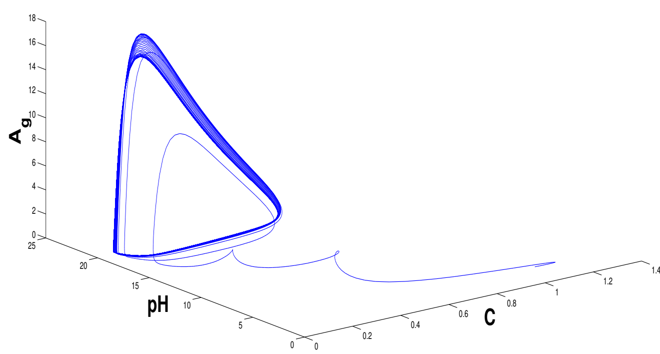

Figure 7.18: Phase potrait between C, pH and A_g showing the existence of limit cycles for h=3.956

deduce that the interior equilibrium point E^* is asymptotically stable for the model parameter values given by equation (7.56). The local stability behaviour of E^* is shown by figure 7.1. Figures 7.2 and 7.3 demonstrate the global stability of E^* showing that all trajectories initiating from different initial values converge to the equilibrium point.

From the stability analysis, it is shown the pH of water decreases as the carbon concentration in water rises which is supported by equation (7.19). Figure 7.4 also shows that as the value of input rate of carbon in water (E) increases, the water becomes more acidic due to formation of carbonic acid and consequently the pH level of water declines. Also, it is shown by figure 7.5 that as the rate of input of carbon components in water (E) rises, the density of algal population also increases. The increase of carbon concentration implies elevated acidity and global warming. In turn, the acidic and warmer waters with high algal growth lead to drop in level of concentration of dissolved oxygen (D) in water as shown by figure 7.6. Further, since the population is dependent on dissolved oxygen for its existence survival, the increase in carbon components also affects the population growth negatively as shown in figure 7.7. Moreover, it can be seen in figure 7.8, that as the value of consumption rate of dissolved oxygen in the algal decomposition process (ψ_1) increases, the equilibrium level of dissolved oxygen concentration declines. Thus, excessive growth of algal blooms can lead to scarcity of dissolved oxygen in water. Furthermore, the excessively grown algal population forms a layer over water and hinders the penetration of dissolved oxygen in the interior parts of the water body. This leads to a situation of insufficient oxygen concentration being available for the aquatic species to survive. The situation of hypoxia, hence pushes the aquatic population towards a state of mass deaths or in worst cases, extinction. This is shown by figure 7.9 that as input rate of dissolved oxygen in water (R) decreases, population density also decreases.

It is further observed that as the value of the algal decay rate (h) is increased to 0.952 and above, keeping the other parameters as given in equation (7.56) unchanged, the stable solutions for the model defined by equations (7.1)-(7.5) transform into oscillatory solutions as shown in figures 7.10, 7.11, and 7.12. Thus, it can be inferred that with the increase in rate of algal decomposition (h) to 0.952 and above, the system bifurcates to a stable limit cycle periodic solution and Hopf-bifurcations are observed as shown in figures 7.13, 7.14, 7.15, 7.16, 7.17 and 7.18.

7.6 Conclusion

From our study, we conclude that simultaneous impacts of environmental pressures such as rising carbon emissions, eutrophication, increasing algal bloom density in water can have far-reaching and devastating consequences for the aquatic ecosystem. These stressors can lead the ecosystem to state of hypoxia which can be very hazardous for the existence, growth and survival of the aquatic populations [80, 94]. The study done by San Diego-McGlone et al. [82] regarding the fish kill event of 2002 in the coastal waters of Bolino, Phillipines owing to low oxygen levels due to increased eutrophication, also support the results of our study. The dissolved oxygen level obtained in their study which led to fish kills was around 2.0. However, since in our study we are considering the simultaneous effects of increased carbon emissions, eutrophication and increased algal bloom concentration, we obtain a dissolved oxygen equilibrium level at 1.5587, which is lower than that available in the study by San Diego-McGlone et al. [82]. Thus, we can further conclude that in comparison with the individual impact of each environmental stressor, the simulatneous effects of all these pressures can cause more havoc in the aquatic ecosystem. Thus, immediate measures need to be devised to curb these environmental hazards which are polluting and deteriorating the aquatic ecosystem.

Bibliography

[1] A.E. Eissa, M.M. Zaki, The impact of global climatic changes on the aquatic environment, Procedia Environ. Sci. 4 (2011) 251-259. https://doi.org/10.1016/j.proenv.2011.03.030.

[2] Y. Sekerci, S. Petrovskii, Mathematical Modelling of Plankton-Oxygen Dynamics Under the Climate Change, Bull. Math. Biol. 77 (2015) 2325-2353. https://doi.org/10.1007/s11538-015-0126-0.

[3] A. K. Misra, Mathematical modelling and analysis of eutrophication of water bodies caused by nutrients, Nonlinear Anal. Model. Control. 12 (2007) 511-524. http://www.lana.lt/journal/27/Misra.pdf.

[4] M. Meerhoff, J.M. Clemente, F.T. de Mello, C. Iglesias, A.R. Pedersen, E. Jeppesen, Can warm climate-related structure of littoral predator assemblies weaken the clear water state in shallow lakes?, Glob. Chang. Biol. 13 (2007) 1888-1897. https://doi.org/10.1111/j.1365-2486.2007.01408.x.

[5] S. Brucet, D. Boix, X.D. Quintana, E. Jensen, L.W. Nathansen, C. Trochine, M. Meerhoff, S. Gasc Jeppesen, Factors influencing zooplankton size structure at contrasting temperatures in coastal shallow lakes: Implications for effects of climate change, Limnol. Oceanogr. 55 (2010) 1697-1711. https://doi.org/10.4319/lo.2010.55.4.1697.

[6] F.X. Fu, A.O. Tatters, D.A. Hutchins, Global change and the future of harmful algal blooms in the ocean, Mar. Ecol. Prog. Ser. 470 (2012) 207-233. https://doi.org/10.3354/meps10047.

[7] O. Kellie-Smith, P.M. Cox, Emergent dynamics of the climate-economy system in the anthropocene, Philos. Trans. R. Soc. A Math. Phys. Eng. Sci. 369 (2011) 868-886. https://doi.org/10.1098/rsta.2010.0305.

[8] J.L. Meyer, M.J. Sale, P.J. Muiholland, N.L. Poff, Impacts of climate change on aquatic ecosystem functioning and health, J. Am. Water Resour. Assoc. 35 (1999) 1373-1386. https://doi.org/10.1111/j.1752-1688.1999.tb04222.x.

[9] P.E. Hulme, Adapting to climate change: is there scope for ecological management in the face of a global threat?, J. Appl. Ecol. 42 (2005) 784-794. https://doi.org/10.1111/j.1365-2664.2005.01082.x.

[10] C.D.G. Harley, A.R. Hughes, K.M. Hultgren, B.G. Miner, C.J.B. Sorte, C.S. Thornber, L.F. Rodriguez, L. Tomanek, S.L. Williams, The impacts of climate change in coastal marine systems, Ecol. Lett. 9 (2006) 228-241. https://doi.org/10.1111/j.1461-0248.2005.00871.x.

[11] B.R. Mackenzie, H. Gislason, C. Mllmann, F.W. Kster, Impact of 21st century climate change on the Baltic Sea fish community and fisheries, Glob. Chang. Biol. 13 (2007) 1348-1367. https://doi.org/10.1111/j.1365-2486.2007.01369.x.

[12] T. Gamo, Y. Nozaki, H. Sakai, T. Nakai, H. Tsubota, Spacial and temporal variations of water characteristics in the Japan Sea bottom layer, J. Mar. Res. 44 (1986) 781-793. https://doi.org/10.1357/002224086788401620.

[13] M.K. Kundzewicz ZW, Mata LJ, Arnell NW, Dll PK, Jimz B, The implications of projected climate change for freshwater resources and their management The implications of projected climate change for freshwater resources and their management, Hydrol. Sci. J. 1 (2008) 3-10. https://doi.org/10.1623/hysj.53.1.3.

[14] I.M. Sokolova, G. Lannig, Interactive effects of metal pollution

and temperature on metabolism in aquatic ectotherms: Implications of global climate change, Clim. Res. 37 (2008) 181-201. https://doi.org/10.3354/cr00764.

[15] C. Vadadi-Flp, C. Sipkay, G. Ms, L. Hufnagel, Climate change and freshwater zooplankton: What does it boil down to?, Aquat. Ecol. 46 (2012) 501-519. https://doi.org/10.1007/s10452-012-9418-8.

[16] M. Collins, S. Il An, W. Cai, A. Ganachaud, E. Guilyardi, F.F. Jin, M. Jochum, M. Lengaigne, S. Power, A. Timmermann, G. Vecchi, A. Wittenberg, The impact of global warming on the tropical Pacific Ocean and El N-o, Nat. Geosci. 3 (2010) 391-397. https://doi.org/10.1038/ngeo868.

[17] O. Hoegh-guldberg, The Impact of Climate Change on the, Ecol. Res. 1523 (2010) 1523-1529. https://doi.org/10.1126/science.1189930.

[18] R. Danovaro, A. Dell-Anno, M. Fabiano, A. Pusceddu, A. Tselepides, Deep-sea ecosystem response to climate changes: the eastern Mediterranean case study, Trends Ecol. Evol. 16 (2001) 505-510. https://doi.org/10.1016/S0169-5347(01)02215-7.

[19] J. Carstensen, J.H. Andersen, B.G. Gustafsson, D.J. Conley, Deoxygenation of the Baltic Sea during the last century, Proc. Natl. Acad. Sci. 111 (2014) 5628-5633. https://doi.org/10.1073/pnas.1323156111.

[20] C. Le Qu, C. Rdenbeck, E.T. Buitenhuis, T.J. Conway, R. Langenfelds, A. Gomez, C. Labuschagne, M. Ramonet, T. Nakazawa, N. Metzl, N. Gillett, Saturation of the Southern Ocean CO2 sink due to recent climate change. Science 316 (2007), 1735-1738. https://doi.org/10.1126/science.1136188.

[21] T. Okunishi, S. ichi Ito, T. Hashioka, T.T. Sakamoto, N. Yoshie, H. Sumata, Y. Yara, N. Okada, Y. Yamanaka, Impacts of climate change on growth, migration and recruitment success of Japanese sardine (Sardinops melanostictus) in

the western North Pacific, Clim. Change. 115 (2012) 485-503. https://doi.org/10.1007/s10584-012-0484-7.

[22] S.R. Kibler, P.A. Tester, K.E. Kunkel, S.K. Moore, R.W. Litaker, Effects of ocean warming on growth and distribution of dinoflagellates associated with ciguatera fish poisoning in the Caribbean, Ecol. Modell. 316 (2015) 194-210. https://doi.org/10.1016/j.ecolmodel.2015.08.020.

[23] C. Deutsch, A. Ferrel, B. Seibel, H.O. Prtner, R.B. Huey, Climate change tightens a metabolic constraint on marine habitats. Science, 348 (2015) 1132-1135. https://doi.org/10.1126/science.aaa1605.

[24] E. Specht, T. Redemann, N. Lorenz, Simplified mathematical model for calculating global warming through anthropogenic CO2, Int. J. Therm. Sci. 102 (2016) 1-8. https://doi.org/10.1016/j.ijthermalsci.2015.10.039.

[25] P.J. Gleckler, P.J. Durack, R.J. Stouffer, G.C. Johnson, C.E. Forest, Industrial-era global ocean heat uptake doubles in recent decades, Nat. Clim. Chang. 6 (2016) 394-398. https://doi.org/10.1038/nclimate2915.

[26] H. Baumann, S.C. Talmage, C.J. Gobler, Reduced early life growth and survival in a fish in direct response to increased carbon dioxide, Nat. Clim. Chang. 2 (2012) 38-41. https://doi.org/10.1038/nclimate1291.

[27] A.K. Sweetman, A.R. Thurber, C.R. Smith, L.A. Levin, C. Mora, C.-L. Wei, A.J. Gooday, D.O.B. Jones, M. Rex, M. Yasuhara, J. Ingels, H.A. Ruhl, C.A. Frieder, R. Danovaro, L. Wrzberg, A. Baco, B.M. Grupe, A. Pasulka, K.S. Meyer, K.M. Dunlop, L.-A. Henry, J.M. Roberts, Major impacts of climate change on deep-sea benthic ecosystems, Elem Sci Anth. 5 (2017) 1-23. https://doi.org/10.1525/elementa.203.

[28] D. Trolle, A. Nielsen, H.E. Andersen, H. Thodsen, J.E. Olesen,

C.D. Brgesen, J.C. Refsgaard, T.O. Sonnenborg, I.B. Karlsson, J.P. Christensen, S. Markager, E. Jeppesen, Effects of changes in land use and climate on aquatic ecosystems: Coupling of models and decomposition of uncertainties, Sci. Total Environ. 657 (2019) 627-633. https://doi.org/10.1016/j.scitotenv.2018.12.055.

[29] V.P. Dymnikov, V.N. Lykosov, E.M. Volodin, Problems of modeling climate and climate change, Izv. - Atmos. Ocean Phys. 42 (2006) 568-585. https://doi.org/10.1134/S0001433806050045.

[30] R.J. Hijmans, C.H. Graham, The ability of climate envelope models to predict the effect of climate change on species distributions, Glob. Chang. Biol. 12 (2006) 2272-2281. https://doi.org/10.1111/j.1365-2486.2006.01256.x.

[31] O.P. Misra, P. Kalra, S.K.S. Rathore, P. Sinha, Effect of increasing temperature due to depletion of ozone layer caused by CFC on the dynamics of two competing populations: A model, J. Appl. Math. Comput. 38 (2012) 279-293. https://doi.org/10.1007/s12190-011-0478-z.

[32] J.B. Shukla, M. Verma, A.K. Misra, Effect of global warming on sea level rise: A modeling study, Ecol. Complex. 32 (2017) 99-110. https://doi.org/10.1016/j.ecocom.2017.10.007.

[33] S.A. Muyibi, A.R. Ambali, G.S. Eissa, The impact of economic development on water pollution: Trends and policy actions in Malaysia, Water Resour. Manag. 22 (2008) 485-508. https://doi.org/10.1007/s11269-007-9174-z.

[34] M.K. Ahmed, M.A. Baki, M.S. Islam, G.K. Kundu, M. Habibullah-Al-Mamun, S.K. Sarkar, M.M. Hossain, Human health risk assessment of heavy metals in tropical fish and shellfish collected from the river Buriganga, Bangladesh, Environ. Sci. Pollut. Res. 22 (2015) 15880-15890. https://doi.org/10.1007/s11356-015-4813-z.

[35] J. Halder, N. Islam, Water Pollution and its Impact on

the Human Health, J. Environ. Hum. 2 (2015) 36-46. https://doi.org/10.15764/EH.2015.01005.

[36] F. Fuentes-Gandara, J. Pinedo-Hernez, J. Marrugo-Negrete, S. D, Human health impacts of exposure to metals through extreme consumption of fish from the Colombian Caribbean Sea, Environ. Geochem. Health. 40 (2016) 229-242. https://doi.org/10.1007/s10653-016-9896-z.

[37] P.B. Hamilton, G. Rolshausen, T.M. Uren Webster, C.R. Tyler, Adaptive capabilities and fitness consequences associated with pollution exposure in fish, Philos. Trans. R. Soc. B Biol. Sci. 372 (2017) 1-9. https://doi.org/10.1098/rstb.2016.0042.

[38] B.S. Zohra, A. Habib, Assessment of heavy metal contamination levels and toxicity in sediments and fishes from the Mediterranean Sea (southern coast of Sfax, Tunisia), Environ. Sci. Pollut. Res. 23 (2016) 13954-13963. https://doi.org/10.1007/s11356-016-6534-3.

[39] N. Corcoll, J. Yang, T. Backhaus, X. Zhang, K.M. Eriksson, Copper affects composition and functioning of microbial communities in marine biofilms at environmentally relevant concentrations, Front. Microbiol. 10 (2019) 1-15. https://doi.org/10.3389/fmicb.2018.03248.

[40] S.A. Sadeq, A.P. Beckerman, The Chronic Effects of Copper and Cadmium on Life History Traits Across Cladocera Species: A Meta-analysis, Arch. Environ. Contam. Toxicol. 76 (2019) 1-16. https://doi.org/10.1007/s00244-018-0555-5.

[41] U.K. Saleem Raja, V. Ebenezer, A. Kumar, P. Sanjeevi, M. Murugesan, Mass mortality of fish and water quality assessment in the tropical Adyar estuary, South India, Environ. Monit. Assess. 191 (2019) 1-12. https://doi.org/10.1007/s10661-019-7636-4.

[42] Z. Wang, K.K.Y. Ho, G.J. Zhou, K.W.Y. Yeung, K.M.Y. Leung, Effects of silver and zinc on tropical freshwater organisms: Implications on water quality guidelines and eco-

logical risk assessment, Chemosphere. 225 (2019) 897-905. https://doi.org/10.1016/j.chemosphere.2019.03.092.

[43] C.G. Avio, S. Gorbi, F. Regoli, Plastics and microplastics in the oceans: From emerging pollutants to emerged threat, Mar. Environ. Res. 128 (2017) 2-11. https://doi.org/10.1016/j.marenvres.2016.05.012.

[44] A.C. Vegter, M. Barletta, C. Beck, J. Borrero, H. Burton, M.L. Campbell, M.F. Costa, M. Eriksen, C. Eriksson, A. Estrades, K.V.K. Gilardi, B.D. Hardesty, J.A. Ivar do Sul, J.L. Lavers, B. Lazar, L. Lebreton, W.J. Nichols, C.A. Ribic, P.G. Ryan, Q.A. Schuyler, S.D.A. Smith, H. Takada, K.A. Townsend, C.C.C. Wabnitz, C. Wilcox, L.C. Young, M. Hamann, Global research priorities to mitigate plastic pollution impacts on marine wildlife, Endanger. Species Res. 25 (2014) 225-247. https://doi.org/10.3354/esr00623.

[45] D. Eerkes-Medrano, R.C. Thompson, D.C. Aldridge, Microplastics in freshwater systems: A review of the emerging threats, identification of knowledge gaps and prioritisation of research needs, Water Res. 75 (2015) 63-82. https://doi.org/10.1016/j.watres.2015.02.012.

[46] K. Mattsson, E. V. Johnson, A. Malmendal, S. Linse, L.A. Hansson, T. Cedervall, Brain damage and behavioural disorders in fish induced by plastic nanoparticles delivered through the food chain, Sci. Rep. 7 (2017) 1-7. https://doi.org/10.1038/s41598-017-10813-0.

[47] J. He, K. Wang, The survival analysis for a population in a polluted environment, Nonlinear Anal. Real World Appl. 10 (2009) 1555-1571. https://doi.org/10.1016/j.nonrwa.2008.01.027.

[48] S. Chakraborty, P.K. Tiwari, A.K. Misra, J. Chattopadhyay, Spatial dynamics of a nutrient-phytoplankton system with toxic effect on phytoplankton, Math. Biosci. 264 (2015) 94-100.

https://doi.org/10.1016/j.mbs.2015.03.010.

[49] K. Chakraborty, K. Das, Modeling and analysis of a two-zooplankton one-phytoplankton system in the presence of toxicity, Appl. Math. Model. 39 (2015) 1241-1265. https://doi.org/10.1016/j.apm.2014.08.004.

[50] A. Kumar, A.K. Agrawal, A. Hasan, A.K. Misra, Modeling the effect of toxicant on the deformity in a subclass of a biological species, Model. Earth Syst. Environ. 2 (2016) 1-14. https://doi.org/10.1007/s40808-016-0086-x.

[51] S.K. Bhatia, S. Chauhan, A. Agarwal, A Stage-Structured Prey-Predator Fishery Model In The Presence Of Toxicity With Taxation As A Control Parameter of Harvesting Effort, J. Nonlinear Anal. Appl. 2017 (2017) 83-104. https://doi.org/10.5899/2017/jnaa-00374.

[52] P.K. Tiwari, I.M. Bulai, A.K. Misra, E. Venturino, Modeling the Direct and Indirect Effects of Pollutants on the Survival of Fish in Water Bodies, J. Biol. Syst. 25 (2017) 521-543. https://doi.org/10.1142/S0218339017500243.

[53] B.I. McNeil, R.J. Matear, Projected climate change impact on oceanic acidification, Carbon Balance Manag. 1 (2006) 1-6. https://doi.org/10.1186/1750-0680-1-2.

[54] J.M. Guinotte, V.J. Fabry, Ocean acidification and its potential effects on marine ecosystems, Ann. N. Y. Acad. Sci. 1134 (2008) 320-342. https://doi.org/10.1196/annals.1439.013.

[55] J. Bijma, H.O. Prtner, C. Yesson, A.D. Rogers, Climate change and the oceans - What does the future hold?, Mar. Pollut. Bull. 74 (2013) 495-505. https://doi.org/10.1016/j.marpolbul.2013.07.022.

[56] G. Cripps, P. Lindeque, K.J. Flynn, Have we been underestimating the effects of ocean acidification in zooplankton?, Glob. Chang. Biol. 20 (2014) 3377-3385. https://doi.org/10.1111/gcb.12582.

[57] D. Breitberg, J. Salisbury, J. Bernhard, W.-J. Cai, S. Dupont, S. Doney, K. Kroeker, L. Levin, W.C. Long, L. Milke, S. Miller, B. Phelan, U. Passow, B. Seibel, A. Todgham, A. Tarrant, And on Top of All That- Coping with Ocean Acidification in the Midst of Many Stressors, Oceanography. 25 (2015) 48-61. https://doi.org/10.5670/oceanog.2015.31.

[58] D.L. Dixson, A.R. Jennings, J. Atema, P.L. Munday, Odor tracking in sharks is reduced under future ocean acidification conditions, Glob. Chang. Biol. 21 (2015) 1454-1462. https://doi.org/10.1111/gcb.12678.

[59] B.M. Jellison, A.T. Ninokawa, T.M. Hill, E. Sanford, B. Gaylord, Ocean acidification alters the response of intertidal snails to a key sea star predator, Proc. R. Soc. B Biol. Sci. 283 (2016) 1-8. https://doi.org/10.1098/rspb.2016.0890.

[60] C. Lewis, R.P. Ellis, E. Vernon, K. Elliot, S. Newbatt, R.W. Wilson, Ocean acidification increases copper toxicity differentially in two key marine invertebrates with distinct acid-base responses, Sci. Rep. 6 (2016) 1-10. https://doi.org/10.1038/srep21554.

[61] I. Nagelkerken, B.D. Russell, B.M. Gillanders, S.D. Connell, Ocean acidification alters fish populations indirectly through habitat modification, Nat. Clim. Chang. 6 (2016) 89-93. https://doi.org/10.1038/nclimate2757.

[62] W. Shi, X. Zhao, Y. Han, Z. Che, X. Chai, G. Liu, Ocean acidification increases cadmium accumulation in marine bivalves: A potential threat to seafood safety, Sci. Rep. 6 (2016) 1-8. https://doi.org/10.1038/srep20197.

[63] D. Qi, L. Chen, B. Chen, Z. Gao, W. Zhong, R.A. Feely, L.G. Anderson, H. Sun, J. Chen, M. Chen, L. Zhan, Y. Zhang, W.J. Cai, Increase in acidifying water in the western Arctic Ocean, Nat. Clim. Chang. 7 (2017) 195-199. https://doi.org/10.1038/nclimate3228.

[64] C.S. Law, J.J. Bell, H.C. Bostock, C.E. Cornwall, V.J. Cummings, K. Currie, S.K. Davy, M. Gammon, C.D. Hepburn, C.L. Hurd, M. Lamare, S.E. Mikaloff-Fletcher, W.A. Nelson, D.M. Parsons, N.L.C. Ragg, M.A. Sewell, A.M. Smith, D.M. Tracey, Ocean acidification in New Zealand waters: trends and impacts, New Zeal. J. Mar. Freshw. Res. 52 (2018) 155-195. https://doi.org/10.1080/00288330.2017.1374983.

[65] A. Wulff, M. Karlberg, M. Olofsson, A. Torstensson, L. Riemann, F.S. Steinhoff, M. Mohlin, N. Ekstrand, M. Chierici, Ocean acidification and desalination: climate-driven change in a Baltic Sea summer microplanktonic community, Mar. Biol. 165 (2018) 1-15. https://doi.org/10.1007/s00227-018-3321-3.

[66] A. Mukherjee, A.R. Bhowmick, J. Mukherjee, M. Moniruzzaman, Physiological response of fish under variable acidic conditions: a molecular approach through the assessment of an ecophysiological marker in the brain, Environ. Sci. Pollut. Res. 26 (2019) 23442-23452. https://doi.org/10.1007/s11356-019-05602-3.

[67] I.B. Kuffner, A.J. Andersson, P.L. Jokiel, K.S. Rodgers, F.T. MacKenzie, Decreased abundance of crustose coralline algae due to ocean acidification, Nat. Geosci. 1 (2008) 114-117. https://doi.org/10.1038/ngeo100.

[68] R.W. Buddemeier, D.R. Lane, J.A. Martinich, Modeling regional coral reef responses to global warming and changes in ocean chemistry: Caribbean case study, Clim. Change. 109 (2011) 375-397. https://doi.org/10.1007/s10584-011-0022-z.

[69] J.M. Pandolfi, S.R. Connolly, D.J. Marshall, A.L. Cohen, Projecting coral reef futures under global warming and ocean acidification, Science (80-.). 333 (2011) 418-422. https://doi.org/10.1126/science.1204794.

[70] P.L. Munday, A.J. Cheal, D.L. Dixson, J.L. Rummer, K.E. Fabricius, Behavioural impairment in reef fishes caused by ocean

acidification at CO2seeps, Nat. Clim. Chang. 4 (2014) 487-492. https://doi.org/10.1038/nclimate2195.

[71] T.P. Hughes, M.L. Barnes, D.R. Bellwood, J.E. Cinner, G.S. Cumming, J.B.C. Jackson, J. Kleypas, I.A. Van De Leemput, J.M. Lough, T.H. Morrison, S.R. Palumbi, E.H. Van Nes, M. Scheffer, Coral reefs in the Anthropocene, Nature. 546 (2017) 82-90. https://doi.org/10.1038/nature22901.

[72] T.M. DeCarlo, A.L. Cohen, G.T.F. Wong, K.A. Davis, P. Lohmann, K. Soong, Mass coral mortality under local amplification of 2°C ocean warming, Sci. Rep. 7 (2017) 1-9. https://doi.org/10.1038/srep44586.

[73] K.R.N. Anthony, D.I. Kline, G. Diaz-Pulido, S. Dove, O. Hoegh-Guldberg, Ocean acidification causes bleaching and productivity loss in coral reef builders, Proc. Natl. Acad. Sci. 105 (2008) 17442-17446. https://doi.org/10.1073/pnas.0804478105.

[74] I.C. Enochs, D.P. Manzello, G. Kolodziej, S.H.C. Noonan, L. Valentino, K.E. Fabricius, Enhanced macroboring and depressed calcification drive net dissolution at high-CO2 coral reefs, Proc. R. Soc. B Biol. Sci. 283 (2016) 1-8. https://doi.org/10.1098/rspb.2016.1742.

[75] J.M. Sunday, K.E. Fabricius, K.J. Kroeker, K.M. Anderson, N.E. Brown, J.P. Barry, S.D. Connell, S. Dupont, B. Gaylord, J.M. Hall-Spencer, T. Klinger, M. Milazzo, P.L. Munday, B.D. Russell, E. Sanford, V. Thiyagarajan, M.L.H. Vaughan, S. Widdicombe, C.D.G. Harley, Ocean acidification can mediate biodiversity shifts by changing biogenic habitat, Nat. Clim. Chang. 7 (2017) 81-85. https://doi.org/10.1038/nclimate3161.

[76] N.N. Rabalais, R.E. Turner, R.J. D, D. Justic, Global change and eutrophication of coastal waters. ICES J. Mar. Sci. 66(7), 1528-1537. https://doi.org/10.5539/enrr.v3n2p37.

[77] G.M. Hallegraeff, Ocean climate change, phytoplank-

ton community responses, and harmful algal blooms: A formidable predictive challenge, J. Phycol. 46 (2010) 220-235. https://doi.org/10.1111/j.1529-8817.2010.00815.x.

[78] P.M. Glibert, J. Icarus Allen, Y. Artioli, A. Beusen, L. Bouwman, J. Harle, R. Holmes, J. Holt, Vulnerability of coastal ecosystems to changes in harmful algal bloom distribution in response to climate change: Projections based on model analysis, Glob. Chang. Biol. 20 (2014) 3845-3858. https://doi.org/10.1111/gcb.12662.

[79] S.J. Mccoy, C.A. Pfister, Historical comparisons reveal altered competitive interactions in a guild of crustose coralline algae, Ecol. Lett. 17 (2014) 475-483. https://doi.org/10.1111/ele.12247.

[80] C.J. Gobler, O.M. Doherty, T.K. Hattenrath-Lehmann, A.W. Griffith, Y. Kang, R.W. Litaker, Ocean warming since 1982 has expanded the niche of toxic algal blooms in the North Atlantic and North Pacific oceans, Proc. Natl. Acad. Sci. 114 (2017) 4975-4980. https://doi.org/10.1073/pnas.1619575114.

[81] M. Snickars, B. Weigel, E. Bonsdorff, Impact of eutrophication and climate change on fish and zoobenthos in coastal waters of the Baltic Sea, Mar. Biol. 162 (2015) 141-151. https://doi.org/10.1007/s00227-014-2579-3.

[82] M.L.S. Diego-mcglone, R. V Azanza, C.L. Villanoy, G.S. Jacinto, Eutrophic waters , algal bloom and fish kill in fish farming areas in Bolinao, Mar. Pollut. Bull. 57 (2008) 295-301. https://doi.org/10.1016/j.marpolbul.2008.03.028.

[83] S. Pal, S. Chatterjee, J. Chattopadhyay, Role of toxin and nutrient for the occurrence and termination of plankton bloom-Results drawn from field observations and a mathematical model, BioSystems. 90 (2007) 87-100. https://doi.org/10.1016/j.biosystems.2006.07.003.

[84] J.B. Shukla, A.K. Misra, P. Chandra, Modeling and analysis of the algal bloom in a lake caused by discharge

of nutrients, Appl. Math. Comput. 196 (2008) 782-790. https://doi.org/10.1016/j.amc.2007.07.010.

[85] J.B. Shukla, A.K. Misra, P. Chandra, Mathematical modeling and analysis of the depletion of dissolved oxygen in eutrophied water bodies affected by organic pollutants, Nonlinear Anal. Real World Appl. 9 (2008) 1851-1865. https://doi.org/10.1016/j.nonrwa.2007.05.016.

[86] A.K. Misra, P.K. Tiwari, E. Venturino, Modeling the impact of awareness on the mitigation of algal bloom in a lake, J. Biol. Phys. 42 (2016) 147-165. https://doi.org/10.1007/s10867-015-9397-9.

[87] H. Nie, S.B. Hsu, J.P. Grover, Algal competition in a water column with excessive dioxide in the atmosphere, J. Math. Biol. 72 (2016) 1845-1892. https://doi.org/10.1007/s00285-015-0926-8.

[88] G.S.K. Wolkowicz, Y. Yuan, Effect of light on the growth of non-nitrogen-fixing and nitrogen-fixing phytoplankton in an aquatic system, J. Math. Biol. 72 (2016) 1663-1692. https://doi.org/10.1007/s00285-015-0924-x.

[89] Z. Jiang, W. Zhang, J. Zhang, T. Zhang, Dynamical analysis of a phytoplankton-zooplankton system with harvesting term and Holling III functional response, Int. J. Bifurc. Chaos. 28 (2018) 1-23. https://doi.org/10.1142/S0218127418501626.

[90] X. Yu, S. Yuan, T. Zhang, The effects of toxin-producing phytoplankton and environmental fluctuations on the planktonic blooms, Nonlinear Dyn. 91 (2018) 1653-1668. https://doi.org/10.1007/s11071-017-3971-6.

[91] J. Zhang, J. Shi, X. Chang, A mathematical model of algae growth in a pelagic-benthic coupled shallow aquatic ecosystem, J. Math. Biol. 76 (2018) 1159-1193. https://doi.org/10.1007/s00285-017-1168-8.

[92] A. Mandal, P. Kumar, S. Samanta, E. Venturino, S. Pal, A nonautonomous model for the effect of environmental

toxins on plankton dynamics, Nonlinear Dyn. (2020) 1-33. https://doi.org/10.1007/s11071-020-05480-2.

[93] A.J. Mearns, D.J. Reish, P.S. Oshida, T. Ginn, M.A. Rempel-Hester, Effects of pollution on marine organisms, Water Environ. Res. 84 (2012) 1737-1823. https://doi.org/10.2175/106143012X13407275695751.

[94] R. Tembo, The Impact of Ocean Acidification on Aquatic Organisms, J. Environ. Anal. Toxicol. 07 (2017) 3-7. https://doi.org/10.4172/2161-0525.1000469.

[95] J.E. Serafy, R.M. Harerell, Behavioural response of fishes to increasing pH and dissolved oxygen: field and laboratory observations, Freshw. Biol. 30 (1993) 53-61. https://doi.org/10.1111/j.1365-2427.1993.tb00788.x.

[96] F. Joos, G.-K. Plattner, T.F. Stocker, A. Krtzinger, D.W.R. Wallace, Trends in marine dissolved oxygen: Implications for ocean circulation changes and the carbon budget, Eos, Trans. Am. Geophys. Soc. 84 (2003) 197-204.

[97] L. Stramma, S. Schmidtko, L.A. Levin, G.C. Johnson, Ocean oxygen minima expansions and their biological impacts, Deep. Res. Part I Oceanogr. Res. Pap. 57 (2010) 587-595. https://doi.org/10.1016/j.dsr.2010.01.005.

[98] G.K. Nurnberg, Quantification of oxygen depletion in lakes and reservoirs with the hypoxic factor, Lake Reserv. Manag. 18 (2002) 299-306. https://doi.org/10.1080/07438140209353936.

[99] R.F. Keeling, A. Krtzinger, N. Gruber, Ocean Deoxygenation in a Warming World, Ann. Rev. Mar. Sci. 2 (2010) 199-229. https://doi.org/10.1146/annurev.marine.010908.163855.

[100] B. Foley, I.D. Jones, S.C. Maberly, B. Rippey, Long-term changes in oxygen depletion in a small temperate lake: Effects of climate change and eutrophication, Freshw. Biol. 57 (2012) 278-289. https://doi.org/10.1111/j.1365-2427.2011.02662.x.

[101] S.Y. Wang, K. Lau, K.P. Lai, J.W. Zhang, A.C.K. Tse, J.W. Li, Y. Tong, T.F. Chan, C.K.C. Wong, J.M.Y. Chiu, D.W.T. Au, A.S.T. Wong, R.Y.C. Kong, R.S.S. Wu, Hypoxia causes transgenerational impairments in reproduction of fish, Nat. Commun. 7 (2016) 1-9. https://doi.org/10.1038/ncomms12114.

[102] J.G. Shepherd, P.G. Brewer, A. Oschlies, A.J. Watson, Ocean ventilation and deoxygenation in a warming world: posters, Philos. Trans. R. Soc. A Math. Phys. Eng. Sci. 375 (2017) 1-9. https://doi.org/10.1098/rsta.2017.0241.

[103] S. Schmidtko, L. Stramma, M. Visbeck, Decline in global oceanic oxygen content during the past five decades, Nature. 542 (2017) 335-339. https://doi.org/10.1038/nature21399.

[104] A.K. Misra, P. Chandra, J.B. Shukla, Mathematical modeling and analysis of the depletion of dissolved oxygen in water bodies, Nonlinear Anal. Real World Appl. 7 (2006) 980-996. https://doi.org/10.1016/j.nonrwa.2005.09.002.

[105] J.B. Shukla, A. K. Misra, P. Chandra, Mathematical Modeling of the Survival of a Biological Species in Polluted Water Bodies, Differ. Equations Dyn. Syst. 15 (2007) 209-230.

[106] S. Khare, S. Kumar, C. Singh, Modelling effect of the depleting dissolved oxygen on the existence of interacting planktonic population, Appl. Math. 55 (2013) 12739-12742.

[107] P. Kalra, Shreya, Study of Effects of Toxicants and Acidity on Oxygen-Dependent Aquatic Population: A Mathematical Model, Int. J. Math. Model. Numer. Optim. 10 (2020) 307-329. https://doi.org/10.1504/IJMMNO.2020.108621.

[108] A.T. Asha Bharathi, A. Chaturvedi, R. Gupta, K. Ramesh, Combined effects of acid and metal on the survival of resource based population incorporating nutrient recycling: A mathematical model, Int. J. Appl. Eng. Res. 10 (2015) 14969-14980.

[109] O.P. Misra, D. Chaturvedi, Fate of dissolved oxygen and sur-

vival of fish population in aquatic ecosystem with nutrient loading: a model, Model. Earth Syst. Environ. 2 (2016) 1-14. https://doi.org/10.1007/s40808-016-0168-9.

[110] E. Venturino, P.K. Tiwari, A.K. Misra, Modeling the depletion of dissolved oxygen in a water body located near a city, Math. Methods Appl. Sci. 40 (2017) 1081-1094. https://doi.org/10.1002/mma.4037.

[111] P.H. Collin, Dictionary of Environment and Ecology, Bloomsbury, 2004.

[112] Mathematical Biology:I. An Introduction,Third Edition, Springer, New York,2002.

[113] J. Bailey, Dictionary Of Ecology And The Environment, Facts On File, New York, 2004.

[114] W. Dubitzky, O. Wolkenhauer, KH. Cho, H. Yokota, Encyclopedia of Systems Biology. Springer, New York,2013.

[115] S. Ahmad, M R. M. Rao, Theory of Ordinary Differential Equations, East West Press, 1999.

[116] W.J.S. Mwegoha, M.E. Kaseva, S.M.M. Sabai, Mathematical Modeling of dissolved oxygen in fish ponds, 4 (2010) 625-638. http://www.academicjournals.org.AJEST.

[117] N. Chitnis, J.M. Hyman, J.M. Cushing, Determining Important Parameters in the Spread of Malaria, 70 (2008) 1272-1296. https://doi.org/10.1007/s11538-008-9299-0.

[118] S. Chakraborty, P.K. Tiwari, S.K. Sasmal, A.K. Misra, J. Chattopadhyay, Effects of fertilizers used in agricultural fields on algal blooms, Eur. Phys. J. Spec. Top. 226 (2017) 2119-2133. https://doi.org/10.1140/epjst/e2017-70031-7.

[119] J. Sirota, B. Baiser, N.J. Gotelli, A.M. Ellison, Organic-matter loading determines regime shifts and alternative states in an aquatic ecosystem, Proc. Natl. Acad. Sci. U. S. A. 110 (2013) 7742-7747. https://doi.org/10.1073/pnas.1221037110.

[120] N.R. Mollica, W. Guo, A.L. Cohen, K.F. Huang, G.L. Foster, H.K. Donald, A.R. Solow, Ocean acidification affects coral growth by reducing skeletal density, Proc. Natl. Acad. Sci. U. S. A. 115 (2018) 1754-1759. https://doi.org/10.1073/pnas.1712806115.

[121] K.E. Fabricius, G. De-ath, S. Noonan, S. Uthicke, Ecological effects of ocean acidification and habitat complexity on reef-associated macroinvertebrate communities, Proc. R. Soc. B Biol. Sci. 281 (2013) 1-8. https://doi.org/10.1098/rspb.2013.2479.

[122] P.B. Hamilton, G. Rolshausen, T.M. Uren Webster, C.R. Tyler, Adaptive capabilities and fitness consequences associated with pollution exposure in fish, Philos. Trans. R. Soc. B Biol. Sci. 372 (2017) 1-7. https://doi.org/10.1098/rstb.2016.0042.

[123] S. Ganguly, Water Pollution From Various Sources and Human Infringements: an Editorial, Ind. J. Sci. Res. Tech. 1 (2013) 54-55. http://www.indjsrt.com.

[124] H. Ali, E. Khan, Trophic transfer, bioaccumulation, and biomagnification of non-essential hazardous heavy metals and metalloids in food chains/webs-Concepts and implications for wildlife and human health, Hum. Ecol. Risk Assess. 25 (2019) 1353-1376. https://doi.org/10.1080/10807039.2018.1469398.

[125] T.I. Moiseenko, Effects of Acidification on Aquatic Ecosystems, Russ. J. Ecol. 36 (2005) 110-119.

[126] U. Riebesell, N. Aberle-malzahn, E.P. Achterberg, M. Alguer S. Alvarez-fernandez, J. Aregui, L.T. Bach, M. Boersma, T. Boxhammer, W. Guan, M. Haunost, H.G. Horn, C.R. Lscher, A. Ludwig, C. Spisla, M. Sswat, P. Stange, J. Taucher, Toxic algal bloom induced by ocean acidification disrupts the pelagic food web, Nat. Clim. Chang. 8 (2018) 1082-1090. https://doi.org/10.1038/s41558-018-0344-1.

[127] M.N. Hassan, L. Asik, J. Kulik, K.R. Long, A. Peace, Environmental seasonality on predator-prey systems under nutri-

ent and toxicant constraints, J. Theor. Biol. 480 (2019) 71-80. https://doi.org/10.1016/j.jtbi.2019.08.001.

[128] B.W. Kooi, D. Bontje, G.A.K. van Voorn, S.A.L.M. Kooijman, Sublethal toxic effects in a simple aquatic food chain, Ecol. Modell. 212 (2008) 304-318. https://doi.org/10.1016/j.ecolmodel.2007.10.042.

[129] D. Chaturvedi, O.P. Misra, Modeling impact of varying pH due to carbondioxide on the dynamics of prey-predator species system, Nonlinear Anal. Real World Appl. 46 (2019) 374-402. https://doi.org/10.1016/j.nonrwa.2018.09.024.

[130] G. Shaffer, S. Olsen, J. Pedersen, Long-term ocean oxygen depletion in response to carbon dioxide emissions from fossil fuels, Nature Geosci. 2 (2009) 105-109. https://doi.org/10.1038/ngeo420.

[131] S. Solomon, G. K. Plattner, R. Knutti, P. Friedlingstein, Irreversible climate change due to carbon dioxide emissions, Proc. Natl. Acad. Sci. 106 (2009) 1704-1709. https://doi.org/10.1073/pnas.0812721106.

[132] H. Sarmento, J.M. Montoya, E. Vuez-Domuez, D. Vaqu.M. Gasol, Warming effects on marine microbial food web processes: How far can we go when it comes to predictions?, Philos. Trans. R. Soc. B Biol. Sci. 365 (2010) 2137-2149. https://doi.org/10.1098/rstb.2010.0045.

[133] G. Yvon-Durocher, J.I. Jones, M. Trimmer, G. Woodward, J.M. Montoya, Warming alters the metabolic balance of ecosystems, Philos. Trans. R. Soc. B Biol. Sci. 365 (2010) 2117-2126. https://doi.org/10.1098/rstb.2010.0038.

[134] C.T. Hasler, J.D. Jeffrey, E.V.C. Schneider, K.D. Hannan, J.A. Tix, C.D. Suski, Biological consequences of weak acidification caused by elevated carbon dioxide in freshwater ecosystems, Hydrobiologia. 806 (2018) 1-12. https://doi.org/10.1007/s10750-017-3332-y.

[135] S. C. Chapra, B. Boehlert, C. Fant, V. J. Bierman Jr, J. Henderson, D. Mills, D. M. Mas, L. Rennels, L. Jantarasami, J. Martinich, K.M. Strzepek, Climate change impacts on harmful algal blooms in US freshwaters: a screening-level assessment, Environ. Sci. Technol. 51 (2017) 8933-8943. https://doi.org/10.1021/acs.est.7b01498.

[136] A. M. Michalak, E. J. Anderson, D. Beletsky, S. Boland, N. S. Bosch, T. B. Bridgeman, J. D. Chaffin, K. Cho, R. Confesor, I. Daloglu, J.V. DePinto, Record-setting algal bloom in Lake Erie caused by agricultural and meteorological trends consistent with expected future conditions, Proc. Natl. Acad. Sci. 110 (2013) 6448-6452. https://doi.org/10.1073/pnas.1216006110.

[137] R. Bhateria, D. Jain, Water quality assessment of lake water: a review, Sustain. Water Resour. Manag., 2 (2016) 161-173. https://doi.org/10.1007/s40899-015-0014-7.

[138] J. Miller, E. Muller, C. Rogers, R. Waara, A. Atkinson, K. R. T. Whelan, M. Patterson, B. Witcher, Coral disease following massive bleaching in 2005 causes 60% decline in coral cover on reefs in the US Virgin Islands. Coral Reefs, 28 (2009) 1-13. https://doi.org/10.1007/s00338-009-0531-7.

[139] N. H. Wolff, P. J. Mumby, M. Devlin, K. R. Anthony, Vulnerability of the Great Barrier Reef to climate change and local pressures, Glob. Chang. Biol. 24 (2018) 1978-1991. https://doi.org/10.1111/gcb.14043.

[140] A. Jansson, J. Norkko, S. Dupont, A. Norkko, Growth and survival in a changing environment: Combined effects of moderate hypoxia and low pH on juvenile bivalve Macoma balthica, J. Sea Res. 102 (2015) 41-47. https://doi.org/10.1016/j.seares.2015.04.006.

[141] Y. Sekerci, S. Petrovskii, Global warming can lead to depletion of oxygen by disrupting phytoplankton photosynthesis:

A mathematical modelling approach, Geosci. 8 (2018) 1-21. https://doi.org/10.3390/geosciences8060201.

[142] A.P. Ballantyne, C.B. Alden, J.B. Miller, P.P. Trans, J.W.C. White, A Newtonian approach to extraordinarily strong negative refraction, Nature. 488 (2012) 70-73. https://doi.org/10.1038/nature11299.

[143] W. E. Forum, the Ellen MacArthur Foundation, The New Plastics Economy: Rethinking the future of plastics, https://www.ellenmacarthurfoundation.org/assets/downloads/news/New-Plastics-Economy_Background-to-Key-Statistics_19022016v2.pdf 2016 (accessed May 25, 2020).

[144] S. Rezania, J. Park, M.F. Md Din, S. Mat Taib, A. Talaiekhozani, K. Kumar Yadav, H. Kamyab, Microplastics pollution in different aquatic environments and biota: A review of recent studies, Mar. Pollut. Bull. 133 (2018) 191-208. https://doi.org/10.1016/j.marpolbul.2018.05.022.

[145] E. Besseling, B. Wang, M. Lrling, A.A. Koelmans, Nanoplastic affects growth of S. obliquus and reproduction of D. magna, Environ. Sci. Technol. 48 (2014) 12336-12343. https://doi.org/10.1021/es503001d.

[146] X. Sun, Q. Li, M. Zhu, J. Liang, S. Zheng, Y. Zhao, Ingestion of microplastics by natural zooplankton groups in the northern South China Sea, Mar. Pollut. Bull. 115 (2017) 217-224. https://doi.org/10.1016/j.marpolbul.2016.12.004.

[147] K. Yokota, H. Waterfield, C. Hastings, E. Davidson, E. Kwietniewski, B. Wells, Finding the missing piece of the aquatic plastic pollution puzzle: Interaction between primary producers and microplastics, Limnol. Oceanogr. Lett. 2 (2017) 91-104. https://doi.org/10.1002/lol2.10040.

[148] G.T. Pecl, M.B. Arajo, J.D. Bell, J. Blanchard, T.C. Bonebrake, I.C. Chen, T.D. Clark, R.K. Colwell, F. Danielsen, B. Eveng,

L. Falconi, S. Ferrier, S. Frusher, R.A. Garcia, R.B. Griffis, A.J. Hobday, C. Janion-Scheepers, M.A. Jarzyna, S. Jennings, J. Lenoir, H.I. Linnetved, V.Y. Martin, P.C. McCormack, J. McDonald, N.J. Mitchell, T. Mustonen, J.M. Pandolfi, N. Pettorelli, E. Popova, S.A. Robinson, B.R. Scheffers, J.D. Shaw, C.J.B. Sorte, J.M. Strugnell, J.M. Sunday, M.N. Tuanmu, A. Verg C. Villanueva, T. Wernberg, E. Wapstra, S.E. Williams, Biodiversity redistribution under climate change: Impacts on ecosystems and human well-being, Science (80-.). 355 (2017) 1-9 https://doi.org/10.1126/science.aai9214.

[149] S.-J. Royer, S. Ferron, S. T. Wilson, D. M. Karl, Production of methane and ethylene from plastic in the environment, PLoS One 13 (2018) 1-13 https://doi.org/10.1371/journal.pone.0200574.

[150] M. Shen, W. Huang, M. Chen, B. Song, G. Zeng, Y. Zhang, (Micro)plastic crisis: Un-ignorable contribution to global greenhouse gas emissions and climate change, J. Clean. Prod. 254 (2020) 1-13 https://doi.org/10.1016/j.jclepro.2020.120138.

[151] J. Zheng, S. Suh, Strategies to reduce the global carbon footprint of plastics, Nat. Clim. Chang. 9 (2019) 374-378. https://doi.org/10.1038/s41558-019-0459-z.

[152] C. Collins, COVID-19 is cutting air pollution, but it will not slow climate change, https://sciencebusiness.net/covid-19/news/covid-19-cutting-air-pollution-it-will-not-slow-climate-change, 2020 (accessed May 25, 2020)).

[153] R. Metzke, Climate action must stay top of the global agenda as we emerge from COVID-19,https://www.weforum.org/agenda/2020/05/climate-action-top-global-agenda-covid-19, 2020 (accessed May 25, 2020).

[154] P. Peduzzi, Record global carbon dioxide concentrations despite COVID-19 crisis, https://www.unenvironment.org/news-and-stories/story/record-global-carbon-dioxide-concentrations-

despite-covid-19-crisis, 2020 (accessed May 25, 2020).

[155] K. Caldeira, M.E. Wickett, Anthropogenic carbon and ocean pH, Nature. 425 (2003) 365. https://doi.org/10.1038/425365a.

[156] L.C. Weiss, L. Ptter, A. Steiger, S. Kruppert, U. Frost, R. Tollrian, Rising pCO2 in Freshwater Ecosystems Has the Potential to Negatively Affect Predator-Induced Defenses in Daphnia, Curr. Biol. 28 (2018) 327-332. https://doi.org/10.1016/j.cub.2017.12.022.

[157] W.J. Cai, X. Hu, W.J. Huang, M.C. Murrell, J.C. Lehrter, S.E. Lohrenz, W.C. Chou, W. Zhai, J.T. Hollibaugh, Y. Wang, P. Zhao, X. Guo, K. Gundersen, M. Dai, G.C. Gong, Acidification of subsurface coastal waters enhanced by eutrophication, Nat. Geosci. 4 (2011) 766-770. https://doi.org/10.1038/ngeo1297.

[158] A. Laurent, K. Fennel, W.J. Cai, W.J. Huang, L. Barbero, R. Wanninkhof, Eutrophication-induced acidification of coastal waters in the northern Gulf of Mexico: Insights into origin and processes from a coupled physical-biogeochemical model, Geophys. Res. Lett. 44 (2017) 946-956. https://doi.org/10.1002/2016GL071881.

[159] R.B. Wallace, H. Baumann, J.S. Grear, R.C. Aller, C.J. Gobler, Coastal ocean acidification: The other eutrophication problem, Estuar. Coast. Shelf Sci. 148 (2014) 1-13. https://doi.org/10.1016/j.ecss.2014.05.027.

[160] P. Bhattacharya, S. Lin, J.P. Turner, P.C. Ke, Physical adsorption of charged plastic nanoparticles affects algal photosynthesis, J. Phys. Chem. C. 114 (2010) 16556-16561. https://doi.org/10.1021/jp1054759.

[161] S.B. Sjollema, P. Redondo-Hasselerharm, H.A. Leslie, M.H.S. Kraak, A.D. Vethaak, Do plastic particles affect microalgal photosynthesis and growth?, Aquat. Toxicol. 170 (2016) 259-261. https://doi.org/10.1016/j.aquatox.2015.12.002.

[162] M. Ghosh, Effect of liming on a fish population in an acidified

lake: A simple mathematical model, Appl. Math. Comput. 135 (2003) 553-560. https://doi.org/10.1016/S0096-3003(02)00068-1.

[163] P. Kalra, Shreya, Impact of water toxicity and acidity on dynamics of prey-predator aquatic populations: A mathematical model, J. Phys. Conf. Ser. 1531 (2020) 1-19. https://doi.org/10.1088/1742-6596/1531/1/012081.

[164] A.K. Misra, M. Verma, A mathematical model to study the dynamics of carbon dioxide gas in the atmosphere, Appl. Math. Comput. 219 (2013) 8595-8609. https://doi.org/10.1016/j.amc.2013.02.058.

[165] A.K. Misra, Modeling the depletion of dissolved oxygen due to algal bloom in a lake by taking Holling type-III interaction, Appl. Math. Comput. 217 (2011) 8367-8376. https://doi.org/10.1016/j.amc.2011.03.034.

[166] S.I. Bartsev, J.I. Gitelson, A mathematical model of the global processes of plastic degradation in the World Ocean with account for the surface temperature distribution, Dokl. Earth Sci. 466 (2016) 153-156. https://doi.org/10.1134/S1028334X16020033.

[167] H.R. Thieme, Convergence results and a Poincarendixson trichotomy for asymptotically autonomous differential equations, J. Math. Biol. 30 (1992) 755-763. https://doi.org/10.1007/BF00173267.

[168] S. Sinha, O.P. Misra, J. Dhar, Modelling a predator-prey system with infected prey in polluted environment, Appl. Math. Model. 34 (2010) 1861-1872. https://doi.org/10.1016/j.apm.2009.10.003.

[169] A.M. Draper, M.J. Weissburg, Impacts of global warming and elevated CO2 on sensory behavior in predator-prey interactions: A review and synthesis, Front. Ecol. Evol. 7 (2019) 1-41. https://doi.org/10.3389/fevo.2019.00072.

[170] A.M. Koltz, A.T. Classen, J.P. Wright, Warming reverses top-down effects of predators on belowground ecosystem function in

Arctic tundra, Proc. Natl. Acad. Sci. U. S. A. 115 (2018) 1-9. https://doi.org/10.1073/pnas.1808754115.

[171] T.F. Stocker, D. Qin, G.K. Plattner, M.M.B. Tignor, S.K. Allen, J. Boschung, A. Nauels, Y. Xia, V. Bex, P.M. Midgley, Climate change 2013 the physical science basis: Working Group I contribution to the fifth assessment report of the intergovernmental panel on climate change, Clim. Chang. 2013 Phys. Sci. Basis Work. Gr. I Contrib. to Fifth Assess. Rep. Intergov. Panel Clim. Chang. 9781107057 (2013) 1-1535. https://doi.org/10.1017/CBO9781107415324.

[172] J.C. Orr, V.J. Fabry, O. Aumont, L. Bopp, S.C. Doney, R.A. Feely, A. Gnanadesikan, N. Gruber, A. Ishida, F. Joos, R.M. Key, K. Lindsay, E. Maier-Reimer, R. Matear, P. Monfray, A. Mouchet, R.G. Najjar, G.K. Plattner, K.B. Rodgers, C.L. Sabine, J.L. Sarmiento, R. Schlitzer, R.D. Slater, I.J. Totterdell, M.F. Weirig, Y. Yamanaka, A. Yool, Anthropogenic ocean acidification over the twenty-first century and its impact on calcifying organisms, Nature. 437 (2005) 681-686. https://doi.org/10.1038/nature04095.

Appendix

Units and Description of Variables and Parameters used in Thesis

In the appendix, the units and description of variables and parameters used in thesis have been given. The units are considered following the metric system, and they have been assumed on the basis of units considered for similar variables in the previously available works and mathematical studies done by researchers in this field [107, 116, 118, 163, 165].

Table 7.1: Units of Variables used in Chapter 2

Variable	**Description**	**Units**
A	Concentration of acid in water	$\mu g L^{-1}$
S	Concentration of toxicant in water	$\mu g L^{-1}$
P	Density of aquatic population like fish	$mg L^{-1}$
D_0	Concentration of favourable resources i.e. dissolved oxygen in water	$mg L^{-1}$

Table 7.2: Units of Variables used in Chapter 3

Variable	**Description**	**Units**
A	Concentration of acid in water	$\mu g L^{-1}$
T	Concentration of toxicant in water	$\mu g L^{-1}$
D_0	Concentration of favourable resources i.e. dissolved oxygen in water	$mg L^{-1}$
N	Density of aquatic prey population like small fishes	$mg L^{-1}$
P	Density of predator population directly dependent on prey for food	$mg L^{-1}$

Table 7.3: Units of Variables used in Chapter 4

Variable	**Description**	**Units**
C	Concentration of carbon in water	mgL^{-1}
pH	pH level of water	
A_l	Density of algal population	mgL^{-1}
D_0	Concentration of dissolved oxygen in water	mgL^{-1}

Table 7.4: Units of Variables used in Chapter 5

Variable	**Description**	**Units**
τ	Average surface temperature	$^{\circ}C$
R	Concentration of atmospheric carbon dioxide	mgL^{-1}
A_g	Density of algal population	mgL^{-1}
O	Concentration of dissolved oxygen in water	mgL^{-1}

Table 7.5: Units of Variables used in Chapter 6

Variable	**Description**	**Units**
P_l	Concentration of plastic waste in water body	μgL^{-1}
G	Concentration of greenhouse gases in the atmosphere	mgL^{-1}
n	Concentration of nutrients entering the water body leading to eutrophication and algal bloom growth	mgL^{-1}
a	Density of algal population	mgL^{-1}
T	Average surface temperature	mgL^{-1}
O	Concentration of dissolved oxygen in water	mgL^{-1}

Table 7.6: Units of Variables used in Chapter 7

Variable	**Description**	**Units**
C	Concentration of carbon in water	mgL^{-1}
pH	pH level of water	
A_g	Density of algal population	mgL^{-1}
D	Concentration of dissolved oxygen in water	mgL^{-1}
P	Density of aquatic population	mgL^{-1}

Table 7.7: Units of Parameters used in Chapter 2

Parameter	Description	Units
p	Input rate of acid in water	$\mu g L^{-1} day^{-1}$
b_1	Rate at which the acid is washed out of the water bodies	day^{-1}
k_1	Rate of increase in water acidity due to increased toxicant amount in water	$L \mu g^{-1} day^{-1}$
q	Rate at which the toxicants and pollutants are introduced in the aquatic ecosystem	$\mu g L^{-1} day^{-1}$
α	Depletion rate of the toxicants and pollutants	day^{-1}
β_{11}	Rate of consumption of dissolved oxygen by the aquatic population	day^{-1}
β_{12}	Half saturation constant	$mg L^{-1}$
d_1	Rate of depletion of population on account of increased acidity	$L \mu g^{-1} day^{-1}$
m	Death rate of the population	day^{-1}
δ_1	Self-restricting rates of growth of population	$L mg^{-1} day^{-1}$
r	Input rate of dissolved oxygen	$mg L^{-1} day^{-1}$
n_1	Natural depletion rate of dissolved oxygen	day^{-1}
n_2	Decomposition rate of the algal biomass and the organic pollutants in water	$L \mu g^{-1} day^{-1}$
t	Time variable	day

Table 7.8: Units of Parameters used in Chapter 3

Parameter	**Description**	**Units**
p_0	Input rate of acid in water	$\mu g L^{-1} day^{-1}$
β	Rate at which the acid is washed out of the water bodies	day^{-1}
k	Rate of increase in water acidity due to increased toxicant amount in water	$L \mu g^{-1} day^{-1}$
q_0	Rate at which the toxicants and pollutants are introduced in the aquatic ecosystem	$\mu g L^{-1} day^{-1}$
a_0	Depletion rate of the toxicants and pollutants	day^{-1}
r	Input rate of dissolved oxygen in water	$mg L^{-1} day^{-1}$
n_{11}	Natural depletion rate of dissolved oxygen in water	day^{-1}
n_{12}	Rate at which the dissolved oxygen decreases due the algal decomposition	$L \mu g^{-1} day^{-1}$
γ	Rate of uptake of dissolved oxygen by the prey population in water	$L mg^{-1} day^{-1}$
h	Natural growth rate of the prey population	$\mu g L^{-1} day^{-1}$
α_{11}	Consumption rate of prey population by predator population	day^{-1}
g	Extent to which the prey population is protected by the environment	$mg L^{-1}$
δ_1	Intraspecific competition between the prey population	$L mg^{-1} day^{-1}$
α_{12}	Assimilation rate of predator	day^{-1}
a_1	Natural mortality rate of the predator population	day^{-1}
t	Time variable	day

Table 7.9: Units of Parameters used in Chapter 4

Parameter	Description	Units
C_E	Input rate of carbon in water	$mgL^{-1}day^{-1}$
τ_c	Latent time period of carbon in water	day
C_0	Threshold level of carbon in water	mgL^{-1}
γ_1	Rate of reaction of dissolved oxygen with carbon	$Lmg^{-1}day^{-1}$
pH_0	Threshold level of pH of water	$mgL^{-1}day^{-1}$
g	Natural lowering rate of pH in water	day^{-1}
α_1	Rate of natural growth of algal population	mgL^{-1}
a	Growth rate of algal blooms on account of increasing carbon concentration in water	day^{-1}
b	Rate of growth of algal blooms on account of decreasing pH	day^{-1}
β_0	Half saturation constant	mgL^{-1}
d_1	Rate of utilization of oxygen in algal respiration process	$Lmg^{-1}day^{-1}$
h	Natural decay rate of algal bloom	day^{-1}
q	Input rate of dissolved oxygen	$mgL^{-1}day^{-1}$
m_1	Natural depletion rate of dissolved oxygen	day^{-1}
n_1	Consumption rate of dissolved oxygen in the decomposition of algal blooms	
t	Time variable	day

Table 7.10: Units of Parameters used in Chapter 5

Parameter	**Description**	**Units**
ϕ	Growth rate coefficient corresponding to average surface temperature	$Lmg^{-1\circ}Cday^{-1}$
δ	Coefficient of depletion of average surface temperature	day^{-1}
R_0	Level of carbon dioxide in absence of pollution and human activities	mgL^{-1}
τ_0	Average surface temperature in absence of rising carbon dioxide levels	$^\circ C$
Q	Rate of increase of carbon dioxide due to human activities	$mgL^{-1}day^{-1}$
α	Natural depletion rate of carbon concentration	day^{-1}
h	Growth rate of algal blooms due to increasing carbon concentration in water	day^{-1}
a	Proportionality constant	
β	Natural death rate of algal blooms	day^{-1}
I	Input rate of oxygen in water	$mgL^{-1}day^{-1}$
d	Depletion rate of dissolved oxygen due to decomposition process of algal blooms in water	$Lmg^{-1}day^{-1}$
n	Natural depletion rate of oxygen	day^{-1}
d_3	Rate of decrease of dissolved oxygen concentration due to low solubility of oxygen in water due to global warming	$^\circ C^{-1}day^{-1}$
t	Time variable	day

Table 7.11: Units of Parameters used in Chapter 6

Parameter	**Description**	**Units**
Q_1	Input rate of plastic in water body	$\mu g L^{-1} day^{-1}$
α_1	Decay and sedimentation rate of plastic	day^{-1}
I_{10}	Emission rate of greenhouse gases due to anthropogenic activities	$mg L^{-1} day^{-1}$
I_{11}	Increase in greenhouse gases due to degradation of plastic particles	day^{-1}
α_2	Natural depletion rate of greenhouse gases	day^{-1}
q_0	Rate of inflow of nutrients due to agricultural run-off or domestic drainage	$mg L^{-1} day^{-1}$
α_{10}	Rate of natural loss of nutrients	day^{-1}
β_{11}	Proportionality constant	day^{-1}
μ_0	Half-saturation constant	$mg L^{-1}$
θ_{11}	Fractional proportionality constant	
θ_{12}	Rate of decrease of algal growth due to reduced photosynthesis by plastics	$L mg^{-1} day^{-1}$
ψ_0	Natural mortality rate of algal population	day^{-1}
ψ_2	Depletion rate of algal population due to crowdings	$L mg^{-1} day^{-1}$
μ_{11}	Rate of increase of water temperature due to rise in greenhouse gases	$L mg^{-1} {}^{\circ}C day^{-1}$
μ_{12}	Coefficient of surface heat transfer	day^{-1}
G_0	Threshold value for greenhouse gases above which temperature will rise due to global warming	$mg L^{-1}$
T_0	Temperature of environment	${}^{\circ}C$
R	Input rate of oxygen in water	$mg L^{-1} day^{-1}$
K_r	Constant of reaction rate under specific temperature T_r	$L mg^{-1} day^{-1}$
γ_1	Coefficient demonstrating rate of reaction increase if temperature rises by 10 degrees Celsius	${}^{\circ}C^{-1}$
T_r	Reference Temperature	${}^{\circ}C$
α_5	Rate of increase in oxygen concentration due to algal photosynthesis	day^{-1}
α_4	Proportionality constant	$L mg^{-1} day^{-1}$
α_3	Coefficient for rate of natural loss of oxygen	day^{-1}
t	Time variable	day

Table 7.12: Units of Parameters used in Chapter 7

Parameter	**Description**	**Units**
E	Input rate of carbon in water	$mgL^{-1}day^{-1}$
τ_l	Latent time period of carbon dioxide in water	day
C_0	Threshold level of carbon in water	mgL^{-1}
a_1	Rate of reaction of dissolved oxygen with carbon	$Lmg^{-1}day^{-1}$
pH_0	Threshold level of pH of water	$mgL^{-1}day^{-1}$
γ_1	Natural lowering rate of pH in water	day^{-1}
β_1	Rate of natural growth of algal population	mgL^{-1}
α_1	Growth rate of algal blooms on account of increasing carbon concentration in water	day^{-1}
α_2	Rate of growth of algal blooms on account of decreasing pH	day^{-1}
β_2	Half saturation constant	mgL^{-1}
γ_2	Rate of utilization of oxygen in algal respiration process	$Lmg^{-1}day^{-1}$
h	Natural decay rate of algal bloom	day^{-1}
R	Input rate of dissolved oxygen	$mgL^{-1}day^{-1}$
ψ_0	Natural depletion rate of dissolved oxygen	day^{-1}
ψ_1	Consumption rate of dissolved oxygen in the decomposition of algal blooms	$Lmg^{-1}day^{-1}$
n_1	Rate of depletion of oxygen due to its consumption in respiration and growth of the oxygen-dependent population	day^{-1}
n_2	Growth rate of oxygen dependent population	day^{-1}
υ_1	Half saturation constant	mgL^{-1}
υ_2	Half saturation constant	mgL^{-1}
θ_1	Natural mortality rate of the population	day^{-1}
θ_2	Rate of intraspecific competition for the aquatic species	$Lmg^{-1}day^{-1}$
t	Time variable	day

Publications and Presentations

Papers Published from the Thesis

i. P. Kalra, Shreya, Impact of water toxicity and acidity on dynamics of prey-predator aquatic populations: A mathematical model, J. Phys. Conf. Ser. 1531 (2020) 1-19. https://doi.org/10.1088/1742-6596/1531/1/012081. (*SCI and Scopus Indexed Journal-SJR=0.23*)

ii. P. Kalra, Shreya, Study of Effects of Toxicants and Acidity on Oxygen-Dependent Aquatic Population: A Mathematical Model, Int. J. Math. Model. Numer. Optim. 10 (2020) 307-329. https://doi.org/10.1504/IJMMNO.2020.108621. (*Scopus Indexed Journal-SJR=0.16*)

iii. Shreya, P. Kalra, Study on Aquatic Population Dynamics under Pollution and Global Warming: Mathematical Review, Plant Arch. 20 (2020) 2647-2652. (*SCI and Scopus Indexed Journal-SJR=0.12*)

iv. Shreya, P. Kalra, Decline in Dissolved Oxygen due to Increasing Temperature and Algal Blooms: Mathematical Model, Plant Arch. 20 (2020) 2653-2359. (*SCI and Scopus Indexed Journal-SJR=0.12*)

Papers Communicated from the Thesis

i. P. Kalra, Shreya, Mathematical Study on Simultaneous Effects of Rising Plastic Waste due to Coronavirus (COVID-19), Global Warming and Eutrophication on Aquatic Ecosystem- *Communicated in a reputed SCI-indexed Journal.*

ii. P. Kalra, Shreya, Impact of Carbon Emissions and Increased Acidity on Aquatic Population: A Mathematical Model- *Communicated in a reputed WoS-indexed Journal.*

Papers Presented in Conferences

i. P. Kalra, Shreya, Study of Combined Effects of Toxicant and Acidity on Survival of Aquatic Population: A Mathematical Model, 106th Indian Science Congress, January 3-7, 2019, Lovely Professional University, Phagwara, Punjab.

ii. P. Kalra, Shreya, Modelling on Combined Effects of Toxicants and Acidity on Dynamics of Aquatic Population, Women's Science Congress (a part of 106th Indian Science Congress), January 5-6, 2019, Lovely Professional University, Phagwara, Punjab.

iii. P. Kalra, Shreya, Impact of Carbon Emissions and Increased Acidity on Aquatic Population: A Mathematical Model, 7th International Conference on Advancements in Engineering And Technology (ICAET-2019), March 15-16, 2019, BGIET, Sangrur, Punjab. Received the "Best Paper Award" at the conference.

iv. P. Kalra, Shreya, Impact of water toxicity and acidity on dynamics of prey-predator aquatic populations: A mathematical model, Recent Advances in Fundamental and Applied Sciences (RAFAS-2019), November 5– 6, 2019, Lovely Professional University, Phagwara, Punjab.